STUDIES ON THE PRECIPITATION OF SOME PHOSPHATES AND CONFORMATIONS OF CYCLIC COMPOUNDS FROM X-RAY DIFFRACTION DATA

VICTOR OLATUNJI AJIBOLA
B.SC (HONS) A.B.U., M.SC

A Thesis Submitted to the postgraduate School, Ahmadu Bello University, Zaria.

In Partial Fulfilment of the Requirements for the Degree of Doctor of Philosophy in Chemistry.

Department of Chemistry
Faculty of Science
Ahmadu Bello University
Zaria, Nigeria.

DECLARATION

I hereby declare that this thesis has been written by me and that it is a record of my own research. It has not been presented in any previous application for a higher degree.

All sources of information are specifically acknowledged by means of references.

Victor O. Ajibola

DEDICATION

To the One who was, who is and who will forever be - The giver of all good things and the embodiment of knowledge.

ACKNOWLEDGEMENT

I thank God and also thank Professor S.A. Thomas whose inputs, efforts and patience in supervising this work has turned a dream into reality.

I wish to also thank Professor J.Y. Olayemi, who co-supervised this work, for his useful suggestions and encouragement. I thank Dr. J.F. Iyun for his encouragement and concern throughout this period.

I express my gratitude to Mr. Gazzino of Structural Chemistry Research Group, University of Bologna, Italy and Mr. David Barak of the Centre for Energy Research, A.B.U., Zaria, for running the X-ray diffraction patterns of the samples. I am also very grateful to Mr. Fagbemi who drew most of the structures and Mall. Sani Shaka for typing and printing this work. I also wish to thank all my friends in Chemistry Department for their support.

I thank my Pastor, Rev. David Bakare and my colleagues in the praise singers' unit of Jesus is Life World Outreach Ministries for their prayers always.

Finally I thank my wife Mrs. M.A. Ajibola, my daughter Toluwani and my son Oluwadamilola for their support, understanding and love. I thank my sisters and Tope Ande for their support in various ways.

CERTIFICATION

This dissertation entitled, "STUDIES ON THE PRECIPITATION OF SOME PHOSPHATES AND CONFORMATIONS OF CYCLIC COMPOUNDS FROM X-RAY DIFFRACTION DATA" by VICTOR O. AJIBOLA meets the regulations governing the award of the degree of Doctor of Philosophy of Ahmadu Bello University, and is approved for its contribution to knowledge and literary presentation.

S.A. Thomas — 22/1/96

Professor S.A. Thomas
B.Sc (Hons), D.Phil.
Chairman, Supervisory Committee

Date

J.Y. Olayemi — 22/1/96

Professor J.Y. Olayemi
B.Sc. D.Phil.
Member, Supervisory Committee

Date

S.B. Sanni — 11/10/95

Professor S.B. Sanni
External Examiner.

Date

S.A. Thomas — 22/1/96

Professor S.A. Thomas
B.Sc. D.Phil.
Head, Chemistry Department

Date

J.Y. Olayemi — 12/5/97

Dean, Postgraduate School

Date

ABSTRACT

In part I of the thesis, studies were carried out on the precipitation of hydroxyapatite. A preliminary experiment **involving** the preparation of calcium hydroxyapatite (HAP) using three different sets of **starting** materials was done. The crystallinity and stoichiometry of the HAP were dependent on the starting materials.

The precipitation of amorphous calcium phosphate (ACP), and its transformation to HA? in the presence of various compounds and ions have also been studied using x-ray diffractometry. The nucleotides, AMP, ADP and ATP (usually regarded as type II inhibitors) caused a slight but discernible decrease in the mean size of the apatitic crystals. However, citrate another type II inhibitor did not appear to alter the mean cryst size in agreement with literature. It would appear that the effect an inhibitor has on the resultant apatitic crystal is dependent on the mechanism of inhibition and not necessarily on whether it is a type I or type II inhibitor. Results obtained for casein and L-glutamate shows that they may be regarded as type II inhibitors. Tetracycline, a broad spectrum antibiotic which may also be classified as type II inhibitor, caused a slight decrease in the mean size of the apatitic crystals.

Inhibition by this compound seems to be more as a result of steric hinderance rather than attachment to the active site of the HAP nuclei.

Preparation of tin hydroxyapatite was attempted using hydrateci cin (II) oxide as the starting material. To the best of our knowledge, a new tin (II) phosphate was obtained which has strong similarit; 3 with calcium hydroxyapatite (HAP) . This new tin (II) phosphate gave a molybdenum blue colouration due to the reduction f molybdophosphoric acid during phosphate determination, indicating that tin existed in the +2 oxidation state. X-ray diffraction patterns of the products obtained in the attempted preparation of tin calcium hydroxyapatite by aqueous and solid state reactions were obtained. Precipitation from aqueous system containing 3 atom % tin in solution gave product which is essentially featureless and characteristic of amorpnous compounds, in agreement with literature. At tin concentration significantly greater than 20 atom %, the products of solid state reaction at both 500° and 700°C were amorphous.

In part II of the thesis, the conformations adopted by some ring compounds in the solid state are describe, and parameterized. The effects of the molecular environment on the geometry and conformation of the rings, have been elucidated based on x-ray diffraction structural data.

For cycloheptane ring derivatives, the boat

TABLE OF CONTENTS

	Page
Title page	i
Declaration	ii
Certification	iii
Dedication	iv
Acknowledgement	v
Abstract	vi
Table of Contents	ix
List of Tables	xv
List of Figures	xviii
List of Charts	xxi
List of Appendices	xxii

PART ONE

CHAPTER ONE

1.0 INTRODUCTION	2
1.1 Historical Background	2
1.2 Precipitation in calcium phosphate system	4
1.2.1 Types of precipitates	4
1.2.2 Mechanism of precipitation	5
1.3 Significance of Study	8
1.4 Research Objectives	11

CHAPTER TWO

2.0 LITERATURE REVIEW	13
2.1 Amorphous calcium phosphate (ACP)	13
2.1.1 Synthetic Amorphous calcium phosphate	14

2.1.2 Conditions for precipitation of ACP 16

2.2 Calcium Hydroxyapatite (HAP) 18

2.2.1 Formation of HAP 18

2.2.2 Substitution into HAP 20

2.3 Octacalcium phosphate (OCP) 21

2.3.1 Chemical properties of OCP 25

2.4 Dicalcium phosphate dihydrate (DCPD) 26

2.5 Transformation of ACP to HAP 27

2.5.1 Intermediate state in transformation of ACP to HAP 31

2.5.2 OCP precursor model 33

2.5.3 Effects of Environment on ACP-HAP Transformation 36

2.6 Inhibition of ACP-HAP Transformation 39

2.6.1 Inhibition 39

2.6.2 Effects of added Macromolecules on ACP-HAP Transformation 40

2.6.3 Structural factors influencing the ability of compounds to inhibit 43

2.6.4 Effect of added ions on ACP-HAP Transformation 49

2.6.5 Effect of inhibitors and reaction medium upon crystal shape of HAP 51

2.7 X-Ray Spectrometry 52

2.7.1 Origin and Generation of X-rays 52

2.7.2 X-ray diffraction by crystalline solid ... 54

2.7.3 Recording the pattern 56

2.7.4 Application of X-ray diffraction methods in studies of calcium phosphate system 57

CHAPTER THREE

3.0 STUDIES ON CALCIUM PHOSPHATE PRECIPITATION... 61

3.1 Introduction 61

3.2 Experimental 63

3.2.1 Precipitation of calcium hydroxyapatite using three different procedures 63

3.2.2 Precipitation of ACP-HAP precipitates 65

3.2.3 Precip;itation of ACP-HAP precipitates in presence of some metal ions and fluoride ion 67

3.2.4 Preparation of ACP-HAP precipitates in presence of inhibitor molecules 68

3.2.5 Effect of tetracycline on HAP crystals ... 70

3.2.6 Chemical Analyses of samples 70

3.2.6.1 Elemental Analysis using Atomic Absorption spectrophatometry 70

3.2.6.2 Colorimetric determination of phosphorus 71

3.2.7 X-Ray Analysis 72

3.3 Results 75

3.4 Discussion 95

CHAPTER FOUR

4.0 Attempted preparation of 'Tin Hydroxyapatite' and studies on Tin Calcium Hydroxyapatite solid solutions 113

4.1 Introduction 113

4.2 Experimental 116

4.2.1 Attempted preparation of tin hydroxyapatite. 116

4.2.2 Attempted preparation of tin calcium hydroxyapatite in aqueous solution 119

4.2.3 Preparation of tin calcium hydroxyapatite by solid state synthesis 120

4.2.4 X-Ray Diffraction Analysis 120

4.2.5 Infra-red Absorption Analysis 120

4.2.6 The quantification of Tin and Phosphorus in powder samples of unknown tin phosphate precipitate 121

4.2.6.1 X-Ray fluorescence Analysis 121

4.3 Results and Discussion 122

CHAPTER FIVE

5.0 Summary, Conclusion and Recommendations 133

5.1 Summary 133

5.2 Conclusion 135

References 137

PART TWO

Page

CHAPTER ONE

1.0 Introduction 144

1.1 Significance and Objective 145

CHAPTER TWO

2.0 LITERATURE REVIEW 147

2.1 X-ray diffraction method of determining total structure 147

2.2 The torsion angle concept 148

2.2.1 Description of Ring geometry 149

2.2.2 Steric relationships at a Ring junction 153

2.2.3 Quantitative Analysis of Ring Conformation.. 156

2.2.4 Symmetry in Rings 157

2.3 Asymmetry parameters 157

2.4 Conformational Analyses 159

2.4.1 Small Rings 159

2.4.2 Medium Rings 163

2.4.3 Cyclohexane 165

CHAPTER THREE

3.0 Molecular conformation of the Cycloheptane ring derivatives in the solid state 168

3.1 Preamble 168

3.2 Experimental Procedure 172

3.2.1 Data for calculation 172

3.2.1.1 Asymmetric parameters 173

3.2.1.2 Conformational parameters Σ_2 and Σ_s 173

3.2.2 Definition of the conformations 175

3.3 Result and Discussion 175

CHAPTER FOUR

4.0 Molecular conformations of Furanose rings in nucleosides and nucleotides in solid state . 194

4.1 Preamble 194

4.2 Experimental Procedure 197

4.2.1 Calculation 197

4.2.1.1 Asymmetry and Geometric parameters 197

4.2.2 Atomic numbering scheme and Nomenclature for conformations 198

4.3 Results and Discussion 200

CHAPTER FIVE

5.0 Molecular conformations of some Ten-membered Rings 222

5.1 Introduction 222

5.2 Experimental Procedure 226

5.2.1 Calculation 226

5.2.1.1 Asymmetry and Geometric parameters 226

5.2.2 Atomic numbering scheme for 10-membered rings of sesquiterpenes and diterpenes 226

5.3 Results and Discussion 227

CHAPTER SIX

6.0 SUMMARY AND CONCLUSION 239

6.1 Summary 239

6.2 Conclusion 240

6.2.1 Seven-membered rings 240

6.2.2 Five-membered rings 240

6.2.3 Ten-membered rings 241

6.3 Recommendation for further studies 241

References 242

LIST OF TABLES

PART ONE

Page

2.1 Some physicochemical properties of OCP and HAP 24

3.1 Inhibitors and experimental conditions used in ACP-HAP transformation 69

3.2 Ca/P molar ratio of HAP obtained from three different procedures 78

3.3 Cell parameters of HAP obtained from three different procedures 78

3.4 Crystallinity index, $1/\beta_{\frac{1}{2}}$ and mean size D of apatite crystals obtained for HAP at pH 9 and 25°C and 50°C 80

3.5 Crystallinity index, $1/\beta_{\frac{1}{2}}$ and mean size, D of apatite crystals obtained in presence of AMP at 25°C, 50°C and pH 9 80

3.6 Crystallinity index, $1/\beta_{\frac{1}{2}}$ and mean size D of apatite crystals obtained in presence of ADP at 25°C, 50°C and pH 9 81

3.7 Crystallinity index, $1/\beta_{\frac{1}{2}}$ and mean size D of apatite crystals obtained in presence of ATP at 50°C and pH 9.0 81

3.8 Crystallinity index, $1/\beta_{\frac{1}{2}}$ and mean size D of apatite crystals obtained in presence of ATP at 37°C, pH 9.0 and 7.4 85

3.9 Crystallinity index, $1/\beta_{\frac{1}{2}}$ and mean size D of apatite crystals obtained in presence of citrate at 25°C, 50°C and pH 9 85

3.10 Crystallinity index, $1/\beta_{\frac{1}{2}}$ and mean size D of apatite crystals obtained in presence of casein at 25°C and pH 9 86

3.11 Crystallinity index, $1/\beta_{\frac{1}{2}}$ and mean size D of apatite crystals obtained in presence of L-glutamate at 25°C and pH 9 86

3.12 Crystallinity index, $1/\beta_{1/4}$ and mean size D of apatite crystals obtained in presence of tetracycline at 37°C and pH 7.4 87

3.13 Crystallinity index, $1/\beta_{1/4}$ and mean size D of apatite crystals obtained in presence of some ions at 25°C and pH 9 88

3.14 Concentrations of Ca^{2+}, PO_4^{3-} and Ca/P molar ratios for ACP-HAP precipitates obtained at different reaction times 89

3.15 Concentrations of Ca^{2+}, Mg^{2+}, PO_4^{3-} and Ca-Mg/P molar ratios for ACP-HAP precipitates obtained in presence of Mg^{2+} 90

3.16 Concentrations of Ca^{2+}, Zn^{2+}, PO_4^{3-} and Ca-Zn/P molar ratios for ACP-HAP precipitates obtained in presence of Zn^{2+} 90

3.17 Concentrations of Ca^{2+}, Cd^{2+}, PO_4^{3-} and Ca-Cd/P molar ratios obtained for ACP-HAP precipitates in presence of Cd^{2+} 91

4.1 Ionic radii and cell parameters for some synthetic hydroxyapatites 127

4.2 Mean wavenumbers for the vibrations of phosphate and hydroxyl groups of synthetic apatites and the new tin phosphate..... 127

PART TWO

Page

3.1 Conformation and Geometric parameters for some cycloheptane ring derivatives in the chair/Twist forms 177

3.2 Endocyclic torsion angles of some cycloheptane ring derivatives in the chair/ Twist-chair conformations 178

3.3 Conformation and Geometric parameters for for some cycloheptane ring derivatives in the Boat/Twist-Boat forms 184

3.4 Endocyclic torsion angles of some cycloheptane ring derivatives in the Boat/ Twist Boat conformations 184

3.5 Stereochemistry of Ring fusion to the cycloheptane derivative 189

4.1 Geometric and conformational parameters for some furanose rings 204

4.2 Geometric and conformational parameters for some furanose rings 205

4.3 Endocyclic torsion angles of some furanose rings 206

5.1 Ring symmetries and conformations of some cyclodecane derivatives 230

5.2 Geometric and conformational parameters for some cyclodecane ring derivatives 231

5.3 Endocyclic torsion angles for some cyclodecane derivatives 232

LIST OF FIGURES

PART ONE

Page

2.1 X-Ray diffraction patterns of amorphous phosphate (ACP) and synthetic hydroxyapatite (HAP) 15

2.2 Structure of calcium hydroxyapatite and Octacalcium phosphate projected through the C-axis on to the basal plane 23

3.1 X-Ray patterns of HAP prepared by methods a, b, and C. 77

3.2 X-Ray patterns of ACP-HAP precipitates prepared at 25°C, 50°C and pH 9 79

3.3 X-Ray patterns of ACP-HAP precipitates prepared in presence of ATP at pH 9/37°C and pH 7.4/37°C 82

3.4 X-Ray patterns of ACP-HAP precipitates in presence of tetracycline (concentrations, 0.025mg/cm^3 and 0.01/mg/cm^3) at pH 7.4 and 37°C 92

3.5 X-Ray patterns showing (a) HAP and (b) HAP treated with tetracycline 93

3.6 Variation of Ca-M^{2+}/P molar ratios with time. 94

3.7 Structures of some of the inhibitors used .. 100

4.1 X-Ray diffraction pattern of the new tin phosphate 124

4.2 Infra-Red spectrum of the new tin phosphate . 125

4.3 Infra-Red spectrum of basic calcium phosphate. 126

4.4 X-Ray diffraction spectra of the product obtained from an aqueous solution containing Sn^{2+} and Ca^{2+} in the ratio 3:97, and solid solutions in the range 0-10 atom % Sn^{2+} obtained at 500°C 129

4.5 X-Ray diffraction spectra of solid solutions in the range 0-30 atom % Sn^{2+} obtained at 700°C 130

PART TWO

2.1 Designation of torsion angles 151

2.2 Geometry as a function of successive torsion 151

2.3 Rules of conformational transmission at a trans junction 154

2.4 Rules of conformational transmission at a Cis junction 154

2.5 Symmetry in five and six-membered rings .. 158

2.6 The nomenclature defining the location of an asymmetry parameter 158

2.7 Torsion angles in cyclopentane 161

2.8 The symbols and rules for use of sign sequence convention 164

2.9 The flexible form of cyclohexane 166

3.1 Atomic numbering scheme used for a cycloheptane ring with two fused 5-membered ring; schematic representations of twist chair, chair and twist boat conformations of cycloheptane illustrating preferred stereochemistry of 5-membered ring fusion..... 169

3.2 Sketches showing symmetry pairs of endocyclic torsion angles (w) used in calculating the conformation parameters Σ_2; Σ_s 174

3.3 Topological conventions of sign sequences of the endocyclic torsion angles in the various conformations. 174

3.4 Correlated variation of principal asymmetry parameters ΔC_s and ΔC_2 for cycloheptane derivatives in the chair and twist chair conformations..... 179

3.5 Correlated variation in the conformation parameters Σ_s and Σ_2 for cycloheptane derivatives in the chair/twist chair conformations. 180

3.6 Correlated variation in principal asymmetry parameters ΔC_s and ΔC_2 for cycloheptane derivatives in the boat and twist boat fonformations 185

3.7 Correlated variation in the conformation parameters Σ_s and Σ_2 for cycloheptane derivatives in the boat and twist boat conformations. 186

4.1 Diagramatic projections of the furanose ring showing the C(3') and C(2') pucker 196

4.2 Atomic numbering scheme and designation of torsion angles for purines and pyrimidines; nomenclature for some symmetric conformations of some furanose rings 199

4.3 Correlated variation in principal asymmetry parameters of some nonplanar ΔC_2 (2-3) versus ΔC_s (3) furanose rings 209

4.4 Correlated variation in principal asymmetry parameters of some nonplaner ΔC_2 (3-4) versus ΔC_s(3) furanose ring 210

4.5 Correlated variation in principal asymmetry parameters of some ΔC_2 (1-2) versus ΔC_s (2) furanose rings 211

4.6 Correlated variation in principal asymmetry parameters of some ΔC_2(2-3) versus ΔC_s (2) furanose rings 212

5.1 Some viable 10-membered rings with planes of symmetry 225

5.2 BCB form of cyclodecane showing substituent positions and ring symmetry 233

5.3 Correlated variation in principal asymmetry parameters ΔC_2 (2-3), ΔC_2 (4-5), ΔC_2(3-4) of some cyclodecane derivative 234

LIST OF CHARTS

PART TWO

Page

3.1 Structural formulae of compounds discussed showing the molecular environments of the cycloheptane derivatives. 191

4.1 Structural formulae of compounds discussed showing the molecular environments of the furanose ring 218

5.1 Structural formulae of compounds discussed showing the molecular environment of the 10-membered ring 237

LIST OF APPENDICES

Appendix		Page
I	X-Ray powder diffraction patters of ACP-HAP precipitates in presence some ions.. 251	
II	X-Ray powder diffraction patterns of ACP-HAP precipitates in presence of some inhibitor compounds	254
III	X-Ray diffraction data for the new Tin phosphate	256
IV	Description of Torsion angle	257
V	Names, codes and References of the sesquiterpenes containing F-membered ring ...	258
VI	Names, codes, and References of the nucleosides and Nucleotides containing the furanose ring	260
VII	Other viable 10-membered rings with planes and axes of symmetry	263
VIII	Names, codes and references of sesquiterpenes containing 10-membered ring.	264

PART ONE

PRECIPITATION OF SOME PHOSPHATES

CHAPTER ONE

1.0 INTRODUCTION

1.1 Historical Background

Bone mineral has been shown to consist of two calcium phosphate pools, a noncrystalline (amorphous) calcium phosphate and a crystalline (apatite) phase (Posner, 1969). The hardness and physical strength of bone, differentiating it from other connective tissues, stem from the extracellular deposition of calcium phosphate within a soft, fibrous, organic matrix. This highly specialised connective tissue not only forms the supportive framework of the body but also enters into metabolic interaction with it (Posner 1969). The chemical nature of the micro-crystals in bone and the physical properties of its surfaces have been the subject of discussion for many years. The conventional view is that hydroxyapatite (HAP) is the relevant compound. About 65% of a mature bone is calcium phosphate, and the two phases are chemically and physically distinct. Thus, the percent crystallinity of bone (that is the percent by weight of the total mineral that is apatitic and not amorphous) is another important physical parameter of this tissue. The basic model is modified in detail by internal lattice faults with entrapped contaminants, and the free surfaces are believed to have suffered

heteroionic exchange with ions such as Sr^{2+}, Mg^{2+}, Na^{+}, CO_3^{2-} and citrate (MacGregor and Brown, 1965). In consequence quantitative analysis of whole bone has yielded no definitive data.

In the formation of bone mineral, the amorphous phase is laid down first by some active process of the bone cell. Subsequently some of the phase is stabilised to remain noncrystalline, while a larger portion is transformed via solubilisation to the crystalline form (Posner 1969, Eanes and Meyer, 1977).

The description of the *in vivo* transformation of the amorphous calcium phosphate to the crystalline calcium phosphate is inferred from studies on synthetic analogues. The reaction of calcium and dibasic phosphate salts in neutral or basic solution has as its final product crystalline hydroxyapatite. During the precipitation of the crystalline material a precursor phase is formed which is amorphous to x-ray diffraction (Eanes et al, 1965). This amorphous phase converts in the presence of water to microcrystalline hydroxyapatite. The lifetime of the metastable amorphous precursor in aqueous solution is a function of the presence of certain macromolecules, interfering ions, pH, viscosity, ionic strength and temperature (Eanes et al, 1965, Termine and Posner, 1970).

1.2 Precipitation in calcium phosphate system

1.2.1 Types of precipitates

The behaviour of supersaturated calcium phosphate solutions in regard to what they may precipitate, is a matter of considerable importance to the physiology of hard tissues. A degree of supersaturation is often encountered in solutions of calcium phosphates and other calcium or phosphate salts, whereas for instance, silver halides precipitate readily from solutions just above saturation. Ignoring different hydrates, five pure orthophosphate of calcium may crystallize from aqueous solution (Laundager Madsen, 1970). They are:

I Primary calcium phosphate, $Ca(H_2PO_4)_2$

II Secondary calcium phosphate, $CaHPO_4$

III Tetracalcium monohydrogen triphosphate, $Ca_4H(PO_4)_3$

IV Tricalcium phosphate, $Ca_3(PO_4)_2$

V Calcium hydroxyapatite $Ca_5(PO_4)_3OH$.

I Crystallizes only from strong phosphoric acid as anhydrous or with one mole of water. II exist in two forms, the anhydrous form (monetite), which is stable above approximately 36^{o}C, and the dihydrate (brushite). Both can be precipitated from slightly acid solution, pH <6. III is the normal product of precipitation in

neutral or slightly basic medium. It is metastable and will slowly recrystallize to hydroxyapatite. IV which is anhydrous is formed by heating HAP at a temperature of 3500°C. V is the stable final product of precipitation from neutral or basic solutions. As its rate of crystallization is very slow at ordinary temperature, it often appears as submicroscopic crystals.

These multitude of possible solid phases which may occur in the calcium phosphate system make the quantitative description of precipitation and dissolution extremely complex (Lundager Madsen, 1970).

1.2.2 Mechanism of precipitation

The formation of a crystalline precipitate from a supersaturated solution is included in the general phenomenon of phase change. Although the precipitation of sparingly soluble salts is important in a wide variety of fields, the mechanism of the crystallization process, is one of the least well understood phenomena in chemistry (Koutsukos et al, 1979). The structure of the precipitate is the result of many kinetic processes which interact with each other. The concept of structure comprises the following: the particle size distribution; the lattice structure of the precipitated crystals; the shapes and morphology of the crystals and in some cases the distribution of the various shapes; the structure of

the surfaces; the presence of dislocations, imperfections, impurities and inclusions in the crystals; and the nature of interparticle interaction resulting from flocculations, aggregation and agglomeration (Dunning, 1973).

In studying precipitation processes it is important to distinguish three different stages in the mechanics of crystallization -

i) The nucleation stage in which the first minute particles of the new phase are generated within the motherphase.

ii) The growth of these nuclei, nurtured by the motherphase to form primary crystalline particles.

iii) The ageing of the primary dispersion or precipitate during which changes in shape, structure, perfection, size, aggregation, agglomeration and flocculation may take place (Wray et al, 1957 and Dunning, 1973).

These processes are not entirely independent of each other. For example, growth processes are involved in nucleation and nucleation takes place during part of the growth stage, while ageing is not confined to the later stages but may occur earlier.

Bone growth is an example of this nucleation phenomena, in that it represents the birth of one phase

from another. The precipitation of calcium phosphate, involving the formation of nonapatitic calcium phosphate phases during the early stages is a complex one. Some of the practical difficulties arising in the study of crystal nucleation from solution are concerned with the elucidation of the relative roles of crystallization, dissolution and agglomeration in the whole precipitation scheme. For these reasons the mechanism of primary processes in precipitation from solution is to some extent obscured, and as a consequence the interpretation of data has often been contradictory (Walton, 1965). Such difficulties as determining the stoichiometry of precipitation from the results of precipitation experiments is due to the appreciable reduction in the concentrations of crystal lattice ions during reaction (Koutsoukos et al, 1980). At each stage, the supersaturated solutions may be metastable with respect to different phases which can form and subsequently redissolve as the concentrations decrease. In the precipitation of calcium phosphates, this probably accounts for the apparent variable stoichiometry and complex kinetics observed experimentally.

It has been shown (Eanes et al, 1967; Walton et al, 1967 and Furedi-Milhofer et al, 1972) that precipitation in basic calcium phosphate system proceeds in at least two steps:

i) The initial formation of metastable colloidal suspensions which forms in neutral or basic solutions.

ii) Secondary precipitation and crystallization which ensue after a period of metastability. Further changes occur mainly due to ageing and hydrolysis.

The complete sequence of events is strongly dependent upon temperature and solution environment (Termine and Posner, 1970).

Although the detail of the nucleation process involved are not known it is possible to establish the composition of the precursor phase (McGregor and Brown, 1965; Walton et al, 1967). The initial stages of nucleation are difficult to investigate owing to problems associated with the detection of nuclei of atomic dimensions. Nucleation and crystal growth are spontaneous processes which lower the energy of the growing particle and the nucleation process has to overcome an activation energy. A physical expression of this energy barrier is the supersaturation which is attained before nucleation and crystal growth ensue.

1.3 Significance of study

The formation and identification of metastable phases during, and subsequent to phase transitions have important implications in many systems particularly those

of biological nature. The type of crystals which are usually involved in metastable phase transitions are those in which there is a large entropy of crystallization (e.g. silicates and some phosphates). Considerable speculation and controversy have surrounded the nature of the calcium phosphate which precipitates under physiological conditions.

In bones there is a mixture of the amorphous phase and the crystalline phase in contact with water. Thus, it is obvious that some factors must exist within living systems which regulate the physicochemical conversion of amorphous calcium phosphate to the crystalline apatite. Knowledge of the mechanism(s) involved is of importance for understanding the growth of bone mineral. Industrially, knowledge of this mechanism could be of importance for water softening and waste water treatment processes (Feenstra et al, 1979). The suggestion that OCP is present in greatest amounts in newly formed bone, whether child or adult means that the chemical properties and interaction of two crystalline species must be taken into account for a full understanding of bone growth and remodelling, bone healing and various pathological conditions. Furthermore studies of calcium phosphate systems will give clearer understanding of:

i) mechanism for prevention of dental caries by fluoride in drinking water;

ii) the unusual variability in the stoichiometry of apatitic precipitates;

iii) the cause of ribbon like and platey morphologies of biological apatitic crystallites;

iv) a possible mechanism for incorporation of impurities and defects into dental enamel;

v) a mechanism of growth of biological apatites; and

vi) a rationale why teeth may vary in their caries susceptibility.

Although the precipitation of sparingly soluble salts is important in a wide variety of fields, the mechanism of crystallization process is one of the least well understood phenomena in chemistry. The crystallization of inorganic salts from aqueous solution is important because of its involvement in areas such as removal of phosphate from waste water, the fate of elements such as Al, Ca, Fe and other heavy metals in the formation of lake and ocean sediments, and in industry where formation of scale on metal surfaces is a continuing problem. In desalination technology the reduction of heat transfer surfaces by growth of magnesium hydroxide and calcium salts such as sulphate hydrates, carbonate polymorphs and phosphates is a serious limitation to the use of evaporative techniques. Calcium phosphate formation is involved in many of these

processes yet the stoichiometry of the precipitated phases is still poorly understood.

1.4 Research objectives

In a preliminary survey, HAP will be prepared using somewhat different starting materials. The aim is to determine whether the crystallinity and stoichiometry of the apatitic products depend on the materials used for preparation. Generally this part of the work is to study the transformation of ACP to HAP, and to determine how some substances (of biological origin), and some ions would affect this conversion. Since the bone of a matured human adult consists of a mixture of ACP and HAP, it would appear that a mechanism exists which regulates the conversion of ACP to HAP *in vivo*. This *in vitro* study was therefore undertaken as part of the on-going search to determine the transformation process. The studies with inhibitors may provide information on the nature of conversion, classification of the inhibitors and structure-activity relationship. X-ray analyses as well as chemical analyses of the solids obtained will be carried out with the aim of determining the extent of conversion, the mean sizes of the particles and the Ca/P molar ratios. The effect of pH and temperature on the transformation process will also be determined.

An attempt is made to prepare tin hydroxyapatite, which has never been prepared. Characterization of the

solid compound obtained will be carried out using X-ray diffraction spectrophotometric and X-ray fluorescence methods. Isomorphous substitution of tin into HAP will also be attempted by aqueous and solid state reactions. The aim here is to compare the interaction of tin with HAP on the one hand, with the interaction of its heavier congener, lead, with the same phosphate. Lead has been shown to substitute for calcium in $Ca_5(PO_4)_3OH$ in the whole range.

CHAPTER TWO

2.0 LITERATURE REVIEW

2.1 Amorphous calcium phosphate (ACP)

On the basis of chemical, x-ray diffraction and electron-microscope studies, it has been assumed that the inorganic constituent of bone tissue is a poorly crystallized calcium phosphate resembling, but not identical to the mineral hydroxyapatite in structure and composition. This single phase description is no longer adequate and bone mineral is now thought to be composed of at least two chemically and physically distinct calcium phosphates (Posner, 1969). Results have indicated that besides an apatite phase, bone mineral contains a large proportion of a noncrystalline (amorphous) calcium phosphate. This noncrystalline phase was found to be extensively and uniformly distributed throughout the osseous tissue of several mammalian species (Termine and Posner, 1967). Approximately 40% of the mineral in the femurs of adult human, cow and rat is amorphous.

The amorphous content of bone however, does apparently vary with age. It appears that the amorphous material predominates in early bone but is superseded by crystalline apatite as bone matures (Posner, 1969).

The little that is known about the properties of *in*

vivo ACP, shows clearly that this phase is not apatitic in structure. When viewed in the electron-microscope, this material consists of aggregates of extremely fine particles and contrasts markedly with the straight edged, solid needle-shaped crystals of bone apatite.

2.1.1 Synthetic Amorphous Calcium Phosphate

The description and knowledge of properties of *in vivo* ACP in mineralised tissue is limited and at present, additional properties can only be inferred from studies on synthetic analogues. In this regard, the initial solid phase that appears in the rapid precipitation of calcium orthophosphate from basic solutions is structurally noncrystalline, though well defined chemically (Eanes et al 1965, Bienenstock and Posner 1968). The molar Ca/PO_4 ratio of this amorphous phase was found to vary from 1.44 - 1.55, depending on the conditions of precipitation and on the calcium salt used in the precipitation (Posner, 1969). The molar Ca/PO_4 ratio is consistent for each salt, a ratio of 1.52 was found when the nitrate solution was used, a value of 1.46 was observed when the chloride solution was used. The amorphous material with a Ca/PO_4 molar ratio 1.50 was found to have the greater solution stability. This observation is a possible chemical justification for

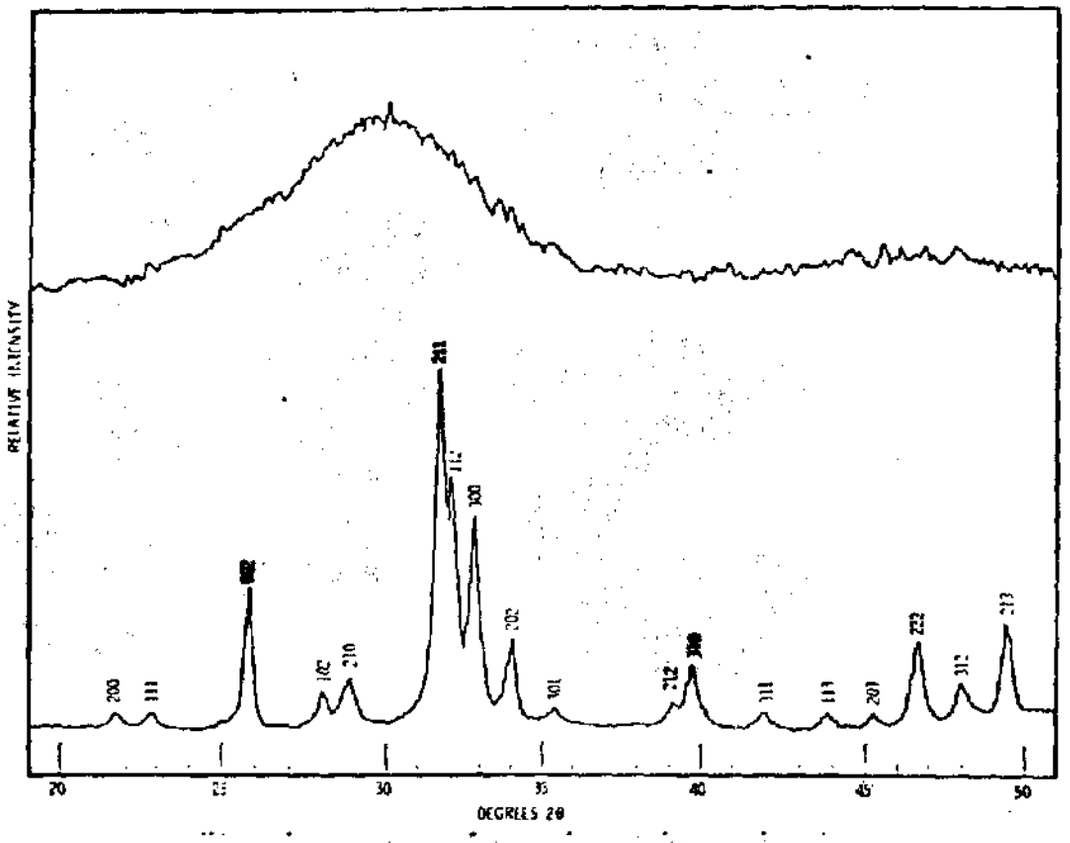


Figure 2.1 X-Ray diffraction patterns of amorphous calcium phosphate (upper) and synthetic hydroxyapatite (lower). The Miller indices are shown on the crystalline pattern (Posner, 1969).

considering the amorphous calcium phosphate as hydrous tricalcium phosphate, TCP having the chemical formula $Ca_3(PO_4)$ $.^xH_2O$ (Lundagar Madsen et al, 1986). The amorphous material has a transient existence when kept in contact with its preparative medium and rapidly converts into crystalline apatite. The degree of instability could be related to the deviation of the composition form the $Ca_3(PO_4)_2$ composition.

The x-ray diffraction patterns of ACP does not contain many sharp Bragg maxima characteristic of crystalline materials, but instead, consist of a few diffuse, ill-defined maxima typical of such commonly recognised noncrystalline substances as glasses and certain polymers (See figure 2.1). A lack of crystalline structure does not imply a lack of local or short range atomic order (Eanes and Posner, 1965). The observation that the Ca/PO_4 molar ratio of this material which is 1.5 is only slightly influenced by the initial Ca/PO_4 molar ratio of the preparative solution, suggests a well defined local structural unit. What is absent in this case is the periodically repetitive spatial array of this local unit unique to crystalline substances (Eanes and Posner, 1965).

2.1.2 Conditions for precipitation of ACP

Knowledge of the conditions for precipitation of ACP is essential for understanding the behaviour of

supersaturated Ca/PO_4 solutions, since it strongly influences the occurrence domains of other phases. It is generally recognised that ACP is formed in the higher pH range pH > 6.7. Whenever formed, ACP normally appears as the first precipitate. Through its consumption of calcium and phosphate as well as its lowering of pH (except in strongly basic solutions). It reduces the supersaturation of other calcium phosphates, often below the critical value for homogeneous nucleation (Posner, 1969).

In solutions containing, apart from calcium and phosphate, only ammonium and nitrate ions, ACP is formed whenever the quantity.

$$Ia = a^3(Ca^{2+})a^{2+}(HPO_4^{2-})a^{-2}(H^+)$$

exceeds a certain critical value. This value decreases strongly with increasing temperature (Lundager Madsen and Thovardarson, 1989). Ia is the formation constant and a the activities of the ions. This mass-action expression corresponds to the reaction -

$$Ca_3(PO_4)_2 + 2H^+ \text{-------} > 3Ca^{2+} + 2HPO_4^{2-}$$

Normally the formation of ACP is instantaneous or nearly so, but in some cases of very dilute solutions, delays of up to several hours can be observed (Lundager Madsen et al, 1986). Decreasing the dielectric constant of the medium by the addition of either dioxane or methanol greatly enhanced ACP formation. Foreign ions such as

$P_2O_7^{4-}$, CO_3^{2-}, F^- and Mg^{2+} all enhance formation of ACP. (Termine and posner 1970). Increasing the intrinsic viscosity of the medium with either glycerol or sucrose inhibited ACP formation considerably.

2.2 Calcium hydroxyapatite, HAP

The basic calcium phosphate mineral, hydroxyapatite, $(Ca_{10}(PO_4)_3(OH)_2$ is a prototype of one of the major constituents of bone and teeth. Studies have been carried out on this material by bone biologists, surgeons, dentists, fertilizer chemists, catalyst chemists, geologists, solid state physicists and so on. Apatites represent a major source of phosphorus and calcium in the earth's crust, and it occurs also in igneous and sedimentary rocks.

Biological apatite is not pure HAP, but is modified by the presence of many other ions such as Cl^-, F^- substituted for some OH^-; Sr^{2+}, Ba^{2+} for some Ca^{2+}, and CO_3^{2-} for PO_4^{3-}. Apatite, in general refers to a family of compounds such as fluoroapatite, $Ca_5(PO_4)_3F$, chloroapatite, $Ca_5(PO_4)_3Cl$ and hydroxyapatite, $Ca_5(PO_4)_3OH$ (Posner, 1969).

2.2.1 Formation of HAP

The formation of HAP as in bone growth is an example of nucleation phenomena, because it represents the birth of one phase from another. In the presence of high concentrations of calcium and phosphate (total Ca and

total PO_4 greater than 10mM) and pH values greater than 6.8, the precipitation of hydroxyapatite is always preceded by the formation of an amorphous precursor (Eanes et al, 1965, Walton et al, 1967; Termine 1972, and Boskey and Posner, 1973). In the absence of such foreign ions as F^- and CO_3^{2-}, HAP is the thermodynamically stable end product of calcium phosphate precipitations carried out at physiological pH (7.4) and temperature (37°C) (Eanes and Meyer, 1977). Boskey et al (1976) found that, in the presence of lower concentration of calcium and phosphate (total Ca and total PO_4 each less than 2mM), the first precipitate formed at pH 7.4 has an x-ray diffraction pattern, morphology and colloidal properties distinct from those of ACP found in the presence of higher concentrations of reactants. This observation contradicts the results of Termine and Posner, (1970) and Eanes (1970), who concluded that ACP was an obligatory precursor to HAP. Furthermore, it is apparent that the pH and specific concentrations of calcium and inorganic phosphate as well as the ionic strength, temperature and presence of heteronuclei rather than calcium phosphate millimolar products alone are critical in determining the initial phase precipitated in the course of HAP formation (Nancollas et al, 1974 and Boskey et al, 1976).

Synthetic basic calcium phosphate prepared from carbonate-free aqueous solutions have x-ray diffraction

stoichiometry by exhibiting low Ca/P molar ratios (Posner, 1969). This has been attributed to the adsorption of HPO_4^{2-} on the surface of the HAP crystal and missing calcium ions either from the surface or interior of the crystal. The calcium-deficient apatites are in reality a continuous series of lamellar intergrowth between octacalcium phosphate and HAP (Brown, 1966). A typical crystal of hydroxyapatite precipitated from solution at room temperature would be needle-like in appearance, with dimensions 200Å x 50Å x 50Å. Such a crystal would have a high reactive surface comparable to many catalysts (Posner, 1969).

2.2.2 Substitution into HAP

The hydroxyapatite structure is subject to isomorphous substitution. The incorporation of foreign ions affects the crystallinity, morphology and lattice parameters, and as a consequence the stability of the apatite structure (Bigi et al, 1991). Furthermore, the presence in solution of foreign ions can prevent the formation of the apatitic phase from solution. The anions F^- and Cl^- replace hydroxyl ions chemically. The closer coordination of the fluoride as compared to the hydroxyl by the calcium accounts in part, for the greater chemical stability of fluoride substituted HAP as evidenced by its resistance to dental caries (Posner, 1969). The entry of carbonate into the crystal structure

especially in the phosphate position causes a lattice distortion (Legeros et al, 1967). Furthermore, HAP precipitated in the presence of carbonate tends to be poorly crystallized, showing broad x-ray diffraction patterns and its weakening effects on the bonds in the structure thus increasing the rate of dissolution and solubility.

The role and location of the many potential substituents for Ca^{2+} in the apatite structure have remained unclarified. Substitution of various cations for calcium in calcium hydroxyapatites is generally related to the size of the ionic radii of the ions compared to that of Ca^{2+} ion (Bigi et al, 1991). In biological apatites many cations have been assumed to be only adsorbed on the apatite surface and not part of the structure (LeGeros et al, 1980).

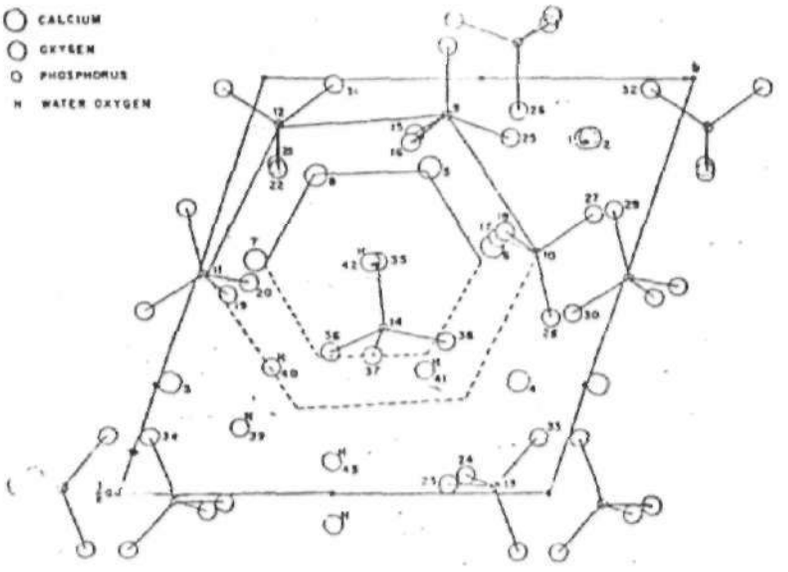
The pH of the solution affects the nature and the extent of incorporation. The concentration of the foreign ion also causes the formation of apatite with differing crystallinity and optical spectra (Posner, 1969).

2.3 Octacalcium Phosphate, OCP

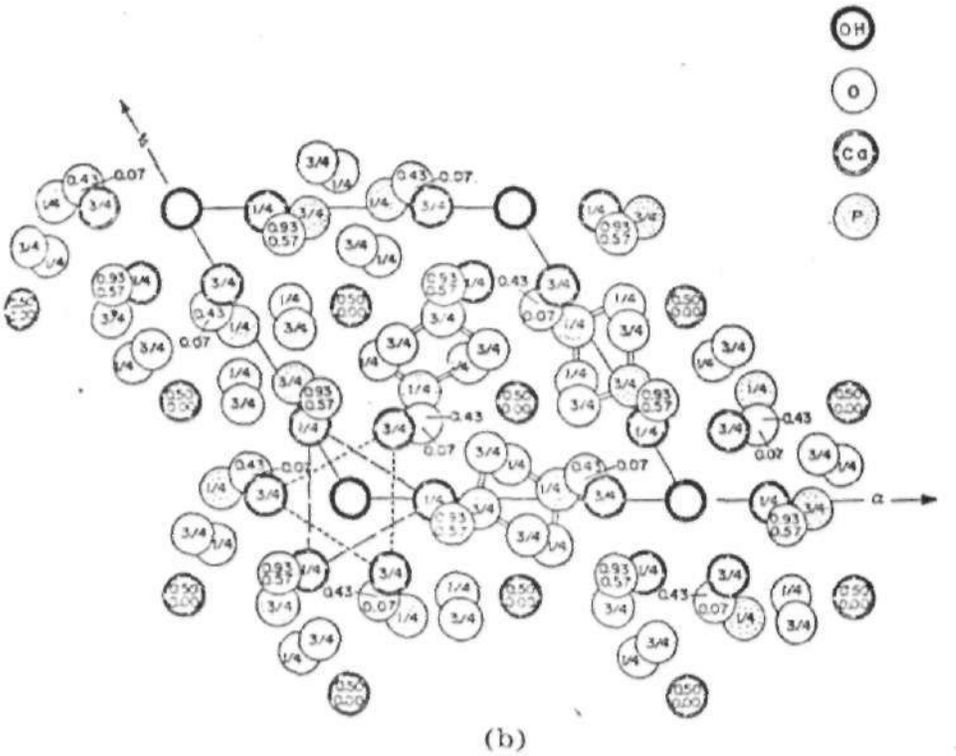
Octacalcium phosphate, $Ca_8H_2(PO4)_6.5H_2O$ is encountered in systems containing calcium phosphates more basic than dicalcium phosphate. OCP has a significant

role in the chemistry of bones, teeth, phosphate fertilizers and other precipitated calcium phosphates (Brown et al, 1962). OCP has distinctive x-ray and optical properties and it contributes additional lines in carlstrom's x-ray pattern for HAP. Single crystal Weissenberg measurements on OCP gave lattice constants, a = 19.70Å b = 9.59Å and c = 6.87Å. The existence of OCP as a distinct crystalline phase, rather than a hydrous defective apatite was established by single crystal and powder diffraction x-ray studies. Its x-ray, optical and chemical properties indicate that OCP is structurally related to HAP, although the two salts are not isostructural (Figure 2.2). OCP is composed of apatitic layers that are parallel to the b-c plane and separated by hydrated layers. Chemical analyses do not yield constant numbers of water of hydration, and this uncertainty reflects the ease with which water enters and leaves the OCP lattice (Brown et al, 1957).

The layer-type structure of OCP and the similarity of parts of its structure to that of HAP are reflected in the chemical and physical properties of OCP. The close correspondence between the atomic positions in apatite layer in OCP and those of HAP, (Figure 2.2) indicates that epitaxial overgrowths of one compound on the other are very likely (Posner, 1969). The water layer, which occupies almost half of the OCP unit cell, rules out



(a)



(b)

Figure 2.2 Structure of octacalcium phosphate (a) and calcium hydroxyapatite (b) projected through the c-axis on to the basal plane (Posner, 1969; Brown et al, 1962).

consideration of OCP as a defect apatite and makes formation of true solid solutions of the two compounds highly unlikely (Brown et al, 1962). The formation of lamellar mixed crystals of the two compounds is more probable. This intracrystalline mixtures not only account for apatitic precipitates with Ca:P ratios less than that in HAP, but also explains observed chemical and physical properties of the precipitated basic calcium phosphates.

Some indications support the idea that OCP may be present in bone. The 'platey' habit of crystallites in bones has been interpreted as indicating that OCP participated in their formation. Thus it is considered that bone mineral is first formed as OCP and that there are spontaneous ageing changes (hydrolysis) which convert OCP into HAP (MacGregor and Brown, 1965). In children where bone growth is maximal, there tends to be more OCP in the microcrystals than in the older subject where the reorganisation of the OCP to HAP overtakes the precipitation process.

Table 2.1 Some Physical Properties of OCP and HAP.

	HAP	OCP
A-axis	9.432A	9.630A
C-axis	6.881A	6.870A
Ca/P ratio	1.67	1.50

2.3.1 Chemical properties of OCP

OCP can be converted to HAP by progressive hydrolysis in boiling water. This is reflected in a gradual increase in indexes of refraction, and decrease in the intensities of the OCP lines in the x-ray powder pattern of the residual solids and the emergence of sharp HAP patterns. The pattern of an OCP crystal that had been boiled is essentially that of HAP alone, indicating that there is considerable reorganisation of the lattice during hydrolysis (Brown et al, 1962).

Anhydrous dicalcium phosphate DCPA having a chemical formular, $CaHPO_4$ is sometimes formed as a separate phase in the hydrolysis of OCP. OCP is not the most stable calcium phosphate under any of the conditions of its preparation, even though OCP precipitates in preference to HAP and DCPA. Brown et al (1970), showed that aggregates of extremely fine acicular crystallites of HAP appeared during the hydrolysis of OCP crystals and that precipitation of HAP was maintained by dissolution of OCP. Thus, HAP apparently is produced by two mechanisms, and its acicular or platey habit shows whether it had been produced by direct precipitation or hydrolysis respectively.

On drying at temperatures slightly above 100^{o}C, OCP loses some of its water of crystallization without apparent change in its x-ray powder diffraction pattern,

although its mean refractive index increases slightly. As drying temperature is raised, the material progressively loses water and the OCP line patterns gradually weaken and disappear at about 180°C (Brown et al, 1962), forming an apatite and DCPA. There is no evidence of HAP and DCPA by direct precipitation or by hydrolysis of OCP.

In aqueous systems containing low concentrations of fluoride ions, fluorapatite is the most stable calcium phosphate (Farr et al, 1962). OCP is reported to react with fluoride to produce an apatite. The apatite reflections are less sharp than the OCP reflections. In contrast to dehydrated or hydrolysed OCP crystals, fluoride-treated OCP crystals are very soft and smear easily. If OCP is present in tooth enamel, fluoride treatment would increase its chemical stability but may decrease its mechanical strength (Brown et al, 1962). HAP also reacts with fluoride, but much slower than OCP, implying that, when a lamellar mixed crystal of HAP and OCP is treated with fluoride solution, the resulting crystal is largely fluorapatite interlayered with HAP.

2.4 Dicalcium phosphate Dihydrate, DCPD

Dicalcium phosphate dihydrate, DCPD is an important product of the application of fertilizers to soils. The main interest in this sparingly soluble salt stems from its participation in the physiological formation of

calcium phosphates. Thus, DCPD has been proposed as an intermediate in the formation of bones and teeth; but there is still much discussion as to the exact nature of the precursor in the formation of HAP under physiological conditions. DCPD may also play an important part in dental caries occurrence. Caries is believed to result from the acid attack upon the dental enamel, mainly HAP, of organic acids produced by the metabolic action of bacteria living in the vicinity of the enamel surface. These organic acids with pKa values in the range 5 to 7, produce acidic conditions with pH from 4 to 6. In aqueous solutions of calcium phosphate under such conditions, the stable solid phase consists of dicalcium phosphate, and a complex species present in the solution are $CaH_2PO_4^+$ and $CaHPO_4$ (Marshal et al, 1969).

2.5 Transformation of ACP to HAP

One of the peculiarities of the aqueous calcium phosphate system is the occurrence of amorphous calcium phosphates which are isothermally unstable over the pH range 6.8-12. If they are in contact with their preparative solution, these materials will hydrolyse nonreversibly into crystalline apatite. The physicochemical mechanisms which govern this precipitate phase transformation process are such that once initiated it would normally proceed to completion, that is, only crystalline apatite is present (Eanes et al, 1965; Eanes

and posner, 1965). Therefore, amorphous calcium, phosphate would be expected to have only a finite suspension lifetime the natural extent of which may be dependent upon the exact experimental conditions used.

In synthetic systems this conversion rate has proved to be strictly proportional to the number of apatitic crystals already formed and not on the amount of material remaining (Posner, 1969). Such autocatalytic behaviour is an example of secondary heterogeneous nucleation, where the crystalline phase evolves through the nucleation of new crystals on the surface of the already developed crystals. Secondary nucleation phenomena can occur only in solutions supersaturated with the ions of the crystallizing phase (in this case with calcium, phosphate and hydroxyl ions). (Posner, 1969; Feenstra et al, 1979). This implies that the amorphous calcium phosphate is more soluble than the crystalline apatite. The fact that the secondary mechanism is the only rate-determining step in the conversion suggests further that the amorphous phase acts essentially as a passive, labile reserviour of calcium and phosphate ensuring a steady-state condition of supersaturation throughout the conversion (Tung et al, 1983).

The isothermal metastability of the ACP in solution implies that the formation of this phase is a kinetic rather than a thermodynamic phenomenon. This initial

interaction between solution calcium and phosphate ions apparently results in collisions leading to irregular coordination complexes, which, upon separating from solution, do not grow into periodic crystalline structures. The spontaneity and rapidity of the appearance of synthetic ACP from solution, is an added evidence for the *in situ* formation of this phase in bone without the assistance of an intervening substrate. Such homogeneous nucleation processes however, occur only at solution concentrations much higher than are needed for heterogeneous nucleations, such as subsequent secondary nucleation of apatite crystals (Posner, 1969). The fact that apatite is not in evidence at such high solution concentrations even though from a thermodynamic view point, their formation should be favoured over that of the amorphous particles, suggests that they can evolve only through relatively slower heterogeneous nucleating mechanisms (Posner, 1969).

The heterogeneous nucleation of the first apatite crystals is of necessity on foreign substrates. These foreign substrates are never absent in synthetic preparations. Their relatively low concentration, together with their lower effectiveness as nucleators, explains why after the appearance of a few crystals of apatitic nature, secondary nucleation, using newly formed crystals as substrates become the dominant and

controlling factor in the conversion of ACP to crystalline apatite. Nevertheless, even secondary nucleation cannot compete with homogeneous nucleation when the degree of supersaturation is high enough to favour the latter, and this is why the amorphous phase appears initially (Posner, 1969).

In the initial stage of the *in vivo* calcification of the collagenous matrix the earliest mineral deposits are extremely small. Changes in the size of bone crystals with age have been noted in x-ray diffraction studies on powdered rat bones (Posner, 1969). The mean size was observed to increase with age of the animal up to maturity. At this point a sharp levelling off of growth rate occurred and the size became relatively constant and independent of age. This could be considered as an evidence for matrix restricted crystal growth (Posner, 1969). However, it could also mean that secondary growth due to dissolution and reprecipitation does not occur for bone crystals in fully mineralised tissue. Secondary growth or ripening is encountered in aqueous (Synthetic) systems of sparingly soluble salts in which the initial precipitate is finely divided (Eanes et al, 1965). Secondary growth is not a continuation of the initial growth of each particle, but is actually a consolidation process in which a decrease in the number of particles occur. This consolidation is accomplished by the

dissolution of the smaller, less stable particles with the dissolved material deposited as growth on the larger, more stable particles (Posner, 1969). Secondary growth occurs in synthetic apatite systems prepared by rapid precipitation in aqueous media. The initial growth of the apatite crystals occurs in a matter of minutes or less (Eanes and Posner, 1965); the average crystal size at the end of this precipitation period is generally smaller than the crystals found in bone (Eanes et al, 1965). The crystal growth with age in synthetic systems continues indefinitely, although at progressively reduced rates. However, water is necessary for the ripening to proceed in these synthetic systems and reducing the water-to-mineral ratio will retard secondary growth.

2.5.1 Intermediate state in Transformation of ACP to HAP

The initial solid phase that precipitates from a calcium ;phosphate solution depends on the degree of supersaturation (Nancollas and Tomazic, 1974). In a solution of low supersaturation, HAP is obtained without precursor phases (Nancollas and Tomazic, 1974; Boskey and Posner, 1976). On the other hand, the first solid to form in highly supersaturated solutions is a noncrystalline calcium phosphate approximating $Ca_9(PO_4)_6$ in composition (Boskey and Posner, 1976). In a study of the transformation and crystal ripening of ACP that had

been precipitated in highly supersaturated and buffered media, initially adjusted to pH 7.4, Furedi-Milhofer et al, (1973), demonstrated that crystalline precipitates were formed by a two-step precipitation via (1) ACP and (2) a precursor, OCP as proposed by Brown et al, (1962). Many assumptions have been made as to the chemical nature of this precursor phase. The calcium phosphate ionic concentrations vary appreciably during reactions. At each stage, therefore, the supersaturated solutions are metastable with respect to different calcium phosphate phases, which could form, and subsequently dissolve as the concentrations in the supersaturated solutions decrease. Since the concentration changes become very small as the reaction proceeds, a relative analytical error of only a few percent in the total calcium or total phosphate concentration could preclude differentiation between the possible crystalline phases (Tomson and Nancollas, 1978, and Koutsoukos et al, 1980).

The hydrolysis of previously prepared amorphous calcium phosphate established that the conversion of ACP to an apatite involves two processes (Tung and Brown, 1933). The first process consumes acid and indicates the formation of a mere acidic calcium phosphate intermediary with the solubility of octacalcium phosphate, (OCP), the second process consumes base and indicates the conversion of the intermediary to apatite and possibly, direct

conversion of ACP to apatite. From experiments involving the mineralization and x-ray analysis of epiphyseal rat cartilage, Posner, (1969) identified an amorphous material of approximately tricalcium phosphate, TCP composition. This phase in addition to OCP and DCPD have been proposed as a precursor to HAP in the formation of teeth and bone. The thermodynamic analysis of solution composition data suggests that ACP converts into a nonstoichiometric apatite when the OCP-like intermediary in formed and a stoichiometric apatite is formed when no OCP-like intermediary is involved (Tung and Brown, 1983). Studies on mineralization kinetics show that, the ratio of Ca/PO_4 in the precursor phase is significantly lower than the 1.50 required for TCP (Tomson and Nancollas, 1978). Hydrolysis is expected only to increase the molar Ca/P ratio, which further rules out TCP as the precursor phase. Results obtained by Brown et al (1957), Tung and Brown (1983), Walton et al (1967), Feenstra et al (1978) and Tomson and Nancollas (1978), show a Ca/PO_4 ratio correspond to OCP in the early stages of the reaction and this phase was confirmed by x-ray analysis.

2.5.2 OCP precursor model

It has been concluded that the stoichiometry of the initial phase in calcium phosphate precipitation at physiological pH is approximately 1.5 and is thus similar to tricalcium phosphate $Ca_3(PO_4)_2$, (Walton et al, 1967).

The formation of this phase, (that is ACP), is detected by a gradual development of opalescence in the solution after a certain lag time (Termine and Posner 1970). This lag time is dependent on concentration, ionic strength and pH. The dependence of the lifetime of ACP on the above mentioned parameters was studied by Termine et al (1970). It appeared that both the long time for the formation and lifetime of ACP are increased at lower supersaturation. The reason for the nucleation of this unstable phase seems to be explainable in terms of classical nucleation theory (Walton et al, 1967). Hydroxyapatite is a hard material of high surface energy and is not readily nucleated with a low thermodynamic driving force (that is low supersaturation). On the other hand, Octacalcium phosphate probably has a much lower surface energy, it undoubtedly has a large entropy of crystallization because of the large number of entities involved in a neutral cluster. The stoichiometry of a product $Ca_3(PO_4)_2$ represents the minimum number of ions in a neutral molecule and may have low entropy of formation. However, the stoichiometry is the same as tricalcium phosphate. The crystalline arrangement is unlikely to resemble that of the latter compound because it, too, is a hard, high surface energy material. Electron diffraction measurements affirm that the product under consideration is amorphous or soft.

The octacalcium phosphate (OCP) precursor model proposed by Brown (1966) to explain the formation of *nonstoichiometric* apatites (Ca/PO_4 < 1.67) provides a possible interpretation of the sequence of events that takes place during the early stages of transformation. The first crystals to form at physiological pH and temperature are postulated to be two-dimensional growths of single unit cell thick OCP (Brown, 1966). They deviate from apatite in morphology, composition, structure and solubility, as exemplified by low Ca/PO_4 molar ratios, high levels of HPO_4^{2-} ions and distorted lattice dimensions. This growth pattern which is known as Ostwald ripening (Walton, 1962; Dunning, 1973), account for the flaky appearance of the earliest crystals (Eanes and Meyer, 1977), as well as for their solubility approaching the value for OCP. These primary crystals are unstable and with a concomitant decrease in solubility. They also change steadily upon solution ageing to compositions and structures more nearly resembling HAP. This post conversion crystallization process is more complicated than can be described by a steady change in the growth and perfection of a highly defective apatite (Eanes and Meyer, 1977).

There are two different hypotheses to explain how this transformation takes place. One hypothesis considers ACP dissolution and subsequent transformation

into crystalline phosphate as the main mechanism (Meyer and Eanes, 1978), while in the second hypothesis, ACP constitutes an expitaxic substrate for secondary nucleation of the crystalline phase (Garcia Ruiz et al, 1980). This phase structurally identified as OCP, takes the form of enlarged prismatic crystals, oriented in all directions of space covering the initial nucleus of ACP. The initial ACP does not change its volume during growth of the ordered phase. OCP formation is thought to be as a consequence of a drop of the calcium and phosphate concentration due to the prior precipitation of ACP.

2.5.3 Effects of Environment on ACP-HAP Transformation

Once initial mineral phase separation (that is precipitation of ACP) takes place during solution-mediated calcium;phosphate formation, the next major event to occur is the transformation of ACP to tiny crystals of HAP. The amount of time that actually elapses during the solution mediated transformation is short and variable. On the other hand, the time required to reach this period of rapid precipitate conversion is strongly dependent upon the exact solution environment (Termine et al, 1970). In as much as initial mineral phase separation is also dependent upon solution environment, it can thus be seen that exact control of initial Ca/PO_4 molar mixing ratio, pH, total ionic

strength, viscosity and temperature, will determine the complete sequence of events occurring within any calcium phosphate-formation system (Termine and Posner, 1970).

The effect of decreasing initial Ca/PO_4 molar mixing ratio upon ACP suspension lifetime, shows that ACP appears to be much more stable if formed from solutions at low levels of initial supersaturation. The initial mineral-phase separation is enhanced by solutions rich in calcium relative to phosphate and poor in total salt concentration. On the other hand, ACP formation is inhibited by solutions rich in inorganic phosphate relative to calcium and high in ionic strength. This lag period (that is the length of time required before ACP precipitates) is directly related to the degree of metastability of the calcifying solution being used (Termine and Posner, 1970).

High pH values enhance ACP formation and affect subsequent transformation to HAP. The total time required for the ACP to HAP transformation to reach completion increases with increasing pH. Under different experimental conditions, observed conversion paths are independent of (i) the nature of buffer, (ii) the type of univalent ions in solution, or (iii) whether the amorphous material was left in contact with the mother liquor or filtered, dried, and added to fresh buffer (Boskey and Posner, 1973).

The effect of increasing temperature enhances ACP formation. It also increases the rate of transformation by both increasing the solubility of the ACP and providing additional energy needed to form a stable primary nucleus (Termine and Posner, 1970; Boskey and Posner, 1973). ACP was found to be three times less stable at 37^{o}C, while sixteen times more stable at 4^{o}C, than at 25^{o}C (Termine and Posner, 1970).

The amorphous particles remain stable in ethanol or acetone, and convert more slowly in a 50% acetone solution than they do in pure buffer. This corroborates the view of Posner (1965) that, the reaction is solution mediated or at least accelerated by the presence of water. The increase in the rate of conversion with increased water solid ratio up to 400:1 further illustrates the necessity for water in the conversion (Boskey and Posner, 1973). The effects of varying ionic strength and dielectric constant show that ACP is least stable when suspended in aqueous media of low dielectric constant and low ionic strength (Termine et al, 1970). In addition ACP is more stable in solutions of high intrinsic viscosity. Addition of either 34% (w/v) glycerol or 26% (w/v) sucrose reduces the transformation of ACP drastically (Termine et al, 1970).

These findings demonstrate that the lag time required for initial mineral phase separation from any

given calcifying solution, (i.e its degree of metastability) is an exact function of many different environmental factors. Therefore it can be seen that in comparing results obtained from different calcification systems, each of these factors must be thoroughly accounted for in each assessment.

2.6 Inhibition of ACP -HAP Transformation

2.6.1 Inhibition

Whenever crystals grow or dissolve, the linear rate of growth or dissolution may be strongly affected by the presence of non-constituent ions or molecules. If the rate is reduced, the components responsible for the reduction are call inhibitors.

The presence of inhibitors may explain why calcium phosphate is not spontaneously precipitated in some biological systems despite the solution being supersaturated with respect to them. However, existing information concerning inhibition of crystal growth and dissolution is mainly of qualitative nature (Nielsen and Christoffersen, 1982). Other problems of inhibition theory is that:

i) it is not easy to devise ways of detecting and describing the effect of inhibitors;

ii) the effect of inhibitors are not easy to explain; and

iii) it is not easy to isolate and identify *in vivo*

inhibitors.

However, it is known that inhibitors cannot influence diffusion in solution (Nielsen and Christoffersen, 1982), therefore the reduced growth rate due to an inhibitor must be surface controlled.

The effect of an inhibitor is in general explained on the basis of the rate controlling mechanism for growth. If the concentration of inhibitors adsorbed is so high that new nuclei can hardly be formed without inhibitor units being removed, the rate of growth will be severely reduced.

2.6.2 Effect of Added Macromolecules on ACP-HAP Transformation

Macromolecules can influence both initial formation of amorphous calcium phosphate and the ultimate formation of apatite through amorphous-crystalline conversion. The exact effect which a given macromolecule exhibits toward amorphous calcium phosphate formation is strongly dependent upon the initial degree of supersaturation of its calcifying solution (Termine and Posner, 1970). For example, at high supersaturation, macromolecular effects would not be expected to compete efficiently with the relatively high driving forces for ACP formation existing within the solvent space itself. Thus under these conditions, macromolecules probably behave only as Ca^{2+} or HPO_4^{2-} binding agents. However at relatively low

levels of initial supersaturation, that is, where solution ACP formation lag times are quite long, specific macromolecules could contain sites either in their internal or solvation-shell space which may actually be favoured locations for ACP nucleation and/or growth. Thus, under these latter condition,s, ACP formation could take place within the protective domain of the macromolecular species and not in free solution (Termine et al, 1970).

Several macromolecules such as the phosphoprotein phospholipids, proteoglycans, free carboxyl-containing polymers, pyrophosphate, some diphosphonates, and others, inhibit amorphous-crystalline transformation or replication from pre-existing crystal seeds in metastable solutions (Termine et al, 1970, Termine et al, 1980 and Nancollas, 1982). Phosphoprotein for example inhibit two stages of the crystal growth. An initial lag period was induced, and this period was prolonged indefinitely when a combination of phosphoprotein precoated seeds were used together with soluble phosphoprotein in the crystal growth reaction. Phosphoproteins prolonged that stage of the reaction where OCP is the predominant mineral phase present prior to its conversion to the final apatite product. Pretreatment of the phosphoprotein with Calcium diminished their inhibitory activity to the seeded crystal growth as towards apatite formation in synthetic

extracellular fluids. The presence of collagen diminished the inhibitory activity of the phosphoprotein towards precipitation but had no effect on phosphoprotein modulated apatite crystal growth in the seeded systems (Termine et al, 1980).

Citrate has minimal effect on ACP-HAP transformation at near physiological conditions, it has a small, measurable stabilising effect in ACP at higher concentrations ($>2x10^{-4}M$), and decreases the rate of recrystallization. Citrate is thought to decrease the rate of conversion of the first formed OCP-like phase to the more apatite-like secondary crystalline phase (Meyer and Selinger, 1980 and Furedi-Milhofer et al, 1972). If crystal ordering of the precursor precedes OCP nucleation, this process could be hindered and secondary nucleation delayed, by the occluded foreign matter (Firedi-Mihofer et al, 1972). The solubilities of the calcium ;phosphate phases are not affected however. This suggests that the specific interactions of citrate with crystalline calcium phosphate may play a casual role in determining the physical and chemical characteristics of the inorganic component of hard tissues (Meyer and Selinger, 1980).

Results obtained in investigation with model macromolecules on initial mineral phase separation and amorphous-crystalline conversion provide ample evidence

that macromolecules definitely interact with calcium phosphate salts (Termine et al, 1970). Specifically, phospholipids, RNA, and the phosphoprotein, phosvitin, casein, and the free carboxyl containing polymers, polyacrylate, poly-l-glutamate and others, indicate that organically bound phosphate and acidic amino acid side chains may well be the most potent sites, for any given macromolecule-mineral interaction (Termine et al, 1970).

2.6.3 Structural factors influencing the ability of compounds to inhibit

Many biological molecules are recognised as having the potential to influence calcification systems through an inhibitory action. Compounds as wide ranging as ATP, fructose 1,6-bisphosphate, phosvitin, casein, pyrophosphate, polyphosphates, phosphonoformate, and phosphocitrate are known inhibitors, and because of the diverse nature of the molecules only few guidelines have ever emerged for predicting the inhibitory ability of compounds (Williams and Sallis 1982).

Polyanionic compounds are potential inhibitors of hydroxyapatite (HAP) formation (Termine et al, 1970, Meyer and Nancollas, 1973), and on the basis of studies with 1-hydroxyethane-1,1-diphosphonate (EHDP), pyrophosphate and imidodiphosphonate (PNP), the suggestion has been made that compounds possessing a $H_2O_3P\text{-}x\text{-}PO_3H$ structure (x may be C, N, O) will inhibit

(Robertson and Fleisch, 1970). Termine and Conn (1976) extended this idea by proposing as a minimum requirement that the two phosphate ester groups need not be closely linked as in for example, fructose 1,6-bisphosphate for inhibition to occur. It has also been proposed that an inhibitor molecule should possess at least one phosphate group and at some other position an acidic group, either another phosphate or a carboxylic moiety (Williams and Sallis, 1979). Although molecules with basic groups are immediately recognised as inhibitors, many other factors must also be responsible for the degree of potency.

In certain situations, this rule needs qualification. Polycarboxylic, phosphate-free molecules will inhibit, but the minimum number of carboxylic groups required for inhibition is unknown (Williams and Sallis, 1982). Structures of some potent inhibitors are given in the next chapter (figure 3.7). Formic and oxalic acids do not inhibit, but citric acid is a weak inhibitor. Notably, the dehydroxyl and dehydro derivatives of citric acid - namely tricarballylic acid and aconitic acid fail to inhibit. In this particular case, the hydroxyl group, perhaps due to its position in a tetrahedral environment, must be associated with the weak inhibitory ability of citrate. However, the ability of phosphonoacetate and phosphonoformate to potently inhibit HAP formation, shows that hydroxyl groups in compounds with phosphate groups

are not needed for potent inhibition (William and Sallis, 1982). The type of functional group present is of primary importance in determining whether a compound inhibits or not. *Secondary factors including:-*

(a) the number of active groups, (b), their proximity

(c) stereochemical arrangement (d), steric factors,

(e) lipophilicity and (f), lability of the molecule also influence inhibitor potency (Williams and Sallis, 1982).

In general, as the number of anionic groups increases, so does the inhibitor power. Thus Adenosine triphosphate (ATP), is more powerful than Adenosine diphosphate (ADP), tripolyphosphate is better than pyrophosphate, and phosphocitrate is stronger than 2- and 3-phosphoglycerate. The proximity of the groups is vital, since the closer the anionic groups, the more strongly a molecule inhibits HAP formation. For example, phosphonoformate is more potent than 2-phosphoglycerate, which is more powerful than 3-phosphoglycerate. Furthermore, a linear arrangement of active groups is less potent than an irregular arrangement, which allows for a closer packing of active groups. The stereochemical arrangement of chelating groups about a tetrahedral sp^3 carbon is more suitable for binding to active sites than about a trigonal nitrogen. If the anionic groups are bound to an sp^2 hybridized carbon

(that is, double-bonded carbon), the molecule no longer inhibits. Substitution of sterically bulky group on to a parent inhibitor reduces the inhibitory capabilities of the inhibitor. This is because of the decreased ability to fully bind to the active sites. The molecular size of the inhibitor also opposes the effects of increasing the number of groups and proximity by rendering binding to active sites less efficient (Williams and Sallis, 1982).

Inhibitors of ACP-HAP transformation have been grouped into two types by Williams and Sallis (1982), based on the manner by which their increasing concentration affect the parameters defining the transition. These are often referred to as Type I and Type II inhibitors. (Table 2.2).

Prior to transformation, ACP spherules are similar in appearance irrespective of the type of inhibitor. After transformation however, the crystals found in presence of type I inhibitors are comparatively small. In contrast, type II inhibitors do not alter the dimensions of the particles involved, even though the on-set of the conversion process is delayed, sometimes as long as with type I inhibitors. *Although needless of HAP* are usually formed after the conversion process, this is not the case when a sufficiently high concentration of type I is present. No transformation occurs and ACP

spherules are indefinitely stabilized (Williams and Sallis, 1982). If the concentration of type I inhibitor is a little less than the amount required to completely block conversion, it is possible to detect a small degree of transformation.

Type I inhibitors are crystal growth inhibitors. Inhibition is not due to chelation but is considered to be as a result of adsorption on to ACP and HAP (Meyer and Nancollas, 1973, williams and Sallis, 1979).

Table 2.2 Examples of Type I and Type II Inhibitors.

Type I Inhibitors	Type II Inhibitors
Pyrophosphate	Adenosine-s-Diphosphate
Phosphocitrate	Adenosine-s-Triphosphate
Tripolyphosphate	Citrate
Immidodiphosphate	Phosphonoformate
1-Hydroxyethane-1,1. diphosphonate (EHDP)	2-phosphoglycerate
	3-phosphoglycerate
	Magnesium iron

* (Williams and Sallis, 1982).

These inhibitors stabilize HAP embryos and inhibit subsequent growth by binding to the active sites and poisoning heterogeneous nucleation. At high concentration of inhibitors, embryos fail to reach their

critical size, and redissolve, hence the decrease in the extent of conversion of ACP to HAP. Type II inhibitors on the other hand are considered to act mainly by decreasing the lability of ACP. Both classes bind to Acp and HAP, and it therefore appears either that type I (Crystal growth) inhibitors bind with higher affinity to the defect sites on HAP from which crystal growth proceeds or that these sites are different from those bound by type II inhibitors or both (Termine and Conn, 1976).

Although inhibitors have been grouped into two types, it does not necessarily indicate that only two mechanisms underly this division. Binding to active sites on HAP is the fundamental mechanism with type I inhibitors while with type II inhibitors, ACP is considered to be the main locus of action, although diverse mechanisms must be responsible for their inhibitory action. It is also suggested that bulky anionic macromolecules can bind to ACP and HAP sufficiently to sterically interfere with the conversion process (Fleisch and Bisaz 1962; Blumenthal et a, 1979).

It is possible to predict compounds that will inhibit HAP formation and offer preliminary estimate of potency. It is also possible to explain the mechanisms at the calcium phosphate surfaces that may underly the separation of inhibitors into two classes, but it is

difficult to elucidate any structural features of molecule that will indicate whether it is type I or typ II inhibitor. No obvious pattern emerges, but type inhibition has been ascribed to the presence of o phosphate group and, in close proximity either to anothe phosphate or multiple carboxylic groups (Williams a Sallis, 1982). In the case of nucleotides, where tripolyphosphate and pyrophosphate are type I inhibitor ATP and ADP are type II inhibitors. The reason given the inability of ADP and ATP to bind as efficiently pyrophosphate and tripolyphosphate to HAP embryos, whi may make them susceptible to surface catalys hydrolysis.

2.6.4 Effect of added ions on ACP-HAP Transformation

Cations and anions separately or in combination a as inhibitors of ACP-HAP transformation. Ions such Mg^{2}, Sr^{2+}, Be^{2+} and F^{-} have been found to inhib calcification in vitro (Bachra and Fischer, 196 Nancollas; 1982). The inhibitory action of Mg^{2+}, Sr and F^{-} ions on apatite formation at high concentration these inhibitors, and of combinations of Mg^{2+} with F^{-} Sr^{2+} ions at lower concentration is due to the inhibiti of apatite nucleation and crystal growth (that is th are type II inhibitors). The inhibitory action of Mg ions on the formation of apatite probably involv

interference with the formation of HAP critical nuclei, by entering the pre-nuclei structures of HAP and creating a structural mismatch (Nancollas, 1982). A molar Mg/Ca ratio greater than 0.2 effectively prevents the transformation of ACP and will also delay the formation of apatite from solutions of low supersaturation. They also slow down the transformation of Octacalcium phosphate, OCP into apatite (Bachra and Fischer, 1969). The relatively large concentration of Mg^{2+} ions in the bone is thought to be the principal component which prevents the precipitation of HAP in vivo (Nancollas, 1982).

Fluorapatite is less soluble than hydroxyapatite, and thus the incorporation of F^- ions within the lattice would be expected to result in a more rapid precipitation of the apatite. However, seeded growth and spontaneous precipitation experiments of HAP in presence of F^- ions have shown that this anion reduces the rate of reaction at low concentrations ($< 10^{-5}M$) but enhances growth at higher concentrations ($> 10^{-5}M$) (Nancollas, 1982). Studies of the ionic molar ratios in the precipitating phase suggest that this phase is not fluorapatite, (FAP) but rather a fluoridated hydroxyapatite in which the degree of substitution of F^- ions for OH^- ions in the lattice varies with the initial F^- concentration in the solution (Nancollas, 1982). Fluoride ions retard the

formation of ACP which precedes the hydrolysis of OCP to HAP and inhibits or even eliminates the formation of OCP-like precursor phase. This is in contrast to the influence of Mg^{2+} ions during precipitation of calcium phosphate which apparently stabilizes TCP-like precursor phases.

2.6.5 Effect of Inhibitors and Reaction medium upon crystal shape of HAP

The initial spontaneous precipitation of ACP due to the addition of base appeared unaltered by the presence of inhibitors. This observation is supported by light scattering and calcium ion activity measurements (Williams and Sallis, 1982). Subsequently as described by Eanes et al (1965), the spheres increased in diameter although addition of an inhibitor decreased the growth rate of the ACP spherules. Just prior to the transformation, all particles appear similar, but during the transformation, a change in morphology is evident with spheres of ACP becoming indistinct and needle-like deposits appearing except when high concentration of type I inhibitors are present. After transformation however, aggregates of needle-like deposits are visible, although dimensions of the individual particles are small.

The particle size and shape of calcium phosphates are determined by the relative rates of several processes. The formation of an amorphous precipitate,

amorphous to crystalline conversion, recrystallization and ageing processes, hydrolysis and so on, bring about morphological as well as chemical and structural changes of the precipitate. Changes in temperature and addition of foreign substances may preferentially affect the rates of one or more processes involved, thus changing the properties of the precipitate.

2.7.0 X-RAY SPECTROMETRY

2.7.1 Origin and generation of x-rays

The portion of the electromagnetic spectrum which lies between ultraviolet and gamma radiation is called the x-ray region. They have much shorter wavelengths than visible light, typically of the order of 1.0.Å (10^{-1}nm), that is they represent a relatively high energy form of radiation.

To produce x-rays, electrons are accelerated by an electric field and directed against a metal target, which slows them down rapidly by multiple collisions. Normally most of the electrons are not brought to a full stop by a single collision and a continuum of radiation is formed (that is a white radiation). X-ray spectra show in addition, a number of sharp peaks of high intensity whose positions change from one material to another. These peaks are the characteristic lines for the element of which the target is made (Dent Glasser, 1979). The most useful metals are usually iron, copper and molybdenum.

when electron bombarding the targets reach certain critical energies they are capable of knocking electrons out of their atomic orbitals. In particular, at energies of about 10kev (for elements with Z approximately 30) they can remove electrons from the innermost (K) shell. The vacancy created in the K-shell is filled either by descent of an electron from the next higher shell (L) or the one above that (M). The decrease in potential energy in going from the higher level to the lower appears as radiation and as the energies of the shells are well defined, each transition gives a nearly monochromatic line. The principal peaks are:

$K_{\alpha 1}$, $K_{\alpha 2}$ L --------» K

$K_{\beta 1}$, $K_{\beta 2}$ M --------» K

Because the difference in energy between L and K shells is less than that between the M and K shells, K_α is always at longer wavelengths than K_β. As the atomic number (Z) of the target element increases, the characteristic lines shift to shorter wavelength, and one can in principle select a target to give almost any desired value for the K_α line which is the x-radiation. The most widely used target is copper (K_α = 1.542Å). In practice however, the choice of targets are limited to materials which are solid, dense, conductive and high-melting. Transition elements of the

first and second long periods meet these requirements and have characteristic radiations in the regions quite useful for x-ray analysis.

2.7.2 X-ray diffraction by crystalline solid

A solid may be composed of particles arranged in a regularly repeating pattern in which case it is said to be crystalline. A solid whose particles show no long-range order is said to be amorphous. The usefulness of x-ray diffraction in the study of solid substances lies in its ability to distinguish ordered from disordered states (Alexander, 1969).

All materials interact to some extent with electromagnetic radiation. Amorphous solids having no long-range order, behave towards incident radiation in much the same way as fluids. They absorb or transmit it equally in all directions, that is, isotropically. In contrast the behaviour of crystalline materials towards radiation is modified by the ordered arrangement of their particles. Crystals may show anisotropy because different directions within the repeating pattern interact differently with the incident radiation. If the wavelength of the incident radiation is of the order of the interatomic distances, scattering or diffraction phenomena become important and these too are modified by the order of arrangement of crystalline materials (Dent Glasser, 1979).

The practical process of obtaining information about a crystal structure from a study of its diffraction pattern falls into two stages (Dent Glasser, 1979). The first step is to study the positions of the diffracted beams with the object of determining the size and shape of the unit cell. The second is to study the intensity of the beams, with the objective of deducing details of the atomic arrangement within the cell. X-ray diffraction studies can be carried out on a single crystal or on a sample consisting of a very large number of randomly oriented crystalline particles, that is a powder. Powder patterns are chiefly used as a rapid means of identification, but they are sometimes used for structural studies, particularly if crystals large enough for single crystal study cannot be obtained. The only condition governing the position of a reflected beam from a powder sample is the Braggs equation which can be written as:

$$n\lambda = 2d_{hkl} \text{ Sin } \theta$$

or

$$n\lambda = 2d \text{ Sin } \theta_{hkl}$$

in order to indicate that the diffraction is by the specific planes (hkl) or at the particular θ_{hkl}, often called the Bragg Angle of the plane (hkl) (Alexander, 1969).

The use of the equation depends on whether one is

concerned with relating the measured angle θ to the interplanar spacing dhkl, as is the case in diffraction experiments in which λ is known, or to the unknown wavelength as is the case in x-ray spectroscopic experiments in which the crystal spacing is known.

2.7.3 Recording the pattern

Diffraction patterns can be recorded on photographic film, using an x-ray camera e.g. a DEBYE-SCHERRER POWDER CAMERA. It can also be recorded using IONISATION or SCINTILLATION DETECTORS mounted in a housing that can be moved in a circular path around the sample. The reason for recording a powder pattern is to identify the phase or phases of which a specimen consist (Dent Glasser, 1979). In general each substance gives its own unique powder pattern which can be used to identify it - hence the term finger-print methods. The patterns, a list of d-spacings and relative intensities for most crystalline phases are usually contained in a powder diffraction file. The unit cell indices and optical data are, if known also included in this file.

Careful measurement of the relative intensities of the lines present in the pattern should enable the amount of the respective phases present in a mixture to be estimated (Alexander, 1969; Dent Glasser, 1979). One difficulty, is to find sufficient lines that are not overlapped by lines from other phases; another is the

possibility of varying degrees of preferred orientation due to changes in morphology. Moreover, the intensity of a pattern depends on the perfection of crystallinity; an apparent increase in the proportions of a given phase may mean that its crystallinity is improving (Dent Glasser, 1979). Amorphous materials cannot be estimated by diffractometry, and if present may prevent absolute values being estimated for crystalline phases. Notwithstanding these reservation for many studies quantitative powder diffractometry may be the best way to follow phase changes that are occurring (Alexander, 1969; Dent Glasser, 1979).

2.7.4 Application of X-ray diffraction methods in studies of calcium phosphate system

The capacity to reveal the degree of ordering in solid substances makes x-ray diffraction well suited to the investigation of crystallinity in calcium phosphate systems. X-ray diffraction analyses are being employed to elucidate certain aspects of nucleation and growth dynamics of emerging solid phase of calcium phosphate systems (Boskey and Posner, 1973; Eanes and Posner, 1965).

X-ray diffraction pattern of the crystalline calcium phosphate, HAP has a strong maximum at approximately 32^{o} 2θ plus some distinct maxima at higher angles. These scattering region (that is $23\text{-}36^{o}2\theta$) have been principally surveyed (Eanes et al, 1965; Bienenstock and

Posner, 1967 and Thomas, 1991). The amorphous material, on the other hand shows a broad maximum at approximately 29^{o} 2θ, and a weaker broad maximum at approximately 45^{o} 2θ (Eanes et al, 1965).

An accepted method of following the extent of conversion of ACP to HAP is the measurement of a degree of crystallinity of each precipitate obtained at a specified reaction time, from its x-ray powder diffraction pattern (Eanes and Posner, 1965; Boskey and Posner, 1973). This index was originally defined to be equivalent to the weight fraction of HAP present in the reaction slurry. In the original method, the integrated intensity of an x-ray diffraction peak (the 002 peak in this case) characteristic of the crystalline material is compared with the integrated intensity of a 100% crystalline sample of the same material of similar size (Eanes and Posner, 1965). The method suffers from the following limitations. First, it involves approximations regarding mass absorption coefficient of a very imperfect calcium hydroxyapatite and an unidentified noncrystalline solid component. Second, peak areas are measured which due to the nature of the diffraction profiles, would always be less than the true areas due to an unavoidable overestimation profiles, would always be less than the true areas due to an unavoidable overestimation of the background level (Eanes and Posner, 1965). Furthermore,

the 100% crystalline sample was arbitrarily assigned in the original paper, but it is now known that an improper assignment could lead to a concealment of valuable information on phase changes during the conversion process (Thomas, 1988). It was also thought that, because crystal faces do not all grow at exactly the same rate, using a single diffraction peak may not sufficiently define the crystal growth profile (Thomas, 1988).

The mean size, D, of the apatite crystals at different sampling intervals is usually estimated approximately from the corresponding line breath at half maximum intensity, $\beta_{1/2}$ (Eanes and Posner, 1965; LeGeros et al, 1967), using the equation:-

$$D = 57.3^{K'} \lambda/\beta_{1/2} \text{ Cos } \theta;$$

where K' is a crystal shape factor with an approximate value of 0.9, λ is the wavelength of the x-radiation employed, and θ is one-half the scattering angle. The constancy in crystal size implies that the crystal nuclei, once formed, grow so rapidly to their final size that at any given point during conversion the majority of crystals present are fully developed. The constancy in size, again implies that the conversion rate is proportional to the number of apatite crystals already formed and to the total interfacial area of the crystalline phase (Eanes and Posner, 1965). Increased x-

ray diffraction line broadening also result from small crystallite size or from strain in the lattice, or from both (LeGeros et al, 1967).

CHAPTER THREE

3.0 STUDIES ON CALCIUM PHOSPHATE PRECIPITATION

3.1 Introduction

The precipitation of calcium phosphates and in particular HAP has been extensively studied. However there remains considerable uncertainty as to the nature of the phases formed during the early stages of the precipitation reaction. The major events comprising their formation from buffered solutions include, (1) initial deposition of ACP, (2) its subsequent transformation into small crystals of apatite and (3) the ultimate growth or ripening of those crystals. The physicochemical mechanisms which govern this precipitate phase transformation process are such that once initiated it would normally proceed to completion (a process known as autocatalysis) (Boskey and Posner, 1973). Therefore ACP would be expected to have only a finite suspension lifetime, the extent of which may be dependent upon experimental conditions used (Termine et al, 1970a). If autocatalytic nucleation is the dominant mechanism in the conversion process, seeding a preparation of uncrystallized calcium phosphate with apatite crystals will bring about a more rapid completion of the transformation (Eanes and Posner, 1969).

The formation and identification of metastable

phases during and subsequent to phase transitions have important implications in many systems, particularly those of biological nature. Bone tissue has always been found to contain substantial amounts of ACP as well as HAP. It would therefore appear that some factors must exist within living systems which regulate the physicochemical conversion of ACP to HAP. If a metastable phase persists for any length of time, it may be identified by crystallographic or analytical procedures.

In this chapter transformation of ACP to HAP was studied under different experimental conditions, with the aim of determining how these conditions would influence nucleation of HAP crystals, extent of conversion and the mean sizes of the resultant HAP crystals. The experiments were carried out in the presence of certain substances thought to be inhibitors of the ACP - HAP transformations. These include Adenosine-5-monophosphate (AMP), Adenosine-5-diphosphate (ADP) Adenosine-5-triphosphate (ATP), L-glutamate, casein, citrate, pyrophosphate, tetracycline powder, some metal ions (Cd^{2+}, Mg^{2+}, Pb^{2+}, Zn^{2+}, Sr^{2+}, Ba^{2+}), and Fluoride ion.

The products of the transformation in each case were examined by x-ray powder diffractometry at various time intervals. The aim is to attempt to decipher the mode of inhibition of the various types (Types I and II) of

inhibiting substances.

In a preliminary experiment HAP was precipitated using three different sets of starting materials in order to determine if the stoichiometry of the apatitic precipitate is influenced by the type of reactants.

3.2 EXPERIMENTAL

3.2.1 Precipitation of calcium hydroxyapatite using three different procedures

Reagents

Unless where stated, all reagents used were of analytical grade. All solutions were prepared using doubly distilled water.

Disodium hydrogen phosphate solution

A solution of 0.019M was prepared by dissolving appropriate amount of the salt in water.

Calcium acetate solution

A solution containing 0.008 mole of Ca^{2+} was prepared by dissolving the calculated amount of the salt in 400cm^3 of water.

Diammonium hydrogen phosphate solution

A solution of 0.019M was prepared by dissolving appropriate amount of the salt in water.

Calcium nitrate solution

The solution was prepared as described for calcium acetate.

Calcium hydroxide solution

A 0.50M solution was prepared by dissolving the appropriate amount of the salt in water.

Orthophosphoric acid solution

A 0.30M solution of the acid was prepared by diluting appropriate amount of the acid (sp. gr. 1.75) with water.

Procedure A

The sodium hydrogen phosphate solution ($1100cm^3$) was heated to boiling and the calcium acetate solution ($400cm^3$) was carefully added drop-wise with constant stirring, using a mechanical stirrer. After precipitation, the contents of the flask were refluxed for about one hour to enhance homogeneity and crystallinity of the apatite. The precipitate was filtered, washed with water and dried at 105^oC for about four hours.

Procedure B

HAP was precipitated as in procedure A, but using ammonium hydrogen phosphate and calcium nitrate as reagents.

Procedure C

HAP was precipitated by allowing calcium hydroxide solution ($500cm^3$) to drop (at a rate of one drop per second) into boiling orthophosphoric acid solution ($700cm^3$). The mixture was stirred constantly using a

mechanical stirrer. After precipitation, the contents of the flask were treated as in procedure A.

3.2.2 Precipitation of ACP - HAP precipitates

Reagents

Buffer solution

pH 9.0

The solution was prepared by mixing together 60cm^3 of 0.50M hydrochloric acid solution and 250cm^3 of 0.60M tris (hydroxy methyl) amino methane solution. The resultant solution was made up to 1000cm^3.

pH 7.4

The solution was prepared by mixing together 42cm^3 of 0.10M hydrochloric acid solution and 50cm^3 of 0.10M tris (hydroxymethyl) amino methane solution. The resultant solution was made up to 1000cm^3.

The buffer solutions were standardized with PYE Unicam (Pw 9418) pH meter.

Calcium nitrate solution

0.04M solution was prepared by dissolving the appropriate amount of the salt in 400cm^3 of the buffer solution.

Diammonium hydrogen phosphate solution

0.036M solution was prepared by dissolving the appropriate amount of the salt in 500cm^3 of the buffer solution.

Ammonia/Acetone solution

One part of ammonia solution (25%) was mixed with one part of acetone (that is 1:1), to give a solution with pH approximately 10.6.

Procedure

The precipitation of ACP was initiated by mixing together the pre-buffered solutions of $Ca(NO_3)_2$ and $(NH_4)_2 HPO_4$. Separate experiments were performed at 25°C and pH 9.0 in a water-thermostated double walled bath (Thomas, 1989).

ACP was allowed to convert to HAP, with stirring at about 250 r.p.m. using a mechanical stirrer. Samples of the precipitated solids were taken into $15cm^3$ ice-cold ammonia/acetone water, and filtered quickly by suction using a vacuum pump. The precipitate was washed with acetone to obtain a free flowing powder. The time of completion of acetone wash was recorded in each case as the time reaction coordinate (Boskey and Posner, 1973; Thomas, 1989). The reaction was carried out for nine hours in each case, and samples were withdrawn at known times. The dry samples were stored in a vacuum desiccator over phosphorus pentoxide.

3.2.3 Preparation of ACP-HAP precipitates in presence of some metal ions and fluoride ion.

Reagents

Buffer solution

Prepared as described in section 3.2.2.

Calcium nitrate solution

Prepared as described in section 3.2.2.

Diammonium hydrogen phosphate solution

This was prepared as described in section 3.1.2.

Metal salts

Metal salts used include, magnesium nitrate, lead nitrate, zinc nitrate, strontium nitrate, cadmium nitrate, barium nitrate and sodium fluoride.

Ammonia/Acetone solution

Prepared as described in section 3.2.2.

Procedure

The crystal growth experiment was initiated by mixing together pre-buffered solutions of $Ca(NO_3)_2$ and $(NH_4)_2 HPO_4$. 0.001M (or 2.5% relative to the molar concentration of Ca^{2+}) each of Cd^{2+}, Mg^{2+}, Pb^{2+}, Zn^{2+}, Sr^{2+}, Ba^{2+} and F^- respectively were added to the mediating solutions in separate experiments. Nitrates of the metals were used to avoid changes in the initial number of ions in solution (Thomas, 1989). The experiments were carried out at pH 9.0 and 25°C over a period of nine hours. Withdrawal of samples were as

described in section 3.2.2.

3.2.4 Preparation of ACP-HAP precipitates in presence of inhibitor molecules

Reagents

Buffer solutions

They were prepared as described in section 3.2.2.

Calcium nitrate solution

The solution was prepared as described in section 3.2.2.

Diammonium hydrogen phosphate solution

The solution was prepared as described in section 3.2.2.

Ammonia/Acetone solution

The solution was prepared as described in section 3.2.2.

Inhibitors

These include, sodium pyrophosphate, trisodium citrate, adenosine-s-monophosphate sodium salt (AMP), adenosine-s-diphosphate sodium salt (ADP), adenosine-s-triphosphate sodium salt (ATP), L-glutamate sodium salt, Casein and tetracycline powder. Concentrations of each inhibitor used for different experiments are shown in table 3.1.

Table 3.1: Inhibitors and experimental conditions used in the Acp-HAP transformation.

Name of Inhibitor	Concentration	pH	Temperature
Adenosine-5-monophosphate	0.002M	9.0	25°C
	0.002M	9.0	50°C
Adenosine-5-diphosphate	0.002M	9.0	25°C
	0.002M	9.0	50°C
Adenosine-5-triphosphate	0.002M	9.0	25°C
	0.002M	9.0	50°C
Tetrasodium pyrophosphate	0.001M	9.0	25°C
	0.002M	9.0	50°C
Trisodium citrate	0.001M	9.0	25°C
	0.002M	9.0	50°C
L-Glutamate (sodium salt)	0.001M	9.0	25°C
Casein	0.5mg/Cm^3	9.0	25°C
Tetracycline powder	0.5mg/Cm^3	7.4	37°C
	0.025mg/cm^3	7.4	37°C

Procedure

The procedure is as described in section 3.2.2. The experiments were carried out at different pH and temperatures for some inhibitors, as shown in table 3.1. The concentration of each inhibitor in the mediating solution is also shown in table 3.1.

3.2.5 Effect of tetracycline on HAP crystals

Reagents

Tetracycline powder

0.01g of the powder was weighted accurately.

HAP Crystals

5g of HAP prepared using procedure C in section 3.2.1 was suspended in 200cm^3 of water.

Procedure

Tetracycline powder was added to the HAP suspension and stirred at room temperature for about one hour. The HAP crystals were recovered by filtration and dried at about 80^{o}C for about three hours.

3.2.6 Chemical analysis of samples

3.2.6.1 Elemental analysis using Atomic Absorption Spectrophotometry

Reagents

Standard solutions for metal ions

Standard solutions were prepared for calcium, magnesium, zinc and cadmium, by dissolving appropriate amounts of their soluble salts in water to give a solution containing 50ppm of each ion (Whiteside, 1975).

Lanthanum solution

10% (w/v) of lanthanum solution was prepared by dissolving 31.20g of lanthanum nitrate hexahydrate in a 100cm^3 volumetric flask and made up to the mark with 50% (v/v) hydrochloric acid.

Procedure

The standard and sample solutions were each treated with 5cm^3 of the lanthanum solution and aspirated into the flame. Absorption intensities were measured and sample concentration were read off from a calibration curve.

A PYE Unicam sp 1900 atomic absorption spectrophotometer was used. Instrumental conditions are as prescribed by Whiteside (1975).

3.2.6.2 Colorimeteric determination of Phosphorus

Reagents

Sodium molybdate solution

The solution was prepared by dissolving 12.5g of the salt in 500cm^3 of 5M sulphuric acid.

Hydrazinium sulphate solution

The solution was prepared by dissolving 1.5g of hydrazinium sulphate in 1000cm^3 of water.

Standard phosphate solution

A stock solution containing 50ppm of phosphate ions was prepared by dissolving 0.2197g of potassium dihydrogen phosphate in 1000cm^3 of water.

Procedure

Different concentrations of the standard solutions were prepared, ranging from 0 to 5ppm. 5cm^3 of the molybdate solution was added to each standard solution in

a $50cm^3$ volumetric flask. This was followed by $2cm^3$ of the hydrazinium sulphate solution and diluted to the mark. After mixing, the volumetric flask was immersed in a boiling water both for about 10 minutes to develop the colour. It was allowed to cool and the absorbance was taken at 830nm. A calibration curve was constructed from the results obtained (Basset et al, 1986).

$2cm^3$ of the sample solutions were transferred into $50cm^3$ volumetric flasks. The procedure for preparing the standard solutions was repeated and the concentration of phosphate ions was read off from the calibration curve.

3.2.7 X-ray Analysis

The x-ray powder diffraction patterns of the dried precipitates were taken using a Philips powder diffractometer (Pw 1730), at the Centre for Energy Research, Ahmadu Bello University Zaria. Nickel-filtered copper K_α radiation was employed. The scattering region $24\text{-}36^\circ$ 2θ was principally surveyed; this portion of the diffraction pattern includes the main hydroxyapatite profile.

At a given time t, the extent of reaction, (that is the fraction of ACP converted), is equivalent to the weight fraction of hydroxyapatite present in the slurry (Boskey and Posner, 1973). In the transformation of ACP to HAP, the integrated intensity of an x-ray diffraction peak characteristic of the crystalline material obtained

in the presence of other ions and inhibitors, were compared to the intensity of samples obtained without inhibitors. The reliability of this x-ray method for determining the fraction of crystalline hydroxyapatite in a given sample has been confirmed using mechanical mixtures of ACP and HAP (Boskey and Posner, 1973).

Because of extensive overlaps, only the 002 peak at about $25.8^{o}2\theta$ was judged to be sufficiently resolved for line-breadth measurements. The width at one-half the maximum height of this peak, $\beta_{1/2}$ was measured in degrees 2θ. The quantity, $1/\beta_{1/2}$ which is proportional to the mean crystallite size and/or degree of perfection in the direction along the c-axis of the crystals was taken as the measure or the crystallinity index (Eanes et al, 1965). Since the variations in the degree of resolution of the remainder of the diffraction pattern reflected the changes in the 002 reflection, this crystallinity index can be taken as representative of the crystal as a whole.

The mean size D, of the apatite crystals at different sampling intervals were estimated from the corresponding $\beta_{1/2}$ by use of scherrer's equation (Eanes and Posner, 1965):-

$$D = 57.3K' \lambda/\beta_{1/2} \text{ Cos } \theta$$

where K' is the crystal shape factor with an approximate value of 0.9, λ is the wavelength of the x-radiation employed (λ = 1.54A) and θ is one-half the scattering

angle.

X-ray diffraction patterns were also taken for the HAP precipitates obtained using three different methods of preparation. Approximate cell parameters, a- and c-axes, for the samples were obtained using the equa for an hexagonal system (Alexander, 1969).

$$d = (4/3a^2 \cdot (h^2 + k^2 + hk) + l^2/c^2)^{-\frac{1}{2}}$$

3.3 Results

X-ray diffraction patterns of precipitates obtained using three different procedures of preparation of HAP are compared in figures 3.1. The Ca/P mole ratios and cell parameters for the different precipitates are compared in tables 3.2 and 3.3 respectively.

X-ray diffraction patterns for the conversion of ACP into HAP at 25^{o}C and 50^{o}C are shown in figure 3.2. The precipitation reactions were carried out using concentrations and pH that allowed for the precipitation of ACP. Samples were regularly taken for analysis over a period of nine hours. The growth of HAP crystals is indicated by the development of distinct Bragg peaks with time of reaction and the region between 19^{o} and 39^{o} 2θ (which is the main diagnostic region) is used in this study. Table 3.4 contains the corresponding crystallinity index; $1/\beta_{\frac{1}{2}}$ and the mean size, D of apatite crystals as a function of time.

The effects of certain inhibitor molecules on the transformation of ACP to HAP are distinct and varied. Appendix I contains the x-ray diffraction patterns for precipitates obtained in the presence of some inhibitor molecules. A short lag time of over 30 minutes was observed in presence of adenosine-5-monophosphate (AMP), at 25^{o}C and pH 9, before a discernible conversion of ACP to HAP was obtained. Increasing the temperature from

25°C to 50°C shows that conversion started in less than 10 minutes. Table 3.5 shows the effects of AMP on the crystallinity index and mean sizes of the apatitic crystals obtained at 25°C and 50°C and pH 9.

Adenosine-5-diphosphate, (ADP) and adenosine-5-triphosphate, (ATP) have been classified as type II inhibitors (Williams and Sallis, 1980). The x-ray patterns of precipitates obtained in presence of these inhibitors are also given in appendix I. At 25°C and pH 9, ADP stabilized ACP for over 4 hours and when the temperature was increased to 50°C conversion of ACP to HAP was almost immediate. Table 3.6 shows the effects of ADP on crystallinity and mean sizes of HAP crystals at reaction temperatures of 25°C and 50°C. At 25°C and pH 9, using ATP as inhibitor there was no conversion of ACP into HAP throughout the period of the experiment (that is 9 hours). Increasing the temperature to 50°C in a separate experiment, transformation started at about 4 hours. The effect of pH on the transformation of ACP to HAP in presence of ATP is compared in figure 3.3. X-ray diffraction patterns of the precipitates obtained at different pH shows that conversion of ACP to HAP in presence of an inhibitor also depends on the pH of the mediating solution. Tables 3.7 and 3.8 contain the corresponding effects of ATP on the mean sizes and crystallinity of HAP crystals under the various

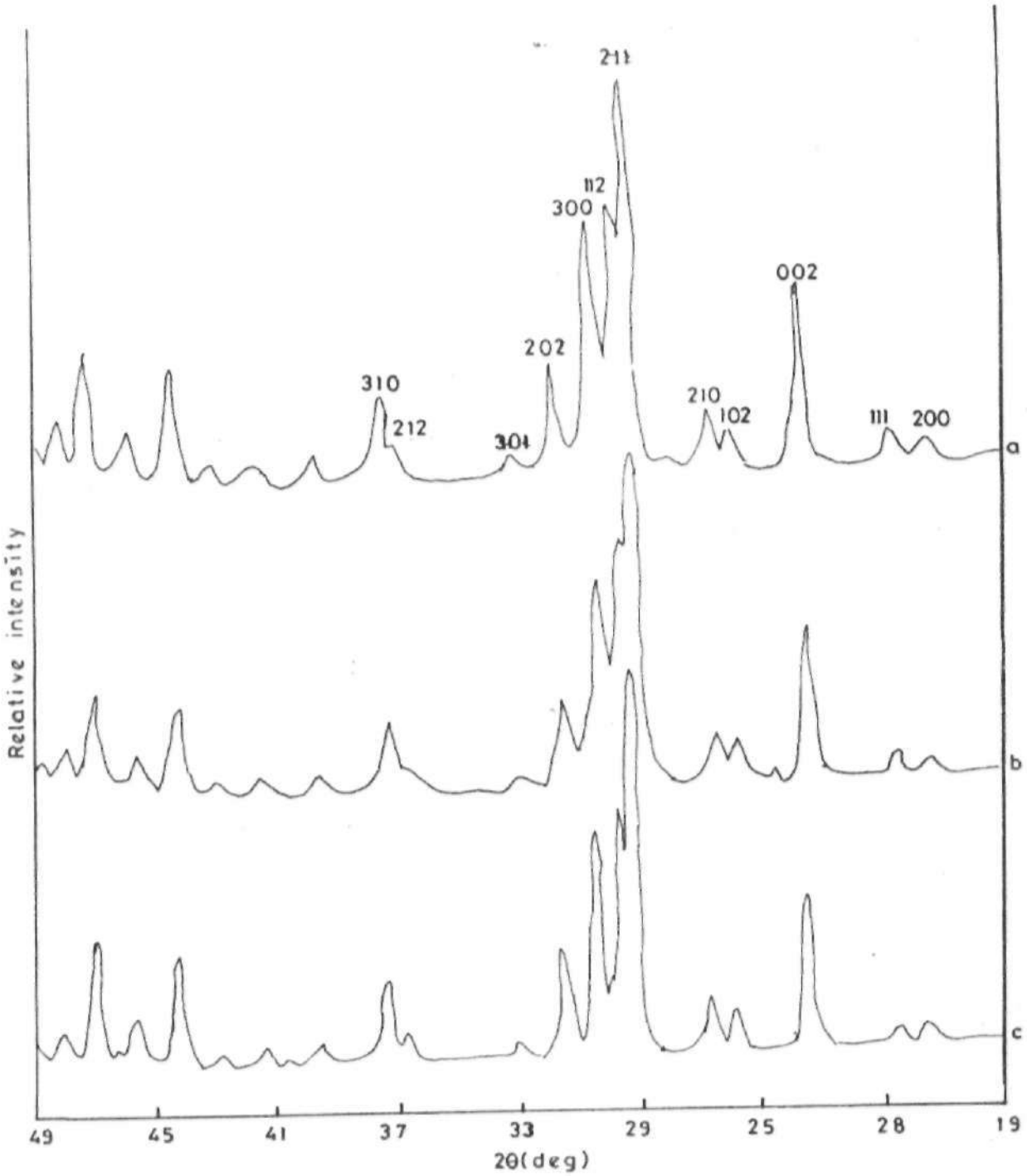


FIG.3.1 : X-RAY PATTERN OF HAP PREPARED BY METHODS a, b AND c SECTION 3.2.4.

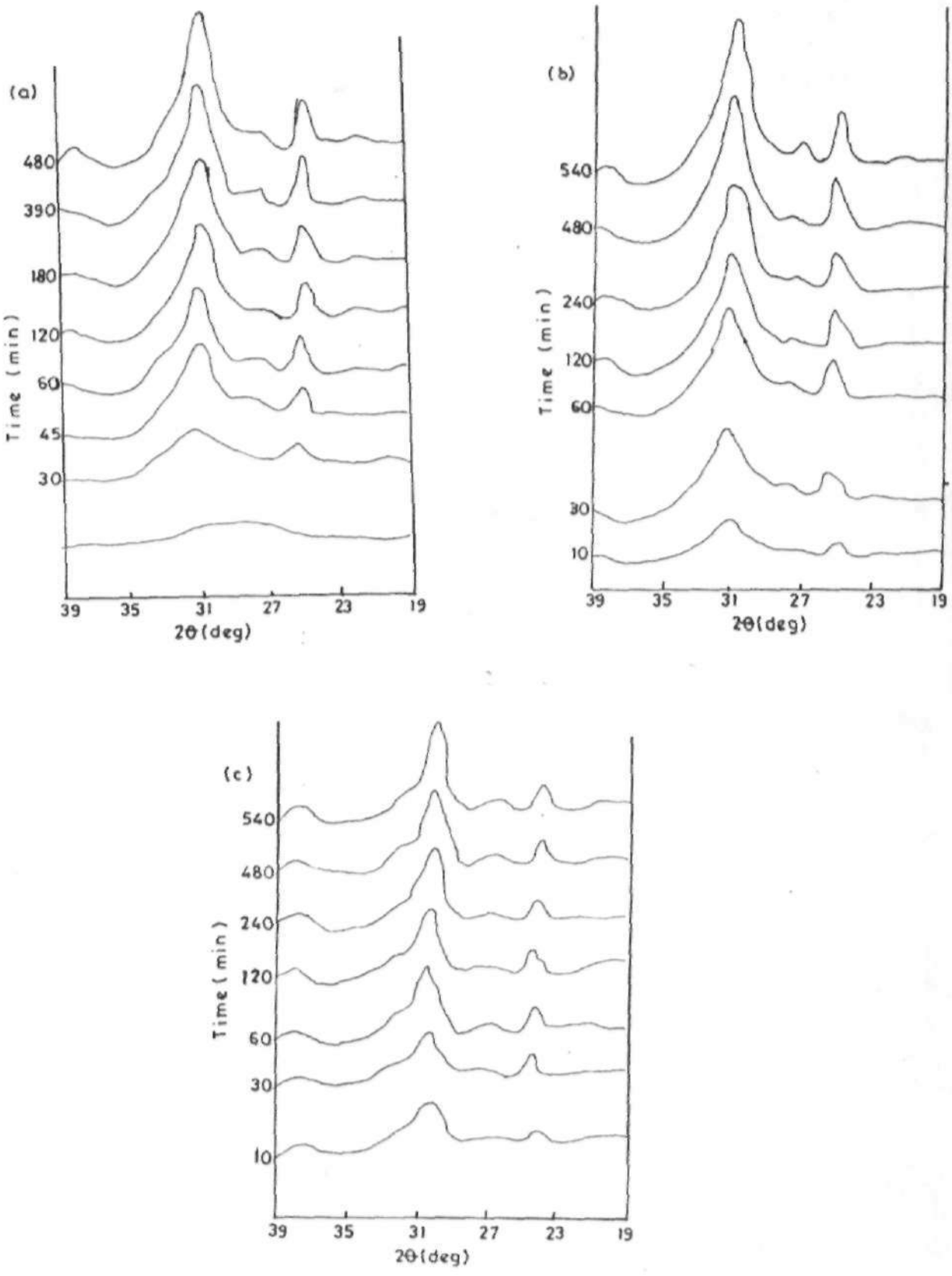
experimental conditions. At the concentration of pyrophosphate used (0.002M), this inhibitor stabilized ACP for over 9 hours. Increasing the temperature from $25^{0}C$ to $50^{o}C$ did not stop the inhibition. X-ray diffraction patterns obtained for the precipitates are given in appendix I.

Table 3.2 Ca/P molar ratio of HAP obtained from three different procedures.

Method of preparation	Ca^{2+} (mole) 10^{-5}	P (mole) 10^{-5}	Ca/P
A	6.18	4.44	1.40
B	6.78	4.55	1.49
C	6.72	4.05	1.66

Table 3.3 Cell parameters of HAP obtained from three different procedures.

Method of preparation	a-axis (Å)	c-axis (Å)
A	9.5292	6.9593
B	9.5148	6.9608
C	9.4724	6.9598
Literature value	9.432	6.881



FIG·3·2: X-RAY PATTERNS OF ACP-HAP PRECIPITATES PREPARED AT 25°C (a), 50°C (b) USING PH 9 AND AT 37°C USING PH 7·4 (c)

Table 3.4 Crystallinity index $1/\beta_{1/2}$ and mean size D of apatite crystals obtained at 25°C and pH 9.

Reaction Temp.	Time (min)	ß½ (θ)	1/ß½	D values
25°C	10	*	*	*
	30	1.00	1.00	77.47
	60	0.80	1.25	96.79
	120	0.80	1.25	96.88
	240	0.80	1.25	96.88
	480	0.80	1.25	96.92
	540	0.80	1.25	96.92
50°C	10	1.00	1.00	77.69
	30	0.90	1.11	88.52
	60	0.80	1.25	96.86
	120	0.80	1.25	96.88
	240	0.80	1.25	96.88
	480	0.80	1.25	96.88
	540	0.79	1.26	97.05

* - values could not be determined, because precipitate was essentially amorphous.

Table 3.5: Crystallinity index, $1/\beta_{1/2}$ and mean size, D of apatite crystals obtained in presence of AMP at 25°C, 50°C and pH 9.

Reaction Temp.	Time (min)	$\beta_{1/2}$ (θ)	$1/\beta_{1/2}$	D values
25°C	10	*	*	*
	30	*	*	*
	60	*	*	*
	120	1.00	1.00	77.82
	240	0.88	1.14	89.79
	480	0.88	1.14	90.23
	540	0.88	1.14	90.23
50°C	10	1.00	1.00	77.82
	30	1.00	1.00	77.82
	60	1.00	1.00	78.24
	120	1.00	1.00	78.69
	240	0.86	1.16	92.35
	480	0.86	1.16	92.35
	540	0.86	1.16	92.35

Table 3.6: Crystallinity index, $1/ß_{½}$ and mean size, D of apatite crystals obtained in presence of ADP at 25°C, 50°C and pH 9.

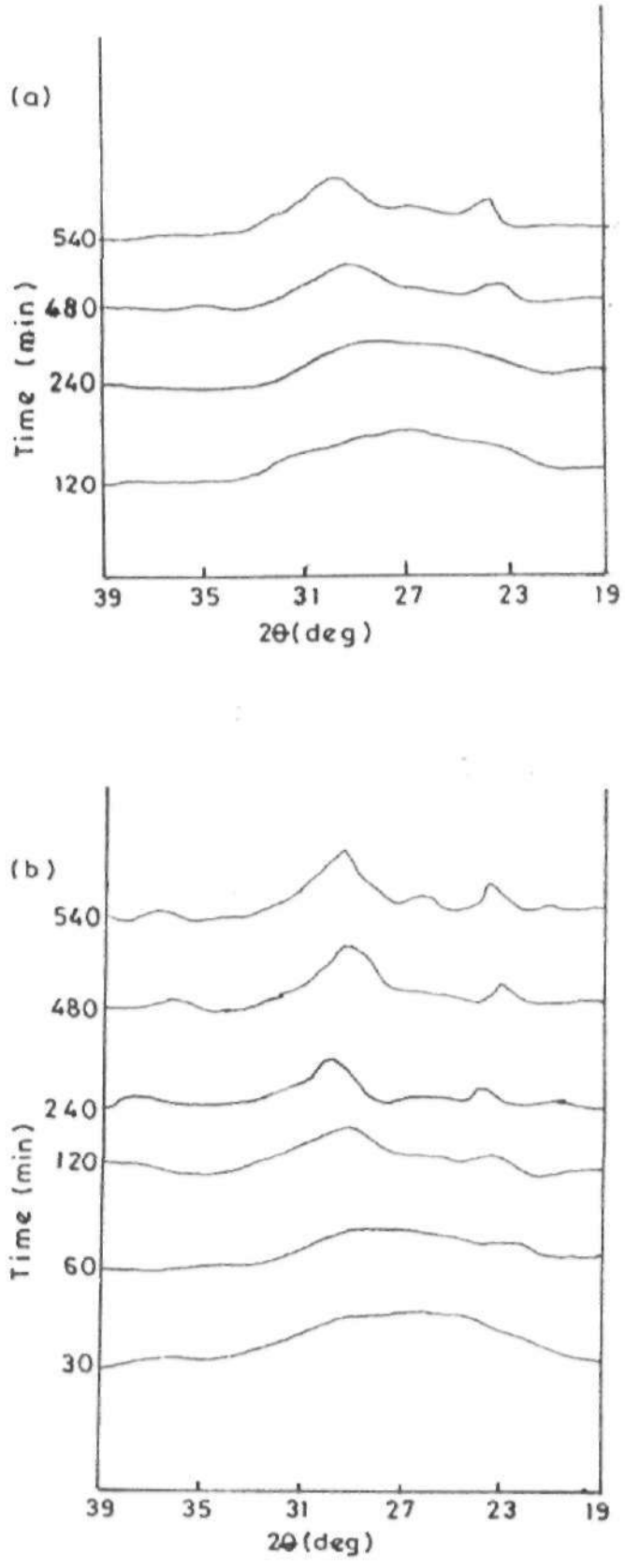
Reaction Temp.	Time (min)	$ß_{½}$ (θ)	$1/ß_{½}$	D values
At 25°C	10	*	*	*
	30	*	*	*
	60	*	*	*
	120	*	*	*
	240	*	*	*
	480	1.00	1.00	77.79
	540	1.00	1.00	77.78
50°C	10	1.00	1.00	77.78
	30	1.00	1.00	77.82
	60	1.00	1.00	78.82
	120	1.00	1.00	77.84
	240	1.00	1.00	77.78
	480	1.00	1.00	77.85
	540	0.90	1.11	86.44

* See table 3.4 for meaning

Table 3.7: Crystallinity index, $1/ß_{½}$ and mean size, D of apatite crystals obtained in presence of ATP at 50°C and pH 9.

Reaction Temp.	Time (min)	$ß_{½}$ (θ)	$1/ß_{½}$	D values
At 50°C	10	*	*	*
	30	*	*	*
	60	*	*	*
	120	*	*	*
	240	*	*	*
	480	1.00	1.00	77.82
	540	1.00	1.00	77.78

* See table 3.4 for meaning.



FIG·3·3 : X–RAY PATTERNS OF ACP HAP PRECIPITATES IN PRESENCE OF ATP AT PH 9/37°C (a) AND PH 7·4 / 37°C (b)

X-ray diffraction patterns for precipitates obtained in the presence of citrate ions at 25^{o}C and 50^{o}C and pH 9 are also given in appendix I. The effects of the citrate ions on the crystallinity and mean sizes of HAP crystals are shown in table 3.9. The effects of casein and glutamate on crystallinity and mean size of HAP crystals are indicated in tables 3.10 and 3.11 respectively.

Figure 3.4 shows x-ray diffraction patterns of ACP-HAP precipitates when tetracycline was used as inhibitor. The precipitation reactions were carried out at physiological conditions (that is pH 7.4 and 37^{o}C Different concentrations of tetracycline powder were used for separate experiments. No precipitate was recovered when 0.05mg/cm^3 of tetracycline was used. Results obtained when 0.025mg/cm^3 and 0.01mg/cm^3 of tetracycline were used are shown in figure 3.4. The effects of tetracycline on crystallinity and mean size of HAP crystals are contained in table 3.12. X-ray diffraction patterns of HAP crystals obtained from procedure C in section 3.2.1 and HAP crystals treated with tetracycline are compared in figure 3.5.

The x-ray diffraction patterns of ACP-HAP precipitates obtained in the presence of metal ions namely, Mg^{2+}, Sr^{2+}, Cd^{2+}, Pb^{2+} and Ba^{2+} are given in appendix II. The various effects of these metal ions on

crystallinity and mean sizes of HAP crystals are given in table 3.13.

X-ray diffraction patterns for ACP-HAP precipitates in presence of F^- are also given in appendix II. The reactions involving all the metal ions and fluoride ion were carried out at 25°C and pH 9.

Chemical analyses were performed on ACP-HAP precipitates obtained at different times for the control experiment as well as those obtained in the presence of Mg^{2+}, Zn^{2+} and Cd^{2+}. Table 3.14 contains the concentrations of Ca^{2+} and PO_4^{3-} as well as the Ca/P molar ratios for each precipitate withdrawn at different times in the control experiment. Table 3.15 contains the concentrations of Ca^{2+}, Mg^{2+}, PO_4^{3-} and $Ca_{10-x}Mg_x/P$ molar ratio. Table 3.16 contains concentrations of Ca^{2+}, Zn^{2+}, PO_4^{3-} and $Ca_{10-x}Zn_{x/}P$ molar ratios. Table 3.17 contains the concentrations of Ca^{2+}, cd^{2+}, PO_4^{3-} and the $Ca_{10-x}Cd_x/P$ molar ratios for each precipitate. Calcium - metal ion/phosphorus (i.e Ca^{2+}-M^{2+}/P) molar ratios for the metal ions in tables 3.14 - 3.17 were plotted against time and shown in figure 3.6. The curves show a typical behaviour of precipitation reactions involving metastable phases (Eanes and Meyer, 1977).

Table 3.9: Crystallinity index, $1/B_{½}$ and mean size of apatite crystals obtained in presence of citrate 25°C, 50°C and pH 9.

Reaction Temp.	Time (min)	$B_{½}$ (θ)	$1/B_{½}$	D values
At 25°C	10	*	*	*
	30	*	*	*
	60	*	*	*
	120	1.00	1.00	77.51
	240	0.80	1.25	96.96
	480	0.80	1.25	96.92
	540	0.80	1.25	96.88
50°C	10	1.00	1.00	77.71
	30	1.00	1.00	77.78
	60	0.80	1.25	97.28
	120	0.80	1.25	97.21
	240	0.80	1.25	97.14
	480	0.80	1.25	97.28
	540	0.80	1.25	97.28

* See table 3.4 for meaning

Table 3.8: Crystallinity index, $1/B_{½}$ and mean size, D of apatite crystals obtained in presence of ATP at 37°C, pH 9.0 and 7.4.

pH	Time (min)	$B_{½}$ (θ)	$1/B_{½}$	D values (A)
7.4	10	*	*	*
	30	*	*	*
	60	*	*	*
	120	*	*	*
	240	1.0	1.0	79.41
	480	1.0	1.0	79.41
	540	0.95	1.05	83.59
9.0	10	*	*	*
	30	*	*	*
	60	*	*	*
	120	*	*	*
	240	*	*	*
	480	1.1	0.91	72.19
	540	1.0	1.0	79.41

* See table 3.4 for meaning

Table 3.10: Crystallinity index, $1/\beta_{1/2}$ and mean size, D of apatite crystals obtained in presence of casein at 25°C, and pH 9.0

Time (min)	$\beta_{1/2}$ (θ)	$1/\beta_{1/2}$	D values (A)
10	1.0	1.0	79.41
30	1.0	1.0	79.41
60	1.0	1.0	79.41
120	1.0	1.0	79.41
240	0.95	1.05	83.59
480	0.95	1.05	83.59
540	0.95	1.05	83.59

Table 3.11: Crystallinity index, $1/\beta_{1/2}$ and mean size, D of apatite crystals obtained in presence of glutamate at 25°C, and pH 9.0

Time (min)	$\beta_{1/2}$ (θ)	$1/\beta_{1/2}$	D values (A)
10	*	*	*
30	1.0	1.0	79.41
60	1.0	1.0	79.41
120	1.0	1.0	79.41
240	0.90	1.1	88.23
480	0.87	1.15	91.29
540	0.85	1.18	93.42

Table 3.12: Crystallinity index, $1/\beta_{1/2}$ and mean size, D of apatite crystals obtained in presence of tetracycline at pH 7.4 and 37°C

Conc of tetracycline	Time (min)	$\beta_{1/2}$ (θ)	$1/\beta_{1/2}$	D values (A)
0.01mg/ml	10	1.0	1.0	79.41
	30	0.90	1.11	88.23
	60	0.90	1.11	88.23
	120	0.90	1.11	88.23
	240	9.84	1.19	94.55
	480	0.80	1.25	99.27
	540	0.80	1.25	99.27
0.025mg/ml	10	1.0	1.0	79.41
	30	1.0	1.0	79.41
	60	0.90	1.11	88.23
	120	0.90	1.11	88.23
	240	0.90	1.11	88.23
	480	0.90	1.11	88.23
	540	0.91	1.09	87.26

Table 3.13: Crystallinity index, $1/\beta_{1/2}$ and mean size, D of apatite crystals obtained in presence of some ions at 25°C and pH 9.

Ions	Time (min)	$\beta_{1/2}$ (θ)	$1/\beta_{1/2}$	D
Mg^{2+}	10	*	*	*
	30	*	*	*
	60	*	*	*
	120	*	*	*
	240	0.80	1.25	97.17
	480	0.80	1.25	97.17
	540	0.80	1.25	97.16
Sr^{2+}	10	*	*	*
	30	*	*	*
	60	*	*	*
	120	1.20	0.83	66.2
	240	0.83	1.20	95.7
	480	0.85	1.18	93.4
	540	0.88	1.14	90.2
Zn^{2+}	10	*	*	*
	30	*	*	*
	60	*	*	*
	120	0.99	1.01	80.2
	240	0.90	1.11	88.2
	480	0.84	1.19	94.5
	540	0.82	1.22	96.8
Cd^{2+}	10	*	*	*
	30	*	*	*
	60	1.00	1.00	79.4
	120	0.89	1.12	89.2
	240	0.90	1.11	88.2
	480	0.88	1.14	90.2
	540	0.88	1.14	90.2
Pb^{2+}	10	*	*	*
	30	*	*	*
	60	*	*	*
	120	0.80	1.25	97.15
	240	0.80	1.25	97.19
	480	0.80	1.25	97.21
	540	0.72	1.40	102.95

Table cont.

Ions	Time (min)	$\beta_{1/2}$ (θ)	$1/\beta_{1/2}$	D
Ba^{2+}	10	*	*	*
	30	*	*	*
	60	*	*	*
	120	1.1	0.91	79.4
	240	0.83	1.20	95.7
	480	0.82	1.22	96.8
	540	0.82	1.22	96.8
F^-	10	*	*	*
	30	*	*	*
	60	1.0	1.0	79.4
	120	0.96	1.04	82.7
	240	0.85	1.18	93.4
	480	0.86	1.16	92.3
	540	0.85	1.18	93.4

* See table 3.4 for meaning.

Table 3.14: Concentrations of Ca^{2+}, PO_4^{3-} and Ca/P molar ratios for ACP-HAP precipitates obtained at different times.

Time (min)	Ca^{2+} (10^{10-5})	$P(10^{-5})$	Ca/P Ratio
10	2.38	2.90	0.82
30	2.92	2.94	0.98
60	2.38	2.20	1.08
120	2.22	2.20	1.00
240	2.88	2.22	1.30
480	2.59	2.00	1.30

Table 3.15: Concentrations of Ca^{2+}, Mg^{2+}, PO_4^{3-} and Ca- Mg/P molar ratios for ACP-HAP precipitates obtained in presence of Mg^{2+}

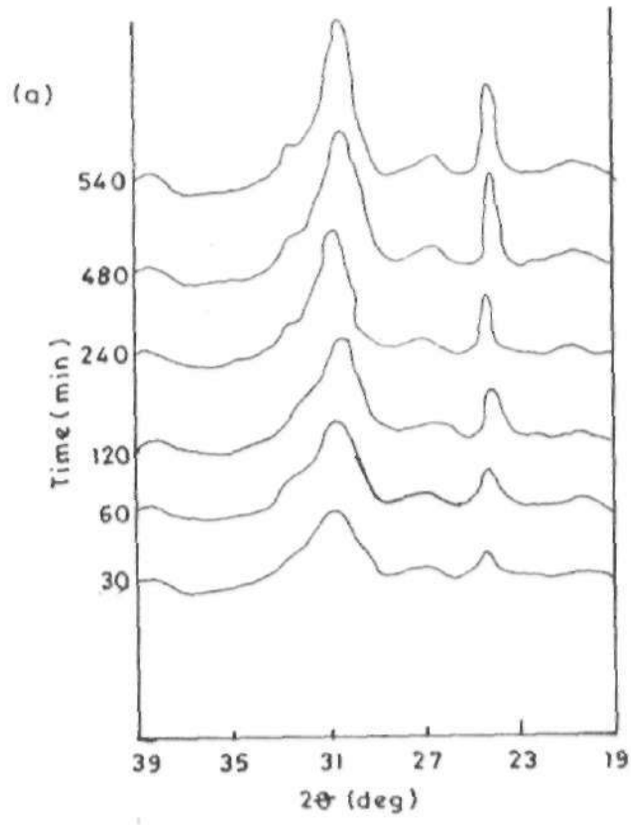
Time (min)	Ca^{2+} (10^{10-5})	Mg^{2+} (10^{-6})	P(10^{-5})	Ca-Mg/P
10	3.75	3.90	3.14	1.24
30	1.81	1.93	2.98	0.65
60	3.81	4.00	2.91	1.34
120	3.81	3.98	3.92	1.02
240	3.12	3.26	3.87	0.84
480	3.25	3.41	2.48	1.40
540	2.72	2.84	2.03	1.40

Table 3.16: Concentrations of Ca^{2+}, Zn^{2+}, PO_4^{3-} and Ca- Zn/P molar ratios for ACP-HAP precipitates obtained in presence of Zn^{2+}

Time (min)	Ca^{2+} (10^{10-5})	Zn(10^{-7})	P(10^{-5})	Ca-Zn/P
10	2.31	2.40	3.15	0.77
30	2.31	2.41	3.02	0.81
60	2.50	2.60	2.91	0.89
120	2.22	3.14	3.90	0.81
240	3.44	3.57	3.90	0.92
480	3.62	3.76	2.50	1.51
540	2.99	3.11	2.04	1.50

Table 3.17: Concentrations of Ca^{2+}, Cd^{2+}, PO_4^{3-} and Ca- Cd/P molar ratios obtained for ACP-HAP precipitates in presence of Cd^{2+}

Time (min)	Ca^{2+} (10^{10-5})M	Cd^{2+}(10^{-6})	P(10^{-5})	Ca-Cd/P
10	3.88	1.38	4.70	0.85
30	2.69	1.08	3.32	0.84
60	2.59	1.03	3.17	0.84
120	3.94	1.46	4.72	0.87
240	2.00	0.91	2.42	0.86
480	2.19	0.97	2.62	0.87



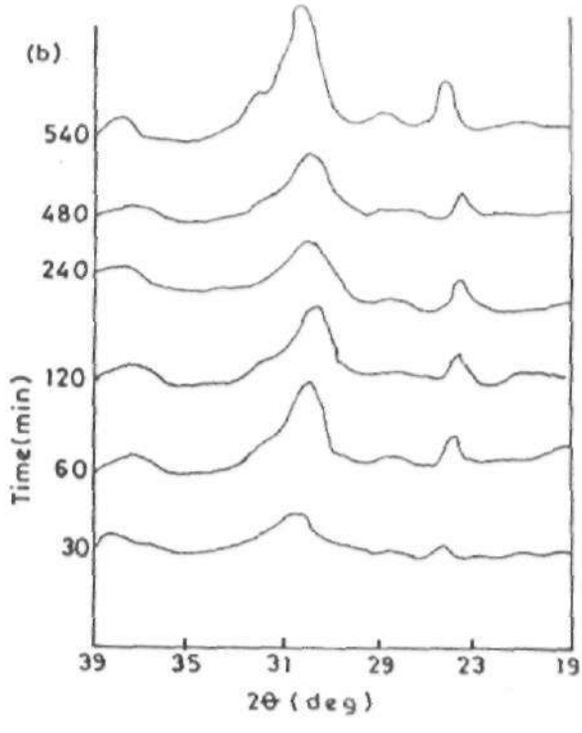
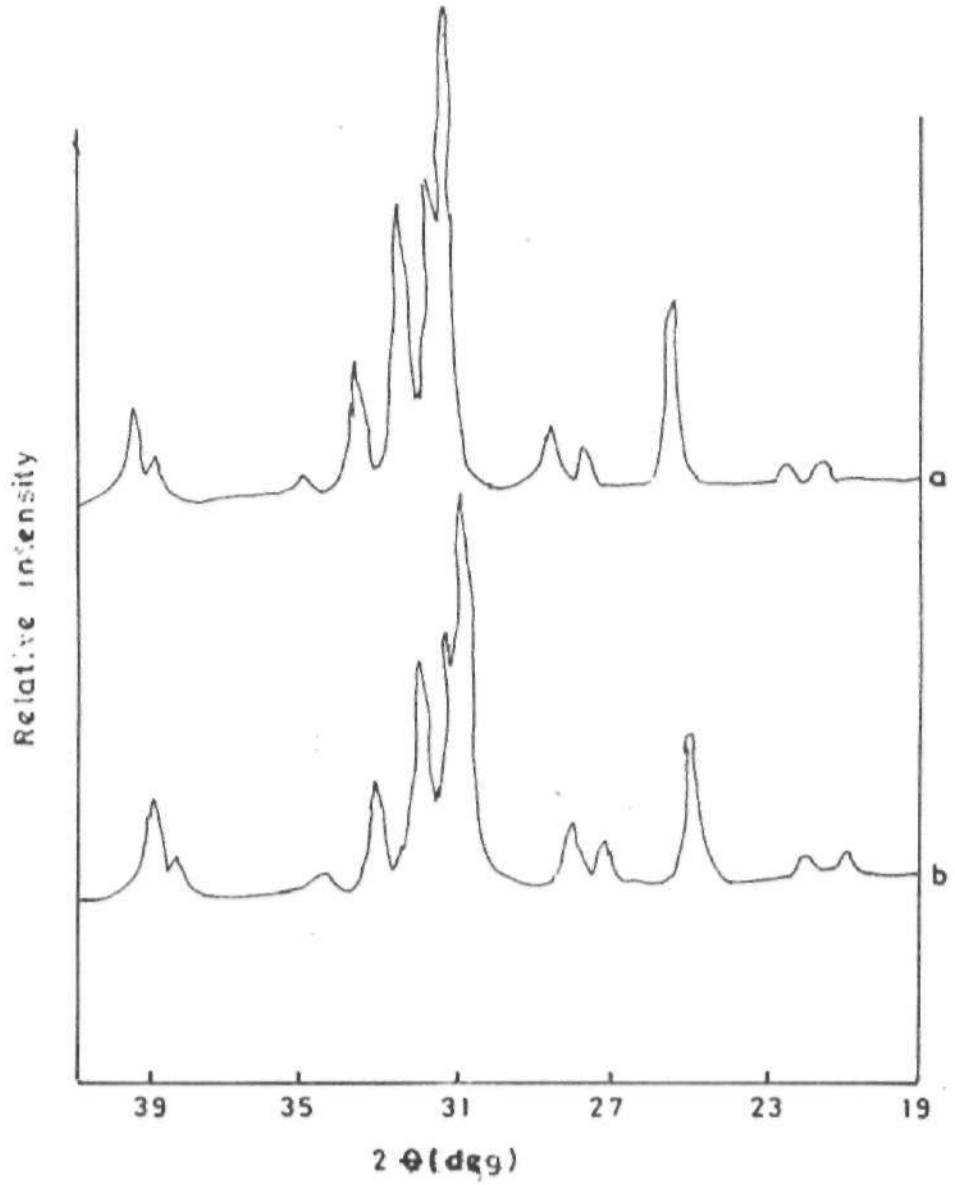


FIG.3·4; X—RAY PATTERNS OF ACP—HAP PRECIPITATES IN PRESENCE OF TETRACYCLINE (CONCENTRATIONS 0·01mg/cm^3 (a) AND 0·025mg/cm^3 (b) AT PH 7·4 AND 37°C.



FIG·3·5 : X-RAY PATTERNS SHOWING (a) HAP AND (b) HAP TREATED WITH 0·05M TETRACYCLINE

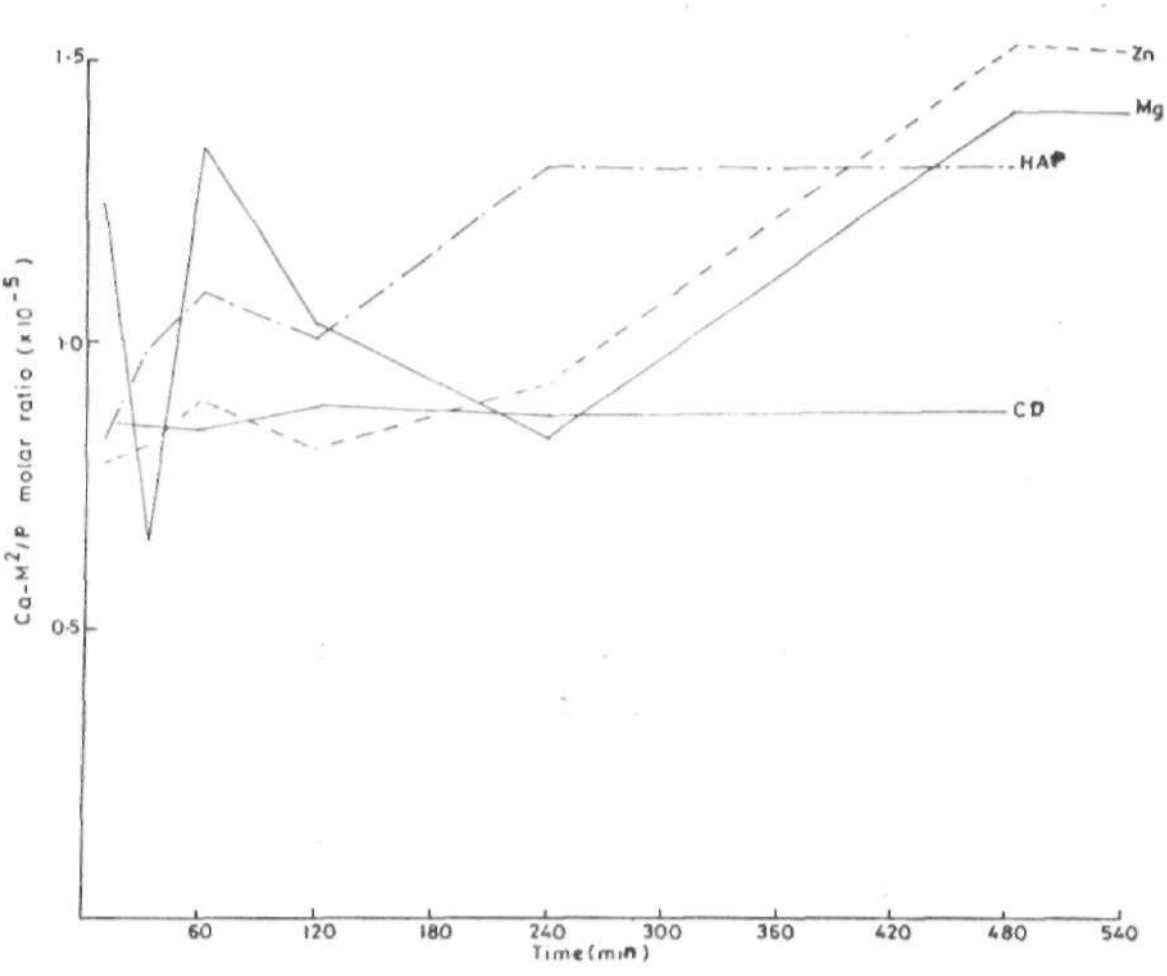


FIG-3.6 : VARIATION OF $Ca\text{-}M^{2+}/P$ MOLAR RATIO WITH TIME

3.4 Discussion

Synthetic basic calcium phosphates prepared from carbonate-free aqueous solutions have x-ray diffraction patterns similar to hydroxyapatite but often depart from its stoichiometry by exhibiting low Ca/P molar ratios between 1.5-1.60 (Posner, 1969). In this work the HAP crystals with the highest and ideal Ca/P molar ratio (1.65) were obtained from the procedure C, which involves the use of $Ca(OH)_2$ and H_3PO_4. The other methods, A and B (that is Na_2HPO_4/CH_3COOCa and $Ca(NO_3)_2/(NH_4)_2$ HPO_4 respectively) gave apatite crystals with 1.41 and 1.49 (table 3.2). Broader peaks corresponding to the 211, 112, 310 and 212 reflections are observed for the more imperfect crystals as shown by the x-ray diffraction patterns obtained for samples from procedures A and B. Generally a low Ca/P molar ratio has been attributed to, first, excess HPO_4^{2-} groups adsorbed on the surface of the stoichiometric HAP crystals and secondly, missing calcium either from the surface or from the interior of the HAP crystals (Posner, 1969). Posner (1969) further suggested that a general formular for all cation-deficient apatites can be written as $M_{10-x}H_{2x}(PO_4)_6(OH)_2$; where M is any divalent cation such as Ca^{2+}.

The x-ray diffraction patterns of ACP-HAP precipitates shown in figure 3.2 is typical of solids undergoing phase changes (Boskey and Posner, 1973). The

values of the crystallinity index, $1/ß_{½}$ and mean size D of apatite crystals show that the mechanism of the transformation is such that once the initial nuclei are present, the rate of proliferation and perfection of the crystalline material is very rapid. The rate of production of these crystalline materials during this proliferation period has been found to be proportional to the fraction of crystalline material already present (Boskey and Posner, 1973). This process is said to be autocatalytic, since it accelerates itself by production of additional crystals. Furthermore, since the mean crystal size, D of apatite formed is nearly the same throughout the conversion, this also implies that conversion rate is proportional to the number of apatite crystals already formed and to the total interfacial area of the crystalline phase. In an attempt to explain the mechanism of conversion, Eanes and Posner (1965), suggested that the precursor phase first dissolves with subsequent solution transport of the dissolved ions to a nucleation site. Crystallization then occurs directly from a supersaturated calcium phosphate solution with some ancillary nucleating mechanism acting as the rate controlling step, making ACP a passive but unstable calcium and phosphate ion reservoir.

Increasing the reaction temperature to 50^{o}C caused the induction time to reduce and the rate of conversion

to increase. The mean size of the apatite crystals did not change significantly (table 3.4). There is some indication then that, there is an energy barrier which must be overcome in order to form the first stable nucleus. According to Boskey and Posner (1973), increasing the temperature decreases the induction time by increasing the solubility of the ACP as well as providing additional energy needed to form a stable primary nucleus. This also agrees with the results obtained by Termine and Posner (1970), that ACP are more stable at lower temperature.

Previous studies (Termine and Posner, 1970; Termine et al, 1970; Williams and Sallis, 1982) on the transformation of ACP into HAP have demonstrated that many compounds inhibit the formation of HAP. It is this finding that has led to this reappraisal of the factors determining whether or not a substance will inhibit HAP formation on one hand, and the effects of such inhibitors on the crystallinity and mean sizes of the resultant HAP crystals. The structures of the inhibitors used in this work are shown in figure 3.7, since these have formed one of the bases of classifying them (Williams and Sallis, 1982). Inhibitors have been grouped into two types based mainly on the manner by which their increasing concentration affects the parameters defining transition.

The nucleotides that is, adenosine-5-monophosphate

(AMP), adenosine-5-diphosphate (ADP) and adenosine-5-triphosphate (ATP) following the classification of Williams and Sallis (1982) are type II inhibitors. With this type of inhibitors ACP is considered to be the main locus of action, although other mechanisms can be responsible for their inhibitory action. AMP shows a weak inhibitory action, delaying conversion for a short time. ADP showed a relatively stronger inhibitory action and ATP showed the strongest inhibitory action among the nucleotides used in this work. At 25^{o}C in the presence of AMP, conversion of ACP into HAP started at about 2 hours, with ADP the conversion started at about 8 hours and with ATP the precipitates were amorphous throughout the period of reaction (appendix 1). This trend can be attributed to the extent to which each of the nucleotide binds to the active sites on the HAP nuclei. The complexing ability of these nucleotides increases as the polyphosphate chain becomes longer (Wazer, 1958). This means that, ATP binds to the active sites on HAP nuclei the most, while AMP binds to it the least. This trend is also supported by measurement of stability constants of ionic complexes of various adenosine phosphates with calcium ions (Smith and Alberty, 1958). The conversion of ACP into HAP at 25^{o}C in presence of AMP and ADP may occur as a result of hydrolysis of the nucleotides with time, or that they bind poorly to the active sites of the

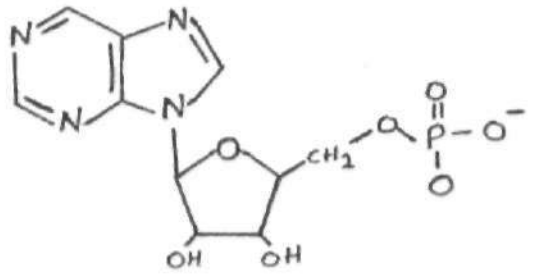
HAP nuclei. The adenosine moiety can also sterically obstructed one active site per molecule, thus decreasing the coverage and therefore permitting HAP crystal growth to continue (Williams and Sallis, 1982). ATP though capable of being hydrolysed, the area of scission of the polyphosphate is thought to be dependent on pH of the media (Corbridge, 1980). In biological processes or reactions at approximately neutral pH, ATP can be hydrolysed successively leading to ADP and AMP, thus releasing high amount of energy.

$$ATP + H_2O \text{ ------» } ADP + H_3PO_4$$

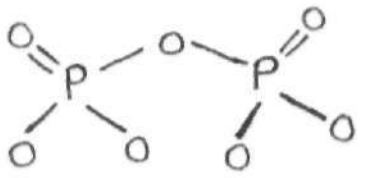
$$ADP + H_2O \text{ ------» } AMP + HPO_4^{2-}$$

$$AMP + H_2O \text{ ------» } A + HPO_4^{2-}$$

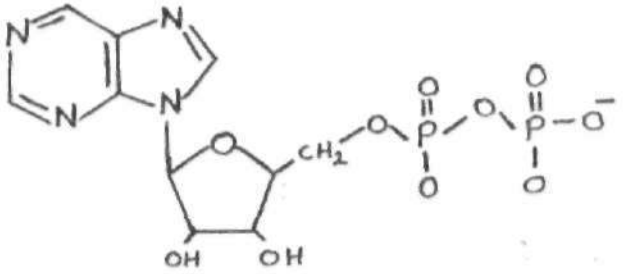
In biological processes, the rates of hydrolysis are greatly increased by the presence of enzymes. In alkaline solution ATP breaks at the second P-O-P linkage (figure 3.7), to give AMP and pyrophosphate (Corbridge, 1980). From the results obtained (appendix I) when precipitation was carried out in alkaline medium (pH 9.0), pyrophosphate was possibly formed as a result of the hydrolysis, and pyrophosphate being a stronger complexing agent (Smith and Alberty, 1958), than AMP, causes a more permanent poisoning of the HAP nuclei. This may explain why the precipitates obtained were amorphous throughout the period of reaction. Increasing the reaction temperature from 25^{o}C to 50^{o}C, caused



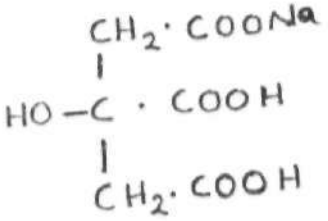
Adenosine-5-monophosphate



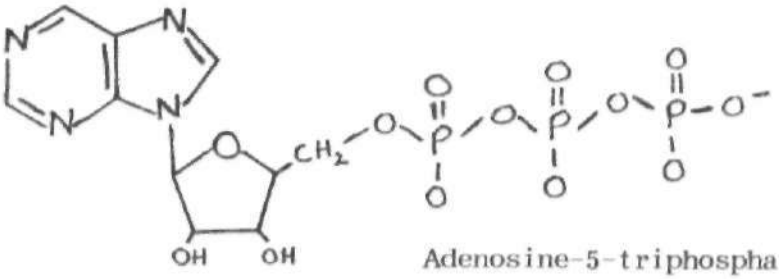
Pyrophosphate



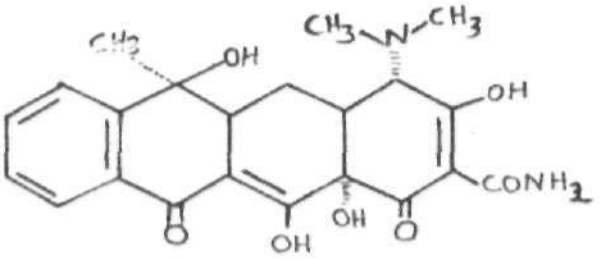
Adnesine-5-diphosphate



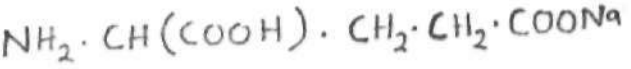
Sodium citrate



Adenosine-5-triphosphate



Tetracycline



L-glutamic acid sodium salt.

Figure 3.7 Structures of some inhibitors used.

conversion of ACP into Hap at approximately 8 hours of reaction. At this temperature ACP converts faster into HAP, and the concentration of the pyrophosphate that resulted from the hydrolysis of ATP may not be enough to cause a permanent inhibition. When the precipitation reaction was carried out under physiological conditions (pH 7.4 and 37^{o}C) in the presence of ATP (figure 3.3), the conversion of ACP into HAP started at approximately 1 hour. Under this condition as discussed earlier, ATP hydrolyses successively to AMP; and since the susceptibility of these nucleotides to hydrolysis is given as AMP > ADP > ATP (Smith and Alberty, 1958), it is expected that ACP should convert at relatively shorter induction time as observed. For AMP and ADP, when the temperature was increased from 25^{o}C to 50^{o}C at pH 9 (appendix I), this appeared to appose their inhibitory effects, and conversion of ACP into HAP started at approximately 10 minutes for both inhibitors.

Williams and Sallis (1982) reported that type II inhibitors do not alter the dimensions of the particles involved in the transition. In this work it was found that the nucleotide inhibitors actually caused a slight reduction in the mean sizes of the crystals (tables 3.5, 3.6 and 3.7), even when the temperature was increased. However, citrate which is also a type II inhibitor did not cause such a reduction in the crystal size (table

457801

1 0 NOV 1995

Bello

3.9). This finding suggests that even though the nucleotides and the citrate are type II inhibitors, they may bind to different sites of the HAP nucleus. Tables 3.5, 3.6 and 3.7 show that increasing the temperature of reaction acts only to reduce the induction time, but does not have any effect on the size of the apatite crystals formed in presence of nucleotide inhibitors. The fact that citrate cannot be hydrolysed further confirms that the mechanism of inhibition is different from that exhibited by the nucleotides. It has also been reported that the solubilities of the apatite crystals obtained in the presence of citrate ions were not different from those obtained in the control experiment (Meyer and Salinger, 1980). It would therefore appear that the effect an inhibitor would have on the resultant apatite crystals is also dependent on the mechanism of inhibition and not necessarily on whether it is a type I or type II inhibitor.

Pyrophosphate on the other hand has been classified as a type I (that is, a crystal growth) inhibitor (Williams and Sallis, 1982). This ion can change either the surface or the internal chemical composition of the initial amorphous phase, thus increasing the activation energy barrier of amorphous calcium phosphate dissolution and initial apatite crystal formation (Termine and Posner 1970). Both classes of inhibitor bind to ACP and HAP,

and it therefore appears either that type I inhibitor bind with higher affinity to the defect sites on HAP from which crystal growth proceeds, or that these sites are different from those bound by type II inhibitors or both with the concentration of pyrophosphate used in this work, no transformation of ACP into HAP occurred and the ACP spherules were stabilized throughout the period of reaction (9 hours). Pyrophosphate is likely to have bound very strongly to ACP, thus changing its chemical composition and showing no evidence of being hydrolysed in the course of the reaction, even when the temperature was increased to 50^{o}C. In the pyrophosphate ion (figure 3.7), the P-O-P bond is more difficult to hydrolyze than polyphosphates attached to organic groups. The pyrophosphate resembles the diphosphate group in ADP structurally and the difference in the inhibitor potency could be because of the size difference. ADP probably acts on the surface of the HAP nuclei (in which case it is prone to surface catalyzed hydrolysis), while the pyrophosphate may enter the HAP nuclei and cause a more permanent poisoning of the HAP nuclei at the temperature used. Since there was no conversion of ACP to HAP, even at 50^{o}C, this could imply that the pyrophosphate was not hydrolysed at this temperature, and ACP was stabilized for a much longer period.

The citrate ion delayed the conversion of ACP into

HAP for approximately 60 minutes at 25^{o}C (appendix I). Table 3.9 shows that the inhibitor did not affect the dimensions of the apatite crystals. Though citrate had earlier been classified as a type II inhibitor, this finding is contrary to the generalization made by Williams and Sallis (1982). Increasing the reaction temperature to 50^{o}C, completely nullifies the inhibitor potency of the citrate ions at the stipulated concentration. The citrate ions have been reported to substitute for phosphate ions on the apatite surface (Cifuentes et al, 1980).

Casein, a protein found in milk did not inhibit ACP to HAP transformation at the concentration (0.1mg/ml) used in this experiments. Termine et al (1970), reported that this protein inhibited the conversion minimally at a higher concentration (0.5mg/ml). Casein probably interferes sterically with the conversion process especially at high inhibitor concentrations. There are also indications that organically bound phosphate and acidic amino acid side chains may be potent sites for any given macromolecule-mineral interaction (Termine et al, 1970). Like inhibitors containing phosphate groups, the use of casein resulted in the reduction of the mean size of the apatitic crystals formed. Based on the mode of inhibition casein may be grouped along with type II inhibitors.

L-Glutamate was found to delay conversion of ACP to HAP for about 30 minutes. Though not classified by Williams and Sallis (1982), L-glutamate possesses one of the structural factor necessary for a potent ACP-HAP inhibitor (that is more than one carboxylic group). L-Glutamate was also found to reduce the mean size of the apatite crystals and may be regarded as a type II inhibitor.

Tetracycline whose structure is shown in figure 3.4, is a broad-spectrum antibiotic. It has been found to be an inhibitor of ACP - HAP transformation. It is an amphoteric compound, and exist as zwitterions in neutral solutions. It forms stable complexes with many metals including calcium and such chelates are usually very insoluble in water. The affinity of tetracycline for calcium causes it to be laid down in newly formed bones and teeth as tetracycline-calcium phosphate complexes (Doerge, 1978). Deposits of this antibiotics in teeth course a yellow discolouration which darkens over a period of time. The precipitation reactions in the presence of tetracycline were carried out at physiological conditions (pH 7.4 and $37^{O}C \pm 0.05$). At a concentration of 0.005mg/ml of tetracycline, no precipitate of calcium phosphate was isolated. This may be as a result of a greater affinity of tetracycline for calcium ions compared to the phosphate ions. When a

lower concentration ($2.5x10^{-3}$ mg/ml) was used, ACP-HAP precipitates were formed. The rate of ACP to HAP conversion, as well as the extent of conversion were affected by tetracycline at this concentration. It was found that at this concentration tetracycline did not significantly stabilize the amorphous phase (figure 3.4). At still a lower concentration of tetracycline ($1.0x10^{-3}$mg/ml) tetracycline cannot be regarded as an inhibitor of ACP - HAP transformation. Table 3.12 shows that the mean size of crystals formed at this concentration ($1.0x10^{-}$mg/ml) showed considerable reduction in the mean size of the HAP crystals. At high concentrations, it is possible that apart from forming chelates with calcium ions, tetracycline probably interferes sterically with the conversion process. Tetracycline may be classified as a type II inhibitor based on the classification used by Williams and Sallis (1982). All precipitates obtained using tetracycline were yellow at first, but darkened with time when exposed to light. In a separate experiment, when HAP crystals were treated with a neutral solution of tetracycline (0.05M) the resultant HAP crystals turned yellow and later darkened. The x-ray diffraction pattern obtained for these HAP crystals (figure 3.5b), is not different from that obtained for the pure HAP crystal (figure 3.5a). It appears from this result that, tetracycline was only adsorbed on the

surface of the HAP crystals, since broadening of the peaks were not observed.

Metal ions apart from sometimes substituting for Ca^{2+} in apatites, also affect the transformation of Acp into HAP and the dimensions of the resultant crystals. Mg^{2+} (a type II inhibitor) was found to inhibit Acp to HAP transformation (Appendix II). Nancollas (1981), considers the inhibitory role of Mg^{2+} to involve interference of this ion with the formation of HAP critical nuclei by entering the prenuclei structure and creating a structural mismatch. At the concentration used in this study (0.001M0. Mg ion inhibited the nucleation of HAP for about 2 hours, but did not inhibit crystal growth. The mean size of apatite crystals obtained in presence Mg^{2+} (table 3.13) are comparable to the control.

Although it has been reported that Sr^{2+} can easily enter the apatite lattice (Koutsoukos and Nancollas, 1981), they similarly compete with Ca^{2+} and prevent the formation of the appropriate nuclei and slow down crystal growth. The presence of Sr^{2+} in the crystallizing solution was found to reduce not only the crystal growth, but also the mean size of the apatite crystals (table 3.13). In the crystallization of hydroxyapatite from aqueous solution, Koutsoukos and Nancollas (1981), obtained Ca-Sr-hydroxyapatite crystals which were much

smaller than HAP crystals. The reason given is that the presence of Sr^{2+} results in the creation of ionic vacancies in the lattice and insignificant incorporation of the strontium ions.

Zn^{2+} which has been found to substitute for Ca^{2+} in HAP only to a little extent (Inikori, 1992), was found to delay the nucleation of HAP crystals for about 2 hours (appendix II). Zn^{2+} like Mg^{2+} did not reduce significantly the mean size of the apatite crystals formed. Cd^{2+} (ionic radius 0.97A) is similar to Ca^{2+} (ionic radius 0.99A) in size, and is therefore expected to substitute for Ca^{2+} in HAP at the low concentration used. Cd^{2+} was found to delay the nucleation of apatite crystals for about 30 minutes, and also reduced the crystal growth and mean size of the apatite crystals. This reduction in size of the apatite crystals is in agreement with the smaller ionic radius of Cd^{2+} with respect to that of Ca^{2+}. However this difference in ionic radii appears too small to justify the observed reduction in size. Instead the reduction may be attributed to the nature of the cation-oxygen interactions (Big et al, 1986).

Pb^{2+} was found to inhibit nucleation process, but enhanced crystal growth. The replacement of lead for calcium in the apatite structure induces an enlargement of the lattice constants in agreement with the larger

ionic radius of lead (1.30A) with respect to that of calcium. However, this cannot be justified on the basis of the difference in ionic radius and nature of the cation-oxygen interaction alone, but may be accounted for more completely by the structural differences caused by the inhomogeneous lead distribution in the two non-equivalent cation sites of the HAP structure (Bigi et al, 1991).

Ba^{2+} substituted to a small extent for Ca^{2+} in HAP in aqueous medium (Bigi et al, 1984). Ba^{2+} like Sr^{2+} inhibited nucleation process for some time (appendix II), but did not reduce the crystal growth, thus giving crystals similar to those obtained for the control. It appears that under the experimental condition used in this reaction, Ba^{2+} did not substitute for Ca^{2+} in HAP.

The F ion was found to inhibit ACP-HAP transformation by reducing the growth rate of the apatitic crystals, and delaying the nucleation of HAP crystals. Fluorapatite (FAP) is less soluble compared with hydroxyapatite and thus incorporation of F^- within the lattice would be expected to result in a more rapid precipitation of the apatite with a lower final calcium and phosphate concentrations (Newesely, 1961). However, studies of the ionic molar ratios in the precipitating phase was reported to be suggestive that this ;phase is not FAP but rather in fluoridated hydroxyapatite

(Nancollas, 1982). Nancollas (1982), also reported that F^- retards the formation of ACP, but this was not observed under the conditions used in this experiment. The effect of F^- on the size of the resultant HAP crystals was not very significant (table 3.13).

Chemical analysis of ACP-HAP precipitates shows an initial increase in the Ca/P molar ratio of the control, and a lowering at about 2 hours, after which a constant value (1.3) was maintained. In the absence of such ions as F and CO_3, HAP is the thermodynamically stable and product of calcium phosphate precipitations carried out in neutral or basic pH. The data obtained in this study (table 3.14), show that the crystals are apatite like in their general structural features. The first crystals to form in the spontaneously precipitating systems deviated markedly from HAP in composition and structural details as exemplified by low Ca/P molar ratios, x-ray diffraction patterns and distorted mean sizes. These primary crystals are unstable and steadily change upon solution ageing to compositions and structure nearly resembling HAP. The rate at which these chemical and structural changes decrease with time suggests a maturation behaviour similar to that observed in either sparingly soluble inorganic precipitates known as Ostwald ripening (Walton, 1967, Dunning, 1973). Eanes and Meyer (1977) observed similar changes in the growth curve of

HAP under physiological conditions. They reported that these phase changes and the final apatitic stage of the maturation process was marked mostly by changes in the chemistry of the solids. Furthermore, the significant increase in the Ca/P ratio of the solid obtained at 1 hour occurred, but was accompanied by very little decrease in solution calcium. This finding they explained, indicate that the increase in crystal mass during this time span from newly deposited material was negligible and consequently could not account for the observed increase in Ca/P ratio. Instead the significant amounts of the earliest apatite formed by hydrolysis change into more stoichiometric material through continuous dissolution/growth process such as ostwald ripening.

The behaviour of the precipitating phases, differ in the presence of the different metal ions, that is Mg^{2+}, Zn^{2+} and Cd^{2+}. The Ca-Mg/P molar ratio shows an initial decrease and then an increase before it finally attains a stable composition of 1.4 (figure 3.6). This increase in Ca-Mg/P ratio indicates maturation of the apatite crystals and this is consistent with result obtained from x-ray analysis of the precipitates discussed earlier. The Ca-Zn/P molar ratio also shows a general increase, giving a value of 1.5, nearing the expected value for apatites. The Ca-Cd/P molar ratio deviated markedly from

the expected value for apatites, which is approximately 1.67. This result is also consistent with the inhibitory role Cd^{2+} plays on the crystal growth of HAP. The low Ca-Cd/P ratio may be as a result of the contribution from the other precipitating phases of calcium phosphate system unable to convert to the apatite in presence of Cd^{2+}.

CHAPTER FOUR

4.0 Attempted Preparation of "Tin hydroxyapatite" and studies on "Tin calcium hydroxyapatite" solid solutions

4.1 Introduction

Pure stoichiometric hydroxyapatites, $M_{10}(PO_4)_6(OH)_2$ are difficult to prepare from solution. The precipitation of calcium hydroxyapatite is usually nonstroichiometric with Ca:P molar ratio less than theoretical and contains acid phosphate, carbonate and excess water. Other hydroxyapatites such as barium, cadmium, lead and strontium hydroxyapatites are known and have been prepared (Sundarsanan and Young, 1972; Fowler, 1974; Okada and Iwai, 1978; Inikori, 1992). These hydroxyapatites are isostructural with calcium hydroxyapatite, and as such they have the possibility of being incorporated into bony tissues and dental enamel. Structural and crystal studies show that the crystals are hexagonal and have the space group P_3/M. Lattice parameters of hydroxyapatites are shown in table 4.1.

Many of the studies on hydroxyapatites have been directed towards defining the exact nature of the interaction of various ions with calcium hydroxyapatite. Usually the substitution of a cation for Ca^{2+} in calcium hydroxyapatite, HAP is accompanied by changes in the apatite lattice or unit cell parameters. These changes

are often related to the size of the ionic or crystal radius of the cation compared to that of the Ca^{2+}. Similarity in the cationic radius has therefore been proposed as a reason for isomorphous substitution for Ca^{2+} in HAP (Chiranjeevirao et al, 1982). This proposal is not always supported by experimental observations. For example cations larger than Ca^{2+}, such as Sr^{2+}, Pb^{2+} substitute for Ca^{2+} giving a complete series of solid solutions of the type $Ca_{5-n}\ Mn(PO_4)_3OH$ (n=o to 5, M refers to the substituting cation) (Koutsoukos and Nancollas, 1981). Cd^{2+} and Mg^{2+} with smaller radii (the latter more so) have also been found to substitute for Ca^{2+} in the whole range (Inikori et al, 1989). Calcium-barium hydroxyapatites on the other hand show a zone of immiscibility between 0 and 64 atom % barium (Bigi et al, 1984).

In a survey of the effects of various cations on calcium hydroxyapatite in aqueous medium at about 100°C, Legeros et al (1980), reported that amorphous precipitates were obtained from solutions with Sn^{2+} and Ca^{2+} mole ratio of 3:97. It was therefore thought that tin does not substitute for Ca^{2+} in HAP to any significant extent, and therefore may not form an apatite. Lead which is just below tin in the ;periodic table forms lead hydroxyapatite which has been prepared in large amounts from a non-conventional procedure using

lead nitrate (Bigi et al, 1991). Lead also substitutes for calcium in HAP in the whole range. While the lattice constant a of the resultant solid solutions varies linearly with composition, the variation of the lattice constant c does not follow Vegard's law but shows a discontinuity at about 50% lead atom content. The variations of the lattice constants of the solid solutions follow the same laws whether samples are obtained from aqueous media or by solid state reaction (Big et al, 1991). The aim of this section was to study the interaction of tin with calcium hydroxyapatite for comparison with the results obtained for lead. An attempt was made to prepare tin hydroxyapatite from hydrous tin (II) oxide.

4.2 EXPERIMENTAL

4.2.1 Attempted preparation of tin hydroxyapatite

Preamble

Like Pb^{2+} salts, Sn^{2+} salts are colourless and generally soluble in water but are extensively hydrolyzed. For example

$$SnCl_2 + H_2O \quad Sn(OH)Cl + HCl$$

Solutions of tin (II) salts react with alkali to yield a white precipitate of hydrated tin(II) oxide, $SnO.xH_2O$. Hydrolysis of Sn(II) salts gives $(Sn_3(OH)_4)^{2+}$ and $(Sn_2(OH)_2)^{2+}$ as minor contributors (Cotton and Wilkinson, 1976).

$$3\ Sn^{2+} + 4H_2O = (Sn_3(OH)_4)^{2+} + 4H^+$$

The trimeric ion appears to provide the nucleus of several basic tin (II) salts obtained from aqueous solutions at fairly low pH, an example of which is the basic tin (II) nitrate, $Sn_3(OH)_4(NO_3)_2$ (Donaldson and Moser, 1961). Lead hydroxyapatite had earlier been prepared from nitrate, $Pb_6O_5(NO_3)_2$ (Thomas, 1988 and Bigi et al, 1991).

Reagents

Copper sulphate pentahydrate

Metallic tin.

1:1%v/v Ammonia solution

This solution was prepared by mixing together one part of ammonia solution (Sp. gr.0.91) to one part of water, to give a total volume of $280cm^3$.

0.5M orthphosphoric acid

This solution was prepared by mixing an appropriate volume ($7cm^3$) of orthophosphoric acid (Sp. gr. 1.75) in $250cm^3$ of water.

Sulphuric acid solution

$20cm^3$ of the acid was taken in $400cm^3$ of water.

Procedure

Hydrous tin (II) oxide was first prepared, using the method described by Donaldson and Moser, (1961). Cu (II) SO_4 (50_g) was dissolved in the sulphuric acid solution and metallic tin (50_g) was then added. The mixture was heated to boiling (without stirring) until the solution turned colourless and the deposited copper was covered with a grey coating of tin. The resulting tin (II) sulphate solution was filtered and the filtrate treated with ammonia solution, to precipitate the hydrous tin (II) oxide. The grey precipitate was washed by centrifugation using distilled water until it was free of ammonia, and then suspended in water.

An attempt was then made to prepare tin hydroxyapatite using the hydrous tin (II) oxide. A paste of the hydrous tin (II) oxide, was transferred into

the orthophosphoric acid solution over a period of about 30 minutes. The mixture was stirred continuously for 1 hour using a magnetic stirrer. The precipitate obtained was filtered by suction and washed several times using warm water. It was dried in an oven at 100^{o}C for about 2 hours.

4.2.2 Attempted preparation of tin calcium hydroxyapatite aqueous medium

Reagents

Sn^{2+}/Ca^{2+} Solution

A solution containing 3:97 mole ratio of Sn^{2+}/Ca^{2+}, giving a total of 0.008 mole of cation was prepared by weighing the calculated amount of tin (II) chloride and calcium nitrate into $400cm^3$ of water.

Ammonium hydrogen diphosphate solution

A solution containing 0.019 mole of phosphate ions in $1100cm^3$ of water was prepared by dissolving appropriate amount of the salt in water.

Procedure

An attempt to prepare synthetic tin calcium hydroxyapatite was made based on the report of Legeros et al (1980); with a solution containing Sn^{2+} and Ca^{2+}, and by precipitating from an aqueous medium. This was done by dropwise addition of the mixed tin/Calcium ions to a boiling and stirring solution of ammonium hydrogen diphosphate.

After precipitation, the content of the reaction flask was refluxed for about 1½ hours to enhance the homogeneity and crystallinity of the precipitate. The precipitate was then filtered, washed with water and dried in an oven at $105^{o}C$.

4.2.3 Preparation of tin calcium hydroxyapatite by solid state synthesis

Reagents

Calcium hydroxyapatite

This was prepared by the method described in section 3.2.4c.

Procedure

Attempts to prepare tin calcium hydroxyapatites were made by heating mixtures of the final precipitate from section 4.2.1, assumed to be tin hydroxyapatite and calcium hydroxyapatite in a furnace at 500^{o}C overnight. Mixtures were made with tin ranging from 0 to 100 atom %.

The synthesis was repeated at 700^{o}C.

4.2.4 X-ray diffraction analysis

X-ray powder diffraction patterns of the final precipitate from section 4.2.1, and tin "calcium hydroxyapatites" were taken as described in section 3.2.7, in the 2θ range of 5^{o} - 50^{o}.

4.2.5 Infra-red absorption analysis

Infra-red absorption analysis was carried out for the unknown tin phosphate precipitate, obtained from the attempt to prepare tin hydroxyapatite in section 4.2.1. About 1.0mg of the powdered sample was mixed intimately with 300mg of potassium bromide (Infra-red grade). Pellets were made under vacuum, and analysed at the Department Chemistry, University of Bologna, Italy.

4.2.6 The quantification of tin and phosphorus in powder samples of unknown tin phosphate precipitate

4.2.6.1 X-ray fluorescence analysis

The high Z elements as well as the low Z elements of the powder samples can be analysed using different radioisotopes and secondary target x-ray tubes. The ;powder samples were prepared without using the binder and pressed with 2 ton pressure. The Am-241 radioisotope source and Cd-109 radioisotope source were used to excite the fluorescent for tin element and the coherent and incoherent scatter of the samples respectively, at the International Energy and Atomic Energy Centre, Austria. The spectra evaluation was done using orthogonal background order of 10. The quantification for Sn was performed with the use of the fundamental parameter method of the AXIL/QXAS package. In the analysis of phosphorus, cellulose was used as the binder and pressed with 5 ton pressure. With the use of tube x-ray fluorescence system, Fe secondary target was used to excite the fluorescence and for the calculation of sensitivity of the P, the Mo target was used for the calculation of absorption. The spectra evaluation were done using Linear Filter background order of 10. The quantification of P was performed with the use of Quantitative Analysis of Light Matrix Materials of the AXIL/QXAS package.

4.3 Results and Discussion

X-ray diffraction pattern obtained for the new compound suspected to be 'tin hydroxyapatite' $Sn_5(PO_4)_2OH$, is shown in figure 4.1. The x-ray diffraction pattern shows distinct peaks between 29 and 31^{o} 2θ (the main diagnostic region of calcium hydroxyapatite) in addition to some distinct maxima at higher angles. The peak observed at $26^{o}2\theta$ for this compound is similar to the 002 peak of calcium hydroxyapatite. The general formular for hydroxyapatites is considered to be $M^5(PO_4)_3OH$ (M = divalent cation), and they belong to the hexagonal Pb_3/M space group. Results obtained from calculation of lattice parameters (using d-spacing values for the compound in appendix III), assuming the centrosymmetric space group (that is Pb_3/M), showed that the a-axis = 9.88Å and C-axis = 7.45Å. These are compared with results obtained for some synthetic hydroxyapatites in table 4.1. There appears to be some correlation between the ionic radii and the lattice parameters, although this is not exact.

The result of infra-red measurement on the compound is shown in figure 4.2 and the spectra for calcium hydroxyapatite is shown in figure 4.3. Mean wave numbers for the vibrations of phosphate and hydroxyl groups of the tin phosphate together with other synthetic hydroxyapatites are shown in table 4.2. The spectra of

apatite substances containing phosphate ions have nine infra-red active internal vibrations of the phosphate groups (Klee and Engel, 1967). Six of these (V_1 V_{2a} V_{3a} V_{3b} V_{4a}, V_{4b}) are vibrations in which the movements of the atoms are symmetric and the remaining three vibrations in which the movements of the atoms are antisymmetric (i.e V_{2b}, V_{3c} and V_{4c}). All bands associated with PO_4 group in hydroxyapatites occur in the range from 400 to 1100cm^{-1} (Klee and Engel, 1969). Bands due to the librational motion of the OH ions in hydroxy compounds may also occur in this region. Such bands have been observed in the case of $Ca_5(PO_4)_3OH$ (at 631cm^{-1}) and $Cd_5(PO_4)_3OH$ at 714cm^{-1}), and in this study (at 630cm^{-1}). The band assignments are as follows for the internal V_1, V_2, V_3 and V_4 PO_4 modes: the band ranging from 980cm^{-1} to 1100cm^{-1} corresponds to the band ranging from 1040cm^{-1} to 1092cm^{-1} observed for calcium hydroxyapatite for the components of triply degenerate V_3 antisymmetric P-O stretching mode; the band at 940cm^{-1} corresponds to the 962cm^{-1} of calcium hydroxyapatite; for V_1, non-degenerate P-O stretching mode; the bands at 520cm^{-1}, 550cm^{-1} and 590cm^{-1} correspond to the 561cm^{-1}, 575cm^{-1} and 601cm^{-1} components of the triply degenerate V_4 O-P-O bending mode; the band at 455cm^{-1} is assigned to the components of the doubly degenerate V_2

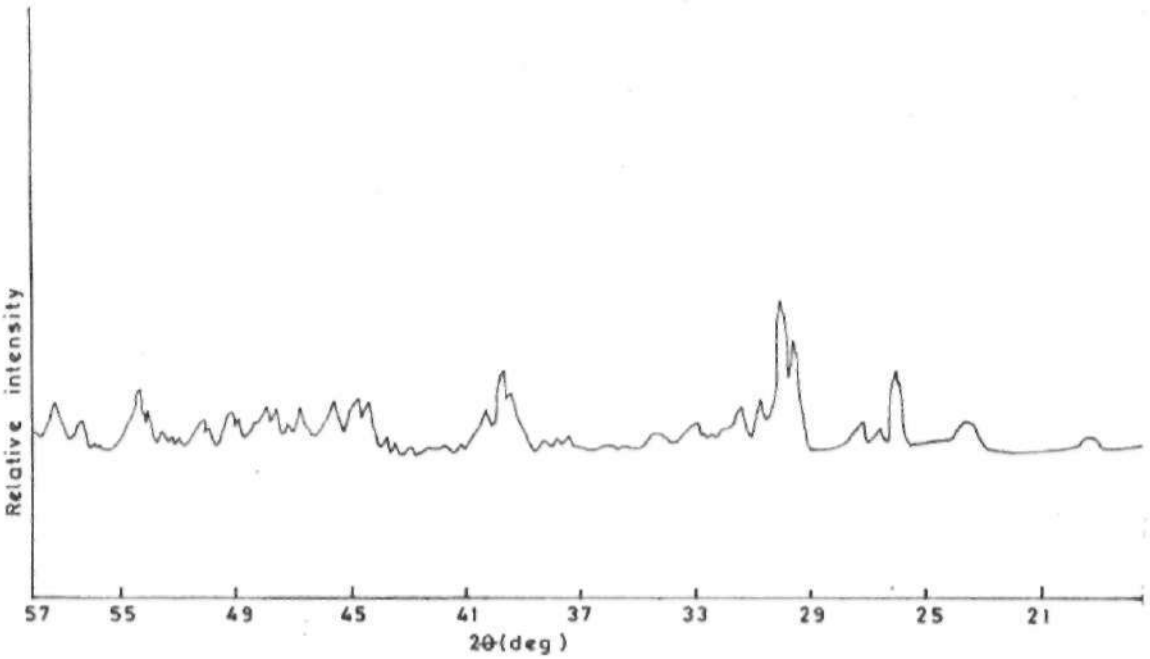


FIG.4.1 : X-RAYDIFFRACTION PATTERN OF THE NEW TIN PHOSPHATE

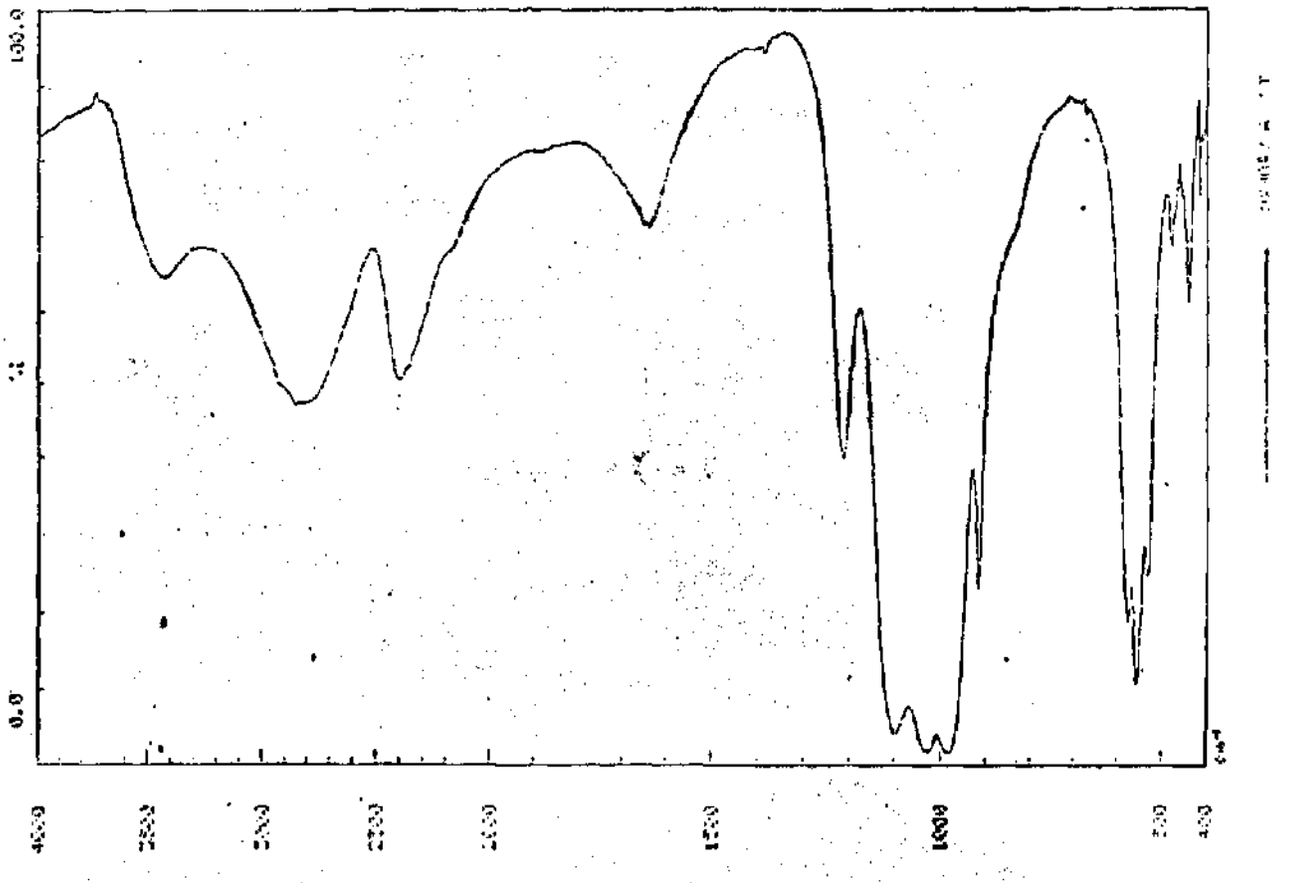


Figure 4.2 Infra-red spectrum of the new tin phosphate

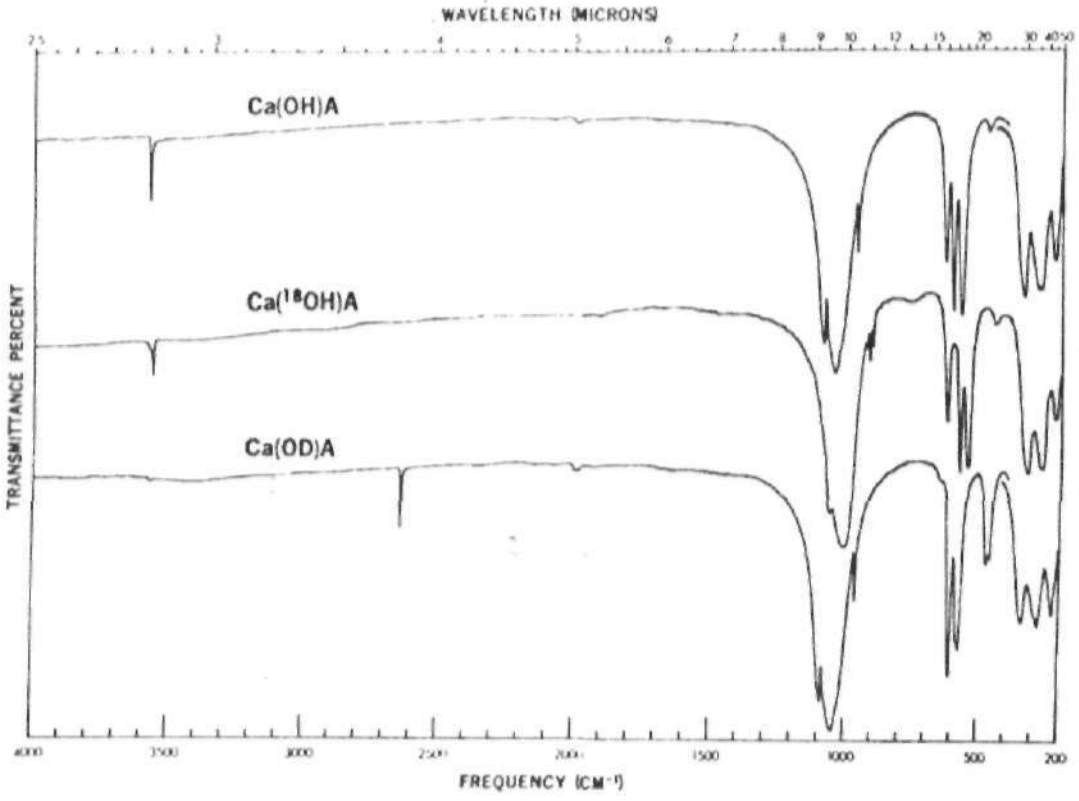


Figure 4.3 Infra-red spectrum of calcium hydroxyapatite

Table 4.1 Ionic radii and Cell parameters for some synthetic hydroxyapatites.

Compound	Ionic radii (Å)	a-axis (Å)	c-axis (Å)	References
$Cd_5(PO_4)_3OH$	0.97	9.335	6.664	Okada and Iwai (1978)
$Ca_5(PO_4)_3OH$	0.99	9.421	6.882	Posner (1969)
$Sr_5(PO_4)_3OH$	1.12	9.765	7.280	Sundarsanam et al (1972)
$Sn_5(PO_4)OH$	1.12	9.884	7.450	This work
$Pb_5(PO_4)_3OH$	1.20	9.890	7.433	Posner (1969)
$Ba_5(PO_4)_3OH$	1.34	10.177	7.731	Fowler (1974)

Table 4.2 Mean wavenumbers for the vibrations of phosphate and hydroxyl groups of "$Sn_5(PO_4)_3OH$" and some synthetic apatites.

Compound	$V_1(PO_4)$	$V_2(PO_4)$	$V_3(PO_4)$	$V_4(PO_4)$	OH	OH
$Ca_5(PO_4)_3OH$	962	473	1057	580	631	3572
$Ca_5(PO_4)_3OH$	950	-	1029	571	714	-
$Sr_5(PO_4)_3OH$	947	457	1045	575	539	3592
$Sn_5(PO_4)_3OH$	940	455	1040	553	630	3540
$Pb_5(PO_4)_3OH^*$	930	-	1030	551	-	3560
$Ba_5(PO_4)_3OH$	933	437	1023	565	430	3606

References Klee and Engel (1970), * Inikori (1992).

of the doubly degenerate V_2 O-P-O bending mode, corresponding to the 473cm^{-1} band in calcium hydroxyapatite. The band 3550cm^{-1} is assigned to the O-H stretching mode for the tin compound.

The results obtained for the new tin phosphate in the x-ray fluorescence analyses (figure 4.3) show that the tin compound has Sn/P molar ratio of 0.92, which is below the expected 1.67 for stoichiometric apatites. In a separate determination for phosphorus on the tin compound by molybdenum blue method (Bassett, 1982), tin in the compound reacted as a reducing agent by leading to the formation of molybdenum blue. This indicates that tin was actually present in the original sample as Sn^{2+}. Various reasons could be attributed to the nonstoichiometry of the compound. The high phosphate concentration could result from adsorption of $H_2PO_4^-$ on the surfaces of the tin hydroxyapatite, or some Sn^{2+} ions could be missing from the crystal lattice, thus creating lattice vacancies and reducing the amount of Sn^{2+} in the crystal.

X-ray diffraction patterns of the products obtained in the preparation of tin calcium hydroxyapatite, in aqueous and solid state reactions were obtained. Figure 4.4 shows the x-ray pattern of the product obtained by precipitation from aqueous system containing 3 atom % tin

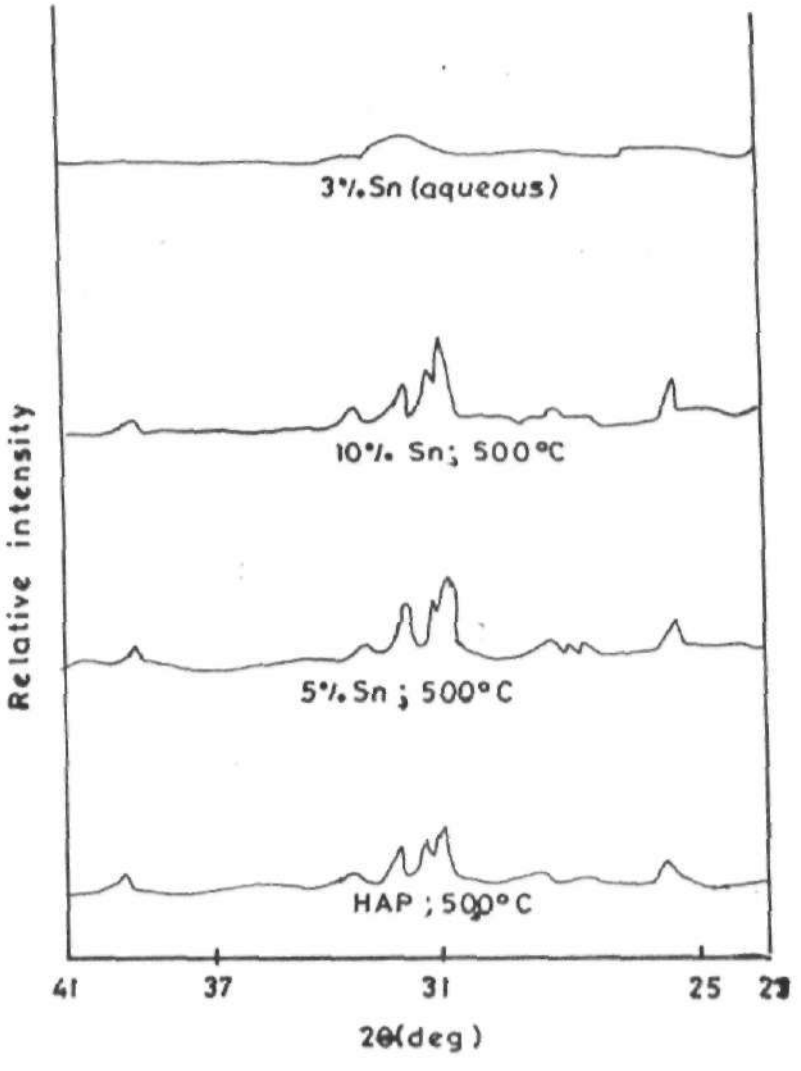


FIG. 4.4 : X-RAY POWDER DIFFRCATION SPECTRA OF THE PRODUCT OBTAINED FROM AN AQUEOUS SOLUTION CONTAINING Sn^{2+} AND Ca^{2+} IN THE RATIO 3:97 AND SOLID SOLUTIONS IN THE RANGE 0–10 ATOM % Sn^{2+} OBTAINED AT 500°C .

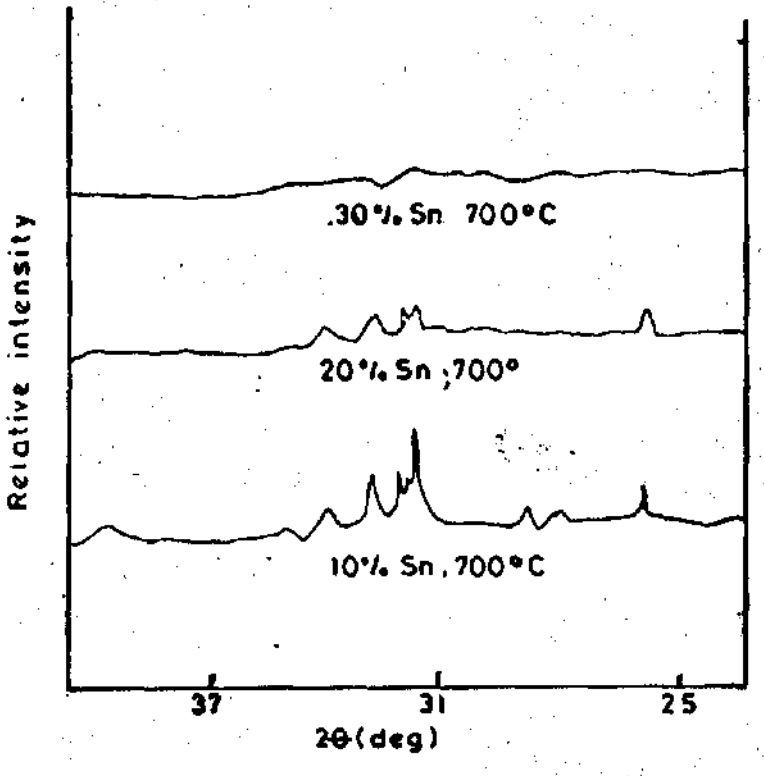


FIG. 4.5 : X-RAY POWDER DIFFRACTION SPECTRA OF SOLID SOLUTIONS IN THE RANGE 0—30 ATOM % Sn^{2+} OBTAINED AT 700°C

in solution together with the patterns of the products of the solid solutions of tin calcium hydroxyapatite in the range 0-10 atom % tin obtained by solid state reaction at 500^{o}C. The pattern of the product from the aqueous system is essentially featureless and characteristic of an amorphous product. This is in agreement with the observation of Legeros et al (1980). At tin concentration significantly greater than 20 atom %, the products of the solid state reaction at both 500^{o}C and 700^{o}C (figure 4.5) were essentially amorphous. This can be seen from figure 4.4 in which the pattern of the product with 30 atom % tin shows no significant peak. The products of the reaction at 500^{o}C and 700^{o} were quite similar, except for a slight increase in crystallinity of the solid solutions (0-10 atom % Sn) at 700^{o}C, as can be seen from a slight sharpening of the peaks for the solid solutions with 10 atom % Sn in figure 4.5. The increase in crystallinity is as would be expected. The structural modifications of hydroxyapatite induced by lead which is directly above tin in the periodic table have also been characterized (Bigi et al, 1991). Lead substitution for Ca^{2+} in HAP structures causes an expansion of the lattice parameters, consistent with the difference in ionic radius. Substitution of Sn^{2+} also shows an expansion of the lattice parameters for the precipitates (in which 0-10% atom tin was used), and this appears to be as a

result of the incorporation of tin in HAP as depicted by the reduced peak intensities of the x-ray patterns (figure 4.4 and 4.5). However, chemical analysis of these products showed that not all the Sn^{2+} in the solid mixtures actually substituted for Ca^{2+} in HAP. For Pb^{2+} the variation of the C parameter with composition does not follow the Vegard's law while the a-axis varies linearly with lead concentration (Bigi et al, 1991). The variations of the cell parameters of the solid solution follow the same laws whether the samples are obtained from aqueous media or by solid-state reaction for the replacement of lead for calcium, but cannot be said to be true for tin substitution of Ca^{2+} in HAP.

CHAPTER FIVE

5.0 Summary and Conclusion

5.1 Summary

The precipitation of calcium phosphates from aqueous solution was studied. The major events comprising the formation of different phases of calcium phosphate solids were monitored in buffered solutions. These events include (a) initial deposition of amorphous calcium phosphate, ACP, (b) its subsequent transformation into small crystals of apatite, and (c) the ultimate growth or ripening of these crystals. The physicochemical mechanisms which govern this precipitate phase transformation process are such that once initiated it would normally proceed to completion (a process known as autocatalysis) (Boskey and Posner, 1973). Therefore, ACP would be expected to have only a finite suspension lifetime, the extent of which was found to be dependent upon experimental conditions used.

In this study a preliminary experiment involving the preparation of HAP using three different sets of starting materials was carried out. It was found that the stoichiometry and crystallinity of HAP crystals obtained were dependent upon the starting materials used. Transformation of ACP to HAP was carried out under different experimental conditions, with the aim of

determining how these conditions would influence nucleation of HAP crystals, extent of conversion and the resultant mean sizes of the HAP crystals. Experiments were also carried out in presence of certain substances thought to be inhibitors of the ACP-HAP transformation. The products of the transformation were examined by x-ray powder diffractometry. Results showed that inhibitors which had been grouped into type I and type II (Williams and Sallis, 1982), inhibited this process to various extents depending on their binding power and experimental conditions such as pH and temperature. Type I inhibitors are stronger binding agents than type II, so ACP was stabilized throughout the period the experiments were carried out. With type II inhibitors, conversion of ACP to HAP started after some time, giving crystals of different sizes for different inhibitors. Adenosine phosphates (type II inhibitors), inhibited ACP-HAP transformation, the extent of which was dependent on the number of phosphate groups attached to the adenosine moiety. Casein, L-glutamate and tetracycline (all classified as type II inhibitors from results obtained in this work), did not inhibit ACP-HAP transformation at low inhibitor concentrations, but gave crystals with relatively small mean sizes.

Transformation of ACP into HAP was also carried out in presence of some metal ions, all of which may be

classified as type II inhibitors. Mg^{2+}, Zn^{2+} and Ba^{2+} delayed nucleation of apatite crystals, but did not reduce the mean size of the resultant crystals. Pb^{2+} delayed nucleation but increased the mean size of the crystals, while Cd^{2+} and Sr^{2+} reduced the mean size of the crystals. F ion (which may also be classified as type II inhibitor), was found to inhibit ACP-HAP transformation by reducing the growth rate of HAP crystals and delaying nucleation.

In another survey of effects of cations on calcium hydroxyapatite in aqueous medium, Sn^{2+} and Ca^{2+} in a mole ratio of 3:92 were allowed to react at about 100°C. Amorphous precipitate was obtained in agreement with results obtained by Legeros et al (1980). An attempt was made to prepare tin hydroxyapatite, since lead which is just below tin in the periodic table forms lead hydroxyapatite. (Thomas, 1988 and Bigi et al, 1991). The tin compound formed was examined using x-ray diffraction analysis and x-ray fluorescence. Results showed that the compound has strong similarities with hydroxyapatite.

5.2 Conclusion

I. The stoichiometry and crystallinity of HAP crystals are dependent upon the starting materials for its preparation.

II. The effect an inhibitor would have on the resultant

apatite crystals is dependent on the mechanism of inhibition and not necessarily on whether it is a type I or type II inhibitor. Furthermore, the nucleation time of HAP crystals in presence of type II inhibitors is dependent on pH and temperature of the reaction media. Type I inhibitors stabilize ACP even at high temperature.

III. Tetracycline may be regarded as a type II inhibitor, which if present in calcifying solution will result in the formation of HAP crystals with small mean sizes. Tetracycline obviously does not enter into the HAP lattice, but is adsorbed on the surface of the HAP crystal.

IV. Foreign metal ions (Divalent) delay the nucleation of HAP and also affect the mean sizes of the resultant crystals. They may be classified as type II inhibitors. The effects of these ions did not show any trend in terms of the ionic radii of the metal ions used.

V. The tin phosphate is not isomorphous with calcium hydroxyapatite, this compound is either a new type of tin phosphate or a very defective tin hydroxyapatite. The oxidation state of tin in the tin compound is +2.

REFERENCES FOR PART I

Alexander, E. Leroy (1969), "X-ray Diffraction methods in Polymer Science". Wiley-Interscience John Weiley and Sons Inc., N.Y. and London. pp. 120.

Bachra, B.N., Trautz, O.K. and Simon, S.L. (1965), "Precipitation of calcium carbonates and phosphates III. The effect of magnesium and fluoride ions on the spontaneous precipitation of calcium carbonates and phosphates". Arch. Oval. Biol. 10, 731-738.

Bachra, B.N. and Fischer (1969), "The effect of some inhibitors on the nucleation and crystal growth of Apatite". Calcif. tissue Res. 3, 348.

Bienstock, A. and Posner, A.S. (1968) "Calculation of the x-ray intensities from arrays of small crystallites of hydroxyapatite". Arch. Biochem. Biophys. 124, 604.

Bigi A., Foresti, E., Marchetti, F., Ripamonti, A. and Roveri, N. (1984). "Barium calcium hydroxyapatite solid solutions". J. Chem. Soc. (Dalton Trans.) 1091-1093.

Bigi, A., Gazzano, M., Ripamonti, A., Foresti, E., and Roveri, N. (1986). "Thermal stability of cadmium calcium hydroxyapatite solid solutions". J. Chem. Soc. (Dalton Trans.) 241 - 244.

Bigi, A., Gandolfi, M., Gazzano, M., Ripamoti A., Roveri, N., Thomas, S.A. (1991). "Structural modifications of hydroxyapatite induced by lead substitution for calcium". J. Chem. Soc. (Dalton Trans.) 2883-2886.

Boskey, A.L., Posner, A.S. (1973). "Conversion of amorphous calcium phosphate to microcrystalline hydroxyapatite. A pH dependent, solution-mediated, soild-solid conversion". J. Phys. Chem. 77, 2313-2317.

Boskey, A.L, Posner, A.S. (1976), "Formation of hydroxyapatite at low supersaturation". J. Phys. Chem. 80, 40-45.

Brown, W.E., Lehr, J.R., Smith, J.P, Frazier, A.W. (1957). "Crystallography of Octacalcium phosphate". J. Amer. Chem. Soc. 79, 5318.

Brown W.E., Smith, J.P., Lehr, J.R. Frazier, A.W. (1962), "Octacalcium phosphate and hydroxyapatite". Nature 196, 1043.

Brown, W.E. (1966) "Crystal growth of bone mineral" Clin. Orthop. 44, 205-220.

Blumethal, N.C., Posner, A.S, Silverman, L.D. and Rosenberg, L.C. (1979). "Effect of proteoglycans on in vitro hydroxyapatite formation". Calcif. Tissue Int. 27, 75.

Chiranjeevirao, S.V., Hemmorce, J., Voegel, J.C. and Frank, R.M. (1982). "A method of preparation and characterization of Mg apatite". Inorganica Chimica Acta 67, 183-187.

Cifuentes, I., Gonzalez-Diaz, P.F., and Cifuentes-Delatte, L. (1980). "Is there a citrate apatite in biological; and calcified systems?" Calcif Tissue Int. 31(2), 147-151.

Collins, R.L. (1959), "Strontium-calcium hydroxyapatite solid solutions precipitated from basic aqueous solutions". J. Amer. Chem. Soc. 81, 5275-5278.

Cotton, F.A. and Wilkinson, G. (1972). Advanced inorganic chemistry 3rd Ed. Inter science pp. 495-687

Dent Glasser S. Lesley (1979). Crystallography and its Applications. ELBS Edition. pp 45-148

Donaldson, J.D. and Moser, W. (161). "Preparation of basic tin (II) nitrate". J. Chem. Soc. 1996-199.

Dunning, W.J. (1973): "Ripening and ageing processes in precipitates". In particle growth in suspensions. Society of chemical industry monograph No. 38. Academic press. London and New York. pp 3-28.

Eanes, E.D., Gillessen, I.H., Posner A.s. (1965). "Intermediate states in the precipitation of hydroxyapatite". Nature 208, 365-367.

Eanes, E.D. and Posner, A.S (1965). "Kinetics and mechanism of conversion of noncrystalline calcium phosphate to crystalline hydroxyapatite". Trans. N.Y. Acad. Sc. 28, 233-241.

Eanes, E.D. and Meyer, J.L. (1977). "The maturation of crystalline calcium phosphate in aqueous suspensions at physiological pH." Calcif. Tiss. Res. 24, 259-269.

Feenstra, T.P. and de Bruyn, P.L. (1979). "Formation of calcium phosphates in moderately supersaturated solutions". J. Phys. Chem. 83, 475.

Flueisch, H. and Bisaz, S. (1962). "Isolation from urine of pyrophosphate, a calcification inhibitor". Amer. J. Physiol. 203, 671.

Fowler, B.O. (1974). "Infra-red studies of Apatite II: Preparation of normal and isotopically substituted calcium strontium and barium hydroxyapatite and spectra structure - *composition correlation*". Inorg. Chem. 13(1), 207.

Harrison, L.G. (1969). "Comprehensive chemical kinetics". Vol. 2, C.H. Banford Ed., Elsevier, Amsterdam, 1969. pp. 377-380.

Inikori, G.O. (1992), "Synthesis and Isomerphous substitution reactions of some hydroxyapatite". PhD Thesis submitted to Ahmadu Bello University, Zaria.

Inikori, G.O., Ayoko, G.A. and Thomas, S.A. (1989). "Solid solutions of Ca-Mg hydroxyapatite". A research paper presented at the 30th annual conference of the Science Association of Nigeria, Nsukka.

Irving, J.I. (1973). "Calcium and phosphorus metabolism. Academic press Inc. N.Y. and London pp 72-78.

Klee, W.E; and Englel, G. (1970). "Infra-red spectra of the phosphate ions in various apatites. J. Inorg. Chem. 32, 1877-1843.

Koutsoukos, P., Amjad, Z., Tomson, M.B. and Nancollas, G.H. (1980). "Crystallization of calcium phosphates. A constant composition study". J. Amer. Chem. Soc. 105, 1554.

Koutsoukos, P.G., Nancollas, G.H. (1981) "Influence of strontium ion on the crystillization of HAP from aqueous solution". J. Phys. Chem. 85, 2403-2408.

Legeros, Z.R., Trautz, R.O., Legeros, P.J. and Klein, e. (1967). "Apatite crystallites. Effect of carbonate on morphology". Science 155, 1409.

Legeros, Z.R., Taheri, M.H., Quirolgico, G.B., and Legeros, J.P. (1980), "Formation and stability of Apatites: Effect of some cationic substituents". In Proc. 2nd international congress on phosphorus compounds, Boston, IMPHOS (Paris). pp. 89-103.

Lundager-Madsen, H.E. (1970). "Nucleation of calcium phosphates: Kinetics of nucleation of tetracalcium monohydrogen phosphate in crystals of calcium monohydrogen dihydrate". Acta. Chemica Scand. 24, 1677-1686.

Laundager-Madsen, H.E., Lopez-Valero, I., Lopez-Acevedo, V., Boistelle, R. (1986), "The formation product of amorphous tricalcium phosphate at 37°C". J. Cryst. Growth 75, 429.

Marshall, W.R. and Nancollas, G.H. (1969). "The kinetics of crystal growth of dicalcium phosphate dihydrate". J. Phys. Chem. 73, 3838.

Meyer, J.L., and Eanes, E.D. (1978). "A thermodynamic analysis of the secondary transition stage in the spontaneous precipitation of calcium phosphate". Calcif. Tissue Res. 25, 209.

Meyer, J.L. and Eanes E.D. (1978) "A Thermodynamic analysis of the precipitate of ACP and its transformation to crystalline apatite". Calcif. Tissue Res. 25, 59.

Meyer, J.L. and Nancollas, G.H. (1973). "The Influence of multidentate organic phosphates on crystal growth of hydroxyapatite" Calcif Tissue Res. 13, 295.

Meyer, J.L. and Selinger, A.H. (1980) "Effect of citrate on calcium phosphate phase transitions" Miner. Electrolyte Metab. 3 (4), 207-216.

Nancollas, G.H. (1982). "Phase transformation during precipitation of calcium salts". Biological *mineralisation and demineralisatio. Dahlem Konferenze* Springer Berlin, pp 79-99.

Nancollas, G.H. and Tomazic, B. (1974). "Growth of calcium phosphate on hydroxyapatite crystals. Effect of supersaturation and ionic medium". J. Phys. Chem. 78, 2218.

Nielsen and J. Christoffersen (1982). "The mechanism of crystal growth and dissolution". Biological mineralisation and demineralisation. Springer, Berlin, pp. 37-77.

Posner, A.S. (1969). "Crystal chemistry of bone mineral". Physio. Rev. 49, 760.

Quinlan, K.P. and Desesa, M.A. (1955). "Spectrophotometric determination of phosphorus". Anal. Chem. 27, 1626.

Robertson W.G. and Fleisch, H. (1970). "The effect of imidodiphosphate (P-N-P) on the precipitation and dissolution of calcium phosphate in vitro". Biochm. Biophys. Acta, 222, 677.

Smith M.R. and Alberty, A.R. (1956). "The apparent stability constants of ionic complexes of various adenosine phosphates with monovalent cations." J. Phys. Chem., 60, 180.

Termine, J.D. and Posner, A.S. (1970). "Calcium phosphate formation in vitro: Factors affecting initial phase separation". Arch. of Biochem. Biophys. 140, 307.

Termine, J.D. Peckauskas, R.A. and Posner, A.S. (1970b) "Calcium phosphate formation in vitro II. Effect of environment on amorphous - crystalline transformation." Arch. Biochm. Biophys. 140, 318.

Termine, J.D., Eanes, E.D. and Conn, K.M. (1980). "Phosphoprotein modulation of apatite crystallization". Calcif. Tissue Int. 31, 247.

Termine, J.D. and Conn, K.M. (1976), "Inhibition of apatite formation by phosphorylated metabolites and macromolecules". Calcif Tissue Res. 22, 149.

Thomas, S.A. (1988). "Studies on some calcium phosphate systems". A report submitted to the third world academy of science, Trieste Italy.

Thomas, S.A. (1989). "On the determination of the degree of conversion of amorphous calcium phosphate to crystalline calcium hydroxyapatite". Nig. J. Chem. Soc. 14, 37.

Tomson, M.B. and Nancollas, G.H. (1978). "Mineralisation kinetics: A constant composition Approach". Science, 200, 1059.

Tung, M.S. and Brown, W.E. (1983). "An Intermediate State in hydrolysis of amorphous calcium phosphate". Calcif. Tissue Int. 35, 783.

Walton, A.G. Bodin, W.J., Furedi, H. and Schwartz, A. (1967). "Nucleation of calcium phosphate from solution." Canad. J. Chem. 45, 2695.

Walton, A.G. (1965). "Nucleation of crystals from solution: mechanisms of precipitation are fundamental to analytical and physiological processes", Science, 148, 601.

Williams, G. and Sallis, J.D. (1979). "Structure activity relationship of inhibitors of hydroxyapatite formation", Biochem. J. 184, 181.

Williams, G. and Sallis, J.D. (1982). "Structural factors influencing the abilityof compounds to inhibit hydroxyapatite formation". Calcif. Tissue Int. 34, 169.

PART TWO

CONFORMATIONS OF SOME RING COMPOUNDS

CHAPTER ONE

1.0 INTRODUCTION

The configuration and conformation of a natural or synthetic product are often determined by conducting X-ray crystal structure studies on the compound. These have been instrumental in defining the composition and constitution of many compounds (Duax et al, 1976). Full X-ray crystal structure studies provide the most precise and accurate details concerning molecular conformation, the most favoured orientation of side chains and the nature of the primary intermolecular interactions that a specific compound has with its environment. These structure determinations provide a wealth of raw data concerning molecular conformation and intermolecular interactions that is ideally suited to analysis of structure - function relationships.

The functions and activities of Compounds are determined by their composition, constitution, configuration and conformation (Duax et al, 1976). Composition defines the number and kinds of atoms that make up the molecule. This is readily represented by its chemical formula. Constitution refers to the connectivity of the molecule and is best illustrated diagrammatically showing which atoms are bonded to one another. Molecular configuration defines the chirality

of all the asymmetric centres in the molecule. Conformation refers to the total geometric distribution or disposition of the atoms in three dimensions. The non-identical arrangement of the atoms in a molecule obtainable by rotation about one or more single bonds result in differences in conformation (Eliel et al, 1967). Only rotation about bonds between atoms carrying at least one other substituent can lead to differences in conformation. When there are more than two substituted atoms which can rotate with respect to each other (like the methyl) group in propane, (CH_3 - CH_2 - CH_3), differences in conformation will result from rotation about any or all of the salient bonds. Rotation about a single bond is in most instances, not free and some conformations are more stable than others (Eliel et al, 1967). The different conformations of a molecule are stereoisomeric, since they differ in spatial arrangement, but not in the number, kind of atoms and the way in which these atoms are linked.

1.1 SIGNIFICANCE AND OBJECTIVE

The significance of a study such as this lies mainly in the elucidation of structure-function relationships and giving suitable reasons for such phenomenon. For example, the way in which a steroid acts in a normal, carcinogenic, or a carcinostatic process is a function of its total structure (Duax et al, 1976). Similarly the

function of different sequiterpenes, nucleosides and nucleotides, in different environments is also a function of the structures of these compounds. The more detailed knowledge obtained about the structures of individual compounds, the easier it will be to correlate specific structural features of that compound with the various functions. Minor changes in the basic makeup of the compound totally alter their conformation and biological functions.

In this part, a quantitative evaluation of the conformation of some ring compounds is carried out interms of some geometric and conformational parameters, which measure the degree of departure from ideal symmetry. The aim is to, as far as possible, elucidate features which determine the conformations of some rings found in some natural products.

CHAPTER TWO

2.0 LITERATURE REVIEW

2.1 X-RAY DIFFRACTION METHOD OF DETERMINING TOTAL STRUCTURE:

Conformational analysis may be described as the interpretation of the reactions and properties of compounds in terms of their conformations (Eliel et al, 1967). These conformational arrangements are almost in variably determined by physical methods. The most important of these total methods is X-ray crystallography, which in principle will give the total structure of any compound which can be obtained in crystalline form.

An X-ray structure determination involves two main steps (Stewart and Hall, 1971). The first is the measurement of diffraction intensities. The Unit cell parameters and space group for the crystal are initially determined by photographic techniques and a more accurate set is subsequently measured with a diffractometer. For a moderately complex organic molecular crystal (30 - 50 non hydrogen atoms in the asymmetric unit of the cell) approximately 2000 - 4000 reflections are needed for a reliable structure study. The more accurate and precise the data, the easier it is to solve the structure, as well as determine the fine details of the molecular and crystal structure of the compound. However, to determine

the gross molecular structure of an organic molecule with one or two heavy atoms (e.g. chlorine), the demand for accurate data is small. The advent of the use of diffractometers has greatly increased the accuracy with which diffracted intensities can be measured.

The second and most critical stage in X-ray structure analysis is a solution to the phase problem. Radiation being scattered from different centres will be more or less out of phase, leading to interference pattern. A variety of techniques for determining phases have been developed and refined (stewart and Hall, 1971). One end result of this method is a well determined stereochemical structure of the molecular crystal. The X-ray diffraction techniques has been of tremendous value in establishing the complete structures of natural products when carried sufficiently far the X-ray method can yield very accurate bond lengths and angles (Eliel et al, 1967).

Other methods used in structure determination include, nuclear magnetic resonance, infrared spectroscopy, dipole moments and kinetic methods. These methods are less reliable compared to diffraction methods.

2.2 THE TORSION ANGLE CONCEPT

Torsion angle or dihedral angle is commonly used to denote the angle which characterizes the steric

relationship between two vicinal bonds in a molecule. The torsion angle concept was introduced to organic chemistry to supply a precise description of steric relationships across single bonds and to provide particularly convenient tool for defining ring geometry. The application of this concept to conformational analysis has led to the formulation of several rules concerning:

a) ring conformations and deformations and their effect upon interactions and

b) geometry at a ring junction and transmission of deformations (Bucourt, 1974). These rules make it convenient to study the stereochemistry of cyclic and polycyclic molecules, since all the conformations a molecule might adopt can be determined in a logical way and easily transcribed onto paper. A description of torsion angle is given in appendix IV.

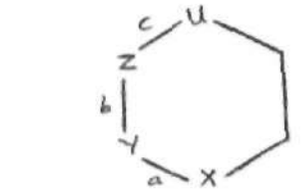
2.2.1 Description of Ring Geometry

The torsion angles of a cycle are those described by each group of three consecutive bonds forming the cycle, as shown by the bonds a, b, and c in the cyclohexane molecule of figure 2.1a. To assign a torsion angle the three successive bonds, a, b, and c or the four connected atoms can be named as Φa, b, c or Φx, y, z, u. Sometimes, only the position of the central bond need to be

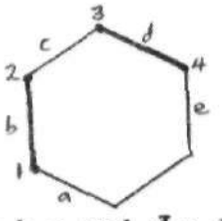
indicated, that is Φb or Φy, z. This means Φb is the torsion angle related to the bond b

The relative positions of the central bonds of two torsion angles are denoted by two numbers. For example, the torsion angles Φb and Φd of figure 2.1(b), are in the 1, 3 position, the direction of numbering being chosen so as to minimize the value of the second number. The exact description of the geometry of a ring is given by the sequence of the algebraic values of its torsion angles. The values are written along each central bond. The information contained in such a sequence is both qualitative and quantitative. The simple sequence of signs of the torsion angles indicates the type of conformation and the absolute values of the torsion angles allow the deformation with respect to a reference conformation to be estimated (Bucourt, 1976). For example the sum of the absolute values of the torsion angles of a ring is taken as a relative measure of the puckering or flattening of a deformed conformation. The greater the sum the greater the puckering, and conversely, the smaller the sum the greater the flattening (Bucourt, 1974). Such a sum may also be calculated for just part of a ring.

Figure 2.2(a) shows a system of four consecutive bonds which forms part of a ring. Suppose the shape of the ring in the region Ai and the orientation of a



Φa,b,c; Φx,y,z,u
or Φb; Φy,z
(a)



Φa,b,c and Φc,d,e
or Φb and Φd are
in 1,3 position
(b)

Figure 2.1 Designation of torsion angles.

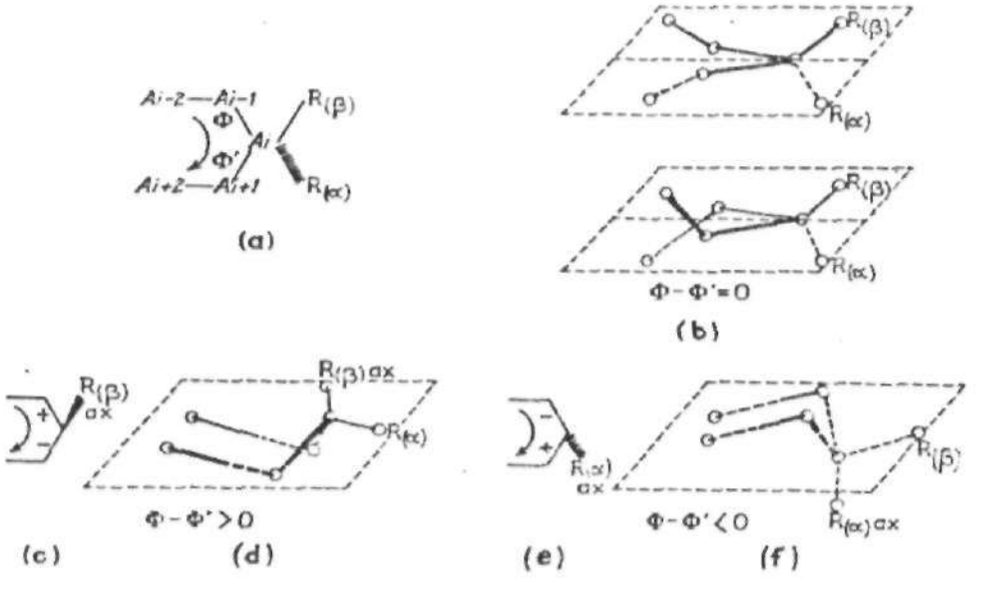


Figure 2.2 Geometry as a function of successive torsion

possible axial substituent on Ai are to be determined. Assume that Ai is a tetragonal atom bearing two substituents. Following the sequence of the torsion angles of the ring in a clockwise direction, the algebraic value of Φ' which precede and follow Ai can give the relative position of Ai relative to other atoms in the ring. When $\Phi - \Phi' = 0$ (or 0), the ring atom Ai lies in the mean plane (that is the least square planes through the five ring atoms (x, y, z, u of figure 2.1) and its two substituents are symmetrically positioned above and below this plane. They are called isoclinal, figure 2.2(b) when $\Phi - \Phi' = 0$, Ai is out of the mean plane defined by the five ring atoms. If the difference is positive, Ai lies above the mean plane and its axial substituent is ß-oriented (above the ring Figure 2.2(c)). If the difference is negative, Ai lies below the mean plane and its axial substituent is said to be α-oriented (below the ring Figure 2.2(d)).

The magnitude of the difference is also of importance since the greater the difference, the greater the distance of Ai from the mean plane and the more axial the substituent, that is the more puckered is this region of the ring. The inspection of the sequence of signs therefore can yield useful information for example, the ideal chair form of cyclohexane is characterized by an arrangement of opposite signs.

The sequence +,- indicates that the ring atom and its axial substituent are pointing upwards, conversely the inverse sequence -, + corresponds to a ring atom and its substituent pointing downwards.

2.2.2 Steric Relationships at a Ring Junction

Steric relationships at a ring junction is of prime importance in the phenomenon of conformational transmission. Fusion between two rings in a polymeric molecule represents where the deformation of one ring can be transmitted to the other.

When two rings are fused in a trans manner the "torsion angles of junction" Φ and Φ' are of opposite signs, figure 2.3. A torsion angle of junction is the torsion angle of each ring which has the common bond as its central bond (Bucourt,1974). The signs are determined by the α- or ß-orientations of the angular substituents R and R', and are consistent with the fact that, in the case of a trans fusion the angular substituents are always axially orientated to both rings. It can be seen from figure 2.3 that the signs of the torsion angles of a junction are related to the orientations of the axial substituents.

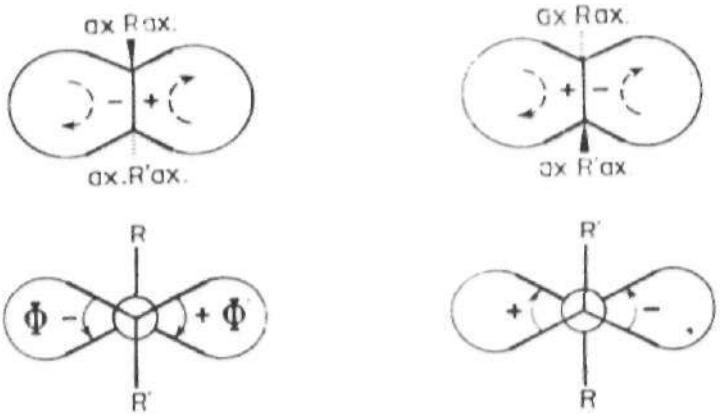


Figure 2.3 Rules of conformational transmission at a trans juction

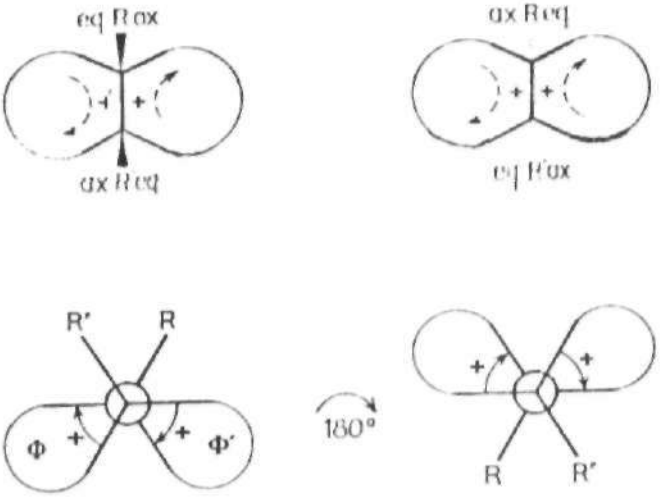


Figure 2.4 Rules of conformational transmission at a Cis junction

A ring deformation which causes an opening of one of the junction torsion angles Φ, will induce a closing of the junction torsion angle, Φ' of the other ring. Conversely a closing of one torsion junction will induce an opening of the torsion at the angle of the junction in the other ring. At trans junction, the deformation is transmitted in the opposite direction to the one by which it is induced (Bucourt, 1974), and the magnitude of the transmitted deformation should be the same as the inducing one.

In cis fusion both torsion angles of junction are usually positive, (figure 2.4), when one torsion angle is closed the torsion angle of junction in the other ring is also closed (and conversely, an opening will give rise to an opening in the other ring). However, at the site of the cis fusion, the signs of the torsion angles can be simultaneously inverted. Contrary to the situation in the trans fusion, the signs of the torsion angles of junction in cis fusion are not fixed (they can both be + or both -). For this reason cis fused junction is flexible while a trans fused junction is rigid.

The signs of the torsion angles of the junction in cis fusion are not related to the α or ß orientations of the angular substituents as in trans fusion. However, the axiality of substituents is always related to the signs of the torsion angles of junction, since each

angular substituent is axial to one ring and equatorial to the other according to the signs of the torsion angle of junction. The values of the two torsion angles of junction at a cis fusion should be the same and the transmitted deformations should also be identical (Bucourt, 1974).

2.2.3 Quantitative Analysis of Ring Conformation

The endocyclic torsion angles redundantly define the conformation in case of five and six - membered rings (Duax et al, 1976). If all bond lengths and angles are held constant, and closure is required, two endocyclic torsion angles having only one common bond will fully define the conformation of a six-membered ring. It has been generally recognised that the symmetry of a ring provides a qualitative means of defining the ring's conformation. The most widely used quantitative descriptors of ring conformation other than torsion angles are pseudorotation parameters (Δ and ϕ) defined by Altona et al (1968). A quantitative evaluation of the conformations of rings of any size from which comparative analysis can be easily made is obtainable from a mathematical combination of torsion angles. This analysis is based upon consideration of approximate symmetry possessed by rings.

2.2.4 Symmetry in Rings

The two types of symmetry considered in order to define ring conformation are mirror planes perpendicular to the dominant ring plane and twofold axes lying in the ring plane. Either of these symmetry elements may be present at any of the three kinds of locations described in figure 2.5. The location of the symmetry in a ring depends on the number of atoms comprising that ring. If there is an odd number of atoms in the ring, all symmetry elements pass through one ring atom and bisect the opposite bond (figure 2.5 a and d). In rings containing an even number of atoms, symmetry elements may pass through two atoms located directly across the ring from each other (figure 2.5 b and e) or bisect two opposite ring bonds (figure 2.5 c and f).

2.3 Asymmetry Parameters

Asymmetry parameters define precisely the confomation of any ring relative to ideal conformations (chair, boat, envelope and so on), and relative to any other ring of similar composition (Duax et al, 1976).

The asymmetry parameters of non-ideal systems measure the degree of departure from ideal symmetry at any of the possible symmetry locations. Related torsion angles are compared in a way that will result in a value of zero if the symmetry in question is present. Mirror related torsion angles are inversely related (same

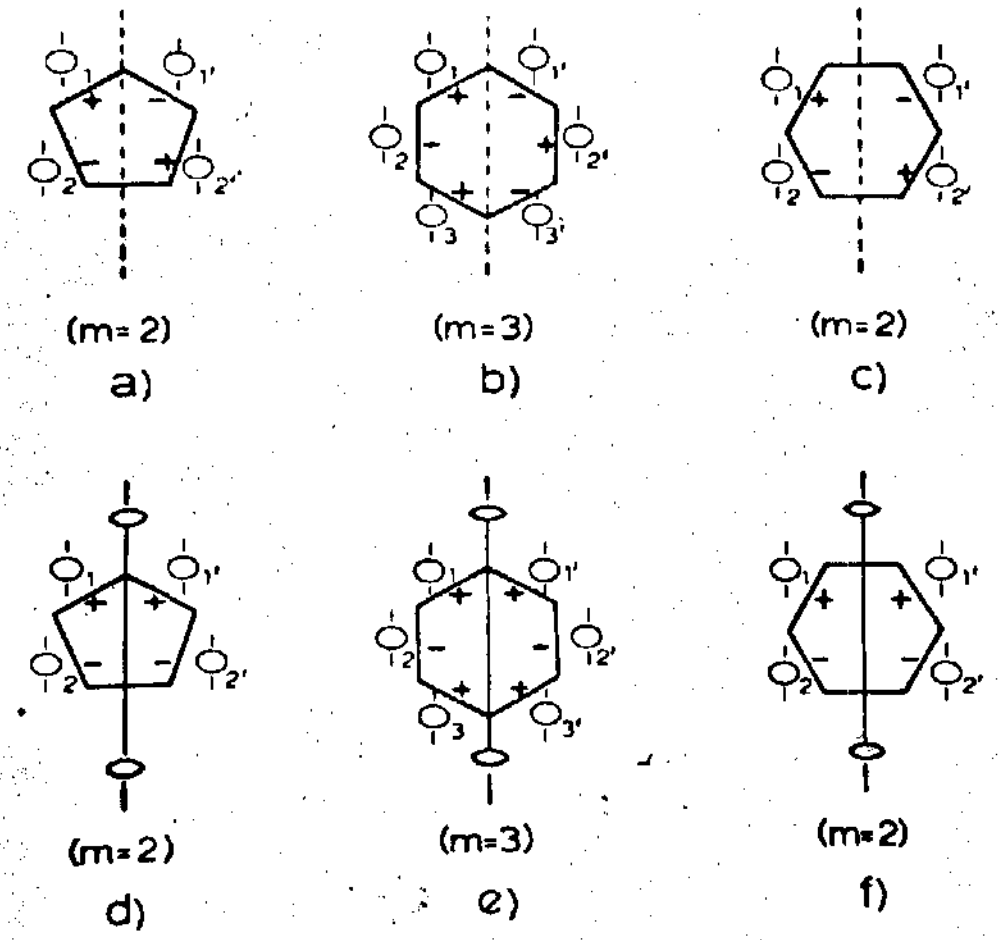


Figure 2.5 Symmetry in five and six-membered rings

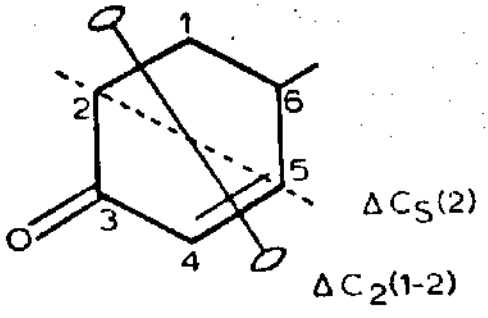


Figure 2.6 The nomenclature defining the location of an asymmetry parameter.

magnitude, opposite sign), and such torsion angles are compared by addition. The two fold related torsion angles are directly related (same magnitude and sign), and are compared by subtraction. The root-mean-square synthesis of these individual discrepancies then yields a measure of the ring's deviation from ideal symmetry at the symmetry location in question. The equations are given in section 3.2.

It is also necessary to define which of the possible locations the asymmetry parameter is describing. Therefore an atom or bond label must be included with the asymmetry parameter that uniquely fixes the location of the parameter in the ring. The atom label for the lower numbered atom present in the symmetry location or the two-atom label of the bisected bond containing the lowest numbered atom will generally be sufficient to locate the position of the asymmetry parameter uniquely. This is shown in figure 2.6. The asymmetry parameters of saturated six-membered rings are useful for detecting the nature of distortions brought about by ring junction and substituent strains.

2.4 CONFORMATIONAL SPECIFICATION

2.4.1 Small Rings

Cyclopropane is a planar molecule and it appears to present no conformational problems (Eliel et al, 1967).

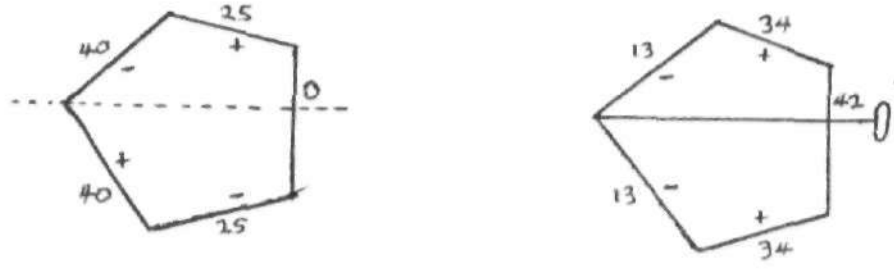
Planar cychobutane rings in the solid state have

been found in a number of simple derivatives in which cychobutane ring is neither conjugated nor fused to another ring (Margulis and Adman, 1968). All of these molecules are centrosymmetric and crystallize in the space group $P2_1/c$ with the molecular centre of symmetry coinciding with the crystallographic centre of symmetry. There has been only slight evidence of the existence of planar rings in gas phase or in solutions puckered rings are also known in the solid state. In the puckered conformation, positions analogous to the equatorial and axial positions of cyclohexane occur, whereas in the planar conformation all positions are equivalent (Margulis and Adman, 1968). The puckered form of cychobutane have been found experimentally to be more stable than the planar one by 1.28kcal/mole (Bucourt, 1970).

The most important ring system smaller than cyclohexane, from the conformational point of view, is cyclopentane. Cyclopentane is a puckered flexible ring characterised by pseudorotation. (Pitzer and Donath, 1959). The puckering rotates around the ring without any significant energy barrier, thus giving rise to an infinity of conformations which differ only in bond and torsion angles. The presence of one or more substituents will in general change the delicate equilibrium between torsional and bond bending energies and introduce steric

factors as well as giving rise to a potential energy barrier opposing pseudorotation (Pitzer and Donath, 1959). Therefore, the importance of a substituent is its power to restrict the flexibility of the ring to a more narrow range depending on the shape and depth of the energy well.

Attention has been focused exclusively on two specific conformations of the cyclopentane ring, they are, the C_s or envelope form with mirror symmetry and the C_2 or half-chair form with a two-fold rotation axis (figure 2.7). These two typical symmetric forms are only two particular points along the essentially strain-free pseudorotation circuit, and there is evidence that certain substituted cyclopentanes exist preferentially with a geometry close to one or the other of these forms.



Envelope (C_s) Half chair (C_2)

Figure 2.7 Torsion angles in Cyclopentane

A method developed by pitzer and Donath (1959), characterizes all these different conformations in terms of common properties. It describes more vigorously the conformation actually encountered in terms of two parameters: the maximum attainable torsion angle. during pseudorotation and a specific phase angle Δ, which locates the exact point on the pseudorotation pathway. If the phase angle Δ is set to zero at the half chair form, then the following equation:

$$\Phi_j \cdot \Phi_{max} \text{ Cos } (\frac{\Delta}{2} + j\delta) \text{ where } j = 0, 1, 2, 3, 4$$
$$\text{and } \delta = 144^{\circ}$$

gives the simultaneous variations of the torsion angles Φ_o, Φ_1, Φ_2, Φ_3 and Φ_4 of the cyclopentane. A variation of Δ from 0 to 720° gives a description of the entire pseudorotation circuit. (Values of Δ varying from 360 to 720° will yield the mirror images of the conformations already encountered from 0 to 360°). (Bucourt, 1974). Duax et al (1976), proposed a two - parameter definition for the conformation of a ring of any size. A quantitative evaluation of the conformations of rings of any size from which comparative analysis can easily be made can be obtained from a mathematical combination of torsion angles. This analysis is based upon consideration of approximate symmetry possessed by most rings.

2.4.2 Medium Rings

The geometry of medium rings has been described in terms of the magnitude of their torsion angles (Hendrickson, 1964 and 1967). The flexibility of these rings allow them to adopt a great number of shapes. The fact that ring families are so characterized by their torsion angles also allow the use of torsion angles for their definition. A family is definable by its symmetry element(s) and its sequence of signs of torsion angles. A topological convention devised by Hendrickson (1964) is based on this and allows all possible symmetric conformations of medium rings to be generated and also gives their interrelations.

In this convention any symmetrical ring is described by a symbol containing a horizontal symmetry line representing the symmetry element (plane or axis) passing through the ring. The cyclic sequence of torsion angle signs of the bonds (+,0,-) arranged around it as in the physical ring. The rules for use of the convention can be summarized as follows:-

a) Bonds opposed across the symmetry element have torsion angles (w_1, w_2 etc) equal in magnitude and equal in sign across an axis but opposite in sign across a plane of symmetry.

b) The symbol is equivalent to the physical ring and so may be turned over or around without changing

its identity.

c) when a symmetry element bisects a bond the sign of its torsion angle appears at the appropriate end of the symmetry line. It is zero (i.e eclipsed) if the symmetry is a plane.

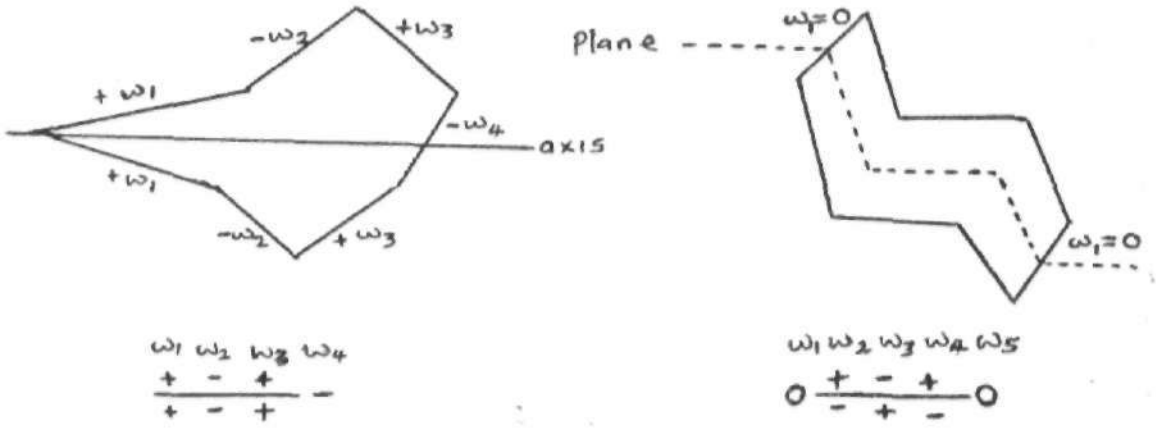


Figure 2.8 The symbols and rules for use of sign sequence convention

d) The mirror image of a ring is generated by reversing all signs; thus it may be shown that a *ring with a plane is identical with its enantiomer* while one with only an axis is not.

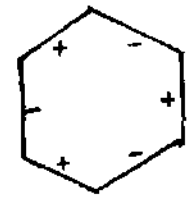
e) Symbols with three or more like signs in sequence are either not real rings or are very highly strained.

With this convention it is not only easy to generate all possible ring forms but it is also possible to follow the torsion angle changes in any mode of interconversion

between families. The convention symbols corresponding to some families of medium rings are discussed in subsequent chapters.

2.4.3 Cyclohexane

The rigid or chair form of cyclohexane is characterized by the regular altenation of the signs of its torsion angles as shown below



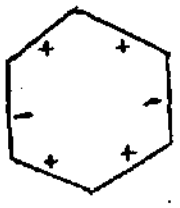
chair form.

In an undistorted chair all the torsion angles have some absolute values (Bucourt, 1974). These two properties reflect the high degree of symmetry of this conformation. It possesses among other elements of symmetry a centre of inversion and a threefold rotation axis perpendicular to the mean plane of the molecule and passing through its centre. As a consequence, the torsion angles in the 1, 4-positions are of opposite sign, whereas they are of the same sign in the 1, 3 positions.

A deformation of the cyclohexane chair form may arise locally, for example, as the result of the fusion with another cycle or through the presence of axial substituents suffering van der waal repulsion (Bucourt, 1974). As a result the torsion angles of the ring is

made to close or open. A decrease in the absolute values of the torsion angles corresponds to a flattening of the rings. An increase corresponds to a puckering.

In the flexible form of cyclohexane, the torsion angles in the 1, 4 positions are of identical sign. This identity reflects the presence of a two-fold symmetry axis perpendicular to the ring at its centre. The sequence of signs is as shown below.



Flexible form

Owing to the flexibility of this form a continuous variation of all the torsion angle values gives rise to an infinite number of conformations (Bucourt, 1974). Among these, the two of highest degree of symmetry are the twist form or stew boat (Figure 2.9), which possess two further two-fold symmetry axis, and the boat form with planes of symmetry.

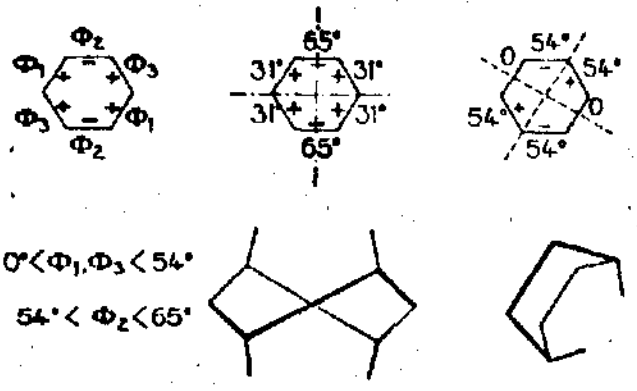


Figure 2.9 The flexible form of cyclohexane

Following the description of the pseudorotating cyclopentane (Altona et al, 1968), the pseudorotation of the flexible form of cyclohexane which interconverts all possible twist and boat forms has been described (Buys and Geise, 1968). Thus, the geometry of any one conformation in cyclohexane pseudorotation circuit may be determined by the expression -

$$\theta_j = \Phi_{max} \cos (\Delta + j\delta)$$

where Φ_{max} represents the greatest value a torsion angle can reach during the pseudorotation, Δ is the pseudorotational phase parameter varying from 0 to 360^{o}, j is an integer (0 to 5) refering to each torsion angle and $\delta = 120^{o}$.

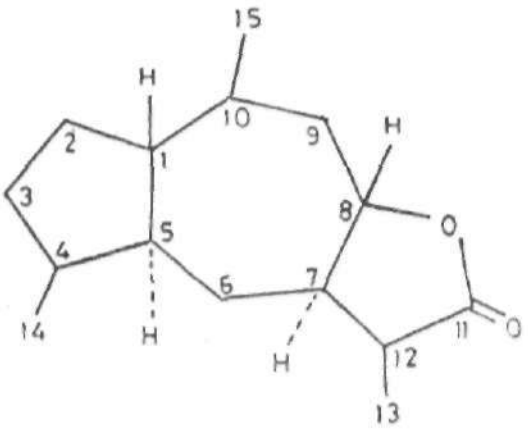
CHAPTER THREE

3.0 MOLECULAR CONFORMATIONS OF THE CYCLOHEPTANE RING DERIVATIVES IN THE SOLID STATE

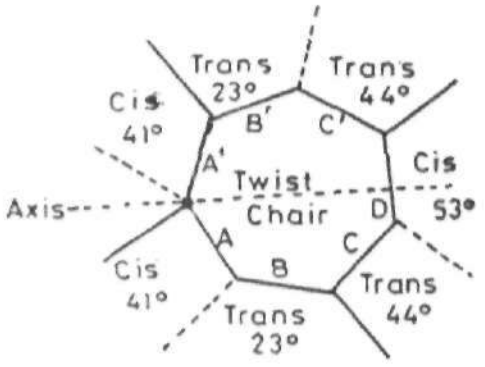
3.1 PREAMBLE

The cycloheptane carbon frame-work constitutes the major structural unit in a rapidly rising number of naturally occurring compounds, particularly in the sesquterpenoids (chart 3.1). While the conformations of cyclopentane and cyclohexane derivatives have been extensively examined (Bucourt, 1975; Duax et al, 1976: Thomas, 1982, 1989, 1991), those of cycloheptane derivatives have not been subjected to such extensive and comparative analyses.

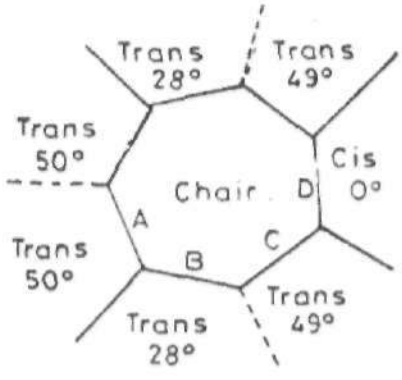
It is known that several conformational differences exist between the higher symmetry cyclohexane and the relatively lower symmetry cycloheptane (Hendrickson, 1963). For instance, cyclohexane has one chair form, while the more flexible cycloheptane has a family of chair forms which are readily interconvertible by pseudorotation. Among the chair forms in the latter sequence, the twist chair with an axis of symmetry (i.e C_2 axis) and a chair with a plane of symmetry (i.e C_s plane of symmetry) are symmetrical with the former thought to be the most stable and the latter least stable in the pseudorotation sequence. The difference in the energy favouring twist - chair form of cycloheptane over



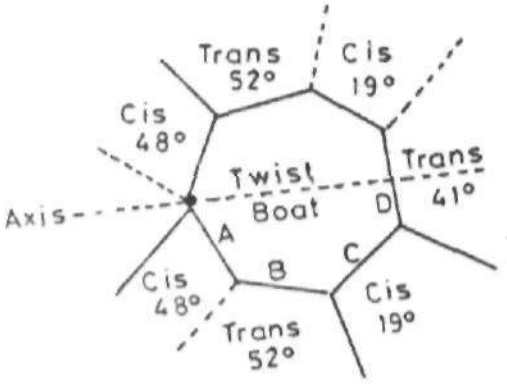
(a)



(b)



(c)



(d)

Figure 3.1 Atomic numbering scheme used for a cycloheptane ring with two fused 5-membered rings; schematic representations of (b) twist chair (c) chair (d) twist boat conformations of cycloheptane illustrating preferred stereochemistry of 5-membered ring fusion. (After Hendrickson).

the chair form is small (i.e 1.4 calories), but since the chair form represents an energy maximum on the pseudorotational sequence it would only have a transient existence (Hendrickson, 1967). Like cyclohexane, the cycloheptane chair forms are also thought to be capable of undergoing a conformational flip into a series of higher energy boat forms. The boat series is normally made of flexible forms interconvertible by pseudorotation. In this sequence, a twist boat form with C_2 axis of symmetry is judged the most stable, while the boat form with a C_s plane of symmetry is the least stable.

The most stable twist - chair form of cycloheptane has seven distinguishable substituent positions. The unique axis-carbon with two identical positions, both equatorial in energetic status, and three other carbons on each side of the axis each with distinguishable axial and equatorial positions. The equatorial position alternates above and below the ring plane as they do in cyclohexane (Hendrickson, 1962). The interconversion between axial and equatorial positions in cycloheptane can all occur by facile pseudorotational passage of the substituent through a sequence of all positions without any flip to the boat forms (Hendrickson, 1967).

Some conflict exists in literature about the possible conformations of some cycloheptane derivatives

in solid state. For example, Sekita et al (1971), attributed a boat conformation to the cycloheptane ring of the compound bromomexicanin-E, while Mcphail and Sim (1973) assigned a conformation midway between the twist chair and chair form to the same ring. The relationship between the conformation of the ring and the stereochemistry of fusion of a five membered ring to the cycloheptane derivative has also been a subject of some discussion in the literature. The fusion of a five membered ring to cycloheptane ring is a very restrictive process, since such a ring will not tolerate fusion at a torsion angle of greater than 45 - 50^{o} without introduction of considerable strain (Hendrickson, 1962). Hendrickson (1963), proposed that cis fusion of a five membered ring to the cycloheptane ring is most favoured at bond A in the twist chair form (figure 3.1b) while trans fusion takes place at either bond B or C (figure 3.1b). Mcphail and Sim (1973), from studying the structures of six cycloheptane derivatives demonstrated that in europatin bromoacetate (H7), (chart 3.1) the cis fused cyclopentene and trans-fused γ-lactone are found at bonds of the D and B types respectively, but the authors erroneously (as shown later) prosposed that in the closely related compounds solstitalian (H8, chart 3.1) and bromodihydroisophotosantonic lactone acetate (H9, chart 3.1), the cis fused five membered rings are

found at bonds of the A type.

The present study was therefore carried out to resolve the above conflicts, and attempt to decipher factors which determine the various conformations adopted by the cycloheptane ring derivatives. Consequently, studies have been carried out on the conformations of carboxylic cycloheptane rings in 28 molecular environments interms of some geometric and conformational parameters (Duax et al, 1976; Bucourt, 1974; Mcphail and Sim, 1973). Some previous conformational assignments in the literature have been revised.

The atomic numbering scheme used is shown in figure 3.1a for a typical sesquiterpenoid. Schematic representations of the twist chair, chair and twist boat forms as proposed by Hendrickson (1963), are shown in figure 3.1b, figure 3.1c and figure 3.1d respectively. The various kinds of bond with respect to the symmetry elements (C_2 or C_s) of the rings are labelled A to D, and A' to C' for symmetry related equivalents in figure 3.1.

3.2 EXPERIMENTAL PROCEDURE

3.2.1 Data for Calculation:

Primary structural data for molecules containing cycloheptane derivatives were obtained from the literature for X-ray analyses with R_f values not exceeding 15%.

3.2.1.1 Asymmetric Parameters:

Asymmetric parameters (ΔC_2 and ΔC_5) were calculated using the expressions defined by Duax and Co-workers (1976) and described by Thomas (1982a,1982b).

$$\Delta C_s = \left(\sum_{i=1}^{m} \frac{(\phi_i + \phi'_i)^2}{m} \right)^{1/2}$$

and

$$\Delta C_2 = \left(\sum_{i=1}^{m} \frac{(\phi_i - \phi'_i)^2}{m} \right)^{1/2}$$

For the ideal chair, $\Delta C_s = 0$, while for ideal twist chair $\Delta C_2 = 0$. Similarly, for the ideal boat $\Delta C_s = 0$ and for the ideal twist boat $\Delta C_2 = 0$.

3.2.1.2 Conformational Parameters Σ_2 and Σ_s

The parameters Σ_2 and Σ_s proposed by Mcphail and Sim (1973), are measures of the deviation of the ring conformation from C_2 and C_s symmetry. They have been estimated in this study using the expressions:

$$\Sigma_2 = (/w_1 - w_6/+/w_2 - w_5/+/w_3 - w_4/).$$

$$\Sigma_s = (/w_1 + w_7/+/w_2 + w_6/+/w_3 + w_5 +/w_4/).$$

where w_1 to w_7 are the endocyclic torsion angles of the rings as illustrated in figure 3.2. Each pair of angles within the modulus sign is a symmetry pair in terms of both the sign and magnitude of the torsion angles. For ideal forms both Σ_2 (for twist chair and twist boat) and Σ_s (for chair or boat) are zero.

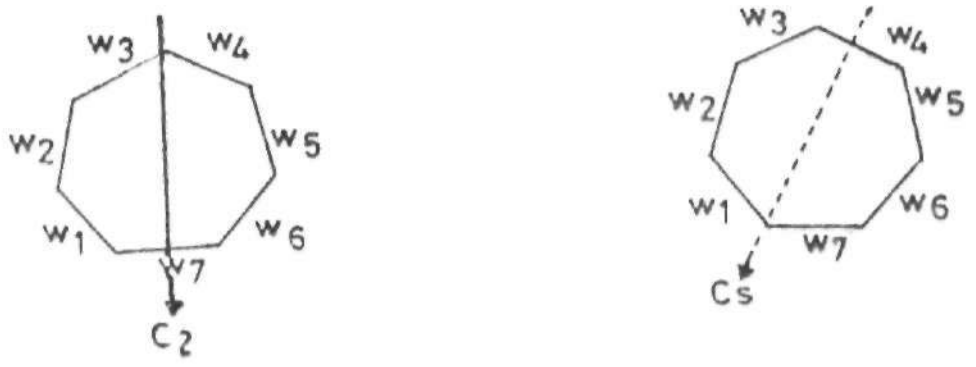


Figure 3.2 Sketches showing symmetry pairs of endocyclic torsion angles (w) used in calculating the conformation parameters

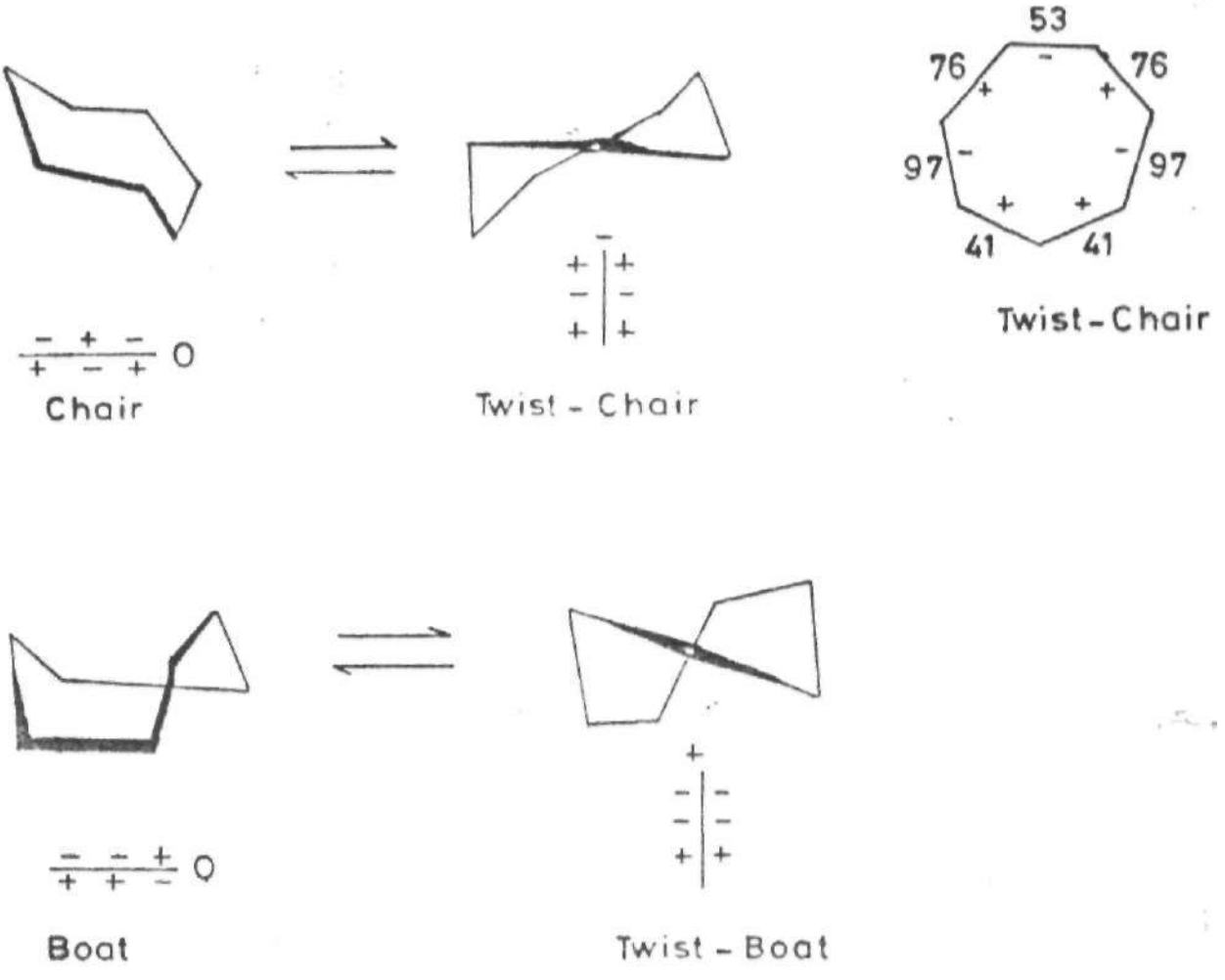


Figure 3.3 Topological conventions of sign sequences of the endocyclic torsion angles in the various conformations

3.2.2 Definition of the Conformations:

The conformations are described as chair, twist chair, boat and twist boat depending on the sign sequence of the endocyclic torsion angles, and the estimated conformational parameters ΔC_s, ΔC_2, Σ_2 and Σ_s. A simplified topological convention in terms of the sign sequence of the endocyclic torsion angles as described in section 2.2.1 is shown in figure 3.3 for the various forms. In the figure, the conventional notations reflect dispositions of the perspective views as indicated in the sketches. For the twist chair and twist boat conformers, the views are along the symmetry axis and this accounts for the way their conventional notations are oriented.

3.3 RESULT AND DISCUSSION

Geometric and conformational parameters (ΔC_2, ΔC_s, Σ_2 and Σ_s) for some cycloheptane ring derivatives (H1 to H19) in the chair/twist chair forms are shown in table 3.1, while the corresponding endocyclic torsion angles are given in table 3.2. Table 3.3 represents a listing of the geometric and conformational parameters for rings (H20 and H28) in the boat/twist boat family of conformations, with endocyclic torsion angles correspondingly listed in table 3.4. It is quite evident from the values of $\Sigma/\phi/$, that the rings in the chair/twist chair conformations are more puckered (with a mean $\Sigma/\phi/ = 425^{o}$) than those in the boat/twist boat

conformation (with mean $\Sigma/\phi/ = 324^{\circ}$). Chart 3.1 shows the molecular environments of the various cycloheptane derivatives examined in this study.

The relative conformations of the rings in the chair/twist chair family (H1 - H19) are displayed in tables 3.2 and 3.3 and figure 3.4. The cycloheptane derivatives fused to two 5-membered rings (H1, H6 and H13) all adopt the chair conformation. The methylene cycloheptane ring represented in this study by the derivatives H5, H8, H10, H14, H16, H19 and H22, has received some attention in the literature (Bovill et al, 1979). Thus, while molecular mechanics calculations for a series of chair and twist chair conformers indicate that the most stable form of an isolated methylene cycloheptane is a twist chair, in which a C_2 axis of the ring passes through the carbon atom adjacent to that bearing the exocyclic methylene group, the rings in H5, H19 and H22 adopt conformations different from the twist chair.

Table 3.1: Conformation and Geometric Parameters for Some Cycloheptane Ring derivatives in the chair/Twist Chair Forms.

Compd. Code	Σ_2	Σ_s	ΔC_2	ΔC_s	$\Sigma/\phi/$	Approx. Symmetry of Torsion of angles	Reference
H1	82.0	13.0	40.2	5.5	421	$C_s(6)$	DullForce et al 1971
H2	7.5	100.3	3.0	36.5	454	$C_2(6)$	Mazhar-ul-Haque et al 1974
H3	7.4	99.7	2.5	36.2	459	$C_2(6)$	"
H4	29,0	61.0	11.9	22.4	401	$C_2(7)$	Mcphail et al 1975a
H5	100.0	20.0	39.3	7.3	433	$C_s(9)$	Bovill et al 1979
H6	74.0	22.0	34.6	7.4	422	$C_s(7)$	Cox and Sim 1975
H7	32.0	107.0	12.7	39.4	407	$C_2(8)$	Mcphail and Sim 1973
H8	19.0	79.0	6.9	28.9	454	$C_2(8)$	"
H9	19.0	49.0	7.3	22.1	446	$C_2(8)$	"
H10	22.0	97.0	7.6	33	426	$C_2(8)$	"
H11	40.0	92.0	18.9	31.3	420	$C_2(8)$	"
H12	62.0	40.0	25.7	13.7	405	$C_s(6)$	Sekila et al 1971
H13	56.0	37.0	21.7	14.7	348	$C_s(7)$	Dullforce et al 1971
H14	30	62.2	13	22.5	462	$C_2(1)$	Chowdhury 1983
H15	95	8.0	37.3	4.1	426	$C_s(8)$	Fronczek 1979
H16	28	77.0	9.7	27.4	437	$C_2(10)$	Cox et al 1975b
H17	27.4	71.0	12.6	24.1	398	$C_2(10)$	Mazhan et al 1969
H18	62	48.0	21.7	16.8	431	$C_s(10)$	Mcphail et al 1975b
H19	102	10.0	40.5	4.4	427	$C_s(1)$	Mcphail et al 1975c

Table 3.2 Endocyclic Torsion Angles of Some Cycloheptane Ring Derivatives in the chair/Twist Chair Conformations.

Compd.	Torsion Angle (deg.)						
Code	C_1-C_5	C_5-C_6	C_6-C_7	C_7-C_8	C_8-C_9	C_9-C_{10}	C_{10}-C_1
H1	76	-66	69	-85	60	4	-61
H2	-95.1	39.8	38.4	-93.8	73.7	-44	68.9
H3	-94.1	37.8	40.8	-91.5	71.5	-49.9	73.3
H4	-84	-62	-18	-31	62	-68	76
H5	64	-3	68	-90	67	62	79
H6	64	-82	64	-57	76	-73	6
H7	25	-63	102	-41	-42	85	-49
H8	51	-74	88	-35	-45	92	-69
H9	63	-78	79	-31	-42	81	-72
H10	44	-59	84	-37	-43	90	-69
H11	-36	59	-81	32	53	-98	61
H12	-36	68	-82	19	60	-86	51
H13	29	-52	74	-93	69	-30	- 1
H14	49.3	-90.7	74.6	-60.9	75.3	-82.4	28.3
H15	- 4	-63	86	-66	65	-79	63
H16	79	-69	57	-75	89	-40	-28
H17	-77	60.6	-36.0	58.7	-81.2	36.6	52.9
H18	-76	87	-51	-23	65	-64	65
H19	62	-87	68	3	-68	80	-59

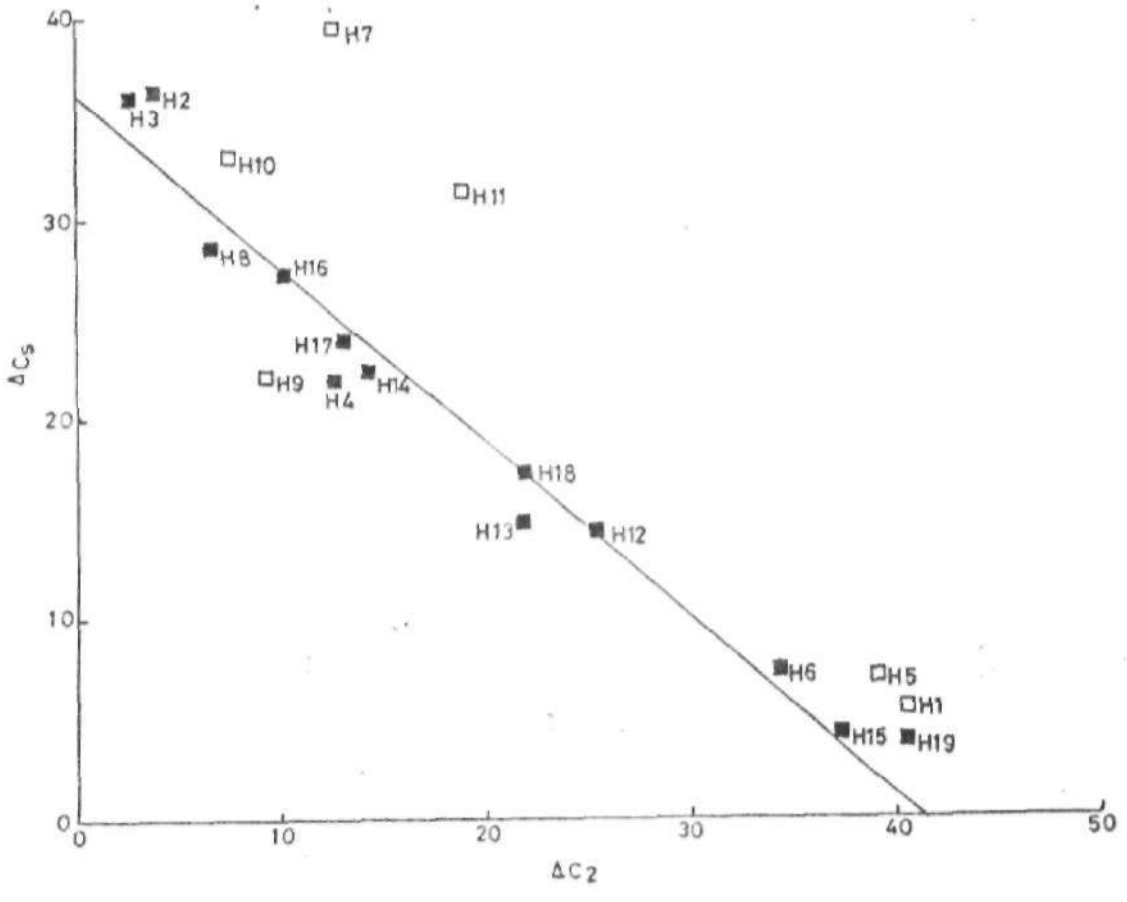


Figure 3.4 Correlated variation in principal asymmetry parameters ΔC_s and ΔC_2 for cycloheptane derivatives in the chair and twist chair conformations. The equation of the line is: $\Delta C_s = 36.44 - 0.896\ \Delta C_2$ ($n = 13$, $r^2 = 0.96$). The points (□) were not included in the least - squares fit.

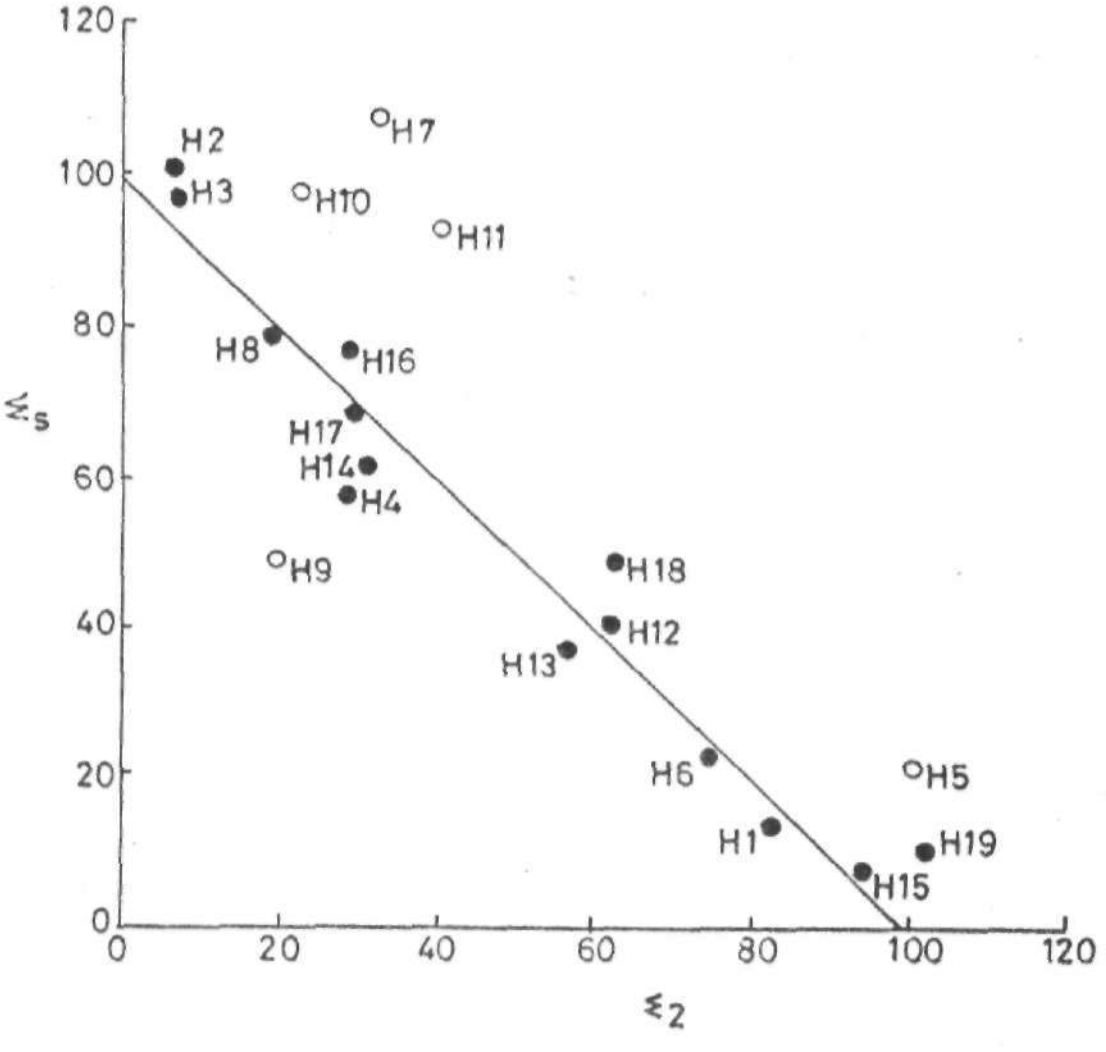


Figure 3.5 Correlated variation in the conformation parameters ξ_s and ξ_2 for cycloheptane derivatives in the chair/twist chair conformations. The equation of the line is:

$\xi_s = 99.44 - 0.974\xi_2$ (n = 14, $r^2 = 0.95$). The points (O) were not included in the least squares fit.

Both H5 and H19 adopt the chair conformation while H22 adopts a twist boat conformation. The latter conformation may be due to constraints arising from the double cis fusion of the two 5-membered rings in H22 to bonds which are in a 1, 3 - relationship. The relative positions of the C_2 axis (for the twist chair) and mirror plane C_s (for the chair) for the fused methylene cycloheptene rings do not necessarily follow the pattern prescribed by molecular mechanics for the free ring. Thus, while the C_2 axis of the ring in H14, H16 and the mirror plane in H19 pass through the required carbon atom, these symmetry elements in H5, H8 and H10 do not pass through the expected carbon atom. It would appear that for the fused ring, other intramolecular constraints may influence the relative position of the symmetry element in the methylene cycloheptane.

In general, a preponderance of 1, 3 - non-bonded interactions among substituents on the cycloheptane derivatives over 1, 4 - nonbonded interactions leads to a preference of conformations in the chair/twist chair family to those in the boat/twist boat forms. The Chair/twist chair sequence also appears preferred when there are equal numbers of 1, 3 - and 1, 4 - nonbonded interactions on the cycloheptane ring derivatives. Within the chair/twist chair family, it is not easy to decipher any distinctive factors which determine what

conformation in the series the ring adopts. The conformation of bromomexicanin - E (H12) in this sequence requires a revision. The cycloheptane ring derivatives in H12 was earlier assigned a boat conformation (Sekita et al, 1971) and later changed to a conformation midway between the chair and twist chair forms (Mcphail and Sim, 1973). Examination of the asymmetry parameters in table 3.2 for H12 and the correlation diagrams (figures 3.4 and 3.5) reflecting the possibility of interconversion by pseudorotation, shows that the ring H12 adopts a conformation closer to the twist chair form than the chair form.

Comparison of figure 3.3 with figure 3.4 and figure 3.5 with figure 3.6 shows that the conformation parameters ΔC_s and ΔC_2 (Duax et al, 1976), and Σ_s and Σ_2 proposed by Mcphail and Sim (1973), give similar conformational information for these rings in the solid state. Thus, any of these parameters may be used to specify the ring conformation with a possibility of obtaining information on the pseudorotational sequences of the two families.

In figure 3.6 and 3.7, tables 3.3 and 3.4 the relative conformations of rings in the boat/twist boat series are presented. It is evident that the twist boat form is the predominant form, as can be seen from figure 3.6 and 3.7. There is clearly a clustering of the points

towards the twist boat end of the pseudorotation inter-conversion lines, suggesting the much higher stability of the twist boat form over the boat form. The conformations in this sequence seem to be adopted when there is, on the ring derivative, a relatively higher preponderance of 1, 4 - nonbonded interactions over 1, 3 - nonbonded interactions (generally in a ratio greater than 2:1 respectively). The derivative H22 appears an exception to this rule. However, the twist boat conformation is probably imposed on this ring by the unusual double cis fusion of two 5-membered rings at the B and D types of bond (figure 3.1). Infact, it is only in the twist boat that bonds B and D can have the same fusion stereochemistry in the same derivative (figure 3.1). The cycloheptene (H27) fused to only one 5-membered ring adopts the twist boat form unlike the derivatives (H1, H6 and H13) fused to two 5-membered rings which adopt the chair conformation. However, in H27, there is clearly a preponderance of 1,4-nonbonded interactions over 1,3-non- bonded interactions. Only two molecules (H23 and H24) in the set studied have the characteristics of the boat form. Even then, the corresponding points in figures 3.6 and 3.7 deviate significantly from the pseudorotation interconversion line. This would suggest that the rings are forced to adopt a particular boat form, possibly by special

Table 3.3 Conformation and Geometric Parameters for some Cycloheptane Ring Derivatives in the Boat/Twist forms.

Compd. Code	Σ_2	Σ_s	ΔC_2	ΔC_s	$\Sigma/\phi/$	Approx. Symmetry of Torsion of angles	Reference
H20	17.7	48.9	6.1	20.2	335	$C_2(10)$	Pettersen and Kim 1976
H21	25.1	47.7	8.5	19.2	330	$C_2(10)$	"
H22	11.7	59.4	4.0	18.4	329	$C_2(10)$	Malone 1980
H23	60.4	52.5	30.5	21.5	334	$C_s(10)$	Nozaki 1979
H24	70.2	57.7	34.6	25.8	346	$C_s(10)$	"
H25	8	54	2.8	21.2	323	$C_2(10)$	Cox and Sim 1977
H26	33.4	46.4	12.1	16.1	326	$C_2(10)$	Von Dreele et al 1975
H27	30	58	12.1	19.9	295	$C_2(9)$	Sundaranman et al 1975
H28	31	69.3	11.1	26.1	302	$C_2(10)$	Herz et al 1980

Table 3.4 Endocyclic Torsion Angles of Some Cycloheptane Ring Derivatives in the Boat/Twist Boat Conformations

Compd. Code	Torsion Angle (deg.) C_1-C_5	C_5-C_6	C_6-C_7	C_7-C_8	C_8-C_9	C_9-C_{10}	C_{10}-C_1
H20	-72.0	-13.7	71.7	-19.9	-64.5	44.5	48.5
H21	-61.3	-21.4	72.5	-12.0	70.8	48.9	42.7
H22	-60.4	-21.1	75.0	-17.9	-65.8	46.0	42.9
H23	78.5	-42.6	- 2.8	42.7	-55.0	-42.0	70.9
H24	77.5	-45.5	- 3.7	44.8	-62.6	-34.8	76.9
H25	70	-11	67	-15	-68	47	45
H26	-69.2	-19.4	65.0	- 4.1	-74.7	40.4	53.5
H27	3	57	-11	-64	49	37	-74
H28	-69	-19.4	65	- 4.1	-74.7	40.1	30.1

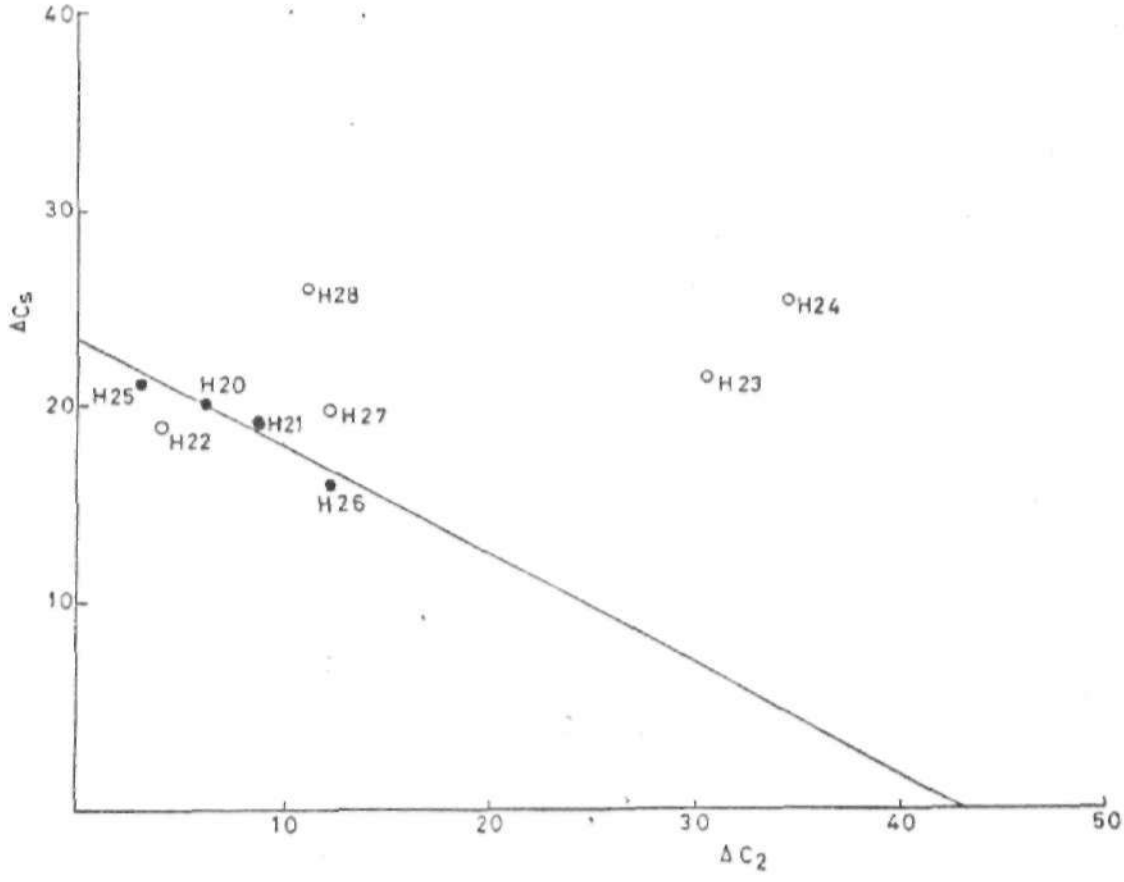


Figure 3.6 Correlated variation in principal asymmetry parameters ΔC_s and ΔC_2 for cycloheptane derivatives in the boat and twist boat conformations. The equation of the line is:

$\Delta C_s = 23.18 - 0.543\ \Delta C_2$ $(n = 4,\ r^2 = 0.93)$.

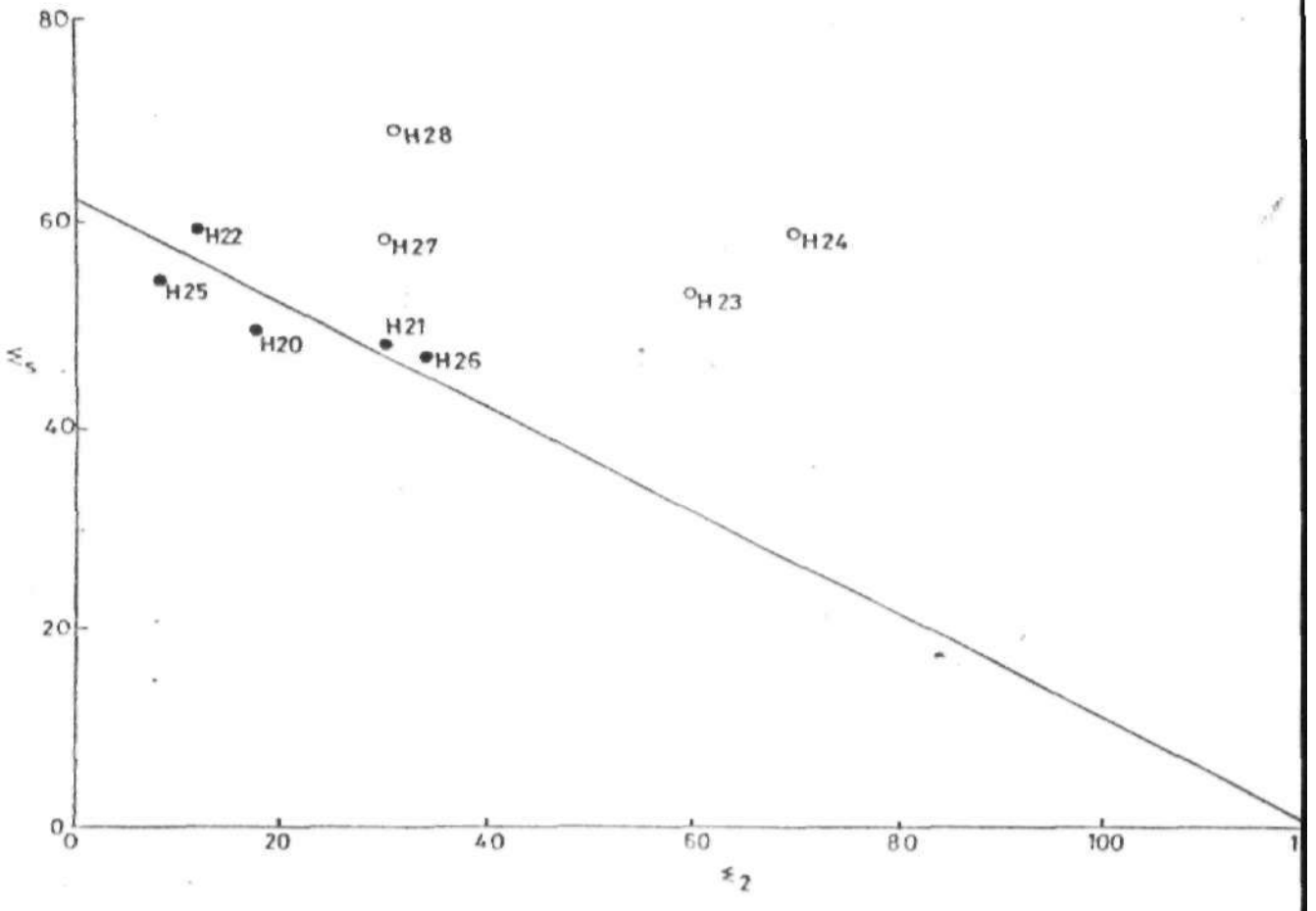


Figure 3.7 Correlated variation in the conformation parameters Σ_6 and Σ_2 for cycloheptane derivatives in the boat and twist boat conformations. The equation of the line is:

$\Sigma_5 = 62.00 - 0.516\,\Sigma_1$ (n = 4, $r^2 = 0.69$).

constraints imposed by the presence of two highly strained cyclopropane rings.

Several of the conformations in the boat/twist boat sequence were inadequately described in the literature. Thus, H20, H21, H27 and H28 were described essentially as distorted boat forms and boat respectively. The sign sequences of the torsion angles in table 3.5, together with figures 3.6 and 3.7 show that these are more of twist boat forms than boat forms. The ring H22 was described as adopting the twist chair conformation, while from this study it is clearly seen to belong to the twist boat form. Examination of the values of the torsion angles in tables 3.1 and 3.3 shows that while the chair and the boat tend towards the monoplanar form (Bucourt, 1974), the twist chair tends towards the 1, 2 - diplanar form and the twist boat towards the 1, 3 - diplanar form.

The stereochemistry of ring fusion to the cycloheptane derivatives in the molecules studied is summarized for the various conformational forms in table 3.5. For the twist chair forms (H4, H7, H8, H9, H10, and H11) the ring is cis fused only at bond A or D. This is in agreement with the proposal by Hendrickson, (1963). However, it would appear that an A/D Cis/Cis fusion is not feasible in the twist chair conformation. Although

most of the fusions at bonds B and C are trans as proposed by Hendrickson, a cis fusion at bond C is observed in H17 and the conformation though closer to the twist chair form, shows a significant deviation ($\Delta C_2(10)$ = 12.6) from the ideal form. It is known that in some cases, a multiplicity of substituents or fused rings often, as in cyclohexane systems, causes ring conformations which are less favourable in the parent to become preferred (Hendrickson, 1963). This may be responsible for the cis fusion at bond C in H17. Similarly, a trans fusion is observed at bond D in H11 instead of the anticipated cis fusion. For solstitalian (H8) and bromodihydroisophotosan tonic lactone acetate (H9), Mcphail and Sim (1973), proposed that the cis fused 5 - membered rings are found at bonds of the A type. It is obvious from table 3.5 that these rings are fused at bonds of the D type as in the related compound euparotin bromoacetate (H7).

Table 3.5 Stereochemistry of Ring Fusion (a) to be Cycloheptane Derivation.

i) chair Forms			ii) Twist chair forms			iii) Twist Boat Forms		
Ring Code	Stereochemistry of Fusion		Ring Code	Stereochemistry of Fusion		Ring Code	Stereochemistry of Fusion	
H1	B/B'	trans/trans	H2	B/B'	trans/trans	H20	B/C'	trans/cis
H5	B/C	trans/(-)(b)	H3	B/B'	trans/trans	H21	B/C'	trans/cis
H6	A/C	trans/(-)	H4	A/C'	Cis/trans	H22	B/D	Cis/Cis
H12	B/B'	Cis/Cis	H7	B/D	trans/cis	H25	B/C'	trans/cis
H13	A'/C	trans/(-)	H8	B/D	trans/cis	H26	B/C'	trans/cis
H15	B/D	trans/cis	H9	B/D	trans/cis	H27	C'	cis
H18	A/D	trans/cis	H10	A/D	Cis/(-)	H28	B/C'	trans/cis
H19	A/D	trans/cis	H11	A/D	cis/trans			
			H14	A/C	(-)/trans			
			H16	B/C	(-)/trans			
			H17	B/C'	trans/cis			

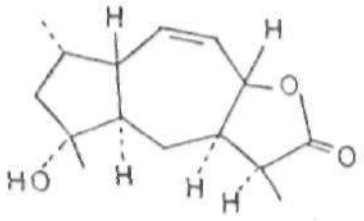
(a) capital letters (A, B, C, D) refer to bond types at which fusion takes place

(b) (-) Refers to the presence of a double bond at ring junction.

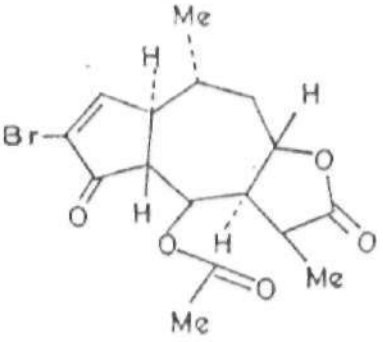
As can be seen from table 3.2 (for H7, H8, H9), the C_2 symmetry axis passes through the C8 carbon atom and bisects the C1 - C5 bond, which is a bond of the D type.

From figure 3.1c, the preferred fusion stereochemistry for the chair forms is a trans fusion at bonds of the type A, B or C, with cis fusion expected preferably at bond D. Generally, this is in agreement with table 3.5. However, it is seen from the table that a B/B' cis fusion is possible as in H12. For the twist boat forms, cis fusion is expected at the A or C bond, while trans fusion is preferred at the B or D bond (Figure 3.1d). As can be seen also from table 3, all observed C bond fusions are cis for the twist boat form, and most observed B bond fusions are trans as anticipated. However, an unexpected B/D - cis/cis fusion is observed in H22. It is not quite obvious why a B/D - cis/cis fusion pattern is adopted, but probably further strain arising from the presence of the C10 - alkene imposes the observed fusion stereochemistry on this ring.

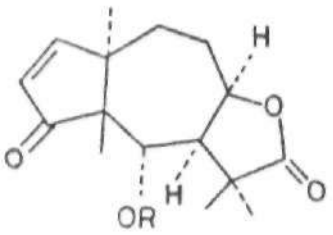
Chart 3.1 Structures of seven membered rings showing the molecular environments



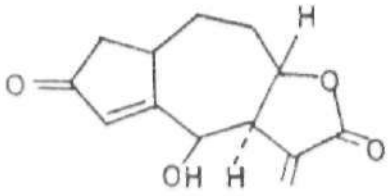
H1



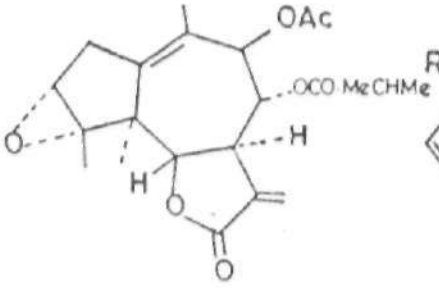
H2 ; H3



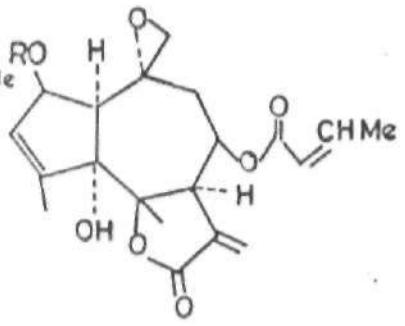
H4



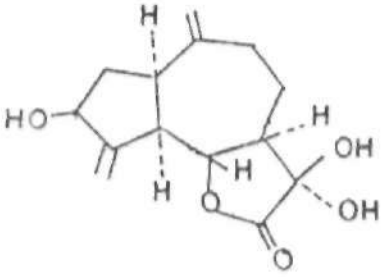
H5



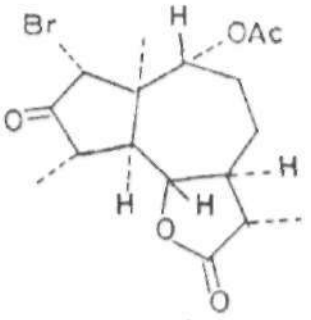
H6



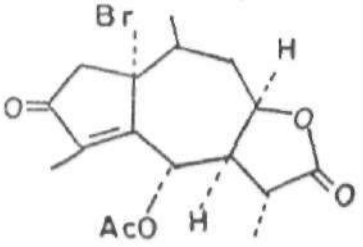
H7



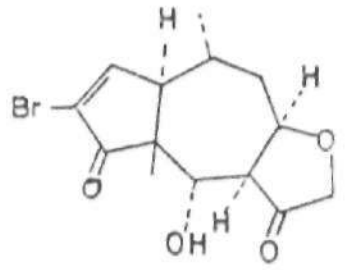
H8



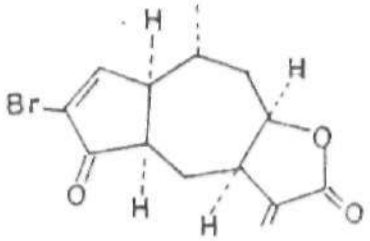
H9



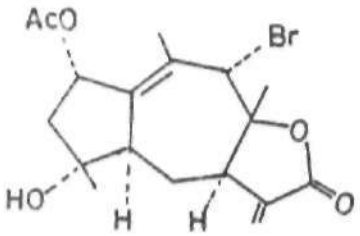
H10



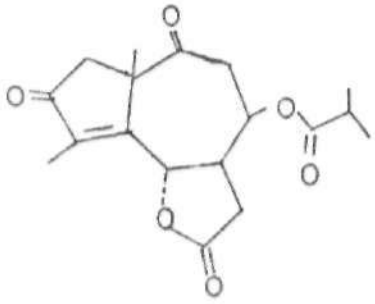
H11



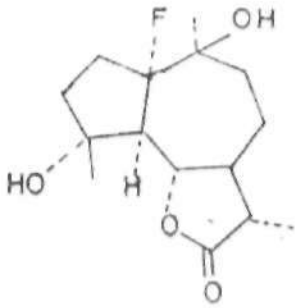
H12



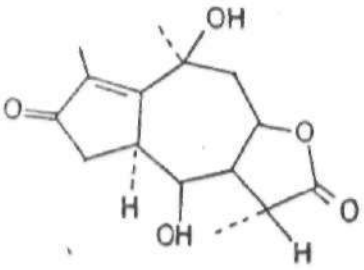
H13



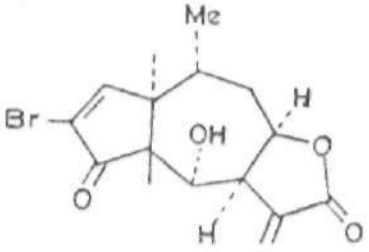
H14



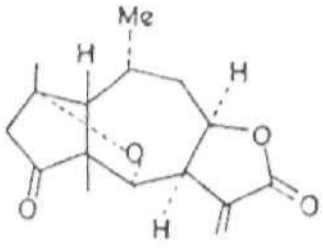
H15



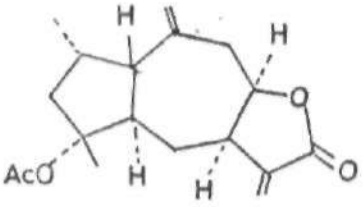
H16



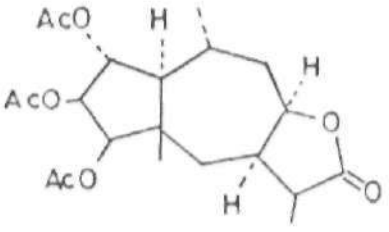
H17



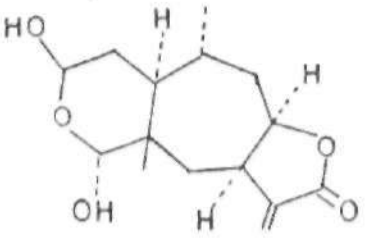
H18



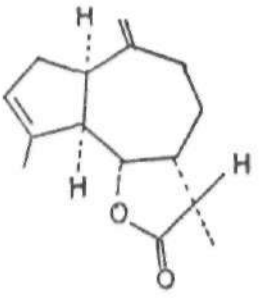
H19



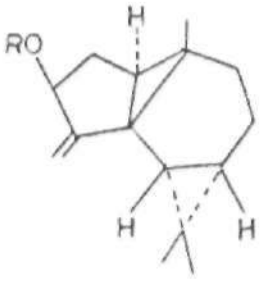
H20



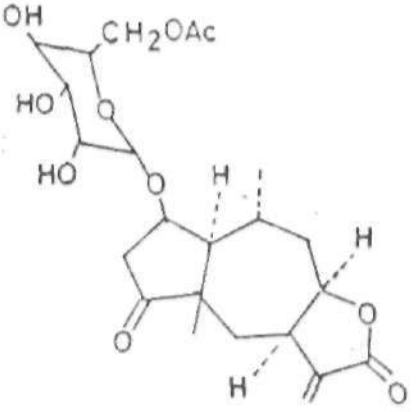
H21



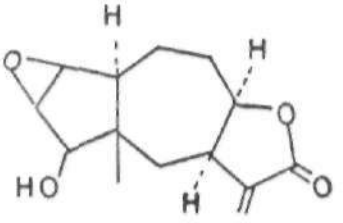
H22



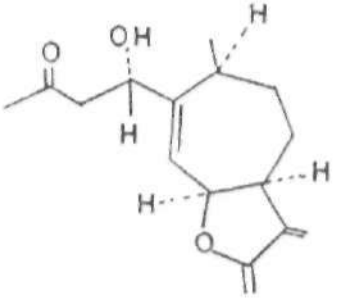
H23;H24



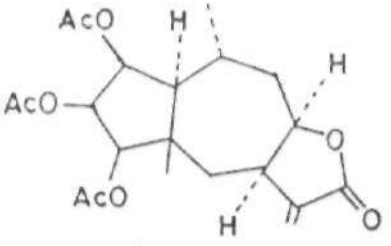
H25



H 26



H27



H 28

CHAPTER FOUR

4.0 MOLECULAR CONFORMATIONS OF FURANOSE RINGS OF NUCLEOSIDES AND NUCLEOTIDES IN SOLID STATE

4.1 PREAMBLE

The furanose ring is centrally located in the sugar phosphate chains of nucleic acids (figure 4.1a). From x-ray studies, it has been suggested (Altona and Sundaralingam, 1972) that this five-membered ring in solid state is not planar but puckered at either the C(2') or C(3') atom (figure 4.1b). Usually, in nucleosides and nucleotides only one puckered state of the five-membered ring is observed (Westhof and Sundaralingam, 1983). In dinucleotides, the conformation of the two sugars are sometimes different but each nucleotide fragment has a precise conformation. The observed differences in conformation of furanose rings in these compounds are probably due to the different hydrogen bonding schemes adopted by the furanoside moieties in the crystal lattice, and some of the differences may be ascribed to the type of substituent in the furanose ring (Sundaralingam, 1965). A change over from one conformer of the furanose ring into the other produces major structural changes in the naturally occurring nucleic acids, and has an important bearing on

their biological functions.

The furanose ring like cyclopentane is a puckered flexible ring characterized by pseudorotation. In cyclopentane the angle of maximum puckering rotates without substantial change in potential energy. However, the presence of one or more substituents, endocyclic or exocyclic will give rise to an induced potential energy barrier opposing free pseudorotation (Pitzer and Donath, 1959). The consequences of limited pseudorotation were studied by Altona et al (1968) and more recently by Thomas (1982), on the conformation of the five-membered D ring in steroids. The puckering in the furanose ring is thought to be mainly due to the torsional forces about the single bonds, arising from nonbonded interactions of the substituent atoms which are in opposition to the forces striving to retain tetrahedral bond angles (Altona et al, 1972).

A quantitative description of puckering and conformation in terms of the maximum angle of torsion (θm) and of the phase angle of pseudorotation (Δ) has been presented (Altona et al, 1968; Altona and Sundaralingam, 1972; Thomas, 1982), based on the interrelationship between the five torsion angles in a nonplanar five membered ring. It has also been demonstrated that both qualitative and quantitative information can be obtained on the geometry of any ring,

from the sequence of the algebraic values of its angles (Bucourt, 1974). The simple sequence of the sign of the torsion angles within the ring indicates the type of conformation, while the absolute values of torsion angles allow the deformation with respect to a reference conformation to be estimated. A quantitative evaluation of the conformation of rings of any size may be obtained in terms of the asymmetry parameters. ΔC_s and ΔC_2 as earlier stated in section 2.3.

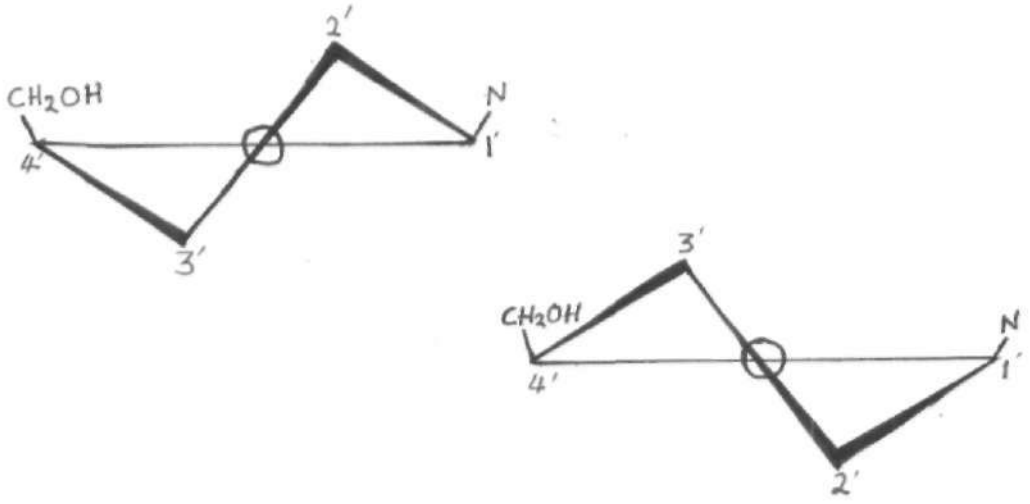


Figure 4.1 diagrammatic projections of the furanose ring showing the C(3′) and C(2′) puckering.

In the crystal structure of the nucleosides and nucleotides, strain in the five-membered ring of the sugar close to intermolecular contact of exocyclic

substituents, and special packing considerations such as intermolecular H- bonding cause puckering of the rings, such that in many cases C(2') or C(3') (figure 4.1b) atom is displaced from the plane of the other four atoms (Munns and Tollin, 1970). It is believed that the ribose conformation is independent of whether the base is a pyrimidine or purine system in nucleosides and nucleotides. In this chapter, the puckering and conformations of furanose rings in a variety of nucleosides and nucleotides have been examined in terms of the sum of the absolute values of the torsion angles ($\Sigma/\phi/$), and asymmetric parameters (ΔC_s and ΔC_2), and some relationships among various parameters derived. Information on the conformations of the furanoside moiety would be of considerable importance in nucleic acid model building and knowledge regarding the shapes of the furanosides would contribute toward a better understanding of their chemical reactions and physical properties. Thus, features which determine the conformations of these rings have also been elucidated.

4.2 EXPERIMENTAL

4.2.1 Calculation

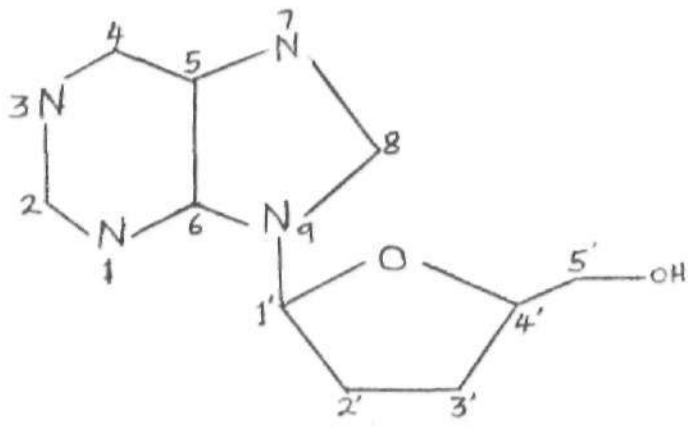
Primary structural data for various compounds of nucleosides and nucleotides were obtained from x-ray analyses in literature with R_f generally less than 15%.

4.2.1.1 Asymmetry and Geometric Parameters

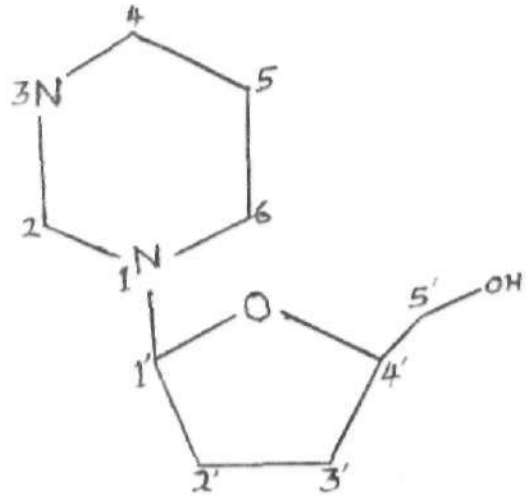
Asymmetry parameters ΔC_2 and ΔC_s were calculated as in Thomas (1982, 1985) using the expressions proposed by Duax and Coworkers (Duax et al, 1976) (see section 3.2.2 for equations). The parameter, $\Sigma/\phi/$, the sum of the moduli of the endocyclic torsion angles, were worked out in each case. The furanose ring is regarded as essentially planar if $\Sigma/\phi/$ is less than 42°, the expected value for the maximum attainable torsion angle in the ideal cyclopentane half-chair form (Bucourt, 1974).

4.2.2 Atomic numbering Scheme and Nomenclature for Conformations

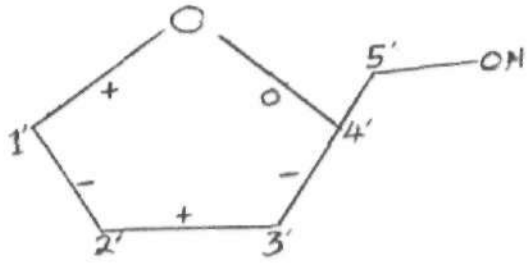
The atomic numbering schemes for the ß-purine and ß-pyrimidine are shown in figure 4.2 (a and b) respectively. The conformations are described in this work as envelope (C_s) and half-chair (C_2) forms. The half-chair conformation is essentially a 1, 2 - diplanar form instead of a monoplanar form of the cyclohexane derivative, the nomenclature proposed by Bucourt (1974). The envelope form, on the other hand, is a monoplanar form as indicated in figure 4.2 (c and d).



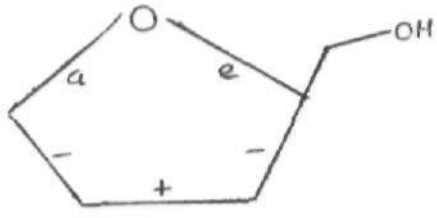
(a) Purine



(b) Pyrimidine



Envelope
(monoplanar)
(c)



Half-chair (a~e<b, c,d)

(d)

Figure 4.2 Atomic numbering scheme and designation of torsion angles for purines and pyrimidines; (c,d) nomenclature for some symmetric conformations of some furanose rings.

4.3 RESULTS AND DISCUSSION

The names, codes and references for all the compounds used in this study are given in appendix VI. The geometric ($\Sigma/\phi/$) and conformational parameters (ΔC_2 and ΔC_S) for the envelope (C_S) and half-chair (C_2) forms of the furanose rings are shown in tables 4.1 and 4.2, while the corresponding endocyclic torsion angles are presented in table 4.3. The relative conformations are displayed in the plots of mirror asymmetry parameter, ΔC_S (3') versus the rotational asymmetry parameter ΔC_2 (2'-3') in figure 4.3 and ΔC_2 (3'-4') are displayed in figures 4.5 and 4.6 respectively. In each case the atoms C(3') or C(2') are the out-of-plane atoms in the envelope forms of these classes of furanose derivatives. It is not easy to decipher any distinctive structural factor that favours either the C(2') or C(3') envelope, even though Munns and Tollin (1970) have attributed it to intermolecular contact of exocyclic substituents and special packing considerations such as inter-molecular hydrogen bonding. In this study also, it appears that in most cases if the torsion angle a (figure 4.2) is less than e, the ring adopts a C_S(3') envelope conformation and if the torsion angle a is greater than e, the ring adopts C_S(2') envelope conformation. From table 4.1 and figure 4.2, it is clear that the conformation of the

furanose ring is independent of whether the base is a pyrimidine or purine system in nucleosides and nucleotides. The values of the sum of moduli of the torsion angles, $\Sigma/\phi/$, also indicate that puckering of the furanose ring is independent of the base system in nucleosides and nucleotides. There is also no exact correspondence between the extent of puckering of the furanose ring and the size of the substituents on the ring.

Figures 4.3 and 4.4 show the possibility of interconversions between the C(3') envelope and either the C(2'), C(3') half-chair or C(3'), C(4') half-chair conformation. These interconversions between the C_s envelope and C_2 half-chair forms are similar to those observed in some 2,4-bridged saturated -lactone rings (Thomas and Agbaji, 1989). However, in the furanose rings, there appears to be a clustering of the conformational forms at intermediate points in the pseudorotation pathway between the C(3') envelope and C(2'), C(3') half-chair (figure 4.3). The structures of the furanose rings in chart 4.1, show that the ring adopts a C_s(3') or C_s(2') envelope conformation when the hydrogen groups on C(2') and C(3') atoms are either both ß- or both α- oriented as in F7, F8, F9, F11 and F12. However, if one of the hydroxy group is ß- oriented and the other α- oriented, the furanose ring adopted a

conformation intermediate between $C_s(3')$ envelope and $C_2(2'-3')$ half-chair forms (F1, F2, F5, F6 and F15).

Table 4.1 Geometric and Conformational Parameters for some furanose rings

Compound Code	$\Sigma/\phi/$	$\Delta C_2(1'-2')$	$\Delta C_2(3'-4')$	$\Delta C_2(3'-4')$	$\Delta C_S(2')$	$\Delta C_S(3')$
F1	134.7		8.9			8.8
F2	112.0		7.7			7.1
F3	129.8		12.5			5.8
F4	127.2		9.4			7.5
F5	116.0		8.8			6.6
F6	124.3		9.6			7.3
F7	123.4		11.8			5.4
F8	123.0		13.2			4.3
F9	127.2		16.7			2.3
F10	114.3		14.2			2.9
F11	126.3		8.1			4.1
F12	129.0		7.2			5.2
F13	129.4		3.7			12.0
F14	122.3		3.5			11.4
F15	114.7		6.3			8.3
F16	124.1		5.5			12.2
F17	130.6			15.0		4.0
F18	112.6			10.6		5.8
F19	121.3			13.4		4.4
F20	119.2			8.4		8.1
F21	120.0			8.2		4.0
F22	104.7			8.4		2.0
F23	132.6			2.1		14.0
F24	106.6			2.3		10.9
F25	107.6			4.7		12.3
F26	138.1	11.2			8.3	
F27	119.2	10.2			6.7	
F28	120.4	11.0			6.1	

Compound Code	$\Sigma/\phi/$	$\Delta C_2(1'-2')$	$\Delta C_2(3'-4')$	$\Delta C_2(3'-4')$	$\Delta C_s(2')$	$\Delta C_s(3')$
F29	126.9	17.3			2.6	
F30	137.6	18.7			2.4	
F31	112.0	17.1			0.1	
F32	123.3	10.0			7.4	
F33	137.4	11.2			8.1	
F34	113.0	17.3			0.7	
F35	118.4	16.7			1.4	
F36	110.7	11.8			1.8	
F37	113.0	10.9			4.9	
F38	133.7	10.2			2.9	
F39	124.0	7.9			4.5	
F40	109.2	9.2			5.8	
F41	133.7	2.1			14.4	
F42	119.5	6.9			9.3	
F43	106.7	6.9			7.6	
F44	149.7	0.25			12.5	
F45	136.3	6.0			11.2	
F46	133.1	7.4			10.4	
F47	127.2	1.98			13.7	
F48	143.2	6.0			11.6	
F49	112.0		17.5		1.2	
F50	119.2		16.7		1.5	
F51	125.0		17.6		1.4	
F52	101.5		13.2		1.9	
F53	116.6		12.4		0.5	
F54	119.6		6.4		8.9	
F55	123.3		0.85		14.7	
F56	121.6		7.9		8.3	
F57	114.8		7.6		8.7	

Table 4.2 Geometric and Conformational Parameters for some furanose rings

Code Code	$\Sigma/\phi/$	$\Delta C_2(01'-4')$	$\Delta C_2(1'-01')$	$\Delta C_2(3'-4')$	$\Delta C_s(1')$	$\Delta C_s(01')$	$\Delta C_s(4')$
F58	115.2	6.9				4.4	
F59	107.0		12.0		4.2		
F60	142.4			**5.7**			7.4
F61	153.9			**5.6**			8.3
F62	132.6		1.9			10.2	

Table 4.3 Endocyclic Torsion Angles of Some Furanose Rings

Compound Code	Torsion Angle * (deg)				
	a	b	c	d	e
F1	7.8	-30.6	40.6	-37.1	18.6
F2	6.5	-25.0	33.8	-31.4	15.3
F3	5.0	-28.7	38.5	-36.9	20.7
F4	6.9	-28.5	38.1	-35.5	18.2
F5	6.3	-25.5	35.2	-32.3	18.7
F6	6.2	-28.0	37.4	-34.7	18.0
F7	4.9	-26.8	37.1	-35.3	19.3
F8	4.1	-25.9	37.2	-35.9	29.9
F9	2.3	-25.7	38.5	-38.2	22.5
F10	-2.4	23.9	-34.4	33.7	-19.9
F11	-19.5	35.7	-37.9	27.7	- 5.5
F12	18.8	-36.0	39.1	-28.7	6.4
F13	9.0	-29.5	37.1	-32.9	15.2
F14	9.8	-29.5	36.9	-31.9	14.2
F15	7.5	-26.6	34.3	-31.0	15.3
F16	-14.7	33.2	-37.7	31.3	- 7.2
F17	-3.8	21.3	38.2	-41.1	26.2
F18	-3.9	17.6	31.2	-34.9	25.0
F19	-3.4	-20.1	34.6	37.6	25.6
F20	-27.3	36.9	-31.9	17.0	6.1
F21	26.2	-36.9	35.5	-19.0	-4.4
F22	31.0	-31.9	21.2	-3.6	-12.0
F23	-11.3	-14.3	33.1	-40.6	33.3
F24	8.8	12.0	-26.9	32.0	-26.3
F25	-25.9	38.6	-26.9	13.9	2.3
F26	-30.5	43.5	-37.8	20.2	6.1

Compound Code	Torsion Angle * (deg)				
	a	b	c	d	e
F27	-26.7	36.9	-32.6	18.0	5.0
F28	-26.5	37.1	-32.2	18.8	4.8
F29	-25.8	39.3	-36.8	23.2	1.3
F30	-24.4	42.0	-41.4	27.7	-2.1
F31	-22.1	34.7	-33.4	21.6	0.2
F32	-27.9	38.1	-33.1	18.7	5.5
F33	-30.7	42.6	-37.6	20.4	6.1
F34	-22.0	35.0	-34.0	22.0	0.0
F35	21.9	35.7	-35.5	23.8	-1.5
F36	-18.0	32.2	-33.2	23.7	-3.6
F37	-17.8	32.3	-33.8	24.6	-4.5
F38	-19.4	37.1	-40.3	30.1	-6.8
F39	5.0	19.4	-34.0	38.1	-27.5
F40	-15.8	31.4	-33.0	23.8	-5.2
F41	-33.4	41.0	33.1	14.6	11.6
F42	-28.1	36.7	-32.0	15.8	6.9
F43	-24.7	32.8	-28.3	14.9	6.0
F44	-14.5	-14.0	37.5	-46.2	37.5
F45	-16.9	36.5	-41.2	32.1	-9.6
F46	-31.2	41.2	-34.8	17.9	8.0
F47	31.7	-39.1	31.6	-13.8	-11.0
F48	-38.5	44.2	-32.4	11.1	17.0
F49	-22.6	37.0	-36.7	24.4	-1.3
F50	-22.6	36.0	-34.4	24.0	-2.2
F51	-23.4	37.7	-37.3	25.3	-1.8
F52	-17.6	30.6	-31.0	20.2	-2.1

Compound Code	Torsion Angle * (deg) a	b	c	d	e
F53	1.1	-22.9	34.7	-35.6	-22.3
F54	-15.6	32.5	35.9	27.2	-7.9
F55	-11.5	30.9	-36.9	31.4	-12.6
F56	-7.0	27.8	-369	33.2	-16.7
F57	-4.6	32.8	-34.3	25.2	-17.9
F58	36.0	-24.4	5.5	16.1	-33.2
F59	-22.6	**1.8**	17.2	-31.2	34.2
F60	38.7	-44.3	31.7	**-9.3**	-18.4
F61	41.5	-48.1	34.6	-10.4	-19.3
F62	34.6	-13.4	-10.5	32.0	-42.1

* The various torsion angles are coded a, b, c, d and e as shown in figure 3.1.

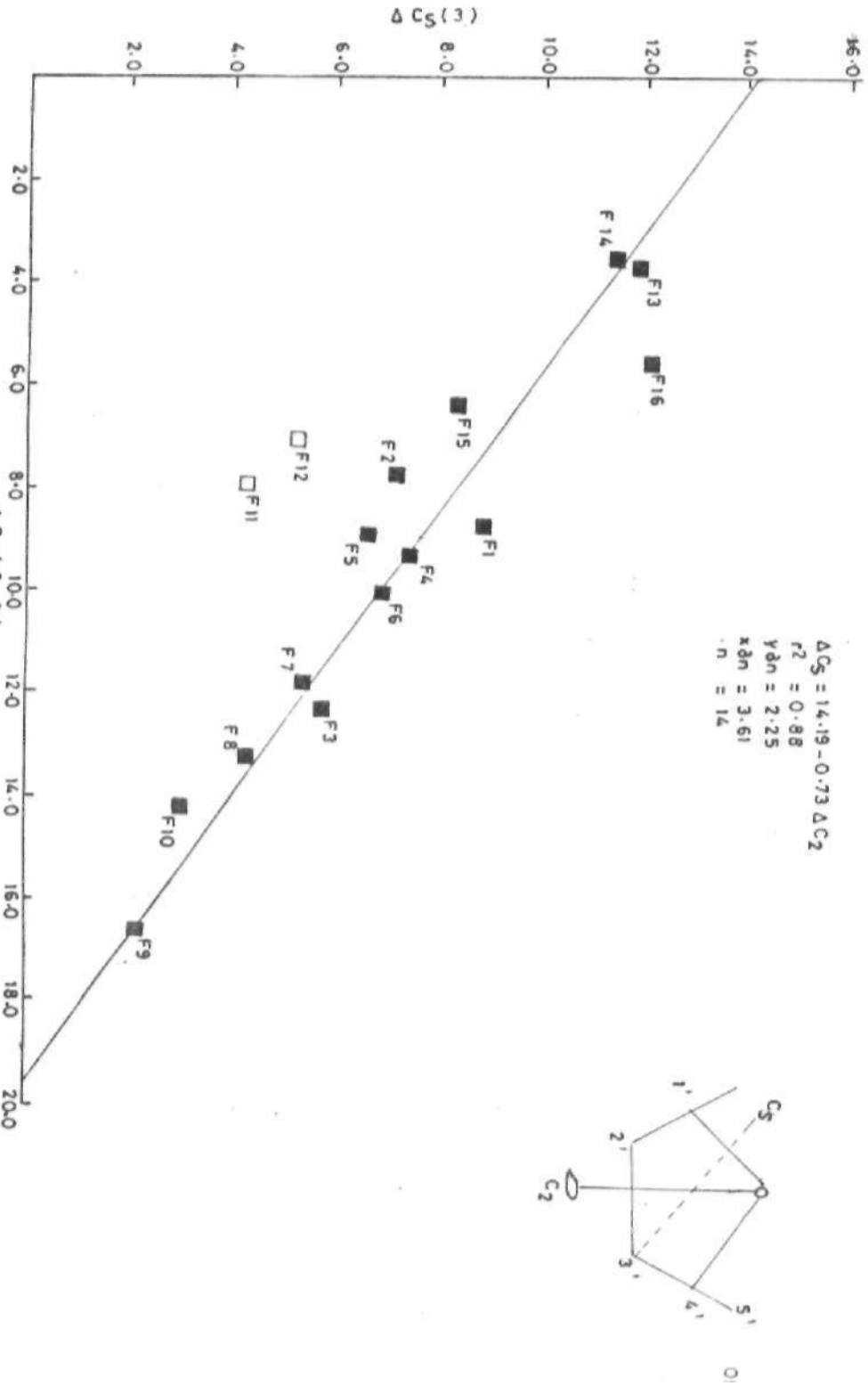


FIG. 4.3 : CORRELATED VARIATION IN PRINCIPAL ASYMMETRY PARAMETERS OF SOME NONPLANAR $\Delta C_2(2\text{-}3)$ VERSUS $\Delta C(3)$ FURANOSE RINGS$_4$. POINTS INDICATED BY □ WERE NOT INCLUDED IN CALCULATION OF THE LEAST SQUARE LINE.

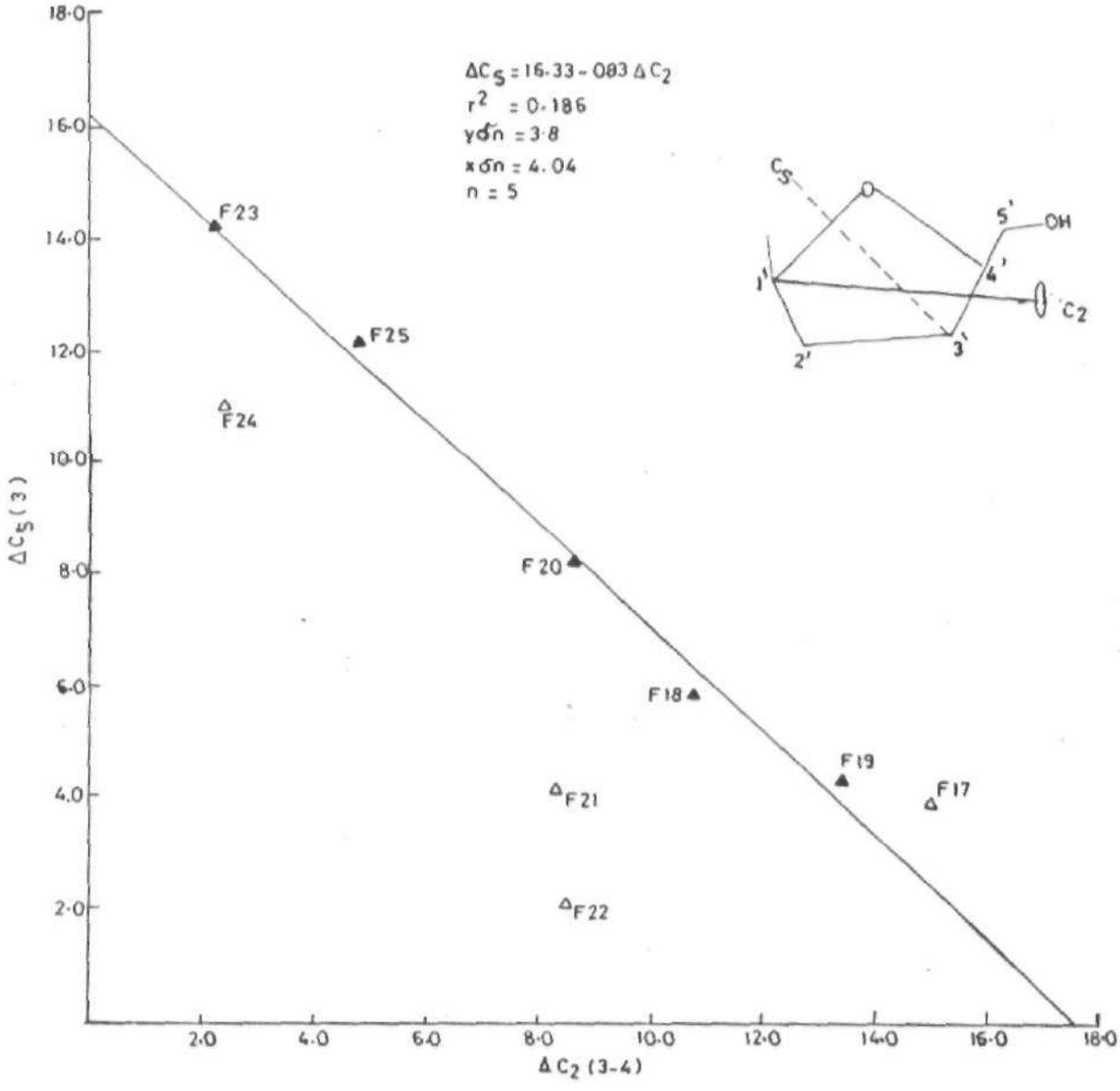


FIG.4.4 : CORRELATED VARIATION IN PRINCIPAL ASYMMETRY PARAMETERS OF SOME MONPLANAR $\Delta C_2(3-4)$ VERSUS $\Delta C_5(3)$ FURANOSE RINGS. POINTS INDICATED BY Δ WERE NOT INCLUED IN CALCULATION OF THE LEAST SQUARE LINE.

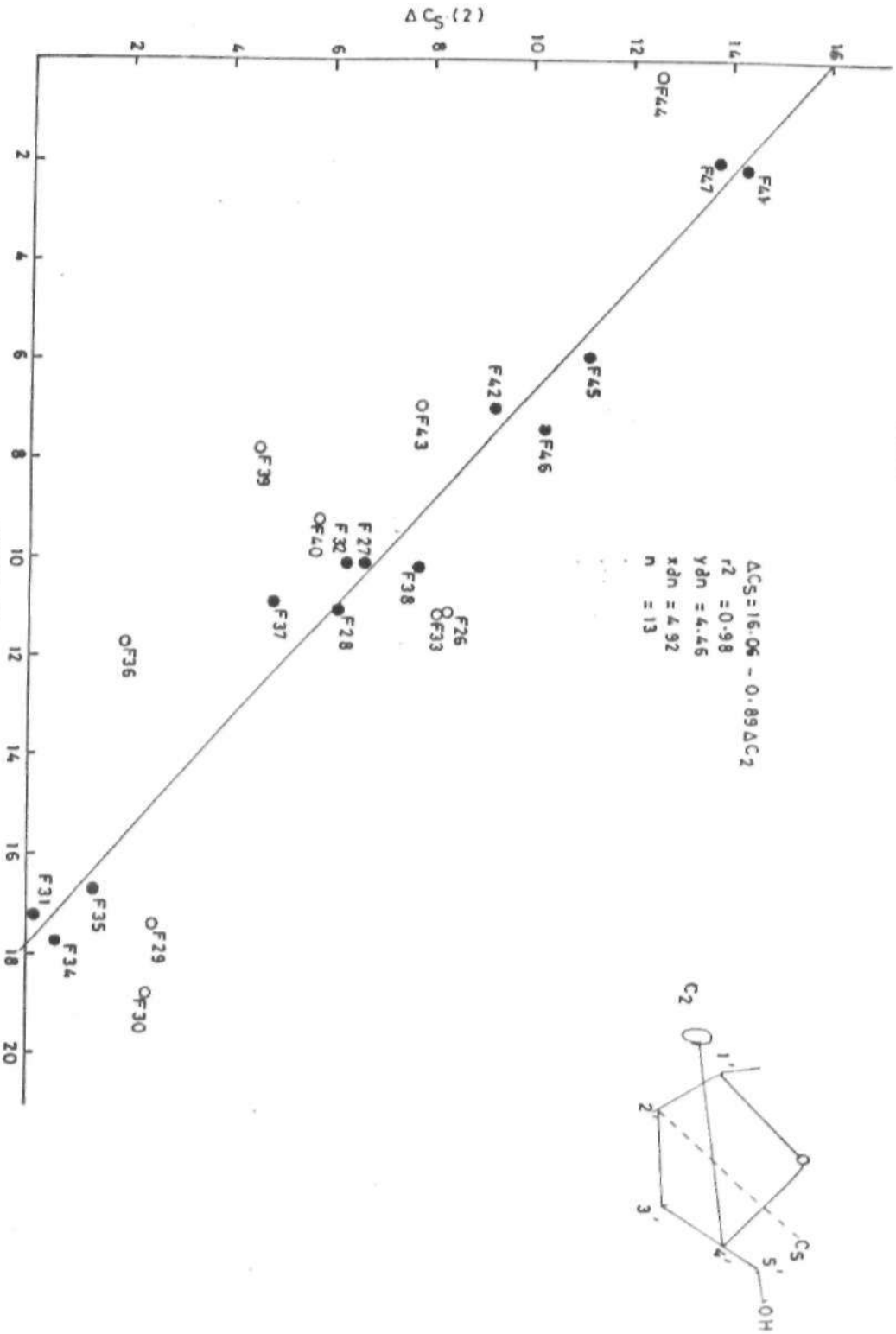


FIG. 4.5: CORRELATED VARIATION IN PRINCIPAL ASYMMETRY PARAMETERS OF SOME $\Delta C_2(1-2)$ VERSUS $\Delta C_S(2)$ FURANOSE RINGS. POINT INDICATED BY (o) WERE NOT INCLUDED IN CALCULATION OF THE LEAST SQUARE LINE.

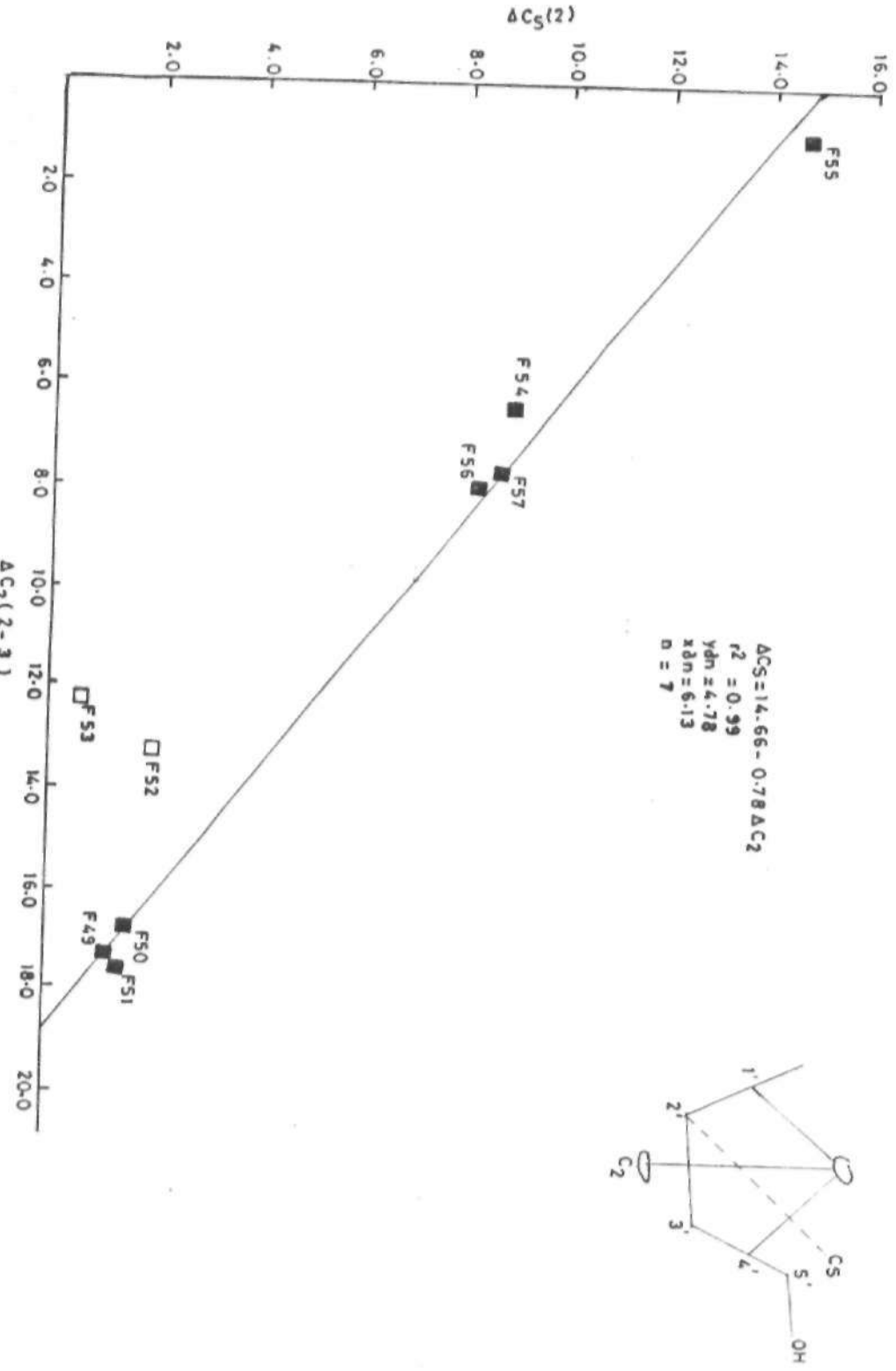


FIG.4.6:CORRELATED VARIATION IN PRINCIPAL ASYMMETRY PARAMETERS OF SOME ΔC_2 (2-3) VERSUS ΔC_5(2) FURANOSE RINGS. POINTS INDICATED BY □ WERE NOT INCLUDED IN CALCULATION OF LEAST SQUARE LINE.

Intermediate conformations are also adopted when bulky substituents such as phosphate or keto group replace the hydroxy group either at the C(2′), C(3′) or C(5′) atom as is the case in F2, F4, F11 and F13. Figure 4.4 shows the possibility of interconversion between the C(3′) envelope and the C(3′), C(4′) half-chair. F21, F22 and F24 show significant deviations from the apparent interconversion line, probably as a result of crystal packing forces or different hydrogen bonding schemes adopted by each molecule. F16 and F25 are two molecules in the same asymmetric unit, but have C(2′), C(3′) and C(3′), C(4′) half-chair conformations respectively. This suggests that crystal packing patterns can modify the conformation of furanose rings in the solid state.

The correlated variation in principal asymmetry parameters in figures 4.5 and 4.6, show the possibility of interconversion between the C(2′) envelope and either the C(1′), C(2′) half-chair or the C(2′), C(3′) half-chair conformations respectively. In figure 4.5, the conformations are clustered midway between the C(2′) envelope forms and the C(1′), C(2′) half-chair forms, while in figure 4.6, the clustering is largely at the C(2′) envelope form and midway in the C(2′) and C(2′), C(3′) pseudoratation pathway. Only few of the rings adopt either the C_2(1′-2′) form (F41, F44, F47) or C_2(2′-3′) form (F55). Furanose rings tends to move closer to

the C_2 half chair form when bulky substituents replace hydroxy group either at C(2'), C(3') or C(5) atom (F28, F40), or when one of the hydroxy groups on C(2') and C(3') atom is α-oriented (F27, F33, F39, F43), or when the ring is a deoxy-furanose ring (F32, F38, F42). Comparison of F27 with F31 suggests that halogen substituents may modify solid state base packing patterns (Buggi and Thewalt, 1969), which in turn modify the conformation of the furanose ring. Similarly, substitution of halogens at the C5 positions of F32, F37, F38 and F42, coupled with the presence of deoxy-furanose rings (F32, F38, F42), tend to force the rings to adopt intermediate forms, even though the halogen did not show a clear trend. This observation suggests that, there exist 1, 5 non-bonded interactions between the halogens at C5 and O(1') in agreement with the suggestion of Camerman et al (1965).

Figure 4.7 shows that F5 and F45 which are two molecules in the same asymmetric unit adopt different conformations. F5 adopts the C_5(3') envelope, while F45 adopts C_2(1'-2') half-chair conformation. This would indicate that packing forces in the crystal and hence environment of the molecule may play a major role in determining the conformation a furanose ring adopts. Other derivatives with two molecules in the same asymmetric units F31 and F48 (guanosine) and F49 and F46

(inosine), also adopt different conformations for each asymmetric unit pairs F31 is $C_s(2')$ envelope F48 is $C_2(1'-2')$ half-chair while F49 is $C_s(2')$ envelope and F46 is $C_2(1'-2')$ half chair forms. These conformations are formed inspite of the fact that inosine (F31 and F48) lacks the amino group at C4 which is an integral part of the hydrogen bonding scheme (Munns and Tollins, 1970). It has been suggested that the parallel stacking of these purine are of preponderant importance in determining the conformation of furanose rings.

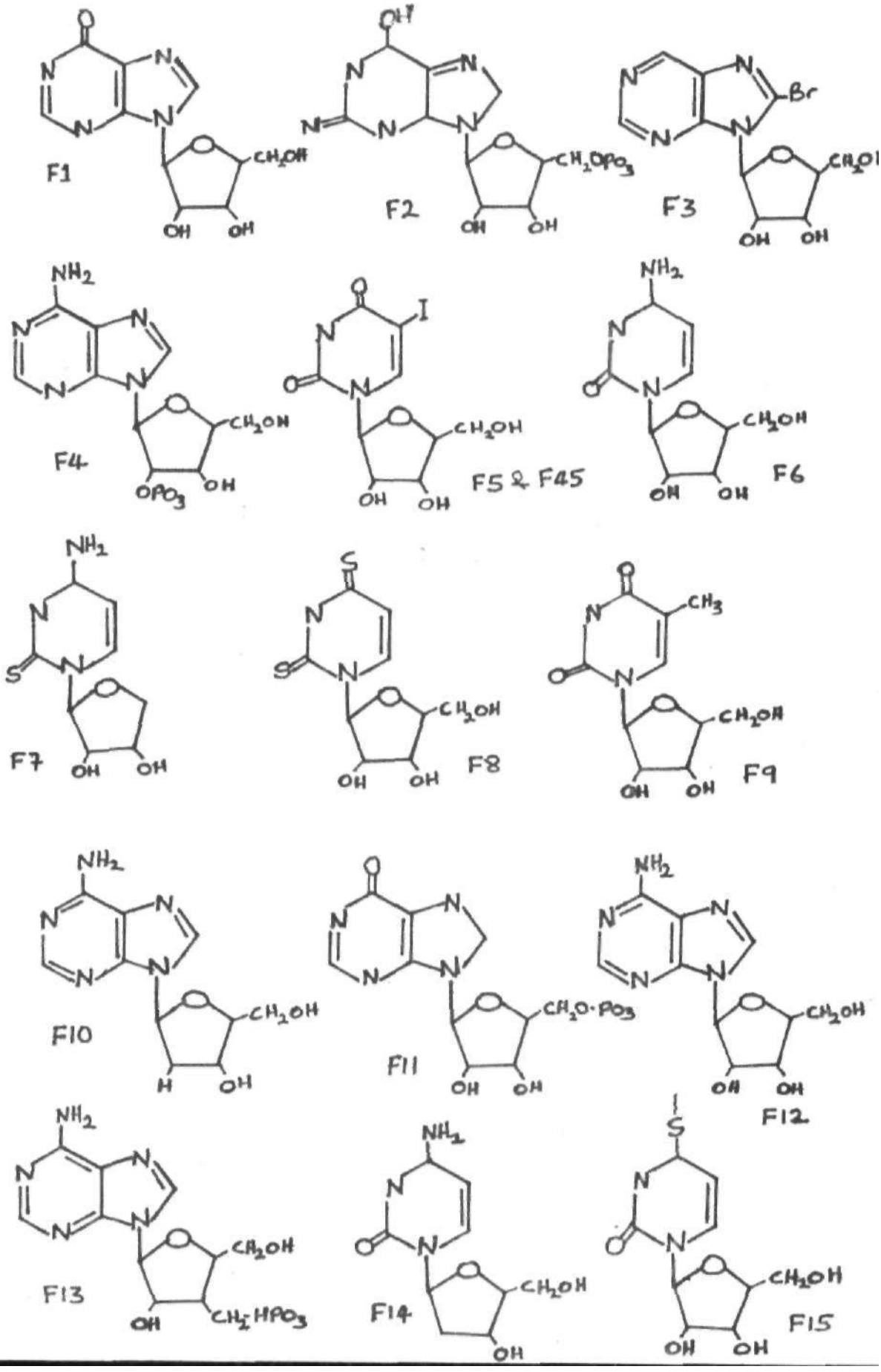
Special constraints may force atoms other than C(2') or C(3') out of the plane of the other ring atoms. The small value of the torsion angle about the bond C(1')-C(2') in F59 shows that the ring atoms C(3'), C(4') and O(1') are close to planarity and C(1') is displaced from the plane (table 4.3). This ring is shown to be distorted slightly from an envelope conformation (table 4.2). This contrasts with the earlier conclusion that puckering of the furanose ring occurs at either C(2') or C(3') or at both atoms in the half-chair form (Sundaralingam, 1965). The observed conformation agrees well with that suggested earlier (Beale et al, 1971). Similarly small value of torsion angle about the bond C(2')-C(3') of F58, as a result of the cyclic phosphate attached to the C(2') and C(3') ring atoms, cause the furanose ring to flatten and making the bonds C(1')-C(2')

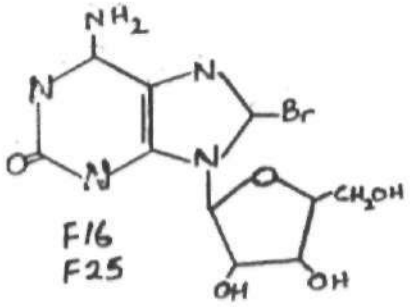
and C(3')-C(4') slightly coplanar. This results in the displacement of O(1') from the plane of the other four atoms giving an O(1') envelope conformation. F60 and F61 also contain cyclic phosphate groups at positions C(3')-C(4') of the furanose ring. The fusion of the cyclic phosphate group is cis, thus causing the ring to adopt a C_2(3'-4') half-chair conformation, while in F44, the cyclic phosphate at position C(3')-C(4') is trans and the ring adopts a C_2(1'-2') half-chair form. From results obtained for F44, F57, F59 and F60, it can be seen that the position and stereochemistry of the cyclic phosphates attached to the furanose ring may determine conformational forms that do not necessarily involve puckering at either the C(2') or C(3') atom.

From this study therefore, and from some previous studies on five-membered rings such as γ-lactone rings (Thomas and agbaji, 1989), D rings in steroids (Thomas, 1982), it has been shown that furanose rings like these other rings can be described in terms of C_s envelope forms with the possibility of any of the ring atoms being the out-of-plane atom and C_2 half-chair forms in which two atoms are displaced by approximately equal amounts on opposite directions from the plane of the remaining three atoms. From these studies (Thomas et al, 1982, 1989 and this work), it seems clear that many of the five-membered rings in natural products tend to adopt conformations

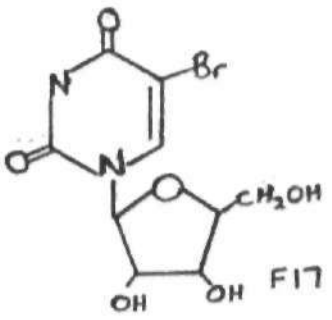
intermediate between the C_s envelope and C_2 half-chair. Only very few rings are found to have conformations at the extremes of the pseudorotational circuit. Reasons such as effects of non-bonded interactions, size and position of substituents, stereochemistry of ring fusion, packing patterns among others, have been deduced for these observations. In furanose rings additional constraints arising from intra and inter-molecular hydrogen bonding may also determine the conformation (Munns and Tollins, 1970).

Chart 4.1 Structural formulae of compounds discussed showing the molecular environments of the furanose rings.

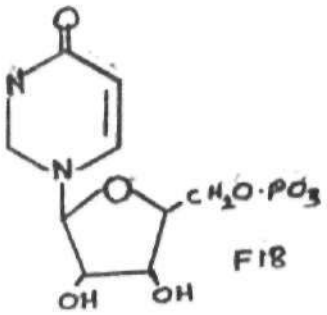




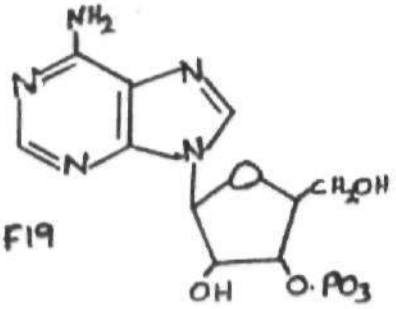
F16
F25



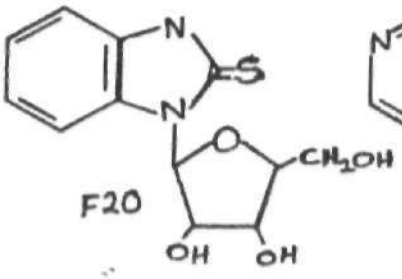
F17



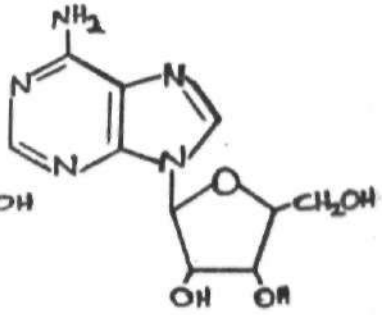
F18



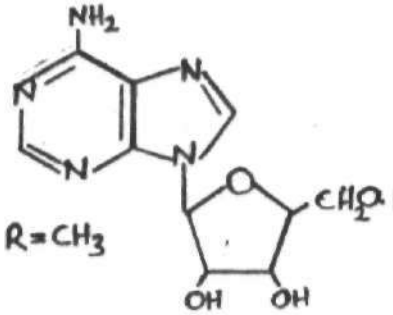
F19



F20

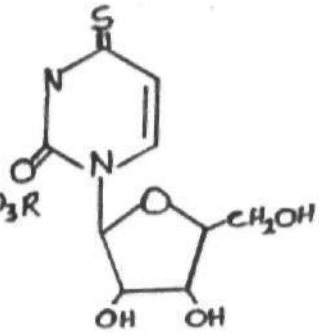


F21

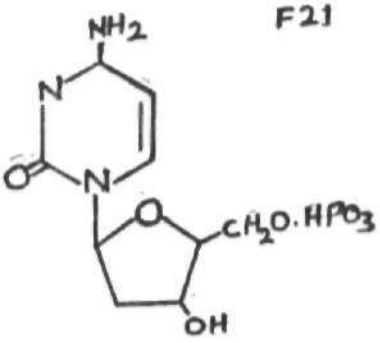


R=CH_3

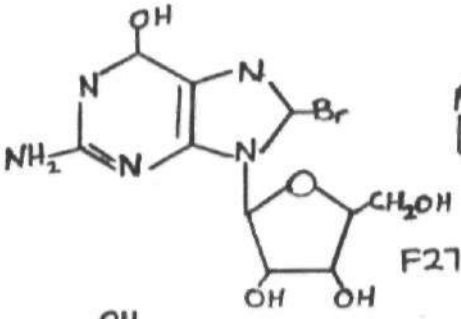
F22



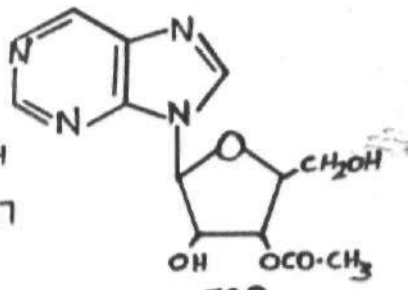
F23



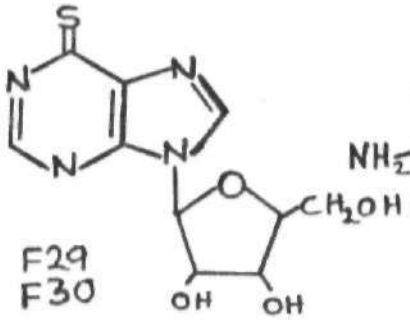
F24



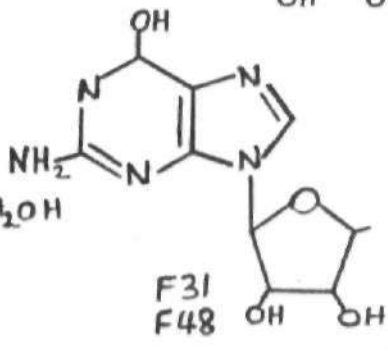
F27



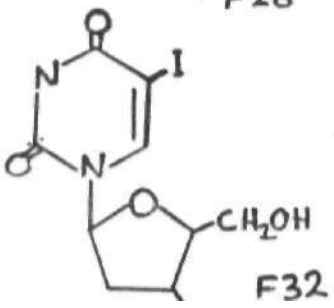
F28



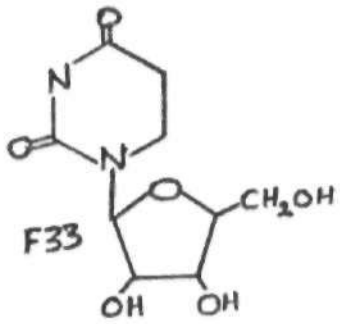
F29
F30

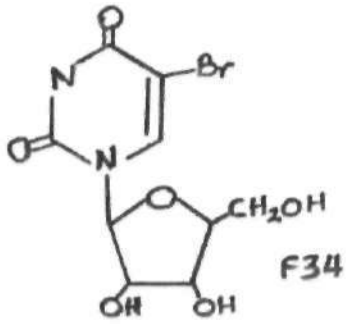


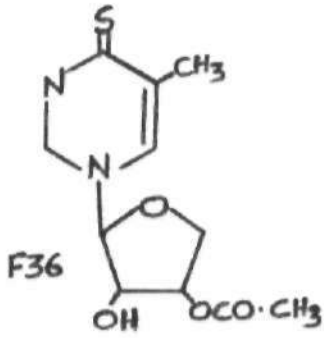
F31
F48

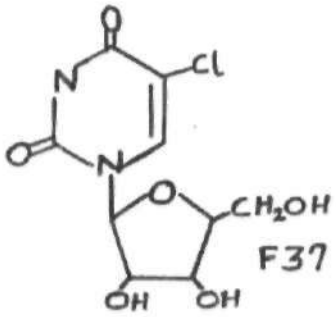


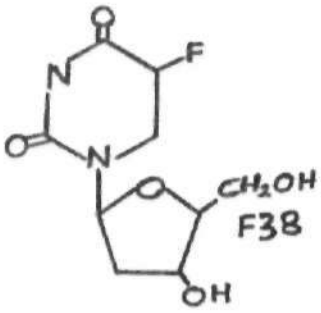
F32

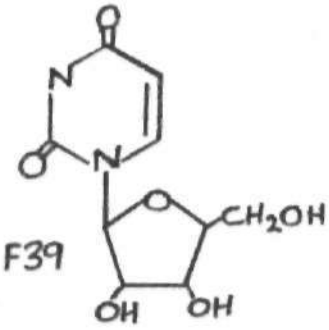

F33
CH2OH
OH
OH

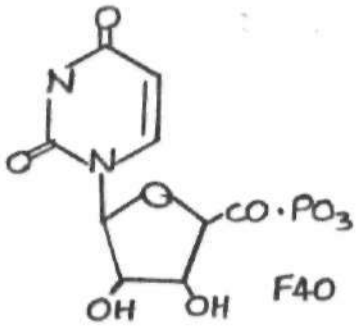

Br
CH2OH
F34
OH
OH

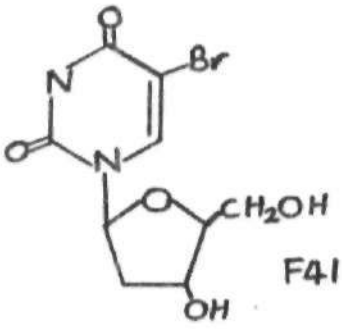

CH3
F36
OH
OCO·CH3

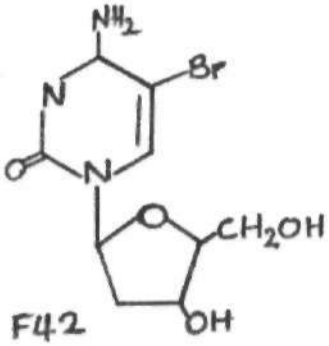

Cl
CH2OH
F37
OH
OH

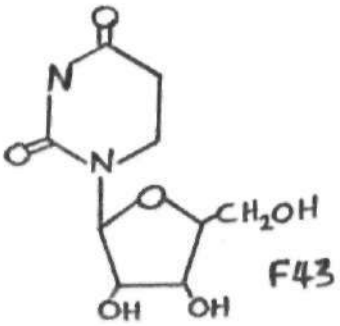

F
CH2OH
F38
OH

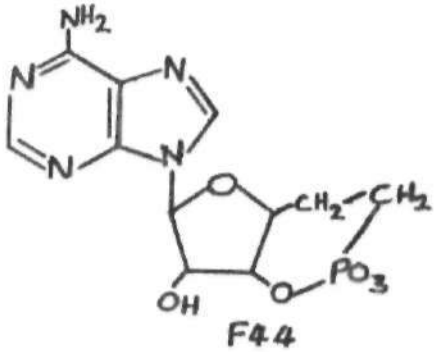

CH2OH
F39
OH
OH

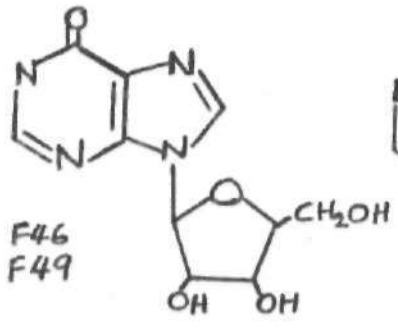

CO·PO3
F40
OH
OH

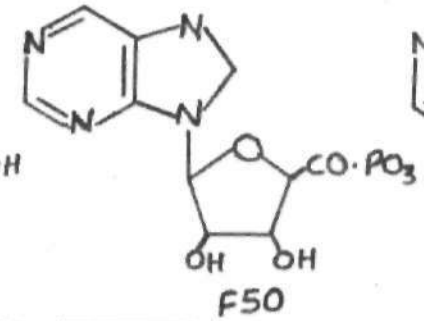

Br
CH2OH
F41
OH

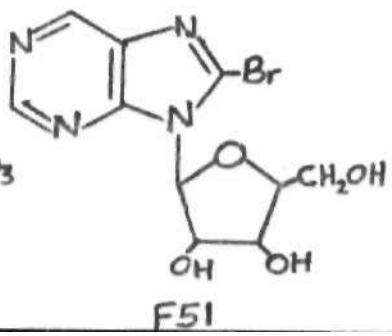

NH2
Br
CH2OH
F42
OH

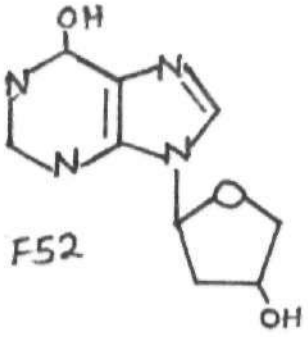

CH2OH
F43
OH
OH


NH2
CH2-CH2
PO3
OH
F44

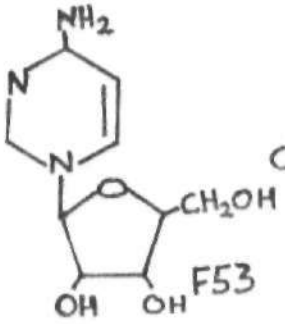

CH2OH
F46
F49
OH
OH


CO·PO3
OH
OH
F50

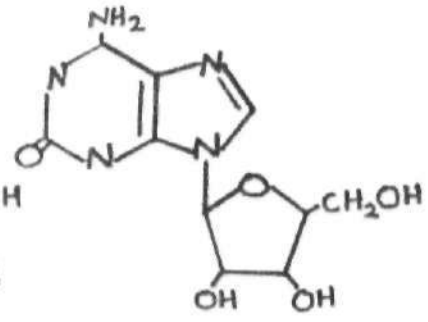

Br
CH2OH
OH
OH
F51



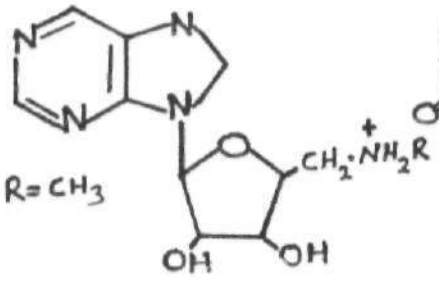
F52



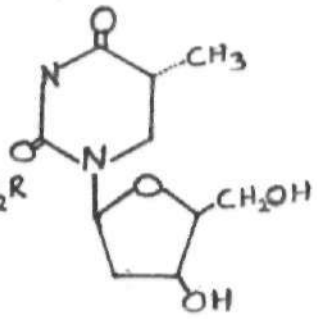
F53



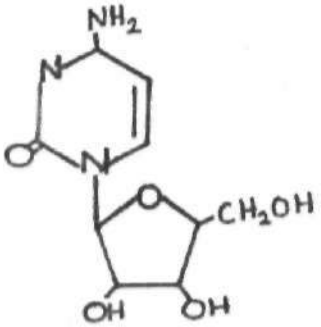
F54



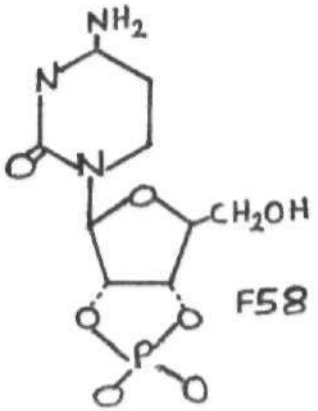
F55



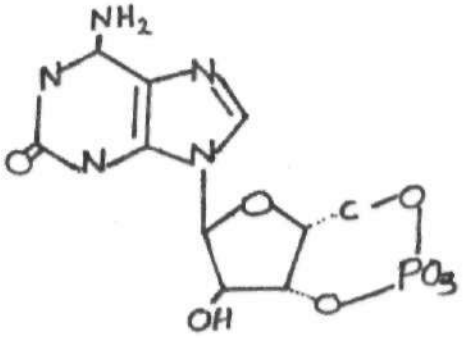
F56



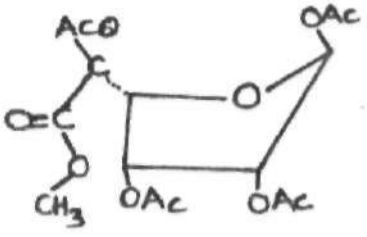
F57



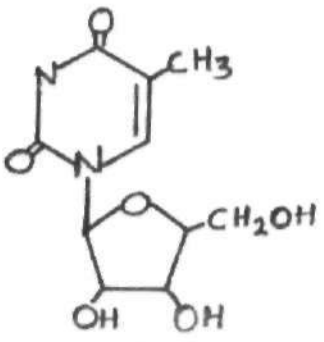
F58



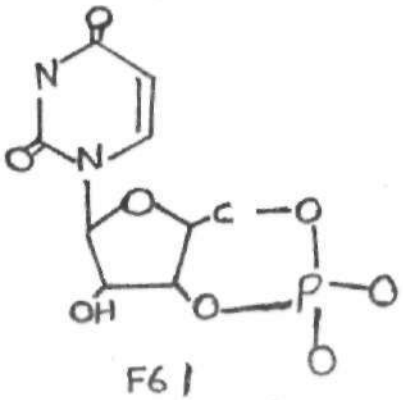
F60



F59



F62



F61

CHAPTER FIVE

5.0 MOLECULAR CONFORMATIONS OF SOME TEN-MEMBERED RINGS

5.1 INTRODUCTION

The methods used to calculate conformations of normal and medium rings have the general limitation of increasing complexity as the ring size increases. For ten-membered rings, no satisfactory systematic method for selecting the types of conformation to be tested has been proposed. Only with cyclopentane was a total solution possible (Altona et al, 1968). With medium rings the greater flexibility affords a large number of different shapes. This is partly because there are more rings representing energy minima of comparable magnitude and partly because these are of lower symmetry than rings like cyclohexane in which all carbons are geometrically identical (Hendrickson, 1964). Evidences are available (Hendrickson, 1967), that implicate only symmetrical conformers as candidates of preferred energy minima, hence the confinement of analyses of medium rings to symmetrical forms.

The basic symmetry elements through a 10-membered ring are either a plane or a two fold axis of symmetry through the molecule, passing through either a pair of opposite atoms (type A) or midpoints of a pair of opposite bonds (type B). Some ring forms have only one

serious candidates for viable molecular conformations. Similarly, viable forms with eclipsed bonds (w=0) are only found when the zeroes in the notation are not adjacent and when their replacement by (+) and (-) yields viable forms (Hendrickson, 1967). This is in effect the rotation of a plane to an axis in the next position around the ring and rotation to the right affords a conformation enantiomeric to the one formed on rotating to the left. Thus, even-membered rings of type A yield type B (of opposite symmetry) and vice versa.

This nomenclature system proposed by Hendrickson (1964), is related not only to the projection of a ring onto its plane of symmetry but also to the torsion angle convention. For example, the all-chair (C, CC, CCC) rings have fully alternating (+) and (-) torsion angles, ignoring eclipsed (w=0) bonds, and the boat regions in a conformation have a pair of like signs together, as can be seen in figure 5.1

The present study was carried out to attempt to parameterize the various conformations of cyclodecane ring derivatives in the solid state using the nomenclature system proposed by Hendrickson (1964) and asymmetric parameters (ΔC_2 and ΔC_s) defined by Duax et al, (1976). Attempts are also made to decipher factors which determine the various conformations adopted by the cyclodecane derivatives.

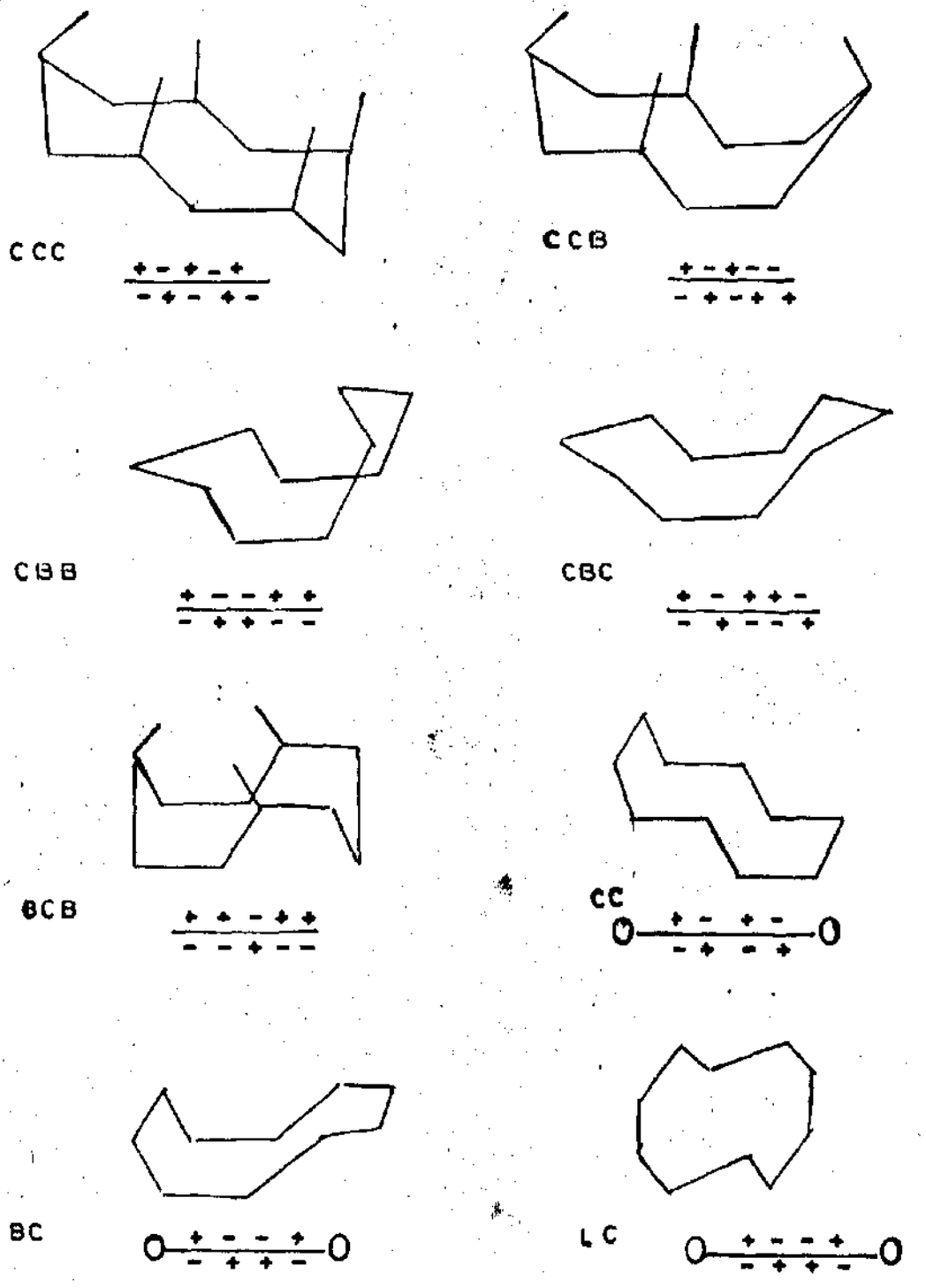


FIG.5.1;SOME VIABLE 10-MEMBERED RINGS WITH PLANES OF SYMMETRY (PLANE / ATOM)

5.2 EXPERIMENTAL

5.2.1 Calculation

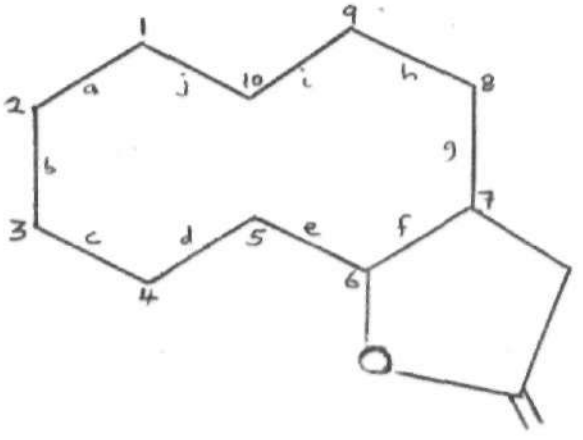
Primary structural data for various compounds of sesquiterpenoid and diterpenoid families were obtained from x-ray analyses with R_f generally less than 10%.

5.2.1.1 Asymmetry and Geometric Parameters

Calculations were made as described in section 3.2.2.

5.2.2 Atomic Numbering Scheme for 10-membered Ring of Sesquiterpenes

This is as shown below:



5.3 RESULTS AND DISCUSSION

Ring symmetries for the cyclodecane ring derivatives under study together with the ring conformations (obtained by the sign sequence of the torsion angles) are shown in table 5.1. The basic symmetry element is either a two-fold rotational axis or a mirror plane through the ring. The most prevalent element being the C_2 rotational axis. The C_s plane is observed clearly, only in structures T3 and T13. In some cases (T10, T11, T22, T23), the mirror plane is destroyed probably because of severe distortions resulting from steric crowding of substituents on the cyclodecane ring. Conformation (ΔC_s and ΔC_2) and geometric ($\Sigma/\phi/$) parameters are given in table 5.2. The corresponding torsion angles are listed in table 5.3. Figure 5.2 shows a plot of the asymmetric parameters ($\Delta C_2(2\text{-}3)$ and $\Delta C_s(3)$ or $\Delta C_s(5)$ of some of the cyclodecane ring derivatives, while chart 5.1 show the molecular environments of the various rings examined in this study. The name and references of the various compounds are given in appendix VIII.

The conformations of the rings with the chair central subunit i.e. Boat-chair-Boat, BCB (T1 -T11) appear to be the most viable owing to the peculiarly favourable torsional energy which outweighs the non-bonded strain situation that is the 1, 2-, 1, 3-, and 1, 4- nonbonded interactions (Hendrickson, 1964; Date,

1973). This form also has an axis perpendicular to its plane of symmetry; two parallel planes of three seriously interacting substituents each found above and below the molecular plane (figure 5.2) and as can be seen from figure 5.3, does not undergo pseudorotation. The boat forms or boat regions in the conformations are identified by a pair of like signs occurring together as can be seen in figure 5.1. It is observed that the cyclodecane ring derivatives adopting the BCB conformation generally have bulky substituents at either the C(3) and/or C(10) positions or may have a -lactone ring attached to C(7) and C(8) positions (figure 5.4). Relatively bulky substituents at the C(1), C(2), or C(3) positions may impose the BCB conformation on the ring (T9). A keto substituent at C(10) as in T3 and T4 also tends to impose a BCB conformation on the ring. It has been reported that the type of conformation adopted by cyclodecane ring derivatives may also depend on the cis- or trans- nature of the C(1)-C(10) and C(4)-C(5) double bonds of germacranolides (T5, T6 and T23) (Rechlewska, 1982). This however, does not apply to other 10-membered ring sesquiterpene.

Table 5.1 shows that T12 and T13 have the CCB and CBC conformations respectively. The CCB which belongs to the same group as BCB (i.e. having a chair central subunit) is intermediate in form between the more

symmetrical CCC and the BCB conformers. With two lactone rings at the C(4)-C(6) and C(7)-C(8) bonds and two epoxide groups at C(1)-C(10) and C(2)-C(3), T12 adopts the CCB conformation. The CBC conformation belong to another groups of boat family, that is the group that has a boat central subunit (BBB, CBB, CBC) (Hendrickson, 1964). All three forms suffer from non-bonded interactions, with the CBC having a 1, 3-nonbonded interaction (figure 5.1).

Table 5.1 Ring Symmetries and Conformations of some Cyclodecane derivatives.

Ser.No.	Compound Code	Ring Symmetry	Conformation
1	T1	C_2	BCB
2	T2	C_2	BCB
3	T3	C_s	BCB
4	T4	C_2	BCB
5	T5	C_2	BCB
6	T6	C_2	BCB
7	T7	C_2	BCB
8	T8	C_2	BCB
9	T9	C_2	BCB
10	T10	C_2	BCB
11	T11	C_2	BCB
12	T12	C_2	CCB
13	T13	C_s	CBC
14	T14	C_2	CCC
15	T15	C_2	CCC
16	T16	C_2	CCC
17	T17	C_2	CCC
18	T18	C_2	CCC
19	T19	C_2	CCC
20	T10	C_2	CCC
21	T21	C_2	CCC
22	T22	C_2	TCCC
23	T23	C_2	TCCC

Table 5.2 Geometric and Conformations at Parameters for some Cyclodecadiene Ring derivatives

	Compound Code	$\Sigma/\phi/$	ΔC_s	ΔC_2	Approx. Sym. of torsion angles
1	**T1**	739	38.3	30.08	C_2(1-2)
2	**T2**	941	25.4	7.2	C_2(1-2)
3	**T3**	942.1	33.03	55.4	C_s(2-3)
4	**T4**	951.9	32.5	51.3	C_s(2-3)
5	**T5**	843	56.1	44.1	C_2(4-5)
6	T6	660	85.5	36.1	C_2(4-5)
7	T7	904	43.8	22.01	C_2(2-3)
8	**T8**	872	56.1	47.8	C_2(2-3)
9	**T9**	**898**	42.3	42.2	C_2(3-4)
10	T10	884.8	-	41.8	C_2(3-4)
11	T11	914.1	-	39.5	C_2(3-4)
12	T12	778	57.96	48.2	C_2(2-3)
13	T13	957.3	43.9	-	C_s(4)
14	T14	1041	32.5	16.3	C_2(2-3)
15	T15	1062	30.15	21.65	C_2(2-3)
16	T16	1038.8	30.3	17.6	C_2(2-3)
17	T17	1056.3	32.2	19.4	C_2(2-3)
18	T18	1054	32.18	19.5	C_2(2-3)
19	T19	1049.1	36.4	12.18	C_2(2-3)
20	T10	1042	33.9	24.17	C_2(2-3)
21	T21	1038	33.2	30.7	C_2(2-3)
22	T22	853.3	-	67.2	C_2(2-3)
23	T23	889	-	70.1	C_2(4-5)

Table 5.3 Endocyclic Torsion Angles of Some Cyclodecadiene Derivative.

CODE	a	b	c	d	e	f	g	h	i	j
T1	-119	48	79	-70	-65	143	-61	-45	105	-4
T2	-143	55	55	-149	102	-57	103	-148	61	68
T3	53.7	30.4	-106.2	164.8	-108.1	65.4	-116.1	74.9	71.8	-150.7
T4	54.9	31.6	-106.9	163.5	-110.9	70.8	-116.2	70.4	73	-153.7
T5	-90	73	-87	165	-121	65	-38	-65	136	-3
T6	-56	14	-54	155	-101	36	-71	-44	125	4
T7	-91.3	53.6	-80.3	-163.2	122.5	14.4	-78.7	43.3	91.3	-166.2
T8	51	-115	109	1	-115	94	-54	113	-169	51
T9	-80	-58	92	4	-124	135	-80	61	-96	168
T10	-110.7	-0.9	92.4	-70.4	-64.8	158.6	-91.7	56.5	-87.6	151.2
T11	-114.6	-3.6	99.1	-69.2	-71.6	157.4	-93.7	66.4	-89.9	148.6
T12	66	-3	55	-163	116	-2	-90	73	57	-153
T13	-71.3	-37	94	158.8	90.2	56	-116.2	78.7	-92.4	162.7
T14	-101	54	-89	156	-132	87	-79	67	-111	165
T15	-107	50	-83	154	-137	93	-87	76	-108	165
T16	97.5	59.4	-85.7	155	-136	89.9	-75.7	66.6	-115.4	166.6
T17	-109.7	52.5	-89.5	145.8	-121.3	95.8	-91.6	76.4	-105.8	167.9
T18	-105.1	53.3	-85.7	147.8	-126.8	95.7	-87.5	74.2	-111.2	168.7
T19	-100.3	50.5	-87.5	157.2	-130.9	86	-82.2	75.2	-114.8	164.8
T20	-100.1	50.1	-87.7	152.1	-133.6	98.6	-80.7	62.4	-108.7	168
T21	-101	55	-82	146	-131	101	-80	55	-111	176
T22	62.6	43.6	115.6	-5.4	129.3	-80.6	56.3	-99.5	132.9	-127.5
T23	-97	75	-92	147	-119	95	-63	**56**	132	13

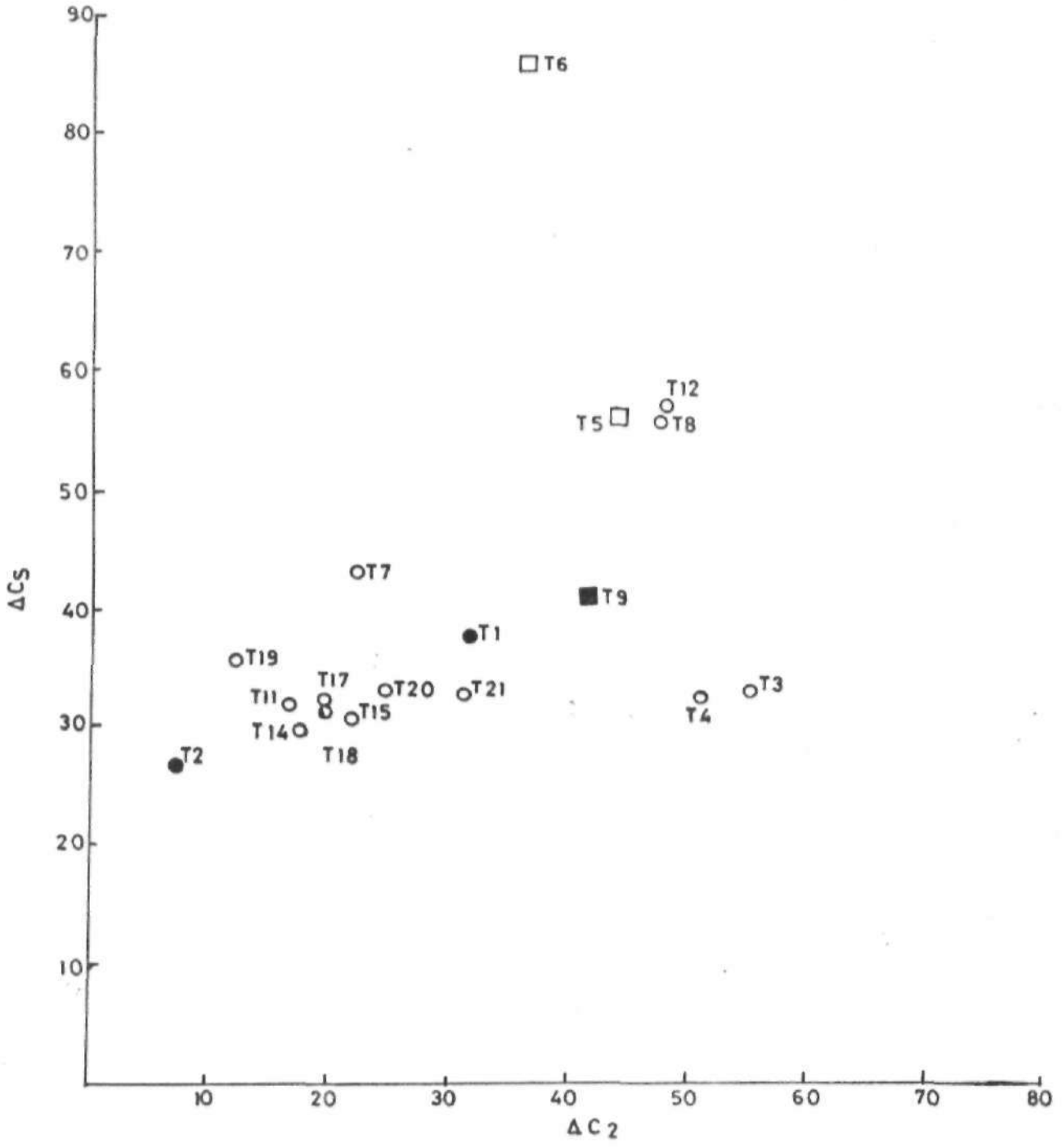


FIG. 5·3 : CORRELATED VARIATION IN PRINCIPAL ASYMMETRY PARAMETERS OF ΔC_2(2-3), o, ΔC_2 (1 2), ●, ΔC_2 (4-5), □, ΔC_2 (3-4), ■, OF SOME CYCLODECANE DERIVATIVES

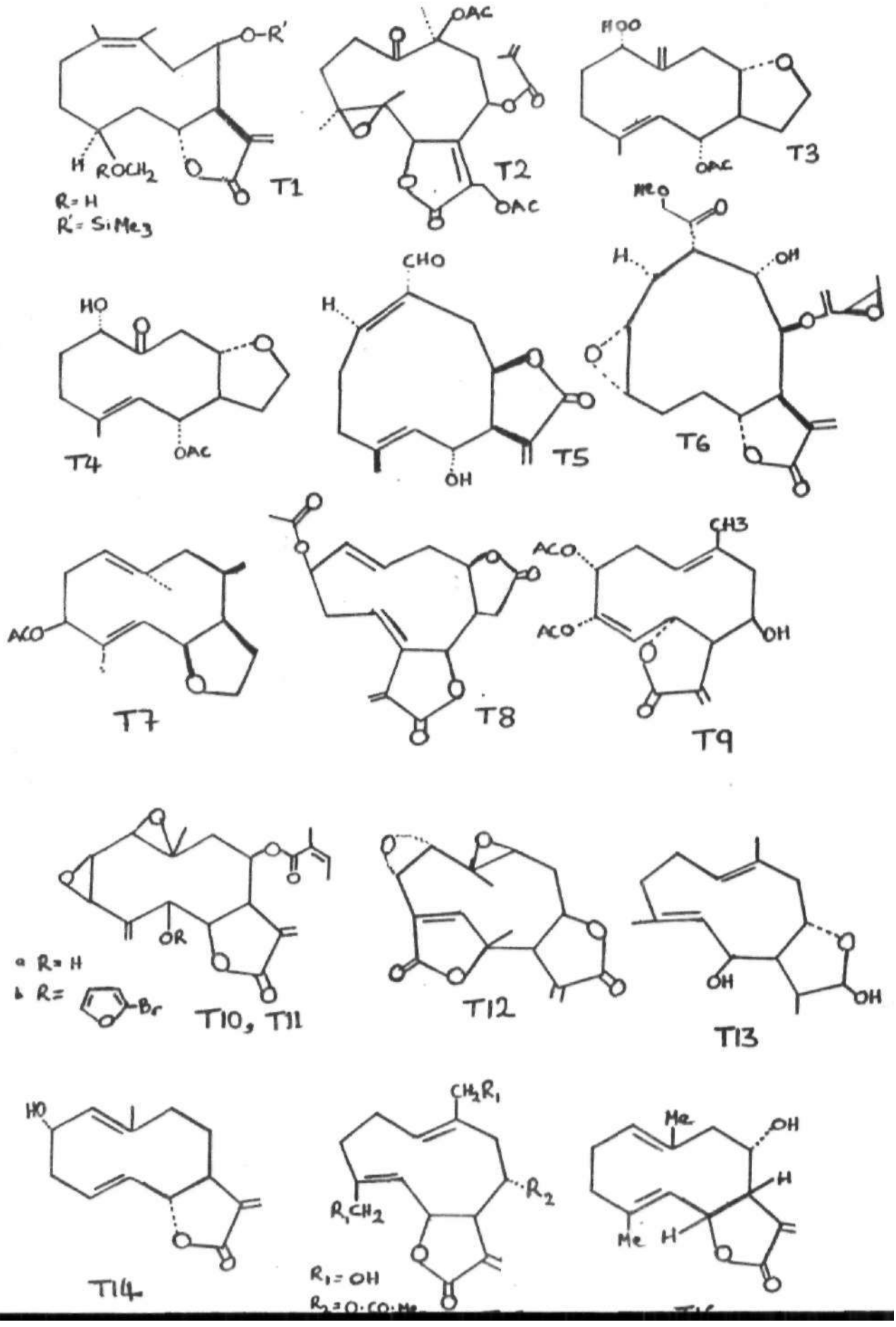
This is as a result of the strain imposed by the Central boat unit and all three have two eclipsed bonds. T13 was reported to have the BB (type B) conformation (Calleri et al, 1983), but is shown to have the CBC conformation (type A) in this study. (Figure 5.1, tables 5.1 and 5.2). The sign sequence of the torsion angles (table 5.3), shows that T13 has a CBC conformation, having an approximate $C_s(4)$ symmetry for the torsion angles. Furthermore, the BB conformation is not a viable form of type B cyclodecanes, having energetically unfavourable eclipsed butane units and severe H-H interpenetrations. The position of the lactol ring (i.e C(7)-C(8) in T13 and the absence of axial substituents may be responsible for the adoption of the transient (i.e CBC) conformation of the cyclodecadiene ring.

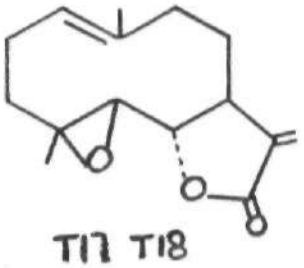
The all-chair (i.e the stair) form, T14 - T21 contain lactone rings fused at positions C(6)-C(7) and in most cases contain double bonds at C(1)-C(10) and C(4)-C(5). T17, T18 and T21 all have a C(4)-C(5) epoxide instead of the double bond. Fusion of the five-membered ring (i.e. whether Cis- or trans-) seem not to affect the conformation of the ten-membered ring. While this is also true for rings adopting the BCB conformation, the position of the five-membered ring seems to be one of the criteria for adopting the CCC conformation. All the rings that adopt the CCC conformation do not have ß-

oriented (i.e. axial) substituents at the C(8) position. T15 and T16 have α-oriented substituents at C(8), but this seem to be of no consequence to the conformation adopted by the rings.

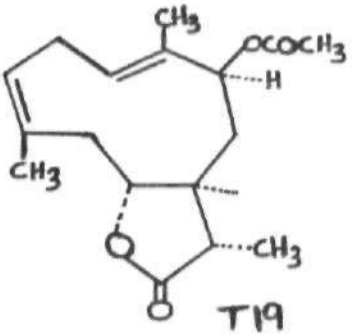
T22 and T23 adopt conformation close to the twist-chair-chair-chair (TCCC). Both have three like signs in sequence (table 5.3), and are either not rings at all or they contain severe interpenetrations of non-bonded substituent groups. Both have bulky and/or sterically demanding substitutions at C(6) to C(10). This unusual conformation is probably adopted to minimize the enhanced unfavourable steric strain introduced into the CCC form by these substituents. A BCB conformation is not adopted in the two cases as this form is known to be sterically more strained than the all chair form.

Chart 5.1 Structures of ten - membered rings showing the molecular environments

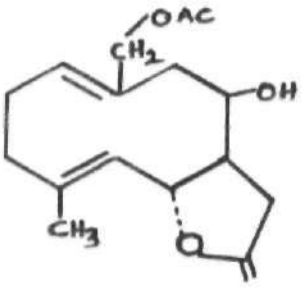




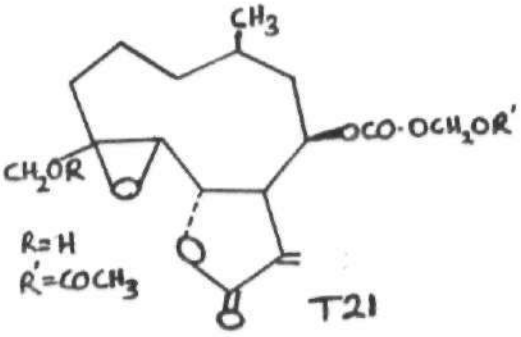
T17 T18



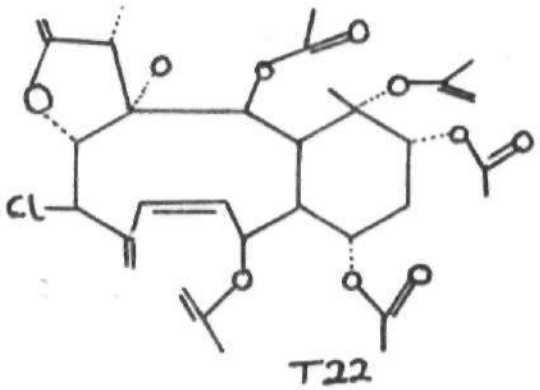
T19



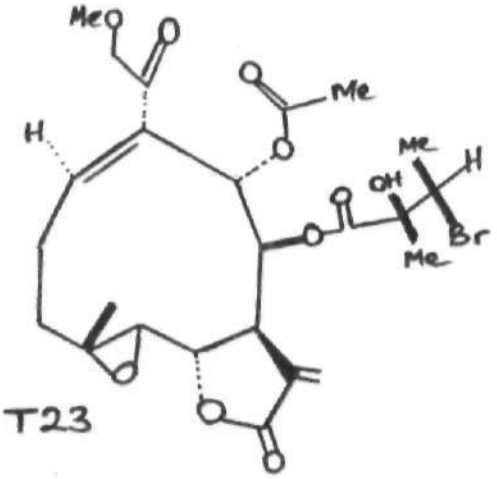
T20



T21



T22



T23

CHAPTER SIX

6.0 SUMMARY AND CONCLUSION

6.1 SUMMARY

The conformations adopted by some five-, seven-, and ten-membered ring derivatives in naturally occurring compounds in the solid state were investigated. The values of endocyclic torsion angles derived from x-ray diffraction structure determinations with R_f values generally less than 15% were obtained from literature and used for this study.

In the conformational study of the various ring types, sign sequences of the endocyclic torsion angles were used to determine the conformation of the ring types, as proposed by Hendrickson (1964) and Bucourt (1974). Asymmetric parameters, ΔC_s and ΔC_2 were calculated using the expression proposed by Duax and co-workers (Duax et al, 1976). The geometric parameter, $\Sigma/\phi/$, the sum of the moduli of the endocyclic torsion angles for each ring type was also calculated in each case and reflect the extent of puckering of the ring. The effects of the molecular environments on the conformation and geometry of these ring types were then elucidated based on the derived structural data.

6.2 CONCLUSION

6.2.1 Seven-membered rings

Although the twist-chair is estimated by energy calculations to be the most stable conformational form in the chair/twist-chair pseudorotational sequence of the cycloheptane, there is relatively no high preponderance of the twist-chair forms (eleven) over the chair forms (eight) among the derivatives reported in this study. On the other hand, the boat form is seldom observed in the boat/twist-boat sequence, with the twist-boat clearly the predominant form based on the structures examined in this study. The stereochemistry of fusion of 5-membered rings to cycloheptane derivatives is generally in agreement with molecular energy calculations. However, multiplicity of substituents on the ring may force a different fusion stereochemistry from the expected one in the solid state.

6.2.2 Five-membered rings

It is apparent that the five-membered furanose rings in nucleosides and nucleotides may adopt other confirmations where the out-of-plane atom is not C(2′) or C(3′). The type, size and stereochemistry of fusion of substituents may determine the type of conformation (i.e. either C_s envelope or C_2 half-chair) or in some cases determine the out-of-plane atom. Like some other five-

membered rings (such as 2.4-bridged γ -lactone and D rings in steroids) furanose rings adopt mainly, forms which are intermediate between the C_s envelope and C_2 half-chair conformations

6.2.3 Ten-membered rings

Although the preferred form of cyclodecane is thought to be the BCB form owing to its peculiarly favourable torsional energy compared to the all-chair form (CCC), a preponderance ratio of 17(BCB) rings to 8 (CCC) rings is observed in this study. The stereochemistry of fusion of the five-membered rings to cyclodecane derivatives seem not to affect the conformation of the 10-membered rings. However, the position of the five-membered ring is important. The (CCC) conformation appears to require fusion of a five-membered γ -lactone ring at the C(6)-C(7) bond. An axial substituent on C(8) or at the C(2) and C(3) atoms of the cyclodecane ring derivatives tend to confer the BCB conformation.

6.3 RECOMMENDATION FOR FURTHER STUDY

The correct orientations of substituents on the furanose rings of nucleosides and nucleotides should be ascertained. This will show how non-bonded interactions of substituents on the five-membered ring contribute to the type of conformation adopted by this ring.

PART II REFERENCES

Adams, W. J., Geise, H. J. and Bartell, L.S. (1970) "Structure, equilibrium conformation and pseudorotation in cyclopentane". J. Amer. Chem. Soc. 92, 5013.

Adman, F. and Margulis (1968) "Planar and Puckered Cyclobutanes". J. Amer. Chem. soc. 90, 4517.

Altona, C., Geise, H. J. and Romers, C. (1968) "Geometry and conformation of Ring D in some steroids from x-ray structure determinations" Tetrahedron, 24, 13.

Altona, C. and sundaralingam (1972) "Conformational analysis of sugar rings in nucleosides and nucleotides. A new description using the concept of pseudorotation" J. Amer. Chem. Soc. 94, 8205.

Barnes, C. L. and Hawkinson, S. W. (1979) "structure of adenosine 5'- methyl-phosphorate hemidydrate", Acta Cryst. B35, 1724.

Beale, J. P, Stephenson, N.C. and Stevens, J. D. (1971) "Conformation of a furanose carbohydrate" Chem. Comm., 25.

Begley, M. J., Combie, L., Gatuma, A. K. (1981) "Germacranolides of Erlangea cordifolia: Structure and absolute stereochemistry of cordifene" J. Chem. Soc. (perkin I), 2702.

Buaks, J. E., Vander Helm, D., Chang, C. Y. and Ciereszko, L. S. (1977), "The crystal and molecular structure of Briareim". Acta cryst. B33, 704.

Bucourt, R. (1974) "The torsion angle concept in conformational analysis" in Topics of stereochemistry. Vol. 8, Interscience publishers PP. 159 - 224.

Bugg, C. E. and Thewalt, U. (1969) "Crystal structure of 8-bromoguanosine". Biochem. Biophys. Res. Comm. 37, 623.

Buggs, C. E. and Marsh, R. E. (19) "Structure of monoclinic form of cytidylic acid b". J. Mol. Biol. 25, 67.

Bunick, G. and Voet, D. (1974) "Crystal and molecular structure of 9-ß-D-arabinofuranosyl adenine" Acta Cryst. B30, 1651.

Buys, H. R. and Geise, H. J. (1968) "Conformation of non aromatic compounds, Part L(1) Boat-Twist-Boat pseudorotation in six-membered ring compounds". Tetrahedron Lett., 5619.

Camerman, N. and Trotter, H. (1965) "The crystal and molecular structure of 5-1odo-2'-deoxy-uridine" Acta cryst. 18, 203.

Chwang, A. and Sundaralingam, M. (1974) "Crystal and molecular structure of a purine arabinonucleoside, 9-ß-D-Arabinofuranosyl adenine Hcl" Acta Cryst B30, 2273.

Chwang, A. and sundaralingam, M. (1974) "The crystal and molecular structure of guanosine 3', 5'- cyclic monophosphate" Acta cryst. B30, 1233.

Coulter, C. L. (1969) "Crystal and molecular structure of triethylammonium salt of cyclic uridine-3',5'-phosphate" Acta cryst. B25, 2055.

Coulter, C. L. (1973) "Crystal and molecular structure of sodium ß-cytidine 2', 3'-cyclic phosphate" J. Amer. Chem. Soc, 95, 570.

Cox, P. J. and Sim, G. A. (1974) "X-ray crystallographic determination of stereochemistry and conformation of Dihydrokanolide, a germacranolide diepoxide", J. Chem. Soc. (Perkin II), 1355.

Cox, P. J. and Sim. G. A. (1975a) "X-ray crystallographic determination of the stereochemistry and conformation of the germacranolide, Glaucolide A". J. Chem. Soc. (Perkin II), 455.

Cox, P. J. and Sim, G. A. (1975b) "X-ray crystallographic determination of the molecular structure of Berlandin, a guaianoside epoxide:. J. Chem. soc. (Perkin II), 459.

Cox, P. J. and Sim, G. A. (1977) "X-ray crystallographic analysis of pancin monohydrate, a pseudoguaianolide glucoside" J. Cehm. Soc. (Perkin II), 259.

Cox, P.J. and Sim. G. A (1976) "X-ray crystallographic determination of the stereochemistry and conformation of deacetylneotunulin" J. chem. soc. (Perkin II), 990.

Dale, J. (1976) "Multistep conformational interconversion mechanisms" in topics in stereochemistry Vol.9, interscience publishers. PP. 221 - 224.

Davis, M. and Hassel, O. (1963) "Electron diffraction investigation of molecules containing a cyclohexane type six-membered ring". Acta chem. scand. 17, 1181.

Duax, W. L., Weeks, C. M., and Rohrer, D. C. (1976) "Crystal structures of steroids: in Topics in stereochemistry. Vol. 9 Interscience publishers. PP. 271 - 383.

Dullforce, T. A., Sim, G. A. and White, D. N. J. (1971) "Stereochemistry of Gaillardin: Crystal and molecular structure of Bromogaillardin and Deacetyl-dihydrogaillardin P-Bromobenzoate" J. chem. Soc. (B), Part 2, 1399.

El-Feraly, F. S., Benigni, D. A. and Mcphail, A. T. (1983) "Biogenetic-type synthesis of santonin, chrysanolide, Dihydrochrysanolide, tulirinol, Arbusculin-c, Tenancetin and artemin". J. Chem. soc. (Perkin I), 355.

Eliel, E. L., Allinger, N. L., Angyal, S. J. and Morrison, G. A. (1967) Conformational analysis. Wiley - Interscience publishers.

Fronczek, F. N. (1979) "X-ray structure of fluor-guainolide derivatives" J. Chem. Soc. (Perkin II), 195.

Fronczek, F. R., Watkins, S. F, and Fischer, N. H. (1980) "Crystal and molecular structure of melampodin B, a 4,5-cis-9, 10-trans-Germacranolile sesguiterpene dilactone" J. Chem. Soc. (Perkin II), 1425.

Furbergs, S., Petersen, C. S. and Rømming, C. (1965) "A refinement of the crystal structure of cytidine" Acta cryst., 18, 313.

Gopalakrishna, E. M., Watson, W. A., Hoeneisen, M. and Silva, M. (1977), "Ovatifolin, a sesquiterpene lactone". J. Cryst Mol. struct. 7, 49.

Haschemeyer, A. E. and Sobell, H. M. (1965). "Crystal structure of a hydrogen bonded complex of adenosine and 5-bromouridine". Acta cryst 18, 525.

Haschemeyer, A. E. and Sobell, H. M. (1965). "The crystal structure of hydrogen bonded complex of deoxy-guanosine and 5-bromodeoxybytidine". Acta cryst. 19, 125.

Hecht, S. M. and Sundaralingam, M. (1972) "Stereochemistry of nucleic acids and their constituents xxvi: 3'-deoxy-3'-(dihydroxyphosphinylmethyl) adenosine: J. Amer. Chem. Soc. 94, 4314.

Hendrickson, J. B. (1967) "Molecular geometry vii. modes of interconversion in the medium rings". J. Amer. Chem. Soc., 89, 7047.

Hendrickson, J.B. (1963). "Conformational analysis in perhydroazulenic sesquiterpenes" Tetrahedron 19, 1387.

Hendrickson, J. B. (1965). "Molecular Geomertry IV. The medium Rings". J. Amer. Chem. Soc., 86, 4854.

Hendrickson, J. B. (1967). "Molecular geometry v. Evaluation of functions and conformation of medium rings". J. Amer. Chem. Soc. 89, 7036.

Hung-yin Lin, G., Sundaralingam, M. and Arora, S. K. (1971). "Stereochemistry of nucleic acids and their constituents xv. crystal structure of 2-Thio cytidine" J. Amer. Chem. soc. 93, 1235.

Hung-yin Lin, G. and sundaralingam, M. (1971). "stereochemistry of nucleic acids and their constituents crystal structure of 2, 4-dithio-uridine" Acta cryst. B27, 961.

Hunt, D. J. and Subramanian, M. (1969). "The crystal structure of 5-methyluridine". Acta cryst. B25, 2144.

Iball, J., Morgan, C. H. and Wilson, H. R. (1966) "The crystal and molecular structures of 5-bromo-2'-deoxyuridine and 5-bromouridine". Proc. Roy. soc. (London) ser. A. 295, 320.

Jones, P. G. and Kennard, O. (1979). "(95, 115)-9-Acetoxydihydrocostunolide (Herbolide A)" Acta cryst. B35, 1273.

Konnert, J., Karle, I.Z. and Karle, J, (1970) "The structure of dihydrothymidine" Acta cryst. B26, 770.

Kua-Hsiung, L. Takeatsu, K. and Masao, O. (1976) "The structure and stereochemistry of Eupahyssopin, A new antitumor germacranolide from Eupatorium hyssopifolium". Tetrahedron Letts., 1051.

Mazhar-ul-Haque, Rogers, D., Caughlan, C. N. (1974). "Crystal structure and absolute configuration of Bromoisotenulin". J. Chem. Soc. (Perkin II), 223.

Mcphail, A. T., and Sim. G. A. (1973). "Conformations of cycloheptane and α-methylene- -lactone rings in sesquiterpenoids: x-ray determination of the constitution, absolute stereochemistry and conformation of Euparotin bromoacetate". Tetrahedron, 29, 1751.

Mcphail, A. T. and Onan, K. D. (1975). "Crystal and Molecular structure of Eupatolide, the major cytotoxic principle from Eupatorium formosanum HAY". J. Chem. Soc. (Perkin II), 1798.

Mcphail, A. T. and Onan, K. D. (1976) "Crystal and Molecular structure of Eupaformonin, a cytotoxic germacranolide from Eupatorium formosanum HAY". J. Chem. Soc. (Perkin II), 578.

Micalleri, Giacomo, C, and Viterbo, D. (1983) "The structure of Hallerol, a Boat-Boat germacrane Lactol". J. Chem. Soc. (Perkin I), 2027.

Munns, A. R. I., Tollin, P. (1970) "The crystal structure of inosine:. Acta cryst. B26, 1101.

Murayama, W., Nagashima, N. and Shimizu, Y. (1969) "The crystal and molecular structure of guanosine - 5'-phosphate trihydrate". Acta Cryst. B25, 2236.

Nagashima, N. and Wakabayashi, K. (1974). "The crystal and molecular structure of inosine - 5'-phosphate". Acta cryst. B30, 320.

Nozaki, H. (1979). "Structure and absolute stereochemistry of the sesquiterpene alcohol (-)-myliol: x-ray analysis of the p-Bromobenozoate". J. Chem. Soc. (Perkin II), 514.

Pettersen, A. and Kim, H. L. (1976). "X-ray structures of Hymenxon and Hymenolane". J. Chem. Soc. (Perkin II), 1399.

Pitzer, K. S. and Donath, W. E. (1959). "Conformation and strain energy in cyclopentane and derivatives". J. Amer. Chem. Soc. 81, 3213.

Pritish, C. K. Nobin, C. U., Ram, P.S. (1983) "Cyclo-tagitinin C and its transformation". J. Org. Chem. 48, 732.

Prusiner, P. and Sundaralingam, M. (1973) "Crystal and molecular structure of 2-Thio-1-(B-D-ribo-furanosyl)-3H-benzimidazole". Acta cryst. B29, 2328.

Quick, A. and Rogers, D. (1976). "Crystal and molecular structure of parthemolide (4,5-epoxygermcra-1(10), 11 (13)-diene-12,6-olactone" J. Chem. Soc. (Perkin II), 465.

Rahman, A. and Wilson, H. K. (1970) "The crystal and molecular structure of 5-1odouridine:. Acta cryst. B26, 1765.

Rao, S. T. and Sundaralingam, M. (1970). "The crystal and molecular structure of 3'-0-acetylodenosine" J. Amer. Chem. Soc. 92, 4963.

Rubin, J., Brenan, T., Sundaralingam, M. (1970). "crystal structure of naturally occurring dinucleotide monophosphate". Acta cryst. B26, 1089.

Rychlewska, U. (1982). "Crystal and molecular structure of Schkuhriolide monohydrate, a cis, trans-Germacra-1(10), 4-diene-cis-8, 12-olide:. J. Chem. soc. (Perkin II), 1641.

Rychlewska, U, (1981). "Stereochemistry of a novel sesquiterpene lactone. X-ray determination of the structure of Ursiniolide-A monohydrate". J. Chem. Soc. (Perkin II), 660.

Saenger, W. (1971). "Molecular and crystal structure of 5'-methylommonium-5'-deoxyadenosine Iodide monohydrate". J. Amer. Chem. Soc. 93, 3035.

Saenger, W. and Scheit, K. H. (1970), "A pyrimidine nucleoside in the conformation. Molecular and crystal structure of 4-thiouridine hydrate". J. Mol. Biol., 50, 153.

Shefter, E. and Trueblood, K. N. (1965). "The crystal and molecular structure of D(+)-Barium Uridine- 5'-phosphate". Acta cryst. 18, 1067.

Shefter, E. (1968). "Crystal and molecular structure of 6-Thiopurine Riboside:. J. Pharm. Sci. 57, 1157.

Shefter, E., Barlow, M., Sparks, R. A. and Trueblood, K. N. (1969). "Crystal and molecular structure of dinucleoside phosphate" Acta cryst. B25, 895.

Sherfinski, J. and Marsh, R. E. (1973). "The crystal structure and absolute configuration of 1-(ß-D-Arabinofuranosyl) cytosine HCl" Acta cryst. B29, 192.

Subrumanian, E. and Hunt, D. J. (1970). "The crystal structure and absolute configuration of 2'-deoxy-cytidine hydrochloride". Acta cryst. B26, 303.

Sundaralingam, M. (1966). "Stereochemistry of nucleic acid constituents molecular structure of adenosine-3'-phosphate dihydrate". Acta cryst. 21, 495.

Sundaralingam, M. and Abola, J. (1972). "The crystal structure of 5'-methyleneadenosine, 3', 5'-cyclic monophosphate monohydrate:. J. Amer. Chem. Soc. 94, 5070.

Sundaralingam, M. and Rao, S. T. (1971). "Molecular conformation of dihydrouridine". Science, 172, 725.

Sundaralingam, M. (1965). "Conformation of the furanose ring in nucleic acids and other carbohydrates derivatives in solid state". J. Amer. Chem. Soc. 87, 599.

Sundaralingam, M. and Jensen, L. M. (1965). "Stereochemistry of nucleic acid constituents. Molecular structure of cytidylic acid". J. Mol. Biol., 13, 914.

Sundaraman, P. and Mcewen, R. S. (1975). "Crystal molecular structure of parthenolin". J. Chem. Soc. (Perkin II), 440.

Stewart, R. F. and Hall, S. R. (1971) "Determination of Organic structures by physical methods". Vol.3 P.74.

Thewalt, U., Bugg, C. E. and Marsh, R. E. (1970) "The crystal structure of guanosine dihydrate and Inosine dihydrate". Acta cryst. B26, 1089.

Thomas, S. A. (1982), "On the conformation of the five-membered D ring in steroids". J. Cryst. and Spec. Res. 12, 167.

Thomas, S. A. (1982). "Chair and non-chair conformations of non-aromatic six-membered ring compounds". Nig. Jour. Sci., 16, 303.

Thomas, S. A. and Bakinzuwo, I. T. (1987) "On molecular structures of tricyclic diterpenoids in the solid state". Nig. Jour. Appl. Sci., 5, 49.

Thomas, S. A. and Agbaji, E. O. (1989) "Molecular conformation of δ-lactone rings from crystal structure data". J. cryst and Spec. Res. 19, 3.

Thomas, S. A. and Agbaji, C. B. (1991) "Conformation of the bicyclo-(3.2.1) Octane ring derivatives in solid state". Indian Jour. Chem. 30B, 732.

Tollin, P. and Wilson, N. R. (1973) "The crystal and molecular structure of uracil-B-D-arabinofuranoside". Acta cryst. B29, 1641.

Tollin, P. and Wilson, H. R. (1969). "The crystal and molecular structure of thymidine". Acta cryst. B25, 1423.

Tougard, P. and Lefebvre-soubeyram, O. (1974) "Stereochemie de la I-ß-D-Arabinofuranosyl-cytosine". Acta cryst B30, 86.

Tougard, P. and Chantot, J. (1974) "Structure cristalline et molelcularie d'une forme N(7)-protone'e de la guanosine le bromohydrate". Acta cryst. B30, 214.

Tougard, P. (1973) "Crystal structure of I-B-D-arabino-furanosyl thymine". Acta cryst. B29, 2227.

Von Dreele, R. B., Pettit, G. R. Cragg, G. M. and Ode, R. H. (1975), "The crystal and molecular structure of the pseudoguaianolide, autumnolide:, J. Amer. Chem. Soc. 97, 5256.

Viswanitra, M. A., Reddy, S. B. and Sundaralingam, M. (1971). "Stereochemistry of nucleic acids and their constituents XVII" J. Amer. Chem. Soc. 93, 4565.

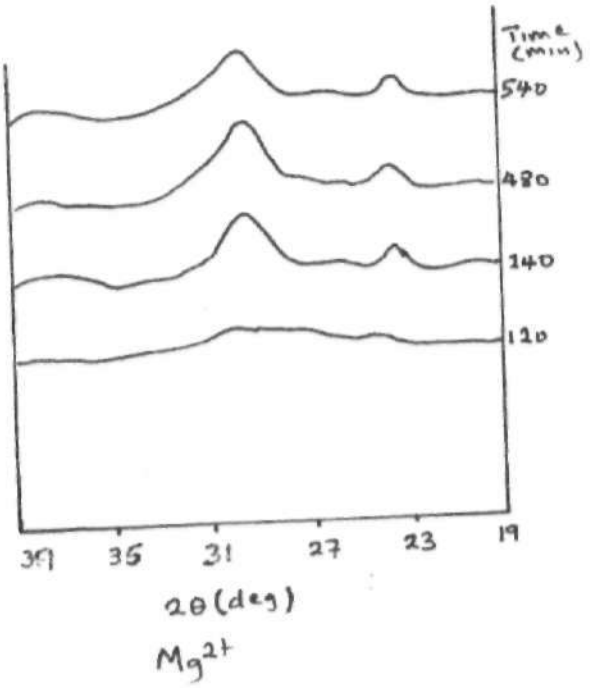
Watkins. S. F., Korp, J. D. and Fischer, N. A. (1978) "Molecular structure of two derivatives of the Germacranolide sesquiterpene lactone, melnerin" J. Chem. Soc. (Perkin II), 599.

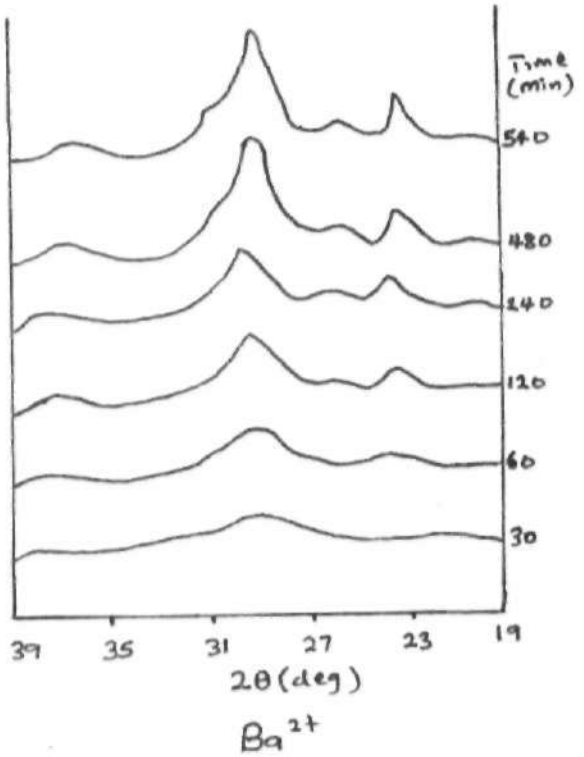
Watson, D. G. (1965). "The crystal structure of deoxyadenosine monohydrate". Acta cryst. 19, 111.

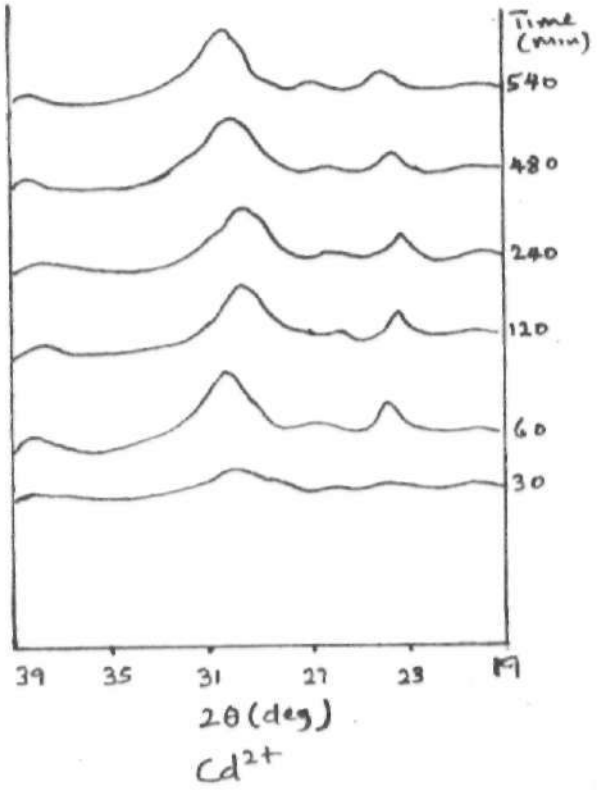
Westhof, E. and Sundaralingam, M (1983) "A method for the analysis of puckering disorder in five-membered rings. J. Amer. Chem. Soc., 106, 970.

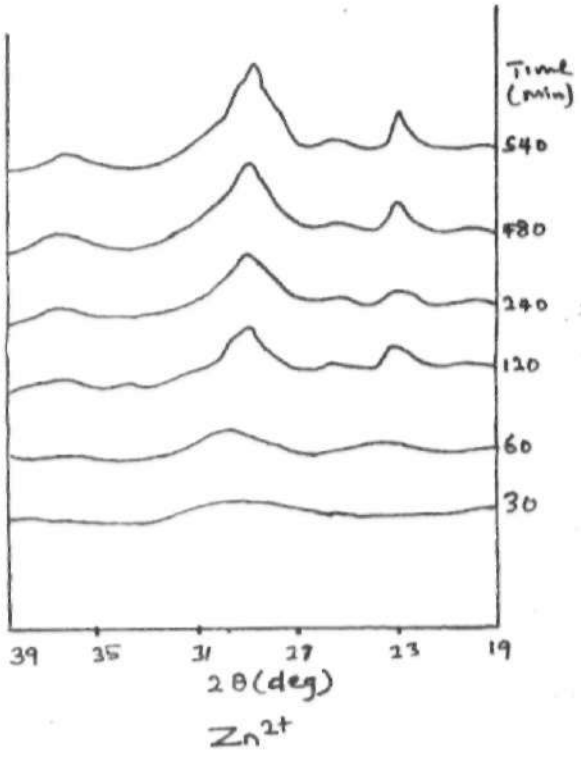
Witt, M. E. and Watkins, S. F. (1978). "Crystal and molecular structure of Tamaulipin-P, a trans, trans-Germacra-1(10), 4-dienolide sesquiterpene lactone". J. Chem. Soc. (Perkin II), 204.

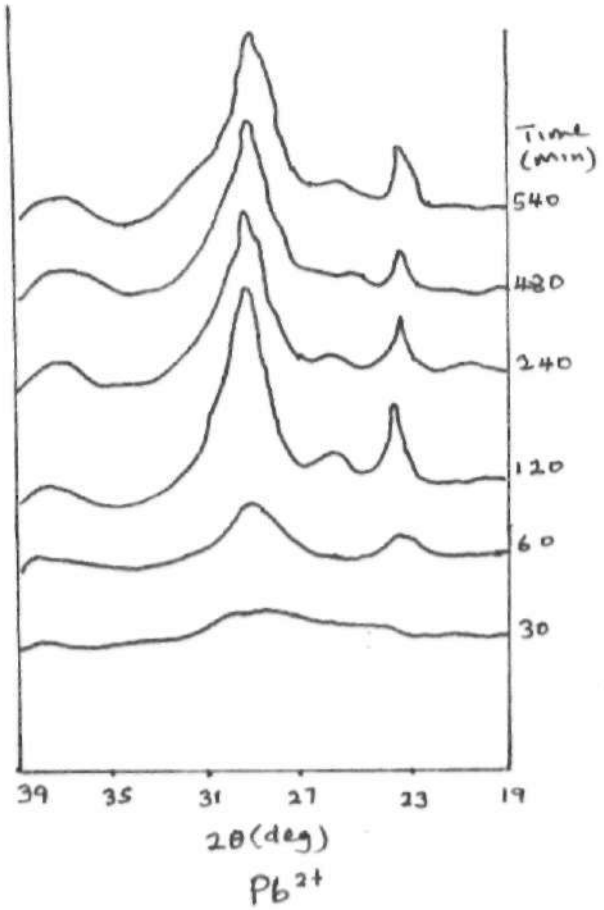
Appendix I X-Ray pattern of ACP-HAP precipitates in presence of metal ions

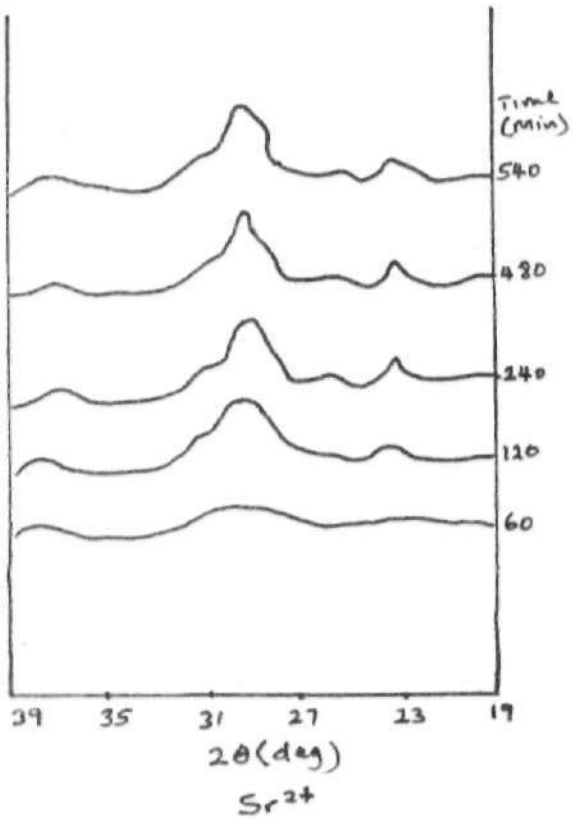


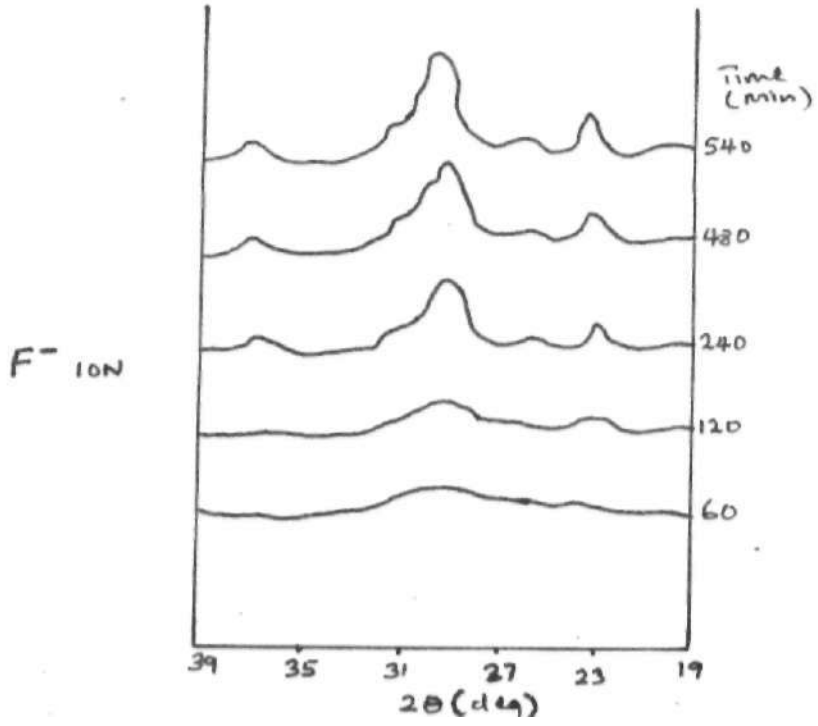




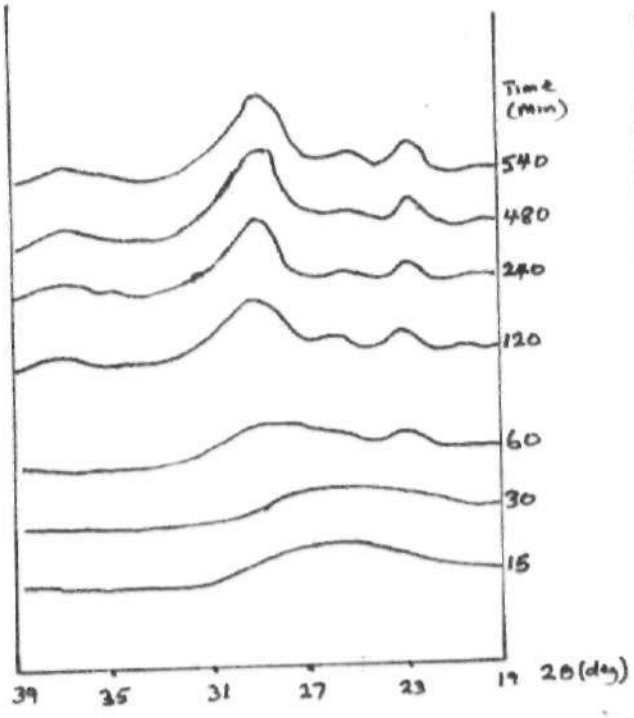



Time (min)
540
480
240
120
60
30
39
35
31
27
23
19
2θ(deg)
Pb2+

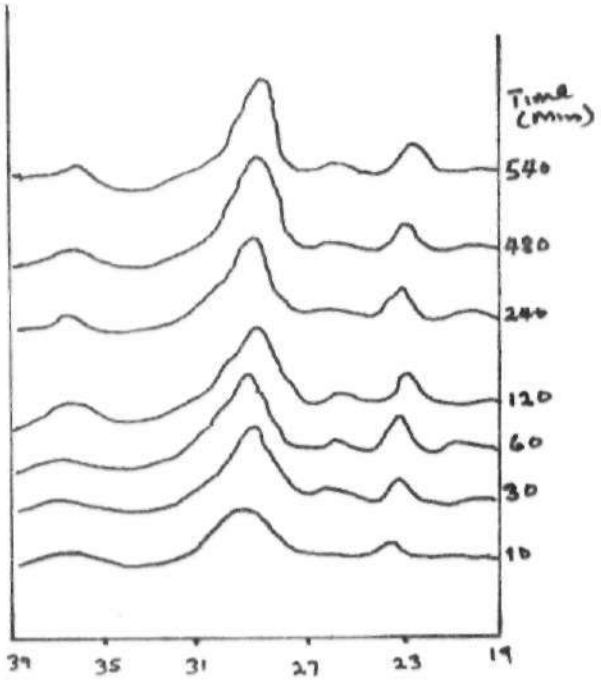

Time (min)
540
480
240
120
60
39
35
31
27
23
19
2θ(deg)
Sr2+


F⁻ ION
Time (min)
540
480
240
120
60
39
35
31
27
23
19
2θ(deg)

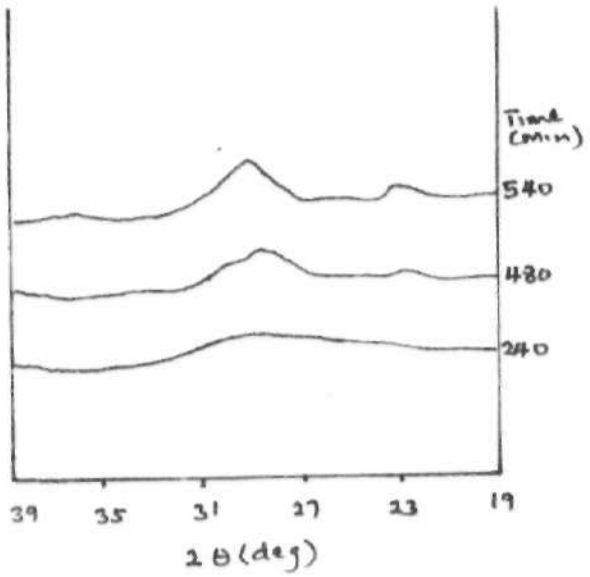
Appendix II X-Ray patterns of ACP-HAP precipitates obtained in presence of some inhibitors



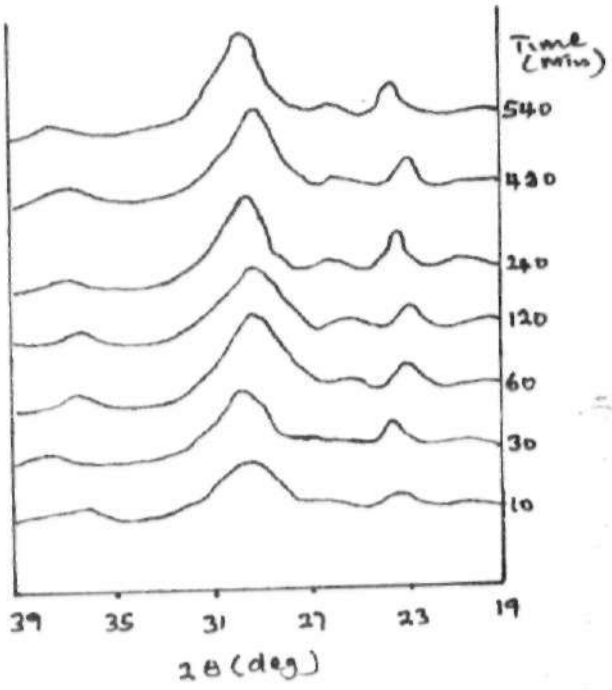
AMP AT pH 9.0/25°C



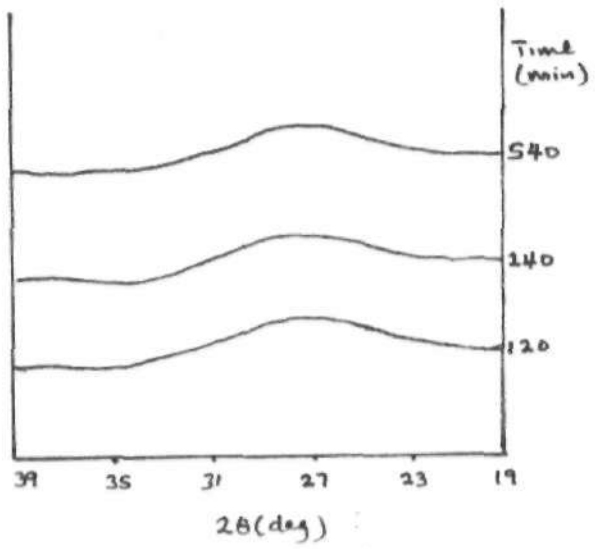
AMP AT pH 9.0/50°C



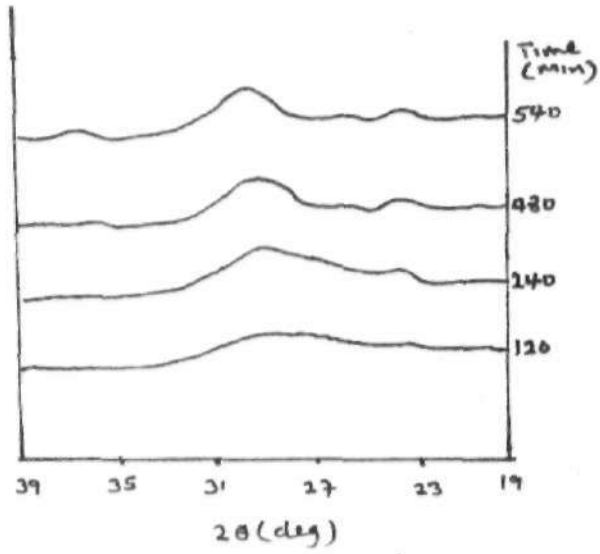
ADP AT pH 9.0/25°C



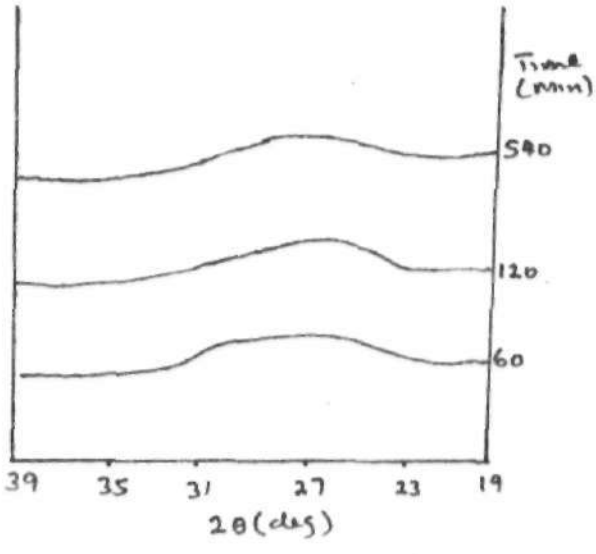
ADP AT pH 9.0/50°C



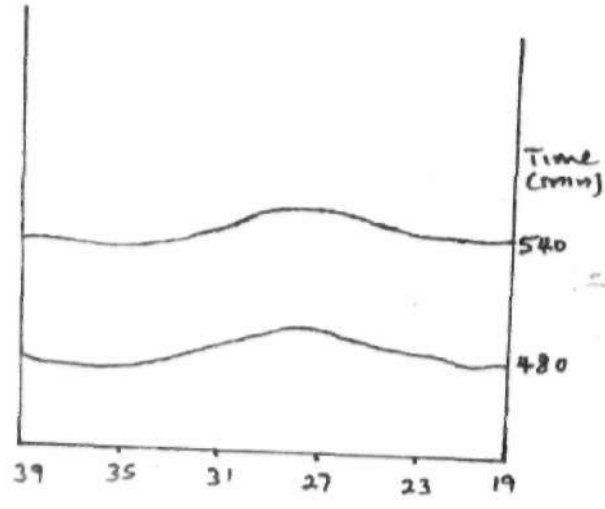
ATP AT PH 9.0/25°C



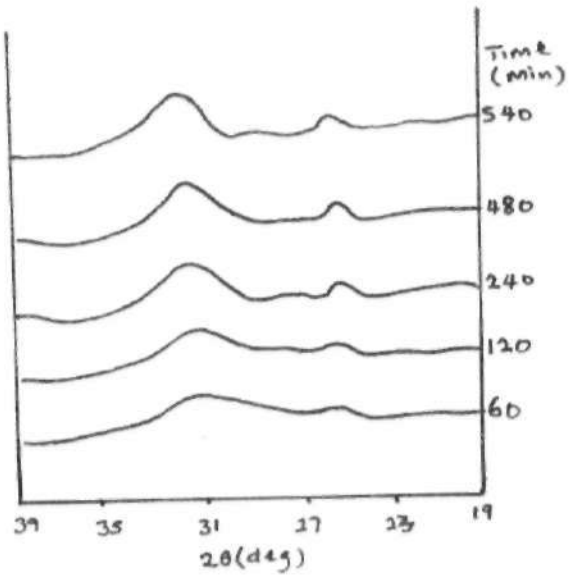
ATP AT PH 9.0/50°C



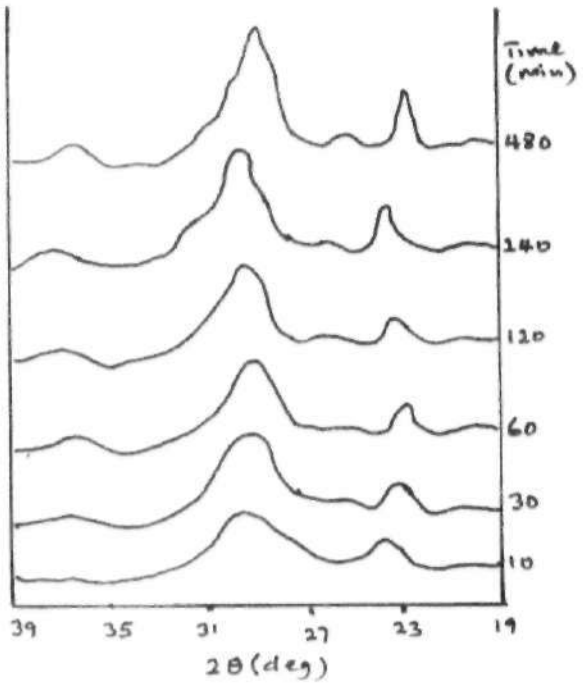
$P_2O_7^{=}$ AT PH 9.0/25°C



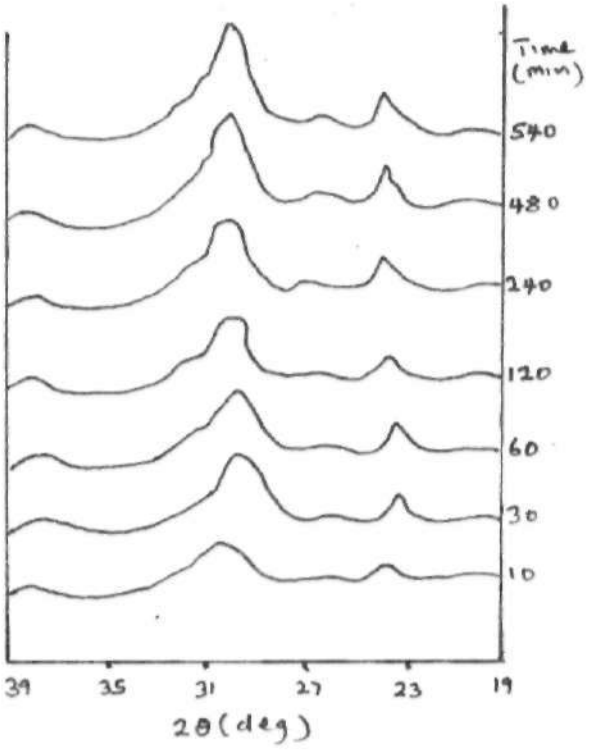
$P_2O_7^{=}$ AT PH 9.0/50°C



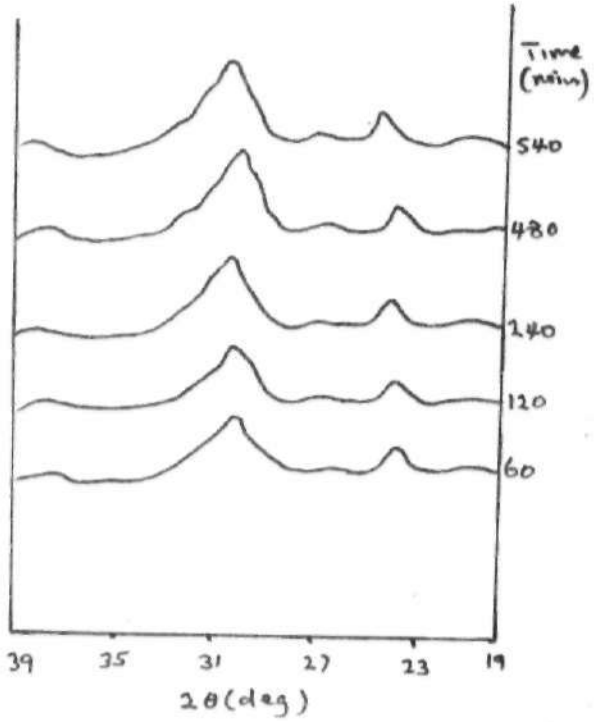
CITRATE AT PH9·0/25°C



CITRATE AT PH9·0/50°C



CASEIN AT PH9·0/25°C



GLUTAMATE AT PH9·0/25°C

APPENDIX III

X-Ray diffraction data for the tin compound, and the equation used for calculating cell parameters for a compound having hexagonal space group.

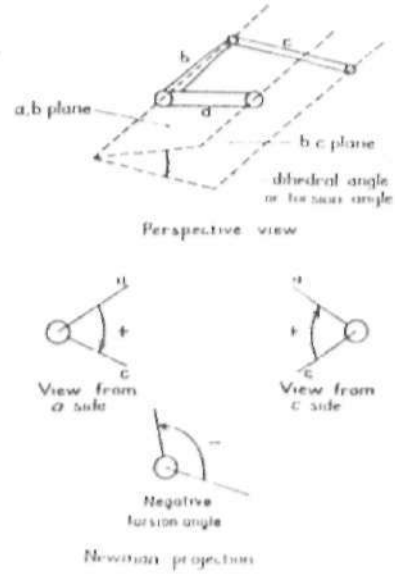
Degrees 2θ	d-spacing
26.0	3.4270
29.8	2.9981
30.2	2.9592
30.9	2.8938
31.5	2.8400
39.6	2.2758
44.3	2.0446
45.0	2.0144
45.6	1.9893
46.8	1.9411
52.9	1.7307

$$\frac{1}{d^2_{hkl}} = \frac{4}{3a^2}(h^2 + hk + k^2) + \frac{l^2}{c^2} \quad)$$

APPENDIX IV

DEFINITION OF TORSION ANGLE CONCEPT

Torsion angle (or dihedral angle) is a term commonly used to denote the angle which characterizes the steric relationship between two vicinal bonds in a molecule. A perspective view is given below. For example a system of three consecutive bonds a, b, c defines two half planes a, b and b, c intersecting along the central bond b. They form a figure known in geometry as a dihedron. The value of this angle gives an accurate evaluation of the relative positions of the vicinal bonds a and c (Bucourt, 1974).



Dihedral or torsion angle.

APPENDIX V

Compound codes, names and references of sesquiterpenes containing the seven-membered ring.

Code	Name	Reference
H1	Dihydrodecaacety/gaillardin-P benzoate	Dullforce, T.A. et al (1971)
H2	Bromoisotenulin Mol. 1	Maxhan-ul-Hague et al (1974)
H3	Bromoisotenulin Mol. 2	" " (1974)
H4	Plenolin	Mcphail and Onan, (1975)
H5	Mikanokngptin	Bovill et al, (1979)
H6	Berladin	Cox and Sim, (1975)
H7	Euparetin	Mcphail and Sim, (1973)
H8	*Solstitlian*	" "
H9	Bromodihydrosophotosan tonic lactone acetate	" "
H10	Bromogeigerin	" "
H11	Bromohelenalin	" "
H12	Bromomexicannin-E	Sekita et al, (1971)
H13	Bromogaillardin	Dullforce et al, (1971)
H14	Cyclotagitinin-C	chowdhury, (1983)
H15	Fluoroguaianolide	Fronczek, (1979)
H16	*Deacetylneotennlin*	*Cox and Sim, (1976)*
H17	Bromohelenalin	Mazhan-ul-Hague, (1969)
H18	Helenalin	Mcphail and Onan, (1975)
H19	4-0--Acetyl-2-0-P-iodobenzoylflorilena-lin.	" " (1975)
H20	Hymenolane	Pettersen et al, (1976)

Code	Name	Reference
H21	Hymenxon	" "
H22		Malone and Kim, (1976)
H23	Alcohol (-)-myliol (A)	Nozaki, (1979)
H24	" " (B)	" "
H25	Paucin monohydrate	Cox and Sim, (1977)
H26	Autunolide	Von Dreele et al, (1975)
H27	Parthemolin	Sundaraman, (1975)
H28		Herz, et al, (1980)

APPENDIX VI

Compound codes, names and references of furanose ring derivatives.

Code	Name	Reference
F1	*Inosine*	*Munns and Tollin, (1970)*
F2	Guanosine-5'-phosphate	Murayama et al, (1969)
F3	Adenosine/5-bromouridine complex	Haschemeyer et al, (1965)
F4	Adenyl-2'-phosphate-5'-Uridine (Uridine res	Shefter et al. (1970)
F5	5-Iodouridine	Rahman et al, (1970)
F6	*Cytidine*	*Furbergs et al, (1965)*
F7	2-Thiocytidine dihydrate	Hung-yin Lin, (1971)
F8	2,4-Dithiouridine dihydrate	" "
F9	5-methyl/uridine	Hunt et al, (1969)
F10	Deoxy adenosine monohydrate	Watson, (1965)
F11	Inosine-5'-phosphate	Nagashima et al, (1974)
F12	9-B-D-arabinofuranosyl adenine HCl	Chwang et al, (1974)
F13	*3'-deoxy-3'-(dihyroxyl phosphine/methyl)* adenosine	Hecht et al, (1972)
F14	Deoxycytidine HCl	*Subramanian et al, (1970)*
F15	4-Thio Uridine disulphide	Altona et al, (1972)
F16	Guanosine hydrobromide Mol.I	Tougard et al, (1974)
F17	5-Bromouridine in complex with Adenosine	*same as F3*
F18	*Calcium thymidine-5'-phosphate*	Altona et al, (1972)
F19	adenosine-3'-phosphate dihydrate	Sundaralingam, (1966)
F20	2-Thio-1-(B-D-ribofuranosyl)-3H-benzimidazole	Prusiner et al, (1973)
F21	9-B-D-Arabinofuranosy/adenine	Bunick et al, (1974)
F22	Adenosine-5'-methlphosphonate Mol.I	*Barnes, (1979)*
F23	4 - Thiouridine monohydrate	Same
F24	Deoxy cytidine-5'-phosphate	Viswamitra et al, (1971)
F25	Guanosine hydrobromide Mol.II	Tougard et al, (1974)
F26	*Adenyl-2'-phosphate-5'-Uridine* (adenyl res.)	Same as F5

F27	8 - Bromoguanosine	Buggi and Thewalt (1969)
F28	3'-0-Acetyladenosine	R0-0 et al, (1970)
F29	6 - Thioinosine Mol. I	Shefter, (1968)
F30	6 - Thioinosine Mol. II	" "
F31	Guanosine dihydrate Mol. I	Thewalt et al, (1970)
F32	5-lodo-2'-deoxyuridine	Cameraman et al, (1965)
F33	dihydrouridine	Sundaralingam, (1971)
F34	5 - Bromouridine	Iball et al, (1971)
F35	5-(1-2'-deoxyuracyl) ethyl sulphide	Altona et al, (1972)
F36	3'-0-Acetyl-4-thiothymidine	" "
F37	5- chorouridine	Coulter et al, (1969)
F38	5- fluoro-2'-deoxy Uridine	" "
F39	Uracil-B-D-arabinofuranoside	Tollin et al, (1973)
F40	D (+)-Barium Uridine 5'-phosphate	Shefter et al, (1965)
F41	5-Bromo-2'-deoxy uridine	Iball et al, (1966)
F42	Bromo deoxyhytidine (in complex with deoxyguanosine)	Haschemeyer, et al (1965)
F43	Diliydrouridine hemihydrate	Sundaralingam, (1976)
F44	5'-Methylene adenosine-3',5'-cyclic phosphate	Sundaralingam, (1974)
F45	5- lodouridine Mol. II	Same as F6
F46	Inosine dihydrate Mol. II	Thewalt et al, (1970)
F47	Adenosine-5'-methlphosphonate Mol.II	Same as F38
F48	Guanosine dihydrate Mol. II	The walt et al, (1970)
F49	Inosine dihydrate Mol. I	" "
F50	Rubidium adenosine-5'- diphosphate	Altona et al, (1972)
F51	8- Bromo adenosine	
F52	Deoxyguanosine (in complex with bromo-deoxycytidine).	Haschemeyer et al, (1965)
F53	1-ß-D-Arabinofuranosyl-cytosine	Tougard et al, (1974)
F54	N^2- Dimethyl/guanosine	Altona et al, (1972)
F55	5-methylammonium-5'-deoxy adenosine	Saenger, (1971)
F56	Thymidine	Tollin and Wilson, (1969)

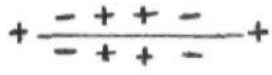
F57	1-ß-D-arabinofuranosyl) cytosine HCl	Sherfinski et al, (1973)
F58	Na-ß-cytidine-2',3'- cyclic phosphate	Coulter, (1973)
F59	Methyl-1,2',3,5-tetra-o-acetyl-ß-D-galacto- furanuronate	Beale, et al, (1971)
F60	Guanosine-3',5'- cyclic monophosphate	Chwang et al, (1974)
F61	Cyclic Uridine - 3',5'-phosphate	Coulter, (1969)
F62	1-(ß-D-arabinofuranosyl) Thymine	Tougard, (1973).

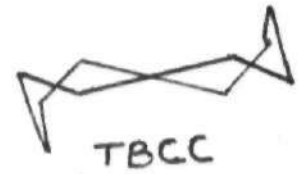
Appendix VII

Some viable ten - membered rings with axis/plane

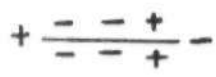


TCBC = TCC



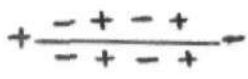


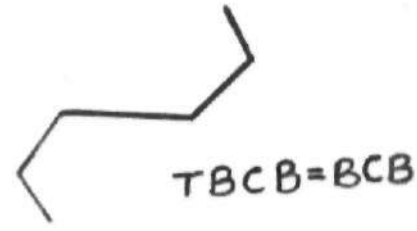
TBCC



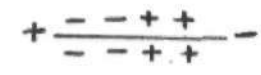


TCCC = CCC



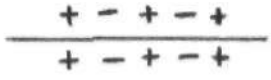


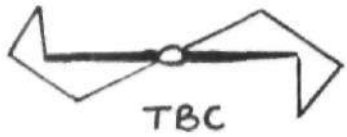
TBCB=BCB



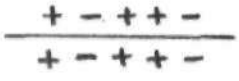


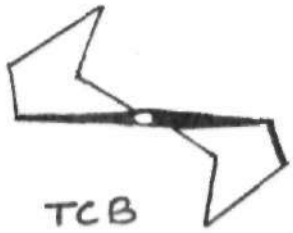
TCC = TCBC



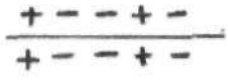


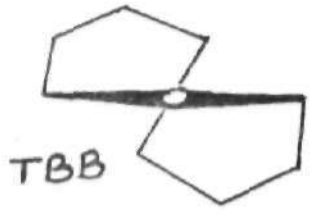
TBC



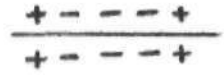


TCB





TBB



APPENDIX VIII

Compound code, Compound name and references of cyclodecadiene ring derivatives.

Compound Code	Name	Reference
T1	Melnerin	Watkins et al, (1978)
T2	Glavcolide	Cox and Sim, (1975)
T3	Dihydrochrysanolide	El-Feraly et al, (1983)
T4	Dihydrochrysanolide	" " "
T5	Schkuhriolid	Rychlewska, (1982)
T6	*Melampodin*	" "
T7	Ursiniolide A monohydrate	" (1981)
T8	Melampodine B	Fronczek et al (1980)
T9	Eupaformonin	Mcphail and Onan, (1976)
T10	Cordifene I	Begcey et al, (1981)
T11	Cordifene II	" " "
T12	Dihydromikanolide	Cox and Sim, (1977)
T13	Hallerol	Calleri et al, (1983)
T14	*Tamaulipin-A*	Witt and Watkins, (1978)
T15	Alatolide monohydrate	Cox and Sim, (1977)
T16	Eupatolide	Mcphail and Onan, (1975)
T17	Parthenolide Mol. I	Quick and Rodger, (1976)
T18	Parthenolide Mol. II	" " "
T19	Herbolide A	Jones and Kennard, (1979)
T20	Ovatifolin	Gopalakrishna et al, (1977)
T21	Eupahyssopin	Kuo-Hsiung hec et al (1976)
T22	Briarein	Bucks et al, (1977)
T23	Enhydrin	*Rychlewska*, (1982).